The role of Pax6 isoforms in embryonic development

By

Jeni Pinson

Thesis submitted for the degree of doctor of philosophy at the University of Edinburgh

2005

Disclaimer

I (Jennifer Pinson) performed all of the experiments presented in this thesis unless otherwise clearly stated in the text. No part of this work has been, or is being submitted for any other degree or qualification.

Signed:

Date: 4/2/05

Acknowledgements

I would like to thank my supervisors David Price, John Mason and Ian Simpson for their endless help, support and advice throughout the course of this study.

I am also grateful to Ben Fenby, Ben Martynoga, Celestial Yap, Dave Tyas, Jane Quinn, Mark Hillen, Martine Manuel, Natasha Tian, Paulette Zaki and Tom Pratt for putting up with my tantrums, imparting their knowledge and generously offering their time and support.

I would also like to thank Linda Wilson for her patience and invaluable expertise in confocal imaging, Shonna Johnston for advice, help and expertise in flow cytometry, and Karen Chapman for critical feedback and advice on the RPA protocol.

Most of all, I'd like to thank all those who have offered me their love and support over the last four years, in particular Mum and Dad, and Des, without whom this piece of work could never have been produced.

When I have fears that I may cease to be
Before my pen has glean'd my teeming brain,
Before high-piled books, in charactery,
Hold like rich garners the full ripen'd grain;
When I behold, upon the night's starr'd face,
Huge cloudy symbols of a high romance,
And think that I may never live to trace
Their shadows, with the magic hand of chance;
And when I feel, fair creature of an hour,
That I shall never look upon thee more,
Never have relish in the faery power
Of unreflecting love;-then on the shore
Of the wide world I stand alone, and think
Till love and fame to nothingness do sink.

John Keats

Table of Contents

Abbreviations

BrdU – 5-bromo-2-deoxyuridine

cDNA – complementary DNA

CNS – Central Nervous System

C-terminus – Carboxy-terminus

dbcAMP - 2'-O-dibutyryladenosine 3', 5'-cyclic monophosphate

DNA – Deoxyribonucleic acid

E12.5 – Embryonic day 12.5

ECACC – European Collection of Cell Cultures

EGL – External granule layer

EMBL – European Molecular Biology Laboratory

ENU – N-ethyl N-nitrosourea

GITC – Guanidine isothiocyanate

HD - Homeodomain

IZ- Intermediate zone

mRNA – messenger RNA

N-terminus – Amino-terminus

OBLS – Olfactory bulb-like structure

ORF – Open reading frame

PD – Paired domain

RNA – Ribonucleic acid

RPA – RNase protection assay

SCO – Sub-commissural organ

ssRNA – Single stranded RNA

TAD – Transactivation domain

TCA – Thalamocortical axon

TPOC – Tract of the post-optic commissure

VZ – Ventricular zone

YAC – Yeast artificial chromosome

Mouse Strains

All strain accession numbers are from Mouse Genome Informatics, www.informatics.jax.org

WT – Wild type (in this study, WT mice were outbred CD-1 strain, Harlan Scientific, UK)

Sey – *Pax6*^{Sey} (MGI:1856155)

Sey^{Neu} – *Pax6*$^{Sey\text{-}Neu}$ (MGI:1856158)

Pax6^{LacZ} – Pax6^{tm1Pgr} (MGI:1934347)

Abstract

During murine development, organogenesis of the central nervous system is a tightly controlled process. Complex regulatory gene networks exist, at the head of which are transcription factors that affect the expression of downstream genes. One such transcription factor, Pax6, is crucial for the correct development of a number of organs, including the brain, eyes and spinal cord.

A number of Pax6 isoforms have been described, many of which involve alterations to the two DNA-binding domains, the paired domain and the homeodomain. In the best characterised of these isoforms, Pax6+5a, the insertion of a 42bp cassette exon by alternative splicing leads to the disruption of a helix-turn-helix motif within the paired domain. The DNA-binding specificity of the Pax6 protein is changed, thereby altering the target genes on which Pax6 can act. Other isoforms exist in which the entire paired domain is absent, and DNA-binding can only occur *via* the homeodomain.

In this way, numerous transcription factors are derived from the *Pax6* locus, all of which are predicted to have the same transactivation properties, but which act on different subsets of downstream genes.

The aims of this study were i) to characterise differences in the spatial and temporal expression of Pax6 isoforms during murine embryonic development ii) to analyse the expression of Pax6 isoforms in various *Pax6* mutant mice during neurogenesis, and iii) to examine the effects of over-expression of the best understood isoforms, in a cell culture system. The overall aim was to elucidate the independent roles of Pax6 isoforms in organogenesis of the central nervous system.

RNase protection assay was used to determine the ratio between *Pax6* and *Pax6+5a* transcripts in a number of tissues of the central nervous system during neurogenesis. In most tissues studied, *Pax6* is much more prevalent than *Pax6+5a* at embryonic day 12.5, but the ratio has fallen by embryonic day 18.5. This may be indicative of a change in the role of Pax6, from controlling proliferation to controlling neuronal differentiation.

Pax6 protein expression was analysed in mice with 0, 1, 2, 8 and 14 functional copies of *Pax6*, in order to compare the levels of Pax6 expression between genotypes, and to

determine if differential expression of one or more isoforms could be responsible for the mutant phenotypes. Most isoforms are down-regulated in the *Pax6*^{Sey}/+ eye, whilst their relative expression is more varied in the *Pax6*^{Sey}/+ brain. Most isoforms are significantly up-regulated in the brain and eye of mice with 8 or 14 copies of *Pax6*, but there are no differences between expression levels in the brain of the two genotypes, indicating that Pax6 is subject to autoregulation. Some Pax6 isoforms are observed in the brain of mice thought to lack functional *Pax6*.

Expression constructs containing *Pax6*, *Pax6+5a* and "paired-less" *Pax6* were introduced into immortalised cell lines. Again, Pax6 autoregulation was demonstrated; the over-expression of *Pax6* leads to the up-regulation of Pax6+5a, and *vice versa*. Pax6 over-expression also promotes neuronal differentiation in a neuroblastoma-derived cell line.

Chapter 1 : Introduction

Pax6 is a transcription factor, belonging to the paired box (*Pax*) gene family (Walther and Gruss, 1991). The *Pax* genes are expressed in discrete domains during development, and are important for the correct control of organogenesis, particularly in the brain (reviewed in Mansouri et al, 1999; see **Figure 1.1**). *Pax6* is expressed throughout neurogenesis in the developing eye, brain, nasal epithelia, spinal cord and pancreas, and is known to be important for the development of all these tissues (Hill et al., 1991; Hogan et al., 1986; St-Onge et al., 1997; Stoykova and Gruss, 1994; Ton et al., 1991).

Within the developing mouse brain, *Pax6* is expressed in the dorsal telencephalon (presumptive cortex), specifically within the ventricular zone (VZ), and in the olfactory bulbs and olfactory epithelia. It is also found in distinct areas of the diencephalon including the ventral thalamus and the epithalamus, and in the cerebellum and the dorsal portion of the hindbrain (Stoykova and Gruss, 1994; Walther and Gruss, 1994; see **Figure 1.1** for a brief outline of the Pax6 expression pattern in the brain during neurogenesis).

1.1: Pax6 Protein Domains

Pax6 is a 422 amino acid transcription factor, which binds to target DNA sequences *via* one or both of two DNA-binding domains; the paired domain (PD), and the homeodomain (HD). Transcriptional regulation of Pax6 target genes is mediated by a C-terminal transactivation domain (TAD; see **Figure 1.2** for an outline of the main Pax6 protein domains).

1.1.1: The Pax6 Paired Domain

The Pax6 PD is situated at the N-terminus of the protein, and the crystal structure of the Pax6 PD – DNA complex has been elucidated (Xu et al., 1999). Within the PD are two separate DNA-binding subdomains, designated PAI and RED, both of which are helix-turn-helix motifs, and can bind target DNA.

The two Pax6 PD subdomains are thought to interact with one another, as the presence of PAI reduces the activity of the RED subdomain on its consensus binding

Figure 1.1 *Pax6* expression in the E13.5 mouse brain (taken from Stoykova and Gruss, 1994). In the telencephalon, *Pax6* expression (in pink) is seen in the olfactory epithelium (OE), the olfactory bulbs (OB), and the ventricular zone of the dorsal telencephalon (CFr, for frontal cortex). In the diencephalon, *Pax6* is expressed in the ventral thalamus (VT), the epithalamus (ET), and a thin strip along the dorsal surface of the dorsal thalamus (DT). *Pax6* is also expressed in the dorsal hindbrain (pons, Pn and myelencephalon, My), the dorsal spinal cord (Sc) and the external granular layer (egl) of the cerebellum (Cb). GE, ganglionic eminence; LV, lateral ventricle; Ms, mesencephalon; ORE, optic recess; PC posterior commissure; POA, Pre-optic area; PT, pretectum; SE, septum; sut, subthalamus; 4V, fourth ventricle.

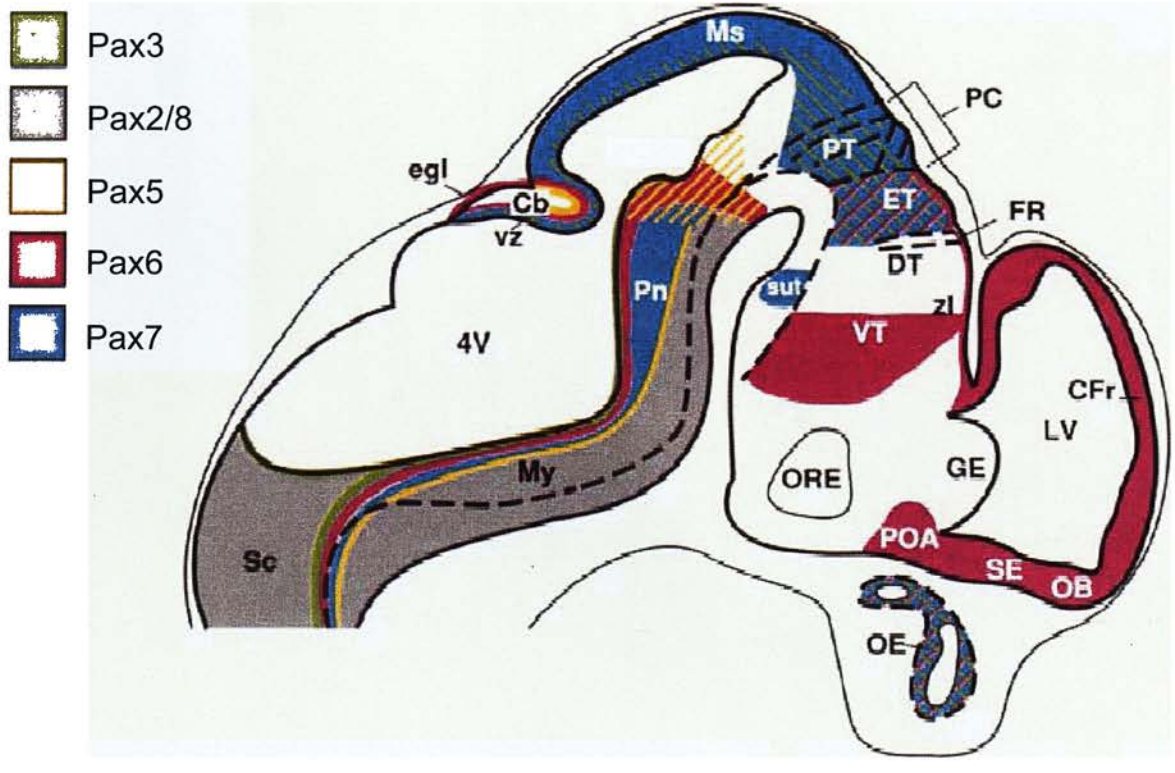
Pax3
Pax2/8
Pax5
Pax6
Pax7
Ms
PC
PT
egl
Cb
ET
FR
vz
DT
Pn
sut
zl
VT
4V
CFr
LV
My
ORE
GE
POA
Sc
SE
OB
OE

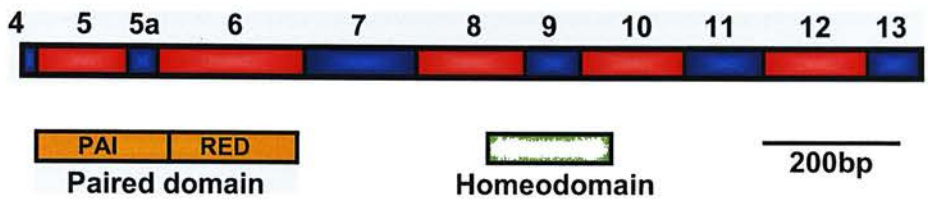

Figure 1.2 Molecular structure Pax6. All known *Pax6* coding exons are shown as red and blue bars. Sections encoding DNA-binding domains are indicated as bars below the coding exons. Canonical translation begins at the 3' end of exon 4, and terminates within exon 13. Immediately at the N-terminus of the protein is a paired domain, a DNA-binding domain characteristic of all Pax genes. In the centre of the protein is a second DNA-binding domain, the paired-type homeodomain. Between these two DNA-binding domains, the protein is rich in glutamine and glycine residues. The C-terminal portion of the gene is the transactivation domain, which dictates the action of Pax6 once it is bound to target DNA.

sequence, and vice versa (Yamaguchi et al., 1997). Also, a naturally-occurring mutation in the RED domain abolishes Pax6-DNA binding via the PAI domain (Singh et al., 2000).

The best characterised *Pax6* alternative splicing event involves the insertion of a 42bp exon, designated exon 5a, into the PD (Walther and Gruss, 1991). As a result of this alternative splicing, two major Pax6 isoforms are produced, Pax6 lacking exon 5a (hereafter designated Pax6-5a), and Pax6 containing exon 5a (hereafter designated Pax6+5a). The insertion of exon 5a is known to alter the DNA-binding properties of the Pax6 PD. The PAI subdomain of Pax6-5a appears to preferentially bind a consensus sequence known as P6CON (Epstein et al., 1994a). When exon 5a is present, it disrupts the PAI subdomain (see **Figure 1.2**), acting as a "molecular toggle", and allowing the RED subdomain to bind its consensus sequence, 5aCON (Epstein et al., 1994b). Although these two consensus sequences were isolated *in vitro* and have not yet been described *in vivo*, they provide evidence that the insertion of exon 5a does alter the sequences on which Pax6 can act.

The alternative splicing of exon 5a, and other alternative splicing events within the Pax6 gene, will be described in greater detail in Section 1.4.

1.1.2: The Pax6 Homeodomain

Pax6 contains a paired-type HD, distinguished from other HDs by a serine rather than a glutamine or a lysine at position 50 (Wilson et al., 1993).

The Pax6 HD is known to bind to a number of target genes, including *Retinoblastoma* (Cvekl et al., 1999), *Engrailed-1* (Plaza et al., 1997) and *Rax* (Mikkola et al., 2001), and is thought to be involved in the transcriptional regulation of a number of other developmentally important genes (reviewed in Simpson and Price, 2002).

The Pax6 PD and HD are known to interact with one another, and affect transactivation *via* consensus binding sequences. As expected of a HD-containing transcription factor, both Pax6+5a and Pax6-5a can activate transcription when bound to consensus HD-binding sequences (Czerny and Busslinger, 1995; Plaza et al., 1994; Singh et al., 2000). Perhaps surprisingly, Pax6-5a has a stronger effect than Pax6+5a, implying that the PD is involved in this interaction (Mishra et al., 2002). An interaction between the PD and the HD was also shown by Singh et al. (2000), as a

naturally-occurring mutation in the PAI subdomain of the PD leads to increased transactivation *via* a HD-binding site. A Pax6 protein lacking the entire HD was created (Mikkola et al., 2001), and this was shown to bind to a Pax6 HD *in vitro*, presumably through the PD.

Evidence from the *Drosophila* gene *Paired,* a member of the *Pax* family, suggests that although both the PD and the HD need to be present for Pax gene activity, they can act *in trans*, and need not be present as part of the same molecule (Miskiewicz et al., 1996). This implies that interactions can occur between protein domains of different Pax6 molecules.

1.1.3: The Pax6 Transactivation Domain

After binding DNA through the PD and/or HD, Pax6 exerts its transcriptional control over target genes *via* the C-terminal portion of the protein, the TAD (Singh et al., 2000; Tang et al., 1998). Various cDNA array-based studies have indicated that Pax6 can act as both an activator and a repressor of transcription (Chauhan et al., 2002a; Chauhan et al., 2002b; Chauhan et al., 2002c). This was also shown with a microarray used to detect Pax3 target genes, and may be a general feature of the *Pax* gene family (Mayanil et al., 2001).

The Pax6 TAD is a complex molecular domain, and deletion studies have shown that a whole, intact TAD is necessary for optimal transcriptional activity (Singh et al., 2000; Tang et al., 1998).

1.2: *Pax6* mutant mice used in this study

For a diagrammatical representation of the *Pax6* mutations in *Sey, Sey*^{Neu} and *Pax6*^{LacZ}, see **Figure 1.3**.

1.2.1: *Small eye (Sey)*

Sey is a spontaneous mutation in the *Pax6* gene, first characterised at the molecular level by Hill *et al.* (1991). A single base pair GGA → TGA substitution results in a glycine → STOP mutation in exon 8 of the murine *Pax6* locus. *Pax6* mRNA is highly expressed in *Sey/Sey* mice (Collinson et al., 2003; Warren and Price, 1997), but the

Figure 1.3 The Pax6 mutations in *Sey*, *Sey*^{Neu} and *Pax6*^{LacZ}. **A**, full-length Pax6. Red and blue bars represent Pax6 exons. Orange bar: paired domain, Green bar: homeodomain, Black bars: internal ATG codons. **B**, *Sey* cDNA, the mutation introducing a STOP codon is indicated with an arrow. Pale blue bar: translated Pax6 transcript. Dark green bar: untranslated mRNA **C**, *Sey*^{Neu} cDNA, the mutation introducing an abnormal splice donor site, and the STOP codon within intron 10 are indicated with arrows. Blue and pink hatched bar: translated region of intron 10. Pink bar: untranslated region of intron 10. **D**, Pax6-LacZ cDNA. Yellow bar represents LacZ cDNA, which replaces Pax6 exons 4-6, including the canonical start ATG. Translation stop site is unknown.

3'-truncated protein has only been detected at very low levels (Engelkamp et al., 1999). Therefore, *Sey/Sey* mice are generally considered to be completely null for Pax6 protein. *Sey/+* mice have a milder phenotype than that seen in the *Sey/Sey* mouse.

Sey/+ mice display micropthalmia, whilst *Sey/Sey* mice do not develop eyes. Homozygous mice can be distinguished from heterozygotes from embryonic day 10.5 (E10.5), when the nasal placodes and lens are entirely absent, and die shortly after birth (Grindley et al., 1995; Hill et al., 1991; Hogan et al., 1986).

The development of the brain is also severely affected in *Sey/Sey* mice (reviewed in Callaerts et al, 1997; Simpson and Price, 2002); the forebrain is reduced in size (Warren and Price, 1997), and shows profound morphological defects (Stoykova et al., 1996). The cerebellum, hindbrain and spinal cord, areas where Pax6 is known to be expressed (Stoykova and Gruss, 1994), are also abnormal in *Sey/Sey* mice (Engelkamp et al., 1999; Ericson et al., 1997; Osumi et al., 1997; Sun et al., 1998).

Sey/+ mice have a mild brain phenotype, with defective development of the subcommissural organ (SCO) (Estivill-Torrus et al., 2001) and the tract of the postoptic commissure (TPOC) (Mastick et al., 1997).

1.2.2: *Small eye^{Neu} (Sey^{Neu})*

The *Sey^{Neu}* allele was created in an ENU-induced mutation screen (Favor et al., 1988). A G→T point mutation at the +1 position of a *Pax6* splice donor site causes a splicing error. A 116bp sequence from intron 10 fails to be spliced out, introducing a premature STOP codon and resulting in a C-terminally truncated transcript (Hill et al., 1991). The phenotype of the *Sey^{Neu}* mutation is generally considered to be the same as that of the *Sey* mutation (Grindley et al., 1997; Hill et al., 1991; Mastick et al., 1997), although there may be subtle differences between the two in the diencephalon (Stoykova et al., 1996).

1.2.3: *Pax6^{LacZ}*

Pax6^{LacZ} mice (St-Onge et al., 1997) contain a copy of the *β-galactosidase* gene inserted in the genomic *Pax6* locus, replacing exons 4 to 6 of the endogenous *Pax6*

gene. This has a two-fold effect, ablating Pax6 expression and replacing it with expression of the β-galactosidase transgene under the control of the *Pax6* promoter(s). The phenotype of the $Pax6^{1.acZ}$ mutation is generally considered to be the same as that of the *Sey* mutation.

1.2.4: PAX77

PAX77 mice (Schedl et al., 1996) are an addition transgenic line containing approximately 6 copies of a YAC spanning the 420kb human *PAX6* locus. This YAC contains not only the *Pax6* coding sequence, but also all the known regulatory elements (Fantes et al., 1995). Although it is an addition transgenic, the inclusion of the human *PAX6* regulatory elements in the YAC should abolish any position effect, and lead to PAX6 over-expression in all tissues in which the endogenous *Pax6* gene is expressed.

Like *Sey*/+ mice, PAX77 hemizygotes and homozygotes show a decrease in eye size, although this effect is highly variable (Schedl et al., 1996). Surprisingly, no brain phenotype has been detected in PAX77 mice (Schedl et al., 1996; M. Manuel, pers. comm.), although the expression domain of a *Neurogenin2* enhancer, E1, is altered in the developing cortex (Scardigli et al., 2003), implying that there may be a mild, as yet undetermined effect of Pax6 over-expression in the brain.

1.3: The role of Pax6 in embryonic development

Pax6 functions as a transcription factor, altering the expression of downstream genes. The transcription of a number of genes is either directly or indirectly affected by Pax6.

The role of Pax6 varies between tissues, and through embryonic development. Most of our knowledge of its function comes from studies of *Pax6* mutant mice, and from experiments involving the expression of Pax6 in cell culture systems. This section will describe what is known about the actions of Pax6 in the tissues used in this study, followed by a discussion of the three main roles that Pax6 is thought to play throughout all tissues; controlling proliferation, neuronal differentiation and cellular adhesion.

1.3.1: Pax6 in the olfactory bulb

Pax6 is known to be crucial for the development of the olfactory bulb. This structure was thought to be absent from *Sey/Sey* mice (Hogan et al., 1986), but subsequent studies have shown that a rudimentary olfactory bulb like structure (OBLS) does develop (Jimenez et al., 2000; Lopez-Mascaraque et al., 1998; Stoykova et al., 1997; Vitalis et al., 2000). A reduction in olfactory bulb size has also been demonstrated in the *Sey/+* mouse (Dellovade et al., 1998).

In the WT mouse, *Pax6* is expressed in the olfactory bulb throughout embryonic development (Stoykova and Gruss, 1994), and expression continues in some cell types into adulthood (reviewed in Callaerts et al., 1997). The exact role of Pax6 in the development of the olfactory bulb is unclear, but it is thought to be an important regulator of cellular adhesion. It is co-expressed with the cellular adhesion molecule *R-cadherin* throughout neurogenesis (Stoykova et al., 1997). These two proteins are thought to interact in the telencephalon (Andrews and Mastick, 2003), and it is likely that this interaction also occurs in the olfactory bulb. Mice lacking NCAM, a cellular adhesion molecule which is directly regulated by Pax6 (Edelman and Jones, 1995; Holst et al., 1997), have a reduced olfactory bulb (Cremer et al., 1994).

Studies of the rat $rSey^2/rSey^2$ brain have shown that abnormalities in olfactory bulb development are in part caused by the abnormal migration of progenitor cells from the telencephalon (Nomura and Osumi, 2004). These cells travel along the rostral migratory stream caudally and away from the OBLS, rather than rostrally and into it, as seen in the WT. This migration occurs between E12.5 and E14.5 in the rat, which roughly corresponds to E11.5 to E13.5 in the mouse. At this age, cells are also created by proliferation of neural precursors within the ventricular zone of the olfactory bulb (reviewed in Lopez-Mascaraque and de Castro, 2002).

1.3.2: Pax6 in the telencephalon

Pax6 expression is first detected in the forebrain at E8.5 (Walther and Gruss, 1991). At E13, it is found in the VZ and the intermediate zone (IZ) of the telencephalon (Stoykova and Gruss, 1994), in a high rostrolateral to low mediocaudal gradient.

In the telencephalon, *Pax6* appears to be vital in controlling both cellular proliferation and neuronal differentiation.

The role of *Pax6* in controlling cellular proliferation is complex, and may vary dependent on the expression of co-factors. It inhibits proliferation in the cortex at E10.5 and E12.5, as demonstrated by a rise in the percentage of cells in S-phase in the *Sey/Sey* VZ (Warren et al., 1999). Consistent with this, Estivill-Torrus *et al.* (2002) described a shortening of the entire cell cycle in the *Sey/Sey* cortex at E12.5, which is reversed by E15.5 as the proportion of cells undergoing asymmetrical division rises. This is in direct contradiction with the role of *Pax6* as an oncogene which promotes proliferation in other tissues, as described by Maulbecker and Gruss (1993) and Yamaoka et al (2000); it is possible that Pax6 acts to repress proliferation in the developing cortex, but can have the opposite effect in different tissues and at different ages.

A rise in the proportion of differentiating cells in the E15.5 *Sey/Sey* cortex is an indication that Pax6 may act to inhibit differentiation at this age (Estivill-Torrus et al., 2002). Another study suggests that the timing of neuronal differentiation is dependent on *Pax6* expression, as differentiation occurs abnormally early in Sey^{Neu}/Sey^{Neu} mice, at E16.5 (Schmahl et al., 1993). One hypothesis is that Pax6 acts in early neurogenesis to hold neural precursor cells in the cell cycle, whilst later in neurogenesis it acts to promote neuronal differentiation. The mechanism behind this proposed change in Pax6 activity is unclear.

1.3.3: Pax6 in the diencephalon

In the developing diencephalon, *Pax6* is important in controlling arealisation and the formation of boundaries, as well as in cellular proliferation and differentiation.

Pax6 expression is high in the presumptive ventral thalamus at E11.5, lower in the dorsal thalamus, and absent in the mesencephalon (Stoykova and Gruss, 1994; Walther and Gruss, 1991). Before E15.5, *Pax6* expression acts as a clear marker of the diencephalon-mesencephalon boundary (Grindley et al., 1997; Stoykova and Gruss, 1994). The boundary between dorsal thalamus and mesencephalon is blurred in *Sey/Sey* and Sey^{Neu}/Sey^{Neu} mice (Mastick et al., 1997), as is that between the diencephalon and telencephalon (Grindley et al., 1997). Mis-expression of *Pax6* in the mesencephalon causes a shift in the diencephalon-mesencephalon boundary

(Matsunaga et al., 2000), suggesting that *Pax6* expression is vital for the correct arealisation of the diencephalon.

In addition to its role in boundary formation, Pax6 is also thought to control proliferation and differentiation in the diencephalon.

In contrast to the results observed in the *Sey/Sey* cortex, proliferation is reduced in the *Sey/Sey* diencephalon at E10.5, and total cell number is reduced by E14.5 (Warren and Price, 1997). This is further indication that there may be cell-type specific differences in the effects of Pax6 on proliferation. The zona incerta of the diencephalon is reduced in size (Grindley et al., 1997; Mastick and Andrews, 2001), perhaps as a result of a reduction in cellular proliferation.

Both *Sey/+* and *Sey/Sey* mice display defects in the differentiation of regions of the diencephalon. In particular, the SCO, posterior commissure and pineal gland do not form in *Sey/Sey* mice, and the differentiation of neurons within the SCO is defective in *Sey/+* mice (Estivill-Torrus et al., 2001).

The proliferative defects in the *Sey/Sey* diencephalon are seen as early as E10.5 (Warren and Price, 1997), whilst the defects in differentiation become more apparent later in development (Estivill-Torrus et al., 2001; Grindley et al., 1997; Warren and Price, 1997), indicating that the role of *Pax6* in the diencephalon might change from controlling proliferation early on in neurogenesis, to controlling differentiation at later stages.

1.3.4: Pax6 in the eye

The role of Pax6 in the developing eye is varied and complex. Experiments involving the expression of human *PAX6* in the *Drosophila melanogaster* leg imaginal disc (Halder et al., 1995) and a reciprocal experiment over-expressing the *D. melanogaster Pax6* homologue *ey* in *Xenopus laevis* (Onuma et al., 2002) (see Section 1.5.1 for a detailed description of the *D. melanogaster Pax6* homologues) have demonstrated that Pax6 is necessary and sufficient for eye formation. This role as a "master regulator" is consistent across the metazoa, and encompasses both compound and single-lens eyes.

The tissues in which Pax6 is expressed in the eye are diverse in origin. For example, the retina, which is derived from the neurectoderm, and the lens, which is formed from head surface ectoderm, both express high levels of *Pax6* (Collinson et al., 2003; Davis and Reed, 1996; Walther and Gruss, 1991). The eye is also the only Pax6-expressing structure in which there is a strong heterozygous phenotype (Hill et al., 1991). The eye seems more sensitive than the brain to *Pax6* gene dosage, which is also evidenced by the presence of an eye phenotype, but no strong brain phenotype in PAX77 mice (Schedl et al., 1996). As homozygous *Sey/Sey*, Sey^{Neu}/Sey^{Neu} and $Pax6^{LacZ\,LacZ}$ mice do not develop eyes, it is the heterozygous phenotype which will be discussed here.

In the retina, the *Pax* genes *Pax2* and *Pax6* have opposing roles, and each represses the other's transcription (Baumer et al., 2002; Schwarz et al., 2000). These two genes are co-expressed early in eye development, and the action of either is required for the correct differentiation of retinal pigmented epithelium (Baumer et al., 2003). *Pax6* alone is crucial for the formation of a boundary between optic cup and optic stalk (Schwarz et al., 2000). Consistent with a role for Pax6 in promoting cellular differentiation, conditional inactivation of the *Pax6* gene in retinal progenitor cells leads to a restriction of potential cell fates, *via* the transcriptional control of proneural genes (Marquardt et al., 2001).

In the lens, Pax6 is thought to act on a different set of target genes (Chauhan et al., 2002a; Chauhan et al., 2002b; Chauhan et al., 2002c). For example, Pax6 is a direct transcriptional activator of *Six3*, and *vice versa* (Goudreau et al., 2002). Both of these genes are thought to be crucial in promoting cellular proliferation in the lens, and *Pax6* is also necessary for the correct differentiation of lens fibre cells (Dimanlig et al., 2001; Goudreau et al., 2002). A specific role for *Pax6+5a* has also been demonstrated in the lens, where over-expression of this isoform leads to the formation of cataracts and up-regulation of the cellular adhesion molecules α5β1 integrin, paxillin and $p120^{ctn}$ (Duncan et al., 2000).

An action of Pax6 which appears to be unique to the lens is in regulating the expression of structural genes, the crystallins (Cvekl et al., 1995b; Duncan et al., 1998; Kralova et al., 2002; Richardson et al., 1995; Sharon-Friling et al., 1998).

Although the effects of Pax6 seem to vary between the retina and the lens, the behaviour of $Pax6^{-/-}$ cells in $Pax6^{+/+} \leftrightarrow Pax6^{-/-}$ chimeras is similar in both tissues.

Pax6$^{-/-}$ cells are excluded during development, suggesting that Pax6 may in fact be playing a similar role in each, perhaps in the control of cellular adhesion (Collinson et al., 2000; Collinson et al., 2003).

The ratio of *Pax6-5a* : *Pax6+5a* has been best described in the eye (see Section 2.2.1), and a number tissue-specific and developmental stage-specific variations have been seen. The differential expression of these two *Pax6* isoforms could play an important role in correct eye development.

1.3.5: Pax6 in the spinal cord

Early in neurogenesis, at E10.5 to E12.5, *Pax6* expression is highest in the dorsal portion of the spinal cord, where, as in the cortex, it is found in the proliferative VZ (Ericson et al., 1997; Stoykova and Gruss, 1994). Its expression is developmentally regulated, and becomes progressively restricted through neurogenesis (Goulding et al., 1993). This regulation is thought to be controlled by sonic hedgehog signalling, and is key to establishing progenitor domains from which different neuronal subtypes emerge (Briscoe and Ericson, 1999; Ericson et al., 1997).

Direct regulation of the cellular adhesion molecule *NCAM* and the proneural gene *Neurogenin2* by Pax6 have been demonstrated in the spinal cord (Holst et al., 1997; Scardigli et al., 2003), but little else is known about direct targets of Pax6 in this tissue.

Pax6 expressing cells in the VZ of the ventral spinal cord can generate either motorneurons or oligodendrocytes, and the determination of both of these fates is affected in *Sey/Sey* mice (Sun et al., 1998). *Sey/Sey* mice also display deficiencies in the formation of spinal cord interneurons (Burrill et al., 1997). Studies of the developing *Sey/Sey* spinal cord show decreased numbers of somatic motorneurons and V1 interneurons, but normal formation of other neuronal subtypes (Takahashi and Osumi, 2002). Again, Pax6 in the spinal cord is crucial in controlling cellular differentiation.

After injury, the Pax6 expressing cell population in the adult rat spinal cord increases, suggesting an involvement of Pax6 in regeneration and renewal (Yamamoto et al., 2001), an involvement that has also been seen in the cornea (Collinson et al., 2004). This is further evidence for a global role of Pax6 in controlling cellular proliferation.

1.3.6: Pax6 in the hindbrain

Pax6 expression is highest in the dorsal hindbrain (Ericson et al., 1997; Stoykova and Gruss, 1994), and is crucial for the correct establishment of neuronal progenitor domains (Ericson et al., 1997; Takahashi and Osumi, 2002).

At E12.5, proliferative rates are increased in the rat $rSey^2/rSey^2$ hindbrain (equivalent to E11.5 in the mouse), as measured by BrdU incorporation (Takahashi and Osumi, 2002). This observation implies that Pax6 is acting in the hindbrain to repress proliferation early in neurogenesis, which is consistent with data from the E12.5 telencephalon (Estivill-Torrus et al., 2002; Warren et al., 1999). In the telencephalon, this phenotype is reversed by E15.5, but the effects of Pax6 on proliferation in the hindbrain have not been studied at later ages.

The effect of Pax6 on differentiation in the developing hindbrain has been studied in greater detail. As in the spinal cord, sonic hedgehog signalling controls the expression of *Pax6*, which in turn controls the formation of neuronal subtypes (Briscoe and Ericson, 1999; Ericson et al., 1997). Whilst somatic motorneurons and V1 interneurons do form in the *Sey/Sey* spinal cord, but in abnormally low numbers, these neuronal subtypes are entirely absent from the *rSey/rSey* hindbrain (Osumi et al., 1997; Takahashi and Osumi, 2002), indicating that the requirement for *Pax6* is stronger for correct neuronal differentiation in the hindbrain.

1.3.7: Pax6 in the cerebellum

Pax6 is expressed in the rhombic lip of the hindbrain from E12.5 onwards (Engelkamp et al., 1999). Post-mitotic neurons migrate away from the rhombic lip, and give rise to the granule cells of the cerebellum, which also express *Pax6* (Kawakami et al., 1997; Walther and Gruss, 1991). Expression persists into adulthood in the granular layer of the cerebellum, although at reduced levels (Stoykova and Gruss, 1994; Walther and Gruss, 1991).

Unlike other *Pax6* expressing tissues, both differentiation and proliferation are largely unaffected in the cerebellum of *Sey/Sey* mice, and Pax6 is thought to influence cellular migration, through the control of cellular adhesion molecules (Engelkamp et

al., 1999). Cell numbers are drastically decreased in the *Sey/Sey* cerebellum at E16.5. Since the percentage of cells labelled by a 1 hour BrdU pulse is the same in *Sey/Sey* precerebellar nuclei and granule cells as in the WT, and there is no increase in cell death in the *Sey/Sey* cerebellum, the reduction in cell number is likely to be due to failed migration of cells from the rhombic lip (Engelkamp et al., 1999).

Similar migratory defects are seen in the rat $rSey^2/rSey^2$ cerebellum. DiI labelling of external granule layer (EGL) cells shows that parallel fibres do not form in the mutant. There is a corresponding increase in the thickness of the EGL, demonstrating that the migration of cell bodies along parallel fibres seen in the WT cannot occur in the $rSey^2/rSey^2$ cerebellum (Yamasaki et al., 2001).

Pax6 also appears to have a role in controlling neurite outgrowth in the cerebellum of both mice and rats. Cultured *Sey/Sey* mouse EGL explants grow fewer neurites than WT explants (Engelkamp et al., 1999). Similarly, $rSey^2/rSey^2$ EGL explants form shorter, thinner neurites than WT explants (Yamasaki et al., 2001). A role for Pax6 in regulating cellular morphology and cytoskeletal organisation has not been demonstrated in any other tissues, and may be unique to the cerebellum.

1.3.8: Pax6 and proliferation

The lack of structures such as the olfactory bulb and the eye in *Sey/Sey* and Sey^{Neu}/Sey^{Neu} mutant mice (Hill et al., 1991; Ton et al., 1991), and the fact that these mice have smaller brains with fewer cells than WT mice (Warren and Price, 1997) and are smaller overall (Vitalis et al., 2000) suggest that Pax6 might play a role in promoting cellular proliferation.

Studies of the cell cycle in *Sey/Sey* mice have provided conflicting insights into the exact nature of the effects which Pax6 exerts on cellular proliferation.

Proliferative rates are increased in the *Sey/Sey* cortex at E10.5 and E12.5, as shown by an increase in the percentage of cells in S-phase (Warren et al., 1999). In contrast, proliferation is reduced in the *Sey/Sey* diencephalon at E10.5 (Warren and Price, 1997). There may be cell-type specific differences in the effects of Pax6 on proliferation.

A more comprehensive comparison between cell cycle times in the cortex of WT and *Sey/Sey* mice showed that WT cortical cells had a longer cell cycle at E12.5, and were therefore proliferating less rapidly. To further illustrate this, *Sey/Sey* cortical cells were cultured *ex vivo*, and shown to have raised levels of cyclin A, a key regulator of the cell cycle. By E15.5, however, this effect was reversed; the cell cycle time was shorter in WT cortex, and *Sey/Sey* cortical cells were now proliferating less rapidly that WT cells (Estivill-Torrus et al., 2002). This study indicated that Pax6 can act to either enhance or repress proliferation, perhaps in a manner that is dependent on the temporally-regulated expression of other genes.

Pax6 is also thought to be an oncogene. The introduction of Pax6 over-expressing cells into adult mice leads to tumour formation (Maulbecker and Gruss, 1993). Ectopic PAX6 expression has since been described in a number of human tumours (Salem et al., 2000), and tumour formation has also been seen in the pancreas of PAX77 mice (Yamaoka et al., 2000).

Taken together, these observations suggest that Pax6 plays an important role in regulating the cell cycle, and thus controlling the proliferation of a number of cell types during embryonic development.

1.3.9: Pax6 and differentiation

Homozygous *Pax6*-null mice (*Sey/Sey*, Sey^{Neu}/Sey^{Neu} and $Pax6^{LacZ/LacZ}$) display defects in the differentiation of cells in the pancreas (Dohrmann et al., 2000; St-Onge et al., 1997), eye (reviewed in Ashery-Padan and Gruss, 2001; Jean et al, 1998; van Heyningen and Williamson, 2002) and brain (reviewed in Simpson and Price, 2002) .

There is a correlation between the onset of WT *Pax6* gene expression and the onset of neurogenesis, which has been most clearly demonstrated in the mouse (Stoykova and Gruss, 1994) and quail (Plaza et al., 1995). A similar correlation between the onset of retinogenesis and WT *Pax6* expression is seen in retinal progenitor cells (Marquardt et al., 2001), whose differentiation is restricted upon the conditional inactivation of *Pax6*.

Differentiation of cell types in the hindbrain (Takahashi and Osumi, 2002) and diencephalon (Warren and Price, 1997) are dependent on Pax6, but the role of Pax6 in neuronal differentiation is perhaps best studied in the developing cortex.

During cortical development, a proportion of cells in the proliferative VZ undergo asymmetrical division. This produces two progenitor cells, one of which continues to divide within the VZ, the other of which exits the cell cycle, migrates out of the VZ and begins to differentiate (Fujita, 1964; Sidman et al., 1959) (see **Figure 1.4**). Early in corticogenesis, the newly differentiated neuron migrates by somal translocation. Later on, as the cortex thickens, radial glia provide a scaffold for neuronal migration (Rakic, 1972; reviewed in Nadarajah and Parnavelas, 2002). The proportion of cells undergoing asymmetrical division in the *Sey/Sey* cortex from E12.5 to E15.5 is abnormally high (Estivill-Torrus et al., 2002), indicating that the rates of neuronal differentiation are increased. In Sey^{Neu}/Sey^{Neu} mice, cortical plate neurons cease differentiation abnormally early, at E16.5, and are deficient in axon formation (Schmahl et al., 1993).

Abnormal differentiation of cells in the absence of Pax6 is also evidenced by the mis-expression of the differentiation marker *Sox11* in the developing *Sey/Sey* brain; *Sox11* immunostaining is seen across a larger than normal area of the proliferating layers of the cortex. This could be an indication either that rates of differentiation are higher in *Sey/Sey* mice, or that differentiation proceeds normally, but migration is impaired, and these cells can no longer leave the proliferative layers of the cortex (Warren et al., 1999).

The role of Pax6 in cortical neuronal differentiation, like its role in proliferation, appears to vary between tissues and developmental ages. This variation is suggestive of a complex and as yet undefined interaction with a number of other genes.

As well as being crucial in neurogenesis, Pax6 is also necessary for gliogenesis to occur in the developing brain. It is expressed in cortical radial glia, and the morphology of these cells is disrupted in *Sey/Sey* mice (Stoykova et al., 1996). It has recently been shown that glial cells can themselves undergo neurogenesis (Heins et al., 2002; Malatesta et al., 2003; Malatesta et al., 2000), and that Pax6 is also critical in this process (Heins et al., 2002).

Taken together, these data imply that Pax6 expression is critical for the correct regulation of numerous kinds of cellular differentiation.

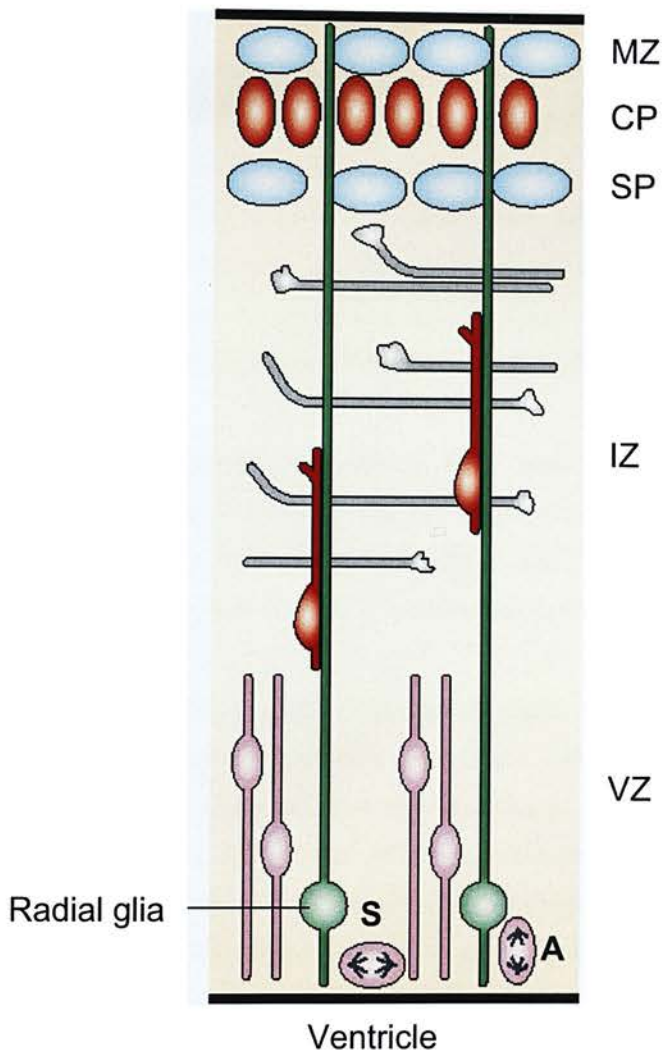

Figure 1.4 Cortical development (taken from Nadarajah and Parnavelas, 2002). The ventricular zone (VZ) contains a proliferating neuronal precursor cell population. Cells either divide symmetrically (S) and remain proliferative, or divide asymmetrically (A) to produce one proliferative cell and one post-mitotic neuron. Postmitotic neurons (red) then migrate through the intermediate zone (IZ) to the outermost layer of the cortex, just above the subplate (SP). Early in neurogenesis, this migration occurs *via* somal translocation. Later on in neurogenesis, as the cortex thickens, postmitotic neurons migrate along radial glia (green). CP, cortical plate. MZ, marginal zone.

1.3.10: Pax6 and cellular adhesion

Pax6 has been shown to directly regulate the expression of the cellular adhesion molecules L1 (Meech et al., 1999) and NCAM (Edelman and Jones, 1995; Holst et al., 1997) and is also thought to act upon R-cadherin (Andrews and Mastick, 2003) in the developing CNS. Mis-expression of these and other cellular adhesion molecules in the *Sey/Sey* mouse has a number of effects on the developing CNS (reviewed in Simpson and Price, 2002). These effects include abnormal regionalisation due to the failure of cells to segregate into discrete populations and abnormal migration of either cell bodies or axons due to differences in the cellular environment through which migration takes place. Each of these three effects will be discussed in turn.

Firstly, numerous regionalisation defects have been described in *Sey/Sey* and Sey^{Neu}/Sey^{Neu} mice, for example in the eye (Baumer et al., 2002), diencephalon (Grindley et al., 1997) and hindbrain (Takahashi and Osumi, 2002). In particular, regionalisation appears to be severely affected in the *Sey/Sey* telencephalon.

A gradient of Pax6 expression, from high rostrolateral to low mediocaudal, is seen in the developing telencephalon (Stoykova and Gruss, 1994; Vitalis et al., 2000). In *Sey/Sey* mice, there is a reduced area of expression of rostrolateral markers of the telencephalon including the cellular adhesion molecule Cad8, and a concomitant increase in the area of expression of mediocaudal markers, including Cad6 (Bishop et al., 2002). This observation implies that Pax6 expression in the anterior forebrain is crucial for establishing anterior cortical identity, and may do so by altering the expression of cellular adhesion molecules. Homozygous double-knockout mice for *Pax6* and *Emx2*, another gene thought to be important in the regionalisation of the cortex, show an almost complete conversion of cerebral cortex into basal ganglia (Muzio et al., 2002a; Muzio et al., 2002b), further evidence for a role of Pax6 in establishing cortical identity.

Studies of $Pax6^{+/+} \leftrightarrow Pax6^{-/-}$ chimeric mice show that $Pax6^{-/-}$ cells exhibit abnormal adhesive properties, and are specifically excluded from the mediocaudal domain of the dorsal telencephalon (Talamillo et al., 2003), various components of the cornea, and the neural retina (Collinson et al., 2003). Similarly, *Sey/Sey* cells segregate out when transplanted into WT cortex (Tyas et al., 2003). Adhesive defects are also thought to be responsible for the abnormal segregation of *Sey/Sey* cortical cells grown

in vitro. Whilst WT cortical and striatal cell aggregates segregate into two separate populations, this segregation is lost in *Sey/Sey* cells (Stoykova et al., 1997).

Secondly, mis-expression of cellular adhesion molecules under the control of Pax6 may have an effect on cellular migration, either by regulating the adhesive properties of the migrating cells, or by regulating the adhesive properties of the cell populations through which they must pass.

A well defined migratory process in the developing brain is the radial migration of neuronal precursors from the VZ to the appropriate cortical layer after differentiation (reviewed in Rakic, 2003; see **Figure 1.4**). Talamillo et al. (2003) looked at radial migration in $Pax6^{+/+} \leftrightarrow Pax6^{-/-}$ chimeric mice, and found that many differentiated $Pax6^{-/-}$ cells do not leave the VZ. Radial migration is also deficient in *Sey/Sey* and Sey^{Neu}/Sey^{Neu} mice, and differentiated cells accumulate in the VZ (Caric et al., 1997; Schmahl et al., 1993; Stoykova et al., 1996). This effect is dependent on Pax6 expression within the cortical layers, as *Sey/Sey* cells do not display radial migration defects when transplanted into a WT cortex (Caric et al., 1997). Pax6 expression therefore appears to be necessary for the process of radial migration, and its expression may alter the adhesive properties of newly-differentiated neurons, or the radial glia along which they migrate (Rakic, 2003).

Radial migration is not the only form of neuronal migration to be affected by Pax6. The migration of mitral cell progenitors from the rostral telencephalon is deficient in $rSey^2/rSey^2$ rats, and is though to be the main reason why an olfactory bulb is not formed in these animals (Nomura and Osumi, 2004). In the mouse and rat cerebellum, Pax6 is also essential for the correct migration of granule cells (Engelkamp et al., 1999; Yamasaki et al., 2001).

A third way in which Pax6 is thought to act *via* cellular adhesion molecules is in controlling the formation of axon tracts. Just as the expression of adhesion molecules can affect the migration of cells, it could also affect the growth and migration of axons from static cell bodies.

The thalamocortical axon (TCA) tract, which runs between the dorsal thalamus and the cerebral cortex, does not form in *Sey/Sey* mice (Jones et al., 2002; Pratt et al., 2002; Pratt et al., 2000). Pax6 is also necessary for the correct formation of the TPOC (Mastick et al., 1997). Although this tract is present in *Sey/Sey* mice, its axons display

pathfinding errors, an effect which can be reversed by the addition of *R-cadherin* (Andrews and Mastick, 2003). Thus, Pax6 can control axon outgrowth, perhaps by controlling the expression of cellular adhesion molecules.

1.4: Alternative splicing of the *Pax6* gene

The alternative splicing of *Pax6* is well documented, and is an important mechanism by which the Pax6 protein structure is regulated. All known splice variants will be described in turn, along with their potential effects on Pax6 activity.

1.4.1: Alternative splicing of *Pax6* exon 5a

As described in section 1.1.1, alternative splicing of exon 5a (Walther and Gruss, 1991) disrupts the PD (see **Figure 1.2**), and alters its DNA binding properties (Epstein et al., 1994a; Epstein et al., 1994b). The phenotypic implications of this alternative splicing event are largely unknown, but a few recent studies have attempted to address this issue.

1.4.1.1: Mouse mutants of *Pax6* exon 5a

Singh et al. (2002) created a mouse mutant in which exon 5a was constitutively deleted. The phenotype was different to that observed in the *Sey/Sey* mouse, and milder. Rather than having no eyes, as seen in *Sey/Sey* mice (Hill et al., 1991; Ton et al., 1991), mice lacking exon 5a displayed iris hypoplasia, alongside defects in the development of the cornea, lens and retina. No phenotype was described in the brain, although this does not preclude the possibility that there was one.

In a complementary experiment, Pax6+5a was over-expressed in the mouse lens (Duncan et al., 2000). This led to the formation of cataracts, and the up-regulation of the cellular adhesion molecules paxillin, $p120^{ctn}$ and $\alpha5\beta1$ integrin.

Both of the studies described above concentrate on the role of alternative splicing of exon 5a in the eye, and little is known about its involvement in the development of other Pax6 expressing tissues.

1.4.1.2: *Pax6* exon 5a affects PD-DNA binding

As described in section 1.1.1, the insertion of exon 5a into the PD is thought to act as a "molecular toggle", switching PD-DNA binding from the PAI subdomain to the RED subdomain (Epstein et al., 1994b). Although a Pax6+5a consensus binding site (5aCON) and a Pax6-5a consensus binding site (P6CON) have been described (Epstein et al., 1994a; Epstein et al., 1994b), it has been shown that both Pax6 isoforms can bind to and activate transcription through both consensus sequences (Chauhan et al., 2004a; Kozmik et al., 1997; Yamaguchi et al., 1997).

The hypothesis that Pax6-5a and Pax6+5a act on different sets of target genes is backed up by data from cDNA micro-array experiments performed using WT, *Pax6-5a* over-expressing and *Pax6+5a* over-expressing lens tissue (Chauhan et al., 2002a; Chauhan et al., 2002b). A total of 27 transcripts were seen to be differentially regulated between WT and *Pax6+5a* over-expressing lens, 13 of which were also mis-regulated in the *Sey/+* lens. The *Pax6-5a* over-expressing lens was seen to have a largely different complement of mis-regulated genes, indicating that the two different Pax6 isoforms exert different roles in the development of the lens.

1.4.1.3: Differential expression of Pax6-5a and Pax6+5a during embryonic development

Ever since the splice variants *Pax6-5a* and *Pax6+5a* were first described (Walther and Gruss, 1991), *Pax6-5a* has been thought to be the more abundant of the two isoforms. Recently, however, evidence has emerged that *Pax6+5a* exists at higher levels in some tissues than was previously thought, and the differential expression of the two splice forms can vary between tissues and developmental stages.

The relative advantages and disadvantages of the techniques used to assess the *Pax6-5a* : *Pax6+5a* mRNA ratio in the following studies will be described in further detail in Section 2.2.1; here a brief outline of the results from each study will be given.

RT-PCR data suggests that 80% of *Pax6* transcripts in the chick retina, but only 2.5% of *Pax6* transcripts in the cornea, contain exon 5a (Koroma et al., 1997). In the bovine eye, *Pax6+5a* is seen to be in excess over *Pax6-5a* in the iris. Levels appear to be approximately equal in the cornea (Jaworski et al., 1997). Taken together, these

results show that there are pronounced tissue-specific differences in the regulation of *Pax6-5a* and *Pax6+5a*.

Semi-quantitative RT-PCR showed that *Pax6-5a* and *Pax6+5a* exist at equal levels in adult human lens epithelium and lens fibres (Zhang et al., 2001), whilst Jaworski et al., (1997) described *Pax6-5a* as being in excess over *Pax6+5a* in total bovine lens. These conflicting data suggest that there may be species-specific differences in differential *Pax6* isoform expression.

RNase protection assay (RPA) has been used to show that *Pax6-5a* is in 8-fold excess over *Pax6+5a* in mouse total head RNA, from E12.5 to E16.5, and in adult brain RNA (Kozmik et al., 1997). Although this study did not separate out mRNA populations from different regions of the head, it is the only absolutely quantitative evaluation of *Pax6-5a* and *Pax6+5a* levels during embryonic development to date.

Protein bands thought to correspond to Pax6-5a and Pax6+5a have been observed by western blot on tissue from species as diverse as quail, mouse and chick. (Engelkamp et al., 1999; Kawakami et al., 1997; Plaza et al., 1993), but little effort has been made to quantitate these bands. As a result, not much is known about the relative abundance of Pax6 protein isoforms throughout embryonic development, and what differential roles these isoforms may be playing.

1.4.1.4: The Pax6-5a : Pax6+5a ratio affects transactivation

One consequence of the differential expression of Pax6-5a and Pax6+5a through development is that the ratio between the two isoforms alters, as well as their absolute quantities. Intriguingly, recent work suggests that this ratio, rather than the absolute amount of an isoform, may be an important determinant of Pax6 activity (Chauhan et al., 2004a). In a cell culture system, a *Pax6-5a* : *Pax6+5a* ratio of either 8:1 or 1:1 leads to strong transcriptional activation from either the P6CON or the 5aCON consensus binding sequences. Intermediate ratios of 2:1 or 4:1, however, show lower levels of transactivation. This suggests that either optimal transactivation of all downstream genes occurs at a ratio of 8:1 or 1:1; or that altering the ratio leads to an alteration in the preferred target DNA-binding sequences, from 5aCON and P6CON to other sequences that weren't used in this particular study. In either case, it seems likely that the Pax6-5a : Pax6+5a ratio is an important determinant of the transcriptional activity of Pax6.

1.4.2: Alternative splicing of *Pax6* exon 6

A number of instances of *Pax6* exon 6 alternative splicing have been documented, and there seem to be multiple mechanisms by which all or part of this exon can be excluded from the mature transcript.

RT-PCR for *Pax6* on mRNA extracted from a human glioblastoma cell line, U373-MG, has identified mRNA species lacking the entire exon 6 in both *Pax6-5a* and *Pax6+5a* forms (T.I. Simpson, pers. comm.). An mRNA has also been isolated from quail neuroretina in which the 3' 198bp of exon 5 (*Pax-QNR* exon 5 corresponds to human and mouse *Pax6* exon 6) is absent. This is due to the usage of an unusual splice donor site 15bp into exon 5, allowing splicing straight onto sequence at the 5' end of exon 6 (human and mouse exon 7) (Carriere et al., 1993). The splice donor site described in this example is conserved across mouse and man. In addition, *Pax6* transcripts lacking exon 6 and also generated by the use of this splice donor site within exon 6 have been described in the bovine eye (Jaworski et al., 1997).

A number of human mutations have also been described in which an alternative, weak splice donor site 3' of exon 6 is used instead of the canonical splice site (www.hgu.mrc.ac.uk/Softdata/Pax6/). This leads to the exclusion of the majority of exon 6 from the mature transcript. It is possible that this weak splice donor site could be employed at a low rate when no mutations are present, leading to a low abundance transcript missing all but a small portion of exon 6, encoding 36 amino acids of the RED subdomain.

1.4.3: Other *Pax6* transcripts

A "paired-less" *Pax6* mRNA lacking exons 2, 4 to 7, and the first 21bp of exon 8 has been described (Mishra et al., 2002), which is expressed in the murine eye, pancreas and brain. As this transcript is lacking the first *Pax6* ATG residue, translation could only initiate from within exon 8, leading to an N-terminally truncated protein without a PD.

This transcript was also isolated using an agarose gel rescue technique (Gorlov and Saunders, 2002). Two further *Pax6* splice variants were found this way. A transcript

was isolated from mouse eye mRNA in which exons 2 to 8 are absent. A third *Pax6* mRNA was found in the mouse brain, with exons 2, 5a to 10, and part of exon 11 missing. It is unclear whether these latter two splice variants represent artefacts or common *Pax6* splice variants, as their relative abundances have yet to be assessed *in vivo*.

Pax6 transcription can also begin from a CpG island within intron 7, a process which has been shown to comprise 1% of *Pax6* transcripts in a lens epithelial cell line (Kleinjan et al., 2004). Again, translation of this mRNA could only begin within exon 8, leading to a "paired-less" Pax6 protein.

As the *Pax6* transcript seems particularly prone to alternative splicing events, it is worth noting that only exons 5a, 6, 8 and 12 could be entirely removed from the transcript whilst leaving an in-frame Pax6 protein. An mRNA in which the whole of exon 12 is absent has also been cloned from the U373-MG cell line (B.T. Fenby, pers. comm.), but this was a single event and may be artefactual.

1.5: Pax6 homologues in invertebrates

The *Pax6* gene is highly conserved in vertebrates. The protein sequence is 100% identical between mouse and human (Hill et al., 1991; Ton et al., 1991), and regulatory elements are highly conserved across species as diverse as human, zebrafish and quail (Griffin et al., 2002; Kleinjan et al., 2004; Morgan, 2004).

This functional conservation of Pax6 is extended across various invertebrates, such as *D. melanogaster, Caenorhabditis elegans* and *Ciona intestinalis* (sea squirt) (Jang et al., 2003; Mazet et al., 2003; Morgan, 2004; Quiring et al., 1994). The invertebrate *Pax6* homologues that are best understood at a molecular level are those found in *D. melanogaster* and *C. elegans*.

1.5.1 *D. melanogaster eyeless* and *eyegone*

The *D. melanogaster* gene eyeless (*ey*) is homologous to Pax6-5a, containing a complete PD, HD and TAD (Quiring et al., 1994). Over-expression of *ey* in *X. laevis* can induce the formation of vertebrate eye-like structures (Onuma et al., 2002), a demonstration of the high levels of *Pax6* conservation between vertebrates and

invertebrates. Similarly, over-expression of human *PAX6* in the *D. melanogaster* leg imaginal disc leads to formation of invertebrate eye-like structures (Halder et al., 1995). Although invertebrate and vertebrate eyes are structurally dissimilar, Pax6 is able to induce the formation of either.

There is a second *Pax6-5a* homologue in *D. melanogaster*, *twin of eyeless (toy)* (Czerny et al., 1999), which appears to have arisen by gene duplication. *toy* and *ey* are most divergent at the C-terminus, suggesting that they might have different transactivational properties (Punzo et al., 2004). The two genes are differentially expressed, implying they play different roles in controlling eye development (Kammermeier et al., 2001). *toy* is expressed earlier in development, and activates the expression of *ey,* although mutations in either gene have a similar effect (Kronhamn et al., 2002).

The alternative splicing of exon 5a, a mechanism by which the DNA-binding properties of vertebrate Pax6 are altered (see Section 1.4.1), is not seen in invertebrates. Intriguingly, *D. melanogaster* expresses a third *Pax6* gene, *eyegone* (*eyg*), which is homologous to the *Pax6+5a* splice variant (Jang et al., 2003). The *eyg* gene is similar to *ey*, but has an incomplete PD. The RED subdomain is intact and can bind target DNA, whilst the PAI subdomain is partially absent. This has the effect of constitutively switching PD-DNA binding from the PAI subdomain to the RED subdomain, an effect which is paralogous to the insertion of exon 5a in vertebrates.

A second *Pax6+5a* homologue, *twin of eyg* (*toe*) is also found in *D. melanogaster.* Like *toy*, this is thought to have arisen by gene duplication (Jang et al., 2003). The function of *toe* is largely unknown.

Functional studies of the four *D. melanogaster Pax6* homologues have been restricted to *ey* and *eyg*, which are known to have different roles during eye development. *eyg* is expressed first in the developing eye, and promotes proliferation of precursor cells. *ey* is expressed later, as *eyg* is switched off. This change in expression is coincident with a switch from proliferation to differentiation in precursor cells (Dominguez et al., 2004; reviewed in Rodrigues and Moses, 2004). As further proof of the molecular similarity between *eyg* and *Pax6+5a*, human *PAX6+5a* was over-expressed in the *D. melanogaster* wing, and caused an increase in cellular proliferation, but had no effect on differentiation (Dominguez et al., 2004).

In *D. melanogaster*, the two *Pax6* homologues, *ey* and *eyg* appear to have distinct functions in eye development. In vertebrates, the differential functions of Pax6-5a and Pax6+5a are harder to assess, for two main reasons. Firstly, Pax6-5a and Pax6+5a are co-expressed in all tissues studied to date (Jaworski et al., 1997; Koroma et al., 1997; Kozmik et al., 1997; Richardson et al., 1995; Zhang et al., 2001), making it hard to assess any differential roles the two isoforms might have. Secondly, whilst *ey* does not control the expression of *eyg* or vice versa (Jang et al., 2003), murine Pax6-5a can regulate the expression of Pax6+5a (Plaza et al., 1993). This interaction can complicate the interpretation of any investigation into the action of one isoform alone.

1.5.2: *C. elegans vab-3* and *mab-18*

The C. *elegans Pax6* homologue, *vab-3*, is important for formation of the adult male tail, and the larval and adult head (Lewis and Hodgkin, 1977).

A second transcript, *mab-18*, is encoded by the same genetic locus, but from an internal promoter. Translation begins within the *vab-3* sequence, resulting in a "paired-less" protein with an intact HD and TAD (Zhang and Emmons, 1995). Similar transcripts can be made from the murine *Pax6* locus (Kleinjan et al., 2004; Mishra et al., 2002) (see Section 1.4.3), but little is known about the function of these "paired-less" forms of Pax6.

Mutations in the HD of the *mab-18* transcript lead to defects in fate determination of sensory ray cells, thought to be a result of defects in cellular adhesion (Zhang and Emmons, 1995). Mutations in the HD of *mab-18* would also be present in the HD of *vab-3*, therefore it is unclear which aspects of this phenotype are due to the mutation in *mab-18*, and which are due to the mutation in *vab-3*. The presence of a "paired-less" *Pax6* in *C. elegans* lends potential functional significance to those observed in other species.

1.6: Pax6 target genes

Pax6 is a transcription factor, containing a PD and a HD that can bind to DNA, and a TAD to modulate transcription of bound target genes. A number of target genes have been shown to be directly regulated by Pax6 activity, and more have been implicated from cDNA micro-array studies.

1.6.1: Known Pax6 target genes

In the eye, Pax6 is known to bind to the promoters of, and affect the transcription of a number of crystallin genes, including *αA-crystallin* (Cvekl et al., 1995a), *β-crystallin* (Duncan et al., 1998), *δ1-crystallin* (Muta et al., 2002), *γE-* and *γF- crystallins* (Kralova et al., 2002), and *ζ-crystallin* (Richardson et al., 1995; Sharon-Friling et al., 1998). Direct interactions between Pax6 and the promoters of both *Six3* and *Sox2* have also been shown (Goudreau et al., 2002; Kamachi et al., 2001), implying that Pax6 acts on the regulators of eye development as well as its structural components.

In the brain, the genes upon which Pax6 acts can be grouped into four main categories; other transcription factors, genes involved in neuronal differentiation, genes involved in cellular proliferation, and genes involved in cellular adhesion.

Transcription factors shown to be directly regulated by Pax6 include *Pax2* (Schwarz et al., 2000) and *Rax* (Mikkola et al., 2001), whilst *Engrailed-1* and *Wnt-7b* are also thought to be regulated by Pax6 (Kim et al., 2001; Matsunaga et al., 2000). These genes are largely involved in patterning of the brain, which is known to be disturbed in homozygous *Pax6* mutant mice (Bishop et al., 2002; Mastick et al., 1997; Muzio et al., 2002a; Muzio et al., 2002b).

The proneural gene *Neurogenin2* is also directly regulated by Pax6 (Marquardt et al., 2001; Scardigli et al., 2003), as are a number of other basic helix-loop-helix transcription factors involved in neuronal differentiation such as *Math5* and *Mash1* (Marquardt et al., 2001).

Cyclin A and $p27^{Kip1}$ are two cell-cycle proteins whose expression is altered in *Sey/Sey* cultured cells (Estivill-Torrus et al., 2002), although it is not known whether this is a direct effect, or an indication of Pax6 acting elsewhere in the cell cycle. A direct interaction between Pax6 and *c-Maf*, an oncogene of the *Maf* family and a regulator of cellular proliferation, has also been demonstrated (Sakai et al., 2001).

The necessity for the Pax6 gene in controlling cellular adhesion in the brain is borne out by the fact that it directly regulates *L1* (Meech et al., 1999) and *NCAM* (Edelman and Jones, 1995; Holst et al., 1997), and is also thought to control the transcription of *R-cadherin* (Andrews and Mastick, 2003).

Importantly, Pax6 can also regulate the activity of its own promoters. This will be discussed in further detail in section 1.6.3.

1.6.2: Potential Pax6 target genes identified from cDNA micro-array analyses

cDNA micro-array analysis has been used to identify genes which are differentially regulated between a number of *Pax6* mutant and WT mice, with particular emphasis on the mouse lens.

Transcripts were compared from the lens of WT mice with those over-expressing *Pax6-5a* specifically in the lens (Chauhan et al., 2002a) Genes involved in differentiation (e.g. *Hoxa7, Atf1*), proliferation (e.g. *Pmp22, neural protein 3.1*) and cellular adhesion (e.g. *L1, NCAM*) were found to be differentially expressed between the two genotypes. It is important to note, however, that mis-regulation of a gene in *Pax6* mutant mice is not necessarily suggestive of direct transcriptional control. Despite this, array-based studies are useful in suggesting candidate genes whose expression may be under the control of Pax6.

A second comparison was made, between WT and *Sey/+* lenses (Chauhan et al., 2002c), and a different cohort of genes involved in differentiation (e.g. *Pitx3*), proliferation (e.g. *p53, pRb*) and cellular adhesion (e.g. *β1-integrin*) was identified alongside a large number of crystallin genes.

Comparing WT lenses with those over-expressing *Pax6+5a* (Chauhan et al., 2002b) again yielded a set of genes involved in differentiation, proliferation and cellular adhesion, including *Hoxa2,* the cyclin gene *Ccne2*, and *paralemmin*. A small subset of these genes was found to be mis-regulated in both *Sey/+* lenses and *Pax6+5a* over-expressing lenses (e.g. *paralemmin* and *Laminin-associated polypeptide 1c*). Although these genes have not previously been associated with Pax6, these array studies show that they are particularly good candidates for direct Pax6 target genes.

1.6.3: Autoregulation of Pax6

The Pax6 protein is known to regulate its own promoters, either directly or through interactions with other proteins, thus affecting transcription of the *Pax6* gene.

Two promoters are thought to be responsible for the majority of *Pax6* expression. They are known as P0 and P1 in the mouse and quail (Anderson et al., 2002; Kammandel et al., 1999; Plaza et al., 1993; Plaza et al., 1995), and PA and PB in the human (Okladnova et al., 1998).

In the quail, it has been shown that PAX-QNR protein (the quail Pax6 homologue), when transfected into quail neuroretina cells, increases the activity from an introduced P0 promoter (Plaza et al., 1993). A similar result was later shown with the P1 promoter (Plaza et al., 1995). This activation depends on PD-DNA binding, but is highest when both PD and HD are present, providing further evidence for the interaction between PD and HD described in section 1.1.2. Only Pax6-5a seems capable of causing *Pax6* autoregulation by this mechanism, as transfection of Pax6+5a and "paired-less" expressing constructs had no effect on either promoter.

In the human, the promoter PA is thought to correspond to quail and mouse P0, whilst PB corresponds to P1. Autoregulation *via* PA has not been studied, but PAX6 protein has been shown to affect the PB promoter (Okladnova et al., 1998). The effect of this autoregulation varies between cell lines; PAX6 can act as either an activator or a repressor if its own transcription, a difference which is presumably dependent on the presence of co-factors. It is unclear whether these cell-line specific differences are consistent across phyla, but *Pax6* autoregulation appears to be a complex phenomenon worthy of further study.

1.7: Aims

The main aim of this study is to analyse the role of *Pax6* isoforms in embryonic development. The mouse is used as a model system throughout, as the murine *Pax6* locus is well characterised (Walther and Gruss, 1991) and the effects of various murine *Pax6* mutations have been described in detail (Hill et al., 1991; Schmahl et al., 1993; St-Onge et al., 1997).

In particular, this study focuses on the two most common *Pax6* splice variants; *Pax6-5a* and *Pax6+5a*. Little is known about their differential expression patterns throughout development, or what independent roles these two isoforms might play.

1.7.1: *Pax6-5a* : *Pax6+5a* mRNA ratio in murine embryonic development

Chapter 2 will describe the use of RNase Protection Assay to determine the relative abundance of *Pax6-5a* and *Pax6+5a* in the olfactory bulb, telencephalon, diencephalon, eye, spinal cord, hindbrain and cerebellum from E12.5 to E18.5.

Spatial and temporal alterations in the ratio of *Pax6-5a* : *Pax6+5a* will be related to alterations in the role that Pax6 is thought to play in the development of different tissues at different embryological ages.

1.7.2: Pax6 protein isoform expression in *Pax6* mutant and WT mice

Chapter 3 will describe the use of western blot to determine the Pax6 protein content of the brain and eye of *Sey/Sey, Sey/+*, WT, $PAX77^{+/-}$ and $PAX77^{+/+}$ mice at E12.5. The relative abundance of each isoform will be compared across the different genotypes, and the alterations in level will be related to the phenotype observed in each mouse. In particular, the role of Pax6 autoregulation in controlling the level of Pax6 protein expression will be discussed.

The Pax6 protein content of *Sey/Sey*, Sey^{Neu}/Sey^{Neu} and $Pax6^{LacZ\,LacZ}$ mouse brains at E12.5 will also be described. The Pax6 isoform which is potentially responsible for any observed protein will be discussed, with reference to the mutation in the *Pax6* gene in each mouse strain.

1.7.3: The effects of *Pax6-5a* and *Pax6+5a* over-expression in a cell culture system

Chapter 4 will describe the introduction of *Pax6-5a* and *Pax6+5a* expression constructs into immortalised cell lines both with and without endogenous Pax6 protein.

The effects of over-expression of each isoform will be described, with particular reference to the effects on Pax6 autoregulation and neuronal differentiation.

Chapter 2: The *Pax6-5a* : *Pax6+5a* ratio in embryonic development

2.1: Summary

The alternative splicing of exon 5a in the paired domain of the Pax6 gene is well documented (Epstein et al., 1994b; Jun and Desplan, 1996; Kozmik et al., 1997; Walther and Gruss, 1991). This chapter details the use of RNase Protection Assay (RPA) to characterise the relative amounts of *Pax6-5a* and *Pax6+5a* mRNA in various tissues at various stages of murine embryonic development.

RPA was performed on total RNA from telencephalon, diencephalon, eye, spinal cord and hindbrain from E12.5, E14.5, E16.5 and E18.5 wild type embryos. From E14.5 onwards, it was also performed on total RNA from the olfactory bulb, and the cerebellum. At all ages, hindfoot mRNA was used as a Pax6 negative control.

A *GAPDH* riboprobe was used to confirm mRNA integrity. A *Pax6* riboprobe corresponding to the transcript between exons 7 and 11 was used to demonstrate the presence of *Pax6* in all tissues studied except hindfoot. A second *Pax6* riboprobe, spanning exons 3 to 5a, allowed determination of the ratio between *Pax6-5a* and *Pax6+5a*.

In all tissues at all ages, the *Pax6-5a* splice variant is predominant over *Pax6+5a*. However, the ratio is consistently lower than previously described in the central nervous system. All CNS tissues examined in this study have a lower *Pax6-5a* : *Pax6+5a* ratio than the eye.

In the telencephalon, diencephalon, spinal cord and hindbrain, a general trend was seen; the ratio falls between E12.5 and E16.5, then rises slightly by E18.5. In the olfactory bulb, on the other hand, the ratio peaks at E16.5. In the eye, the ratio peaks at E14.5, then drops steeply. In the cerebellum, the ratio remains fairly constant across all ages studied.

At E12.5, using a riboprobe spanning *Pax6* exons 6 and 7, transcripts lacking exon 6 are not detected in any tissues.

The observed trends in *Pax6-5a* : *Pax6+5a* ratio indicate that it is regulated in both a tissue-specific and a developmental stage-specific manner, and this regulation may be important in changing the role of Pax6 during development.

2.2: Introduction

2.2.1: Methods previously used to analyse the presence of *Pax6* splice variants during embryonic development

A number of methods have been used to assess the prevalence of *Pax6-5a* and *Pax6+5a* transcripts in various tissues. The variation in techniques employed, and in the species and developmental stages studied, makes it difficult to collate this information into one coherent data set.

Cloning of *Pax6* transcripts after PCR amplification of a cDNA population from adult mouse lens and brain indicated that *Pax6-5a* and *Pax6+5a* were of "similar abundance" in brain tissue, whilst *Pax6-5a* "greatly predominated" in the lens (Richardson et al., 1995). Such an analysis, however, is at best qualitative, as it incorporates a PCR step that can lead to the preferential amplification of one cDNA, and relies on the in-depth analysis of a very small number of cDNA clones.

An estimation of the relative abundance of the two splice forms in chick embryonic tissues, based on the quantitation of RT-PCR products, suggested that 80% of *Pax6* transcript in the retina, but only 2.5% of *Pax6* transcript in the cornea, contained exon 5a (Koroma et al., 1997). In the bovine eye, RT-PCR data indicated that *Pax6+5a* was in excess over *Pax6-5a* in the iris, but the reverse was true in the retina and lens. Levels appeared to be approximately equal in the cornea (Jaworski et al., 1997). Analyses such as these are often highly inaccurate, as they are based on the levels of RT-PCR product after a high number of amplificatory cycles, and can be affected by factors such as cDNA salt content, as much as they are by template concentration (reviewed in Bustin, 2000).

A more rigorous approach, semi-quantitative RT-PCR, involves the use of "mimic" template fragments, in competitive RT-PCR. The levels of an unknown cDNA template can be inferred from gel electrophoresis of a PCR product, by comparison with the levels of a "mimic" fragment of known quantity. This technique allows a

"quantitative approximation" of *Pax6* mRNA content, and showed that *Pax6-5a* and *Pax6+5a* exist at equal levels in adult human lens epithelium and lens fibres (Zhang et al., 2001). This technique is also not entirely quantitative, as it relies on the levels of PCR product being proportional to the levels of PCR template.

RNase protection assay (RPA), on the other hand, does not include an amplificatory step; it can therefore be considered an accurate method of quantitating the mRNA content of a tissue. This technique has been used to show that *Pax6-5a* is in 8-fold excess over *Pax6+5a* in total head RNA, from mice at embryonic day 12.5 (E12.5) to E16.5, and in adult brain RNA (Kozmik et al., 1997). It is important to note, however, that the use of whole head RNA will have masked any potential tissue-specific differences and developmental stage-specific differences within tissues.

2.2.2: RNase Protection Assay

RNase Protection Assay (RPA) is a highly sensitive technique used to analyse the RNA content of a tissue in a target-specific, non-amplificatory manner.

The basic principle behind RPA is illustrated in **Figure 2.1.** Total RNA is extracted from a tissue sample, and hybridised with radio-labelled single-stranded RNA (ssRNA) riboprobes complementary to the mRNA sequence under investigation (**Figure 2.1 B**). It is this hybridisation step which is both target-specific and non-amplificatory, creating a radio-labelled double-stranded RNA (dsRNA) population of known sequence. Provided that the riboprobe is in molar excess over the target mRNA, the dsRNA population will also be of the same quantity as the target mRNA in the original sample. All non-hybridised riboprobe and sample RNAs are digested away by RNases (**Figure 2.1 C**), and the remaining dsRNA molecules are resolved by denaturing polyacrylamide gel electrophoresis (**Figure 2.1 D**).

2.2.3: Aims

The aim of Chapter 2 was to study the relative expression levels of *Pax6-5a* and *Pax6+5a* in the developing CNS by RNase protection assay.

Figure 2.1. The basic principle behind RNase protection assay. **A**, a radio-labelled ssRNA riboprobe is synthesised from a sense cDNA template. **B**, ssRNA riboprobe is hybridised to target mRNA. **C**, un-hybridised ssRNA (either template or riboprobe) is digested with RNase, leaving only hybridised dsRNA duplexes of known fragment sizes. **D**, dsRNA duplexes are resolved by polyacrylamide gel electrophoresis. Red and blue bars, exons. Black arrows, ssRNA riboprobes. Green stars, ^{32}P UTP.

mRNA was obtained from E12.5 to E18.5, as this corresponds to the peak period of neurogenesis in the developing mouse (Gillies and Price, 1993; Levers et al., 2001), and also the period of highest *Pax6* expression (Walther and Gruss, 1991).

The *Pax6-5a* : *Pax6+5a* ratio was ascertained in WT telencephalon, diencephalon, eye, spinal cord and hindbrain at E12.5, E14.5, E16.5 and E18.5. The olfactory bulb and cerebellum were also studied from E14.5 onwards, when these tissues first emerge. The presence of *Pax6* transcripts lacking exon 6 (*Pax6Δ6*) was also assessed at E12.5.

This analysis aims to correlate differences in the *Pax6+5a* : *Pax6-5a* mRNA ratio in these tissues with discrete processes in which Pax6 activity is thought to be involved.

2.3: Methods

See **Appendix 1** for detailed protocols.

2.3.1: RNA extraction from embryonic tissue

CD1 mice were used as the wild type strain in this analysis.

For all matings, the day on which a plug was found was designated embryonic day 0.5 (E0.5).

Embryos were harvested at a range of embryonic ages, from E12.5 to E18.5. See **Figure 2.2** for a detailed description of dissected tissues. All dissections were carried out within 90 minutes in ice cold, sterile PBS. Tissues were snap-frozen in liquid nitrogen, and stored at -70°C until RNA extraction.

RNA extractions from embryonic tissue were performed using the RNAgents kit (***Promega***). Briefly, tissue was thoroughly homogenised using a motorised homogeniser with RNase-free disposable pestles, in a denaturing solution containing guanidium isothiocyantate (GITC). This inhibits RNA digestion by endogenous RNases, allowing the cellular contents to be released with minimal RNA degradation. RNA was then separated out of the solution by acid phenol:chloroform extraction,

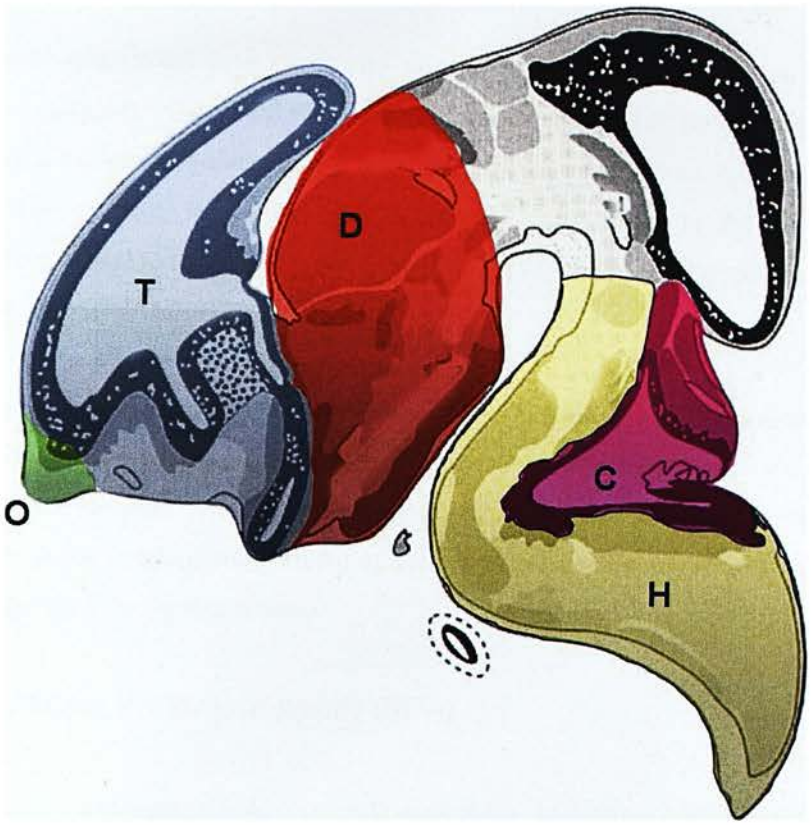

Figure 2.2 Schematic representation of brain areas from which total RNA was taken for use in RNase Protection Assays. E14.5 mouse brain saggital section, taken from Kaufmann (1995). O, olfactory bulb. T, telencephalon. D, diencephalon. H, hindbrain. C, cerebellum. At E12.5, olfactory bulb was included with telencephalon, and cerebellum was included with hindbrain. From E14.5 to E18.5, tissues were dissected as described here.

and excess salts were removed by successive isopropanol precipitations. RNA pellets were resuspended in ddH_2O and stored at -70°C for up to 18 months.

2.3.2: RNA quantitation

RNA was quantitated prior to RNase protection assays, to assure even loading between samples. Quantitations were performed using RiboGreen (***Molecular Probes***), a nucleic acid-intercalating agent that fluoresces at 500nm upon binding to RNA. The intensity of fluorescence is directly proportional to the amount of RiboGreen bound to target RNA, and thus directly proportional to the total amount of RNA in a sample.

Fluorescence intensity was measured using a PicoFluor bench-top fluorimeter. Yeast tRNA standards were used to plot a standard curve of fluorescence against ng RNA, and a fresh standard curve was generated each time. The RiboGreen reagent is sensitive down to <1ng RNA in 80µl of sample, therefore minimal amounts of RNA were expended during quantitation.

2.3.3: RNase Protection Assay (RPA)

RPAs were performed on wild type embryonic RNA, to determine the absolute Pax6 content of various tissues.

2.3.3.1: Riboprobe design

Sections of murine *Pax6* cDNA were cloned into pCR-BluntII-TOPO (***Invitrogen***) to allow the synthesis of riboprobes for use in RPA. For each riboprobe template, *Pax6* cDNA was cloned from whole mouse E12.5 cDNA.

See **Figure 2.3** for a graphical representation of Pax6 mRNA sequences protected by the three riboprobes.

To create a riboprobe spanning exons 3 to 5a, which would differentially recognise *Pax6+5a* and *Pax6-5a* (Probe 5.22), cDNA was amplified with the primers "Pax6 MMu exon 3F" and "Pax6 MMu exon 5aR" (see Appendix 2 for primer sequences and optimal annealing temperatures).

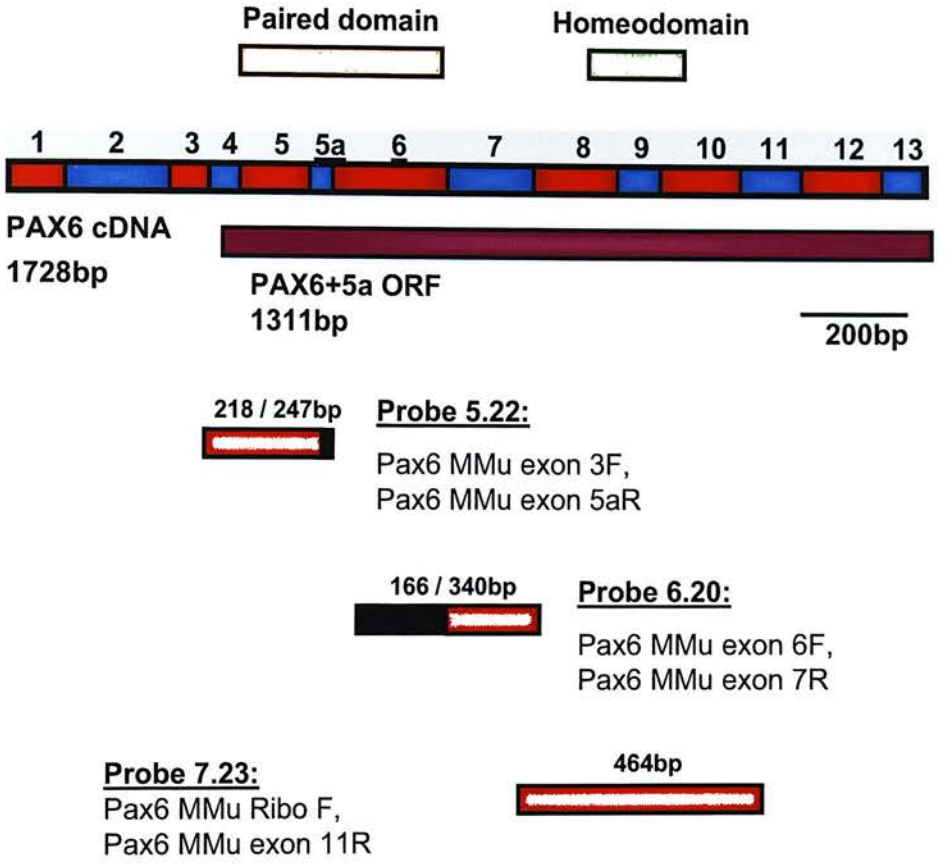

Figure 2.3: Pax6 Riboprobes. Red and blue bars represent Pax6 exons. The alternatively spliced exons 5a and 6 are underlined. Purple bar: Pax6 open reading frame; canonical translation begins at the 3' end of exon 4. Orange bar: paired domain. Green bar: homeodomain. Protected fragments covered by the three riboprobes are depicted by red (unspliced) and black (spliced) bars, with predicted fragment lengths in base pairs. Probe names, and the names of the PCR primers used to create them, are also given.

To create a riboprobe spanning exons 6 and 7, which would differentially recognise *Pax6* and *Pax6Δ6* (Probe 6.20), cDNA was amplified using the primers "Pax6 MMu exon 6F" and "Pax6 MMu exon 7R"

To create a riboprobe spanning the unspliced *Pax6* exons 7 to 11 (Probe 7.23), which would act as a control probe to detect full-length *Pax6*, cDNA was amplified using the primers "Pax6 MMu RiboF" and "Pax6 MMu Exon 11R". All PCR amplifications were performed using Expand DNA polymerase (***Roche***), combining high-fidelity amplification by the proofreading *Pfu* DNA polymerase with the speed of *Taq* DNA polymerase, to minimise the risk of amplification errors.

After PCR amplification, blunt-ended fragments were cloned using the Zero Blunt TOPO cloning system (***Invitrogen***) into the pCR-Blunt-II-TOPO vector (***Invitrogen***). Four clones from each cloning reaction were sequenced across the *Pax6* insert in both directions to ascertain the orientation in which the template had entered pCR-BluntII-TOPO, and to confirm that their sequence corresponded exactly to European Molecular Biology Laboratory (EMBL) entry X63963.1.

pJP5.22 (exons 3 to 5a), pJP6.20 (exons 6 and 7), and pJP7.23 (exons 7-11) were used for all riboprobe synthesis reactions, as they contained the desired *Pax6* sequence with no mutations, in the antisense orientation. Transcription from these templates creates sense-oriented single-stranded RNA, which can bind to and form duplexes with antisense single-stranded mRNA.

The plasmid pTRI-GAPDH (***Ambion***) was also used, for synthesis of a murine glyceraldehyde-3-phosphate dehydrogenase (GAPDH) riboprobe, to confirm the presence of non-degraded mRNA in each sample.

2.3.3.2: Sequencing

All Pax6 expression constructs and riboprobe templates were fully sequenced across the Pax6 locus in both directions. Plasmid backbones were not sequenced, but were understood to be as described by the supplier. Sequencing was performed on ethanol-precipitated plasmid DNA obtained by miniprep, using the MWG-Biotech Value Read sequencing service. For sequencing primers, see Appendix 2.

2.3.3.3: Riboprobe synthesis

Single-stranded, ^{32}P-labelled riboprobes were synthesised antisense to the target RNA. Transcription was carried out using SP6 RNA polymerase in the presence of α-^{32}P-UTP. For *GAPDH* probes, a small amount of unlabelled UTP was included in the reaction to decrease the specific activity of the riboprobe, allowing the visualisation of *GAPDH* and *Pax6* on the same gel, even though *GAPDH* was in great excess over *Pax6*. Riboprobes were purified using a sepharose column (***Promega***) to remove unincorporated nucleotides, and a small aliquot was analysed by polyacrylamide gel electrophoresis to confirm the presence of a single labelled RNA of the expected size. Riboprobes were then quantitated by Cerenkov scintillation counting.

2.3.3.4: HybSpeed RPA

RPAs were carried out using the HybSpeed kit (***Ambion***).

Template RNA, riboprobe and yeast tRNA were combined, ethanol co-precipitated, resuspended in hybridisation buffer, and target RNA – riboprobe hybridisation was allowed to proceed overnight. See **Figure 2.2** for a detailed description of target RNAs. RNAs represented tissues of the central nervous system that were known to express *Pax6* during development, and were taken from E12.5, E14.5, E16.5 and E18.5 embryos, spanning the peak period of neurogenesis. At E12.5 and E14.5, 1μg of total RNA was used per reaction. For E16.5 and E18.5 samples, this was increased to 4μg, as total *Pax6* expression falls at these ages, but greater amounts of RNA can be collected. For each reaction, 80,000cpm of *Pax6* riboprobes and 40,000cpm of *GAPDH* riboprobes were used. Despite *GAPDH* mRNA being more abundant than *Pax6* mRNA in the tissues analysed, a lower cpm of *GAPDH* riboprobe was used. This was because the riboprobe had been spiked with unlabelled UTP, therefore a lower specific activity still represented a higher amount of riboprobe. Yeast tRNA was included to make the total amount of RNA up to 50μg in order to aid ethanol co-precipitation. For each RPA, two control tubes consisting of probe and yeast tRNA with no target RNA were also prepared.

After overnight target RNA – riboprobe hybridisation, all single-stranded target RNA (ssRNA) had hybridised to single-stranded probe RNA, making double-stranded

RNA-RNA (dsRNS) duplexes. Each reaction was treated with a cocktail of RNaseA and RNase T1 to digest away all unbound ssRNA, leaving only dsRNA and NTPs. One negative control reaction was also treated in this way to ensure that RNase digestion progressed to completion. The second negative control reaction was incubated in RNase digestion buffer without RNase cocktail, allowing whole undigested riboprobe to be carried through to the end of the reaction. If this undigested riboprobe was intact on the final polyacrylamide gel, this was an indication that no RNases were present elsewhere in the procedure, and negative samples were indeed negative rather than just a result of unwanted RNase digestion.

Double-stranded RNA-RNA duplexes were then isopropanol precipitated to eliminate digested NTPs, and resuspended in gel loading buffer containing formamide to denature the duplexes. This process was aided by heating samples to 95^0C for 5 minutes. RNA was then resolved on a 6% polyacrylamide, 8M urea denaturing gel, alongside a α-^{32}P-labelled double-stranded DNA ladder to allow approximate sizing of bands.

2.3.4: Densitometric analysis of gel films

Bands on X-ray films were quantitated using a BioRad GS-710 densitometer. Gels were scanned at a high resolution (usually 42.3μm X 42.3μm per pixel), in greyscale spanning 400-750nm wavelengths, using transmitted light. Analysis was performed using the Quantity One software (***BioRad***). Lanes were created, and a rolling disc background subtraction method was used to ensure data was comparable between lanes. Bands were then manually created, and peak area was taken as a measurement of band intensity.

2.4: Results

RNase Protection Assay is a highly sensitive, non-amplificatory, target-specific technique for analysing the mRNA content of a tissue sample. *Pax6* mRNA is detectable from as little as 1μg total RNA at E12.5. As the protocol involves no amplificatory steps, and theoretically no target RNA is lost during an RPA, it allows absolute quantitation of mRNA levels. In practice, some mRNA is lost during the procedure; therefore direct comparison between mRNA samples is not possible. Within a sample, however, the ratio between splice variants should be an accurate

representation of the ratio within a tissue. Careful riboprobe design leads to the production of dsRNA fragments of known size which can be resolved by polyacrylamide gel electrophoresis.

2.4.1: *GAPDH* mRNA is present in all tissues examined

The quality of all total RNA samples was first assessed using a *GAPDH* riboprobe. Where a single, discrete band of 316bp was seen, it was an indication that no RNase digestion had occurred (See **Figure 2.4** for a sample gel). Identical amounts of total RNA were loaded in each lane. Where *GAPDH* signal was weak, this was a sign that protein or DNA contamination had led to inaccurate RNA quantitation, and these samples were excluded from subsequent analyses.

2.4.2: *Pax6* mRNA is present in all tissues examined, except hindfoot

The riboprobe pJP7.23 protects *Pax6* mRNA from exons 7 to 11, an area in which no alternative splicing had been described at the time of probe design. RPA on all tissues with this probe gave a 464bp, full-length band (**Figure 2.5**). A second, lower band of approximately 240bp was occasionally seen, although this was not present in all samples. It is unclear whether this is a *Pax6*-specific band.

Exact sizing of this ectopic band is difficult, as the dsDNA ladder only allows an approximation of dsRNA fragment length. Knowing the predicted size of full-length *GAPDH* and *Pax6* bands shows that dsRNA is retarded on polyacrylamide gels, when compared to dsDNA ladder. Therefore a dsRNA band travelling alongside a 242bp dsDNA band is likely to be slightly smaller than this.

There is no clear explanation for the presence of a ~240bp protected fragment from the riboprobe pJP7.23. Two *Pax6* cDNAs have been cloned from the mouse in which exons 2 to 8, or 2 to 10 are absent (Gorlov and Saunders, 2002). These would give predicted fragment sizes of 176bp or 54bp, respectively. Another *Pax6* transcript, beginning in intron 7 (Kleinjan et al., 2004) would give a 447bp protected fragment. An alternative explanation would involve the alternative splicing of exon 10. In this case, the probe pJP7.23 would protect a 259bp RNA fragment, covering exons 7, 8 and 9. This is approximately the size of the ectopic band observed in **Figure 2.5**, but

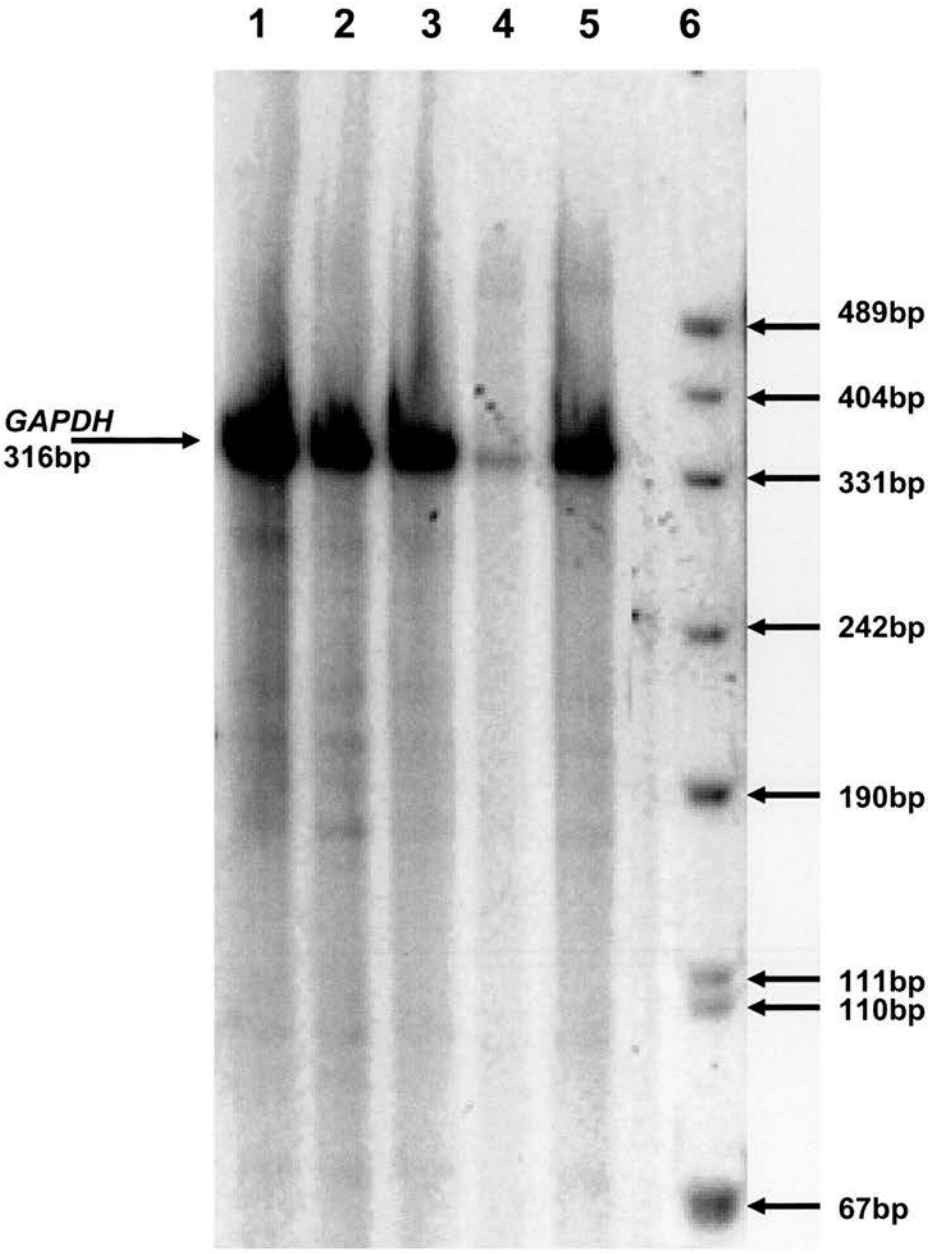

Figure 2.4, *GAPDH* signal in total RNA from telencephalon (lane 1), diencephalon (2), eye (3), spinal cord (4) and hindfoot (5) at E12.5. 1µg total RNA was used in each sample. In this example, spinal cord RNA (lane 4) was discarded, as levels were lower than RNA quantitation suggested, implying protein or DNA contamination. Lane 6, dsDNA ladder. This allows an estimation of dsRNA fragment size.

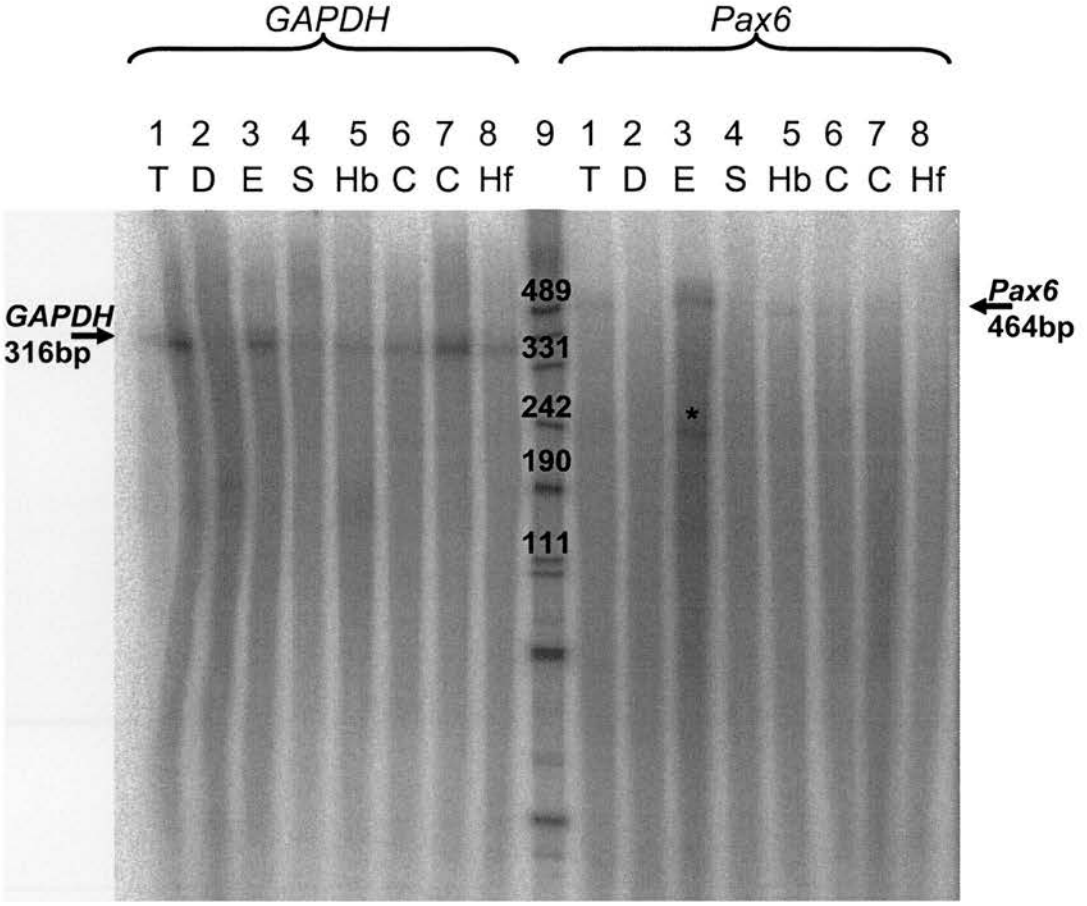

Figure 2.5, Example of GAPDH and *Pax6* signal detected by pTri-GAPDH and pJP7.23 (Pax6 exons 7-11) in total RNA from E14.5 telencephalon (lane 1), diencephalon (2), eye (3), spinal cord (4), hindbrain (5) cerebellum (6+7) and hindfoot (8). 1µg total RNA was used in each sample. In this example, diencephalon RNA (lane 2) was discarded, as levels were lower than RNA quantitation suggested, implying protein or DNA contamination. dsDNA ladder (9) allows approximate sizing of bands, fragment sizes are indicated above bands. A ~240bp band (*) was occasionally seen with the probe pJP7.23.

would not leave the *Pax6* transcript in-frame, and such a splice event has not been documented *in vivo*. Alternative splicing of exon 8 would leave two protected RNA fragments, one of 83bp corresponding to the 5' portion of the probe, the second of 288bp, corresponding to the 3' portion of the probe. This is probably too large a predicted fragment size to account for the ~240bp band, and has also not been documented *in vivo*.

Pax6 mRNA was shown by the riboprobe pJP7.23 to be present in all tissues studied, except hindfoot.

2.4.3: *Pax6-5a* : *Pax6+5a* ratio in the developing mouse telencephalon, diencephalon, spinal cord and hindbrain

All *Pax6* expressing tissues contained both splice variants (**Figure 2.6**). This is consistent with previous studies (Jaworski et al., 1997; Kozmik et al., 1997; Zhang et al., 2001), as exclusive expression of one isoform within a tissue has never been documented. It is also consistent with data presented in Chapter 4, which indicates that regulatory mechanisms are in place to ensure that these two isoforms are usually co-expressed.

The ratio of *Pax6-5a* to *Pax6+5a* is similar between telencephalon, diencephalon, spinal cord and hindbrain between E14.5 and E18.5 (**Figures 2.7-2.9**). At E12.5 it varies between these four tissues, and is highest in the diencephalon, where it approaches 9:1, and lowest in the spinal cord, where it is closer to 3:1. A high degree of variation is seen in samples from the hindbrain, with values ranging between 18:1 and 2:1, whilst results for the other tissues are more consistent. It is important to note that E12.5 telencephalon samples included the developing olfactory bulb, which is shown to behave differently at later ages (see Section 2.4.4). E12.5 hindbrain also included the developing cerebellum, which also seems to follow a different pattern of *Pax6* expression later in development (see Section 2.4.6).

By E14.5, the ratio has fallen in all four tissues, and is around 3:1 in all cases. It drops slightly at E16.5 to 2:1, then rises again by E18.5, back to approximately 3:1.

The other tissues analysed seem to follow separate trends in *Pax6-5a* : *Pax6+5a* ratio, and will be described in turn.

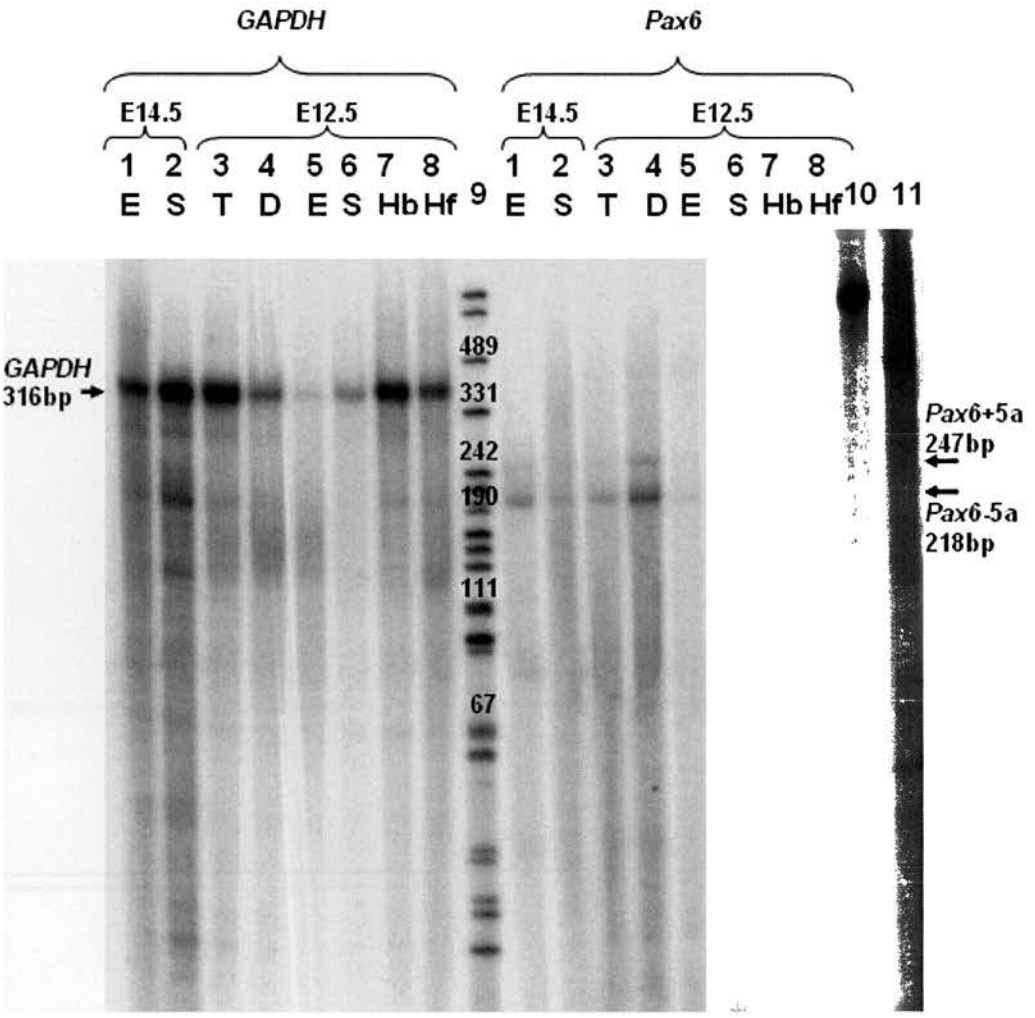

Figure 2.6, Example of GAPDH and *Pax6* signal detected by pTri-GAPDH and pJP5.22 (*Pax6* exons 3 to 5a) in total RNA from E14.5 eye (lane 1), E14.5 spinal cord (2), E12.5 telencephalon (3), E12.5 diencephalon (4), E12.5 eye (5) E12.5 spinal cord (6), E12.5 hindbrain (7) and E12.5 hindfoot (8) 1µg total RNA was used in each sample. dsDNA ladder (9) allows approximate sizing of bands, fragment sizes are indicated above bands. Lane 10, undigested *GAPDH* probe. Lane 11, undigested *Pax6* probe.

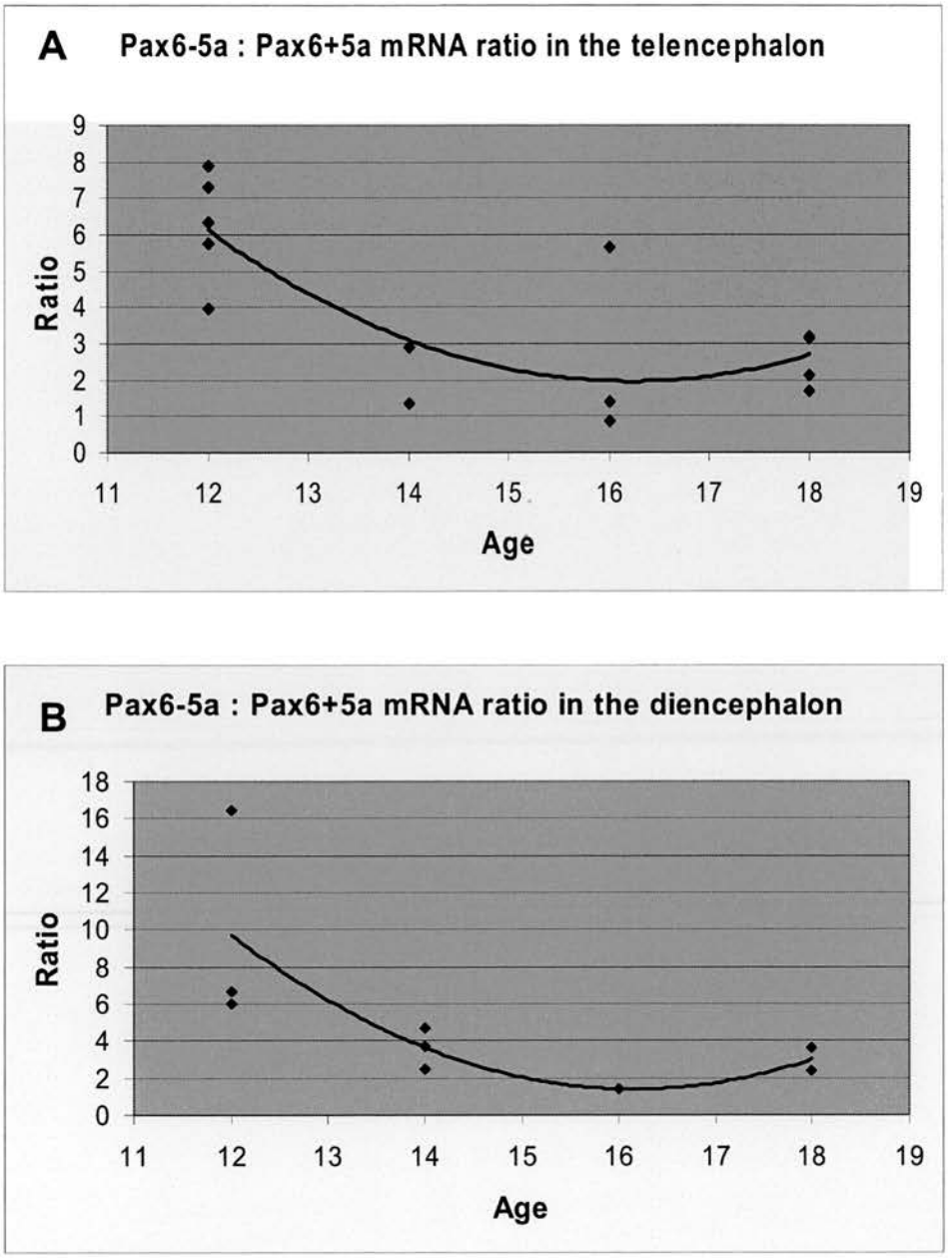

Figure 2.7 Scatter plot of *Pax6-5a* : *Pax6+5a* ratio in **A**, telencephalon from E12.5 to E18.5. **B**, diencephalon from E12.5 to E18.5.

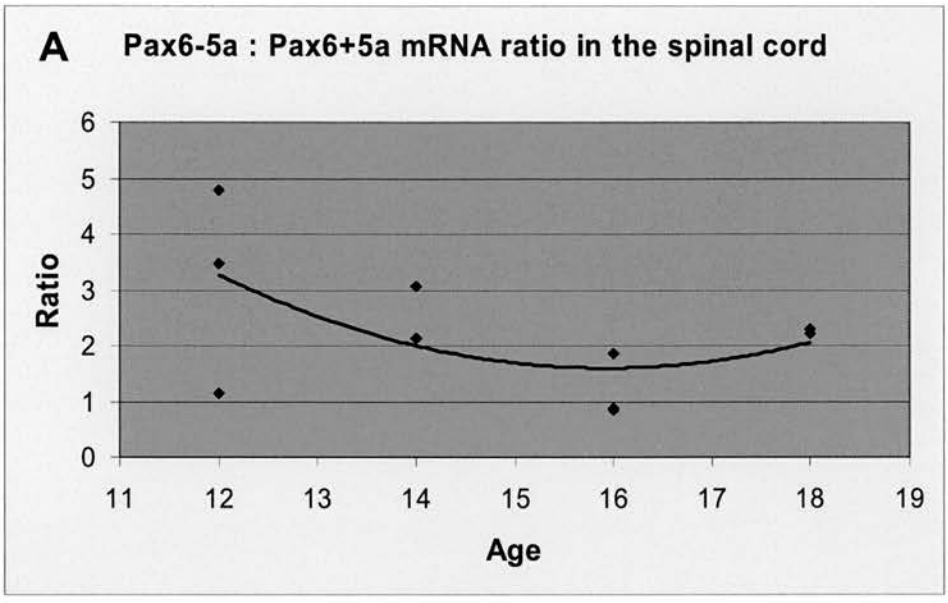

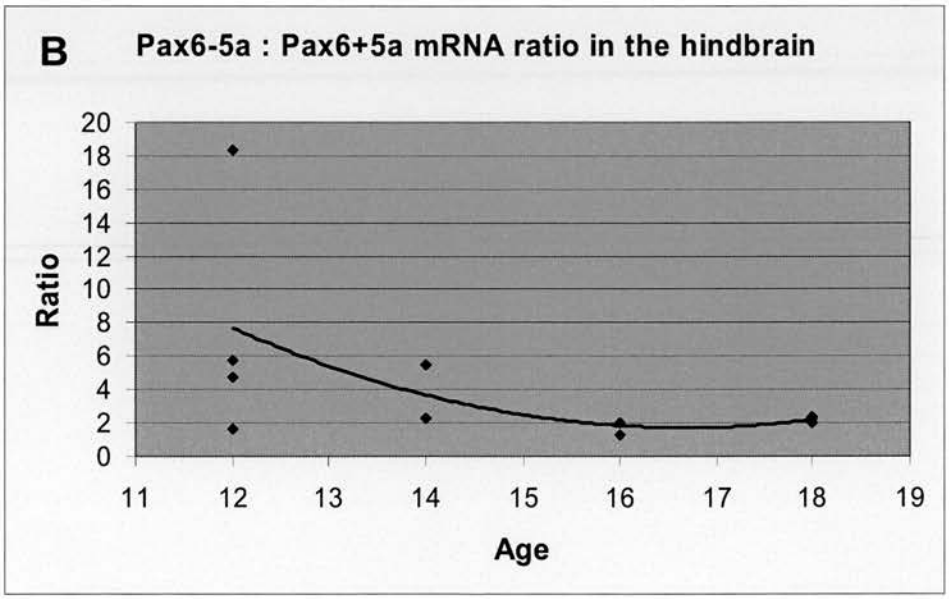

Figure 2.8 Scatter plot of *Pax6-5a* : *Pax6+5a* ratio in **A**, spinal cord from E12.5 to E18.5. **B**, hindbrain from E12.5 to E18.5.

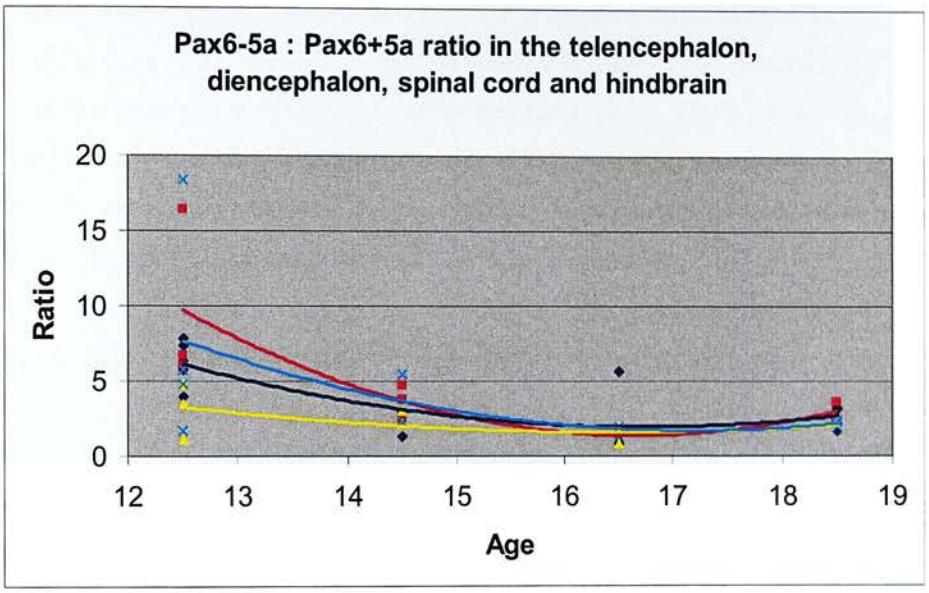

Figure 2.9 Scatter plot of *Pax6-5a* : *Pax6+5a* ratio in telencephalon, diencephalon, spinal cord and hindbrain from E12.5 to E18.5.

2.4.4: *Pax6-5a* : *Pax6+5a* ratio in the developing mouse olfactory bulb

The developing mouse olfactory bulb cannot be distinguished from the telencephalon at E12.5, therefore at this age the two tissues were pooled, and classed as telencephalon. From E14.5, separate olfactory bulb mRNA samples could be obtained. However, sample number is low as the tissue was difficult to collect. The observed *Pax6-5a* : *Pax6+5a* ratio is low, around 2:1 at E14.5 (**Figure 2.10 A**). This is similar that seen in the other CNS tissues described above. Unlike these tissues, however, the ratio rises in the olfactory bulb at E16.5, then falls again at E18.5. It is unclear whether variation between the two olfactory bulb samples from E16.5 is real or experimental, but data from the other two ages is less variable.

2.4.5: *Pax6-5a* : *Pax6+5a* ratio in the developing mouse eye

Data from the developing eye (**Figure 2.10 B**) indicates that the *Pax6-5a* : *Pax6+5a* ratio is higher than that observed in most tissues of the brain and in the spinal cord at E12.5 and E14.5; it is around 8:1. It then drops, and by E18.5 has fallen to approximately 3:1. This drop in ratio is similar to that observed in the telencephalon, diencephalon, spinal cord and hindbrain. In these tissues, however, it is lowest at E16.5, whilst in the eye it is still falling at E18.5.

2.4.6: *Pax6-5a* : *Pax6+5a* ratio in the developing mouse cerebellum

The mouse cerebellum is not apparent at E12.5, being indistinguishable from the rest of the developing hindbrain. By E14.5, a presumptive cerebellum can be seen, and mRNA samples were collected from this age onwards.

Although there is only one data point at E14.5, there appears to be no change in the *Pax6-5a* : *Pax6+5a* ratio in the cerebellum at the observed ages (**Figure 2.11**). On average, the ratio remains at about 4:1. Unlike all the other tissues used in this analysis, it does not fall throughout development, and is no lower at E18.5 than at E14.5.

2.4.7: *Pax6Δ6* is not observed in any tissue at E12.5

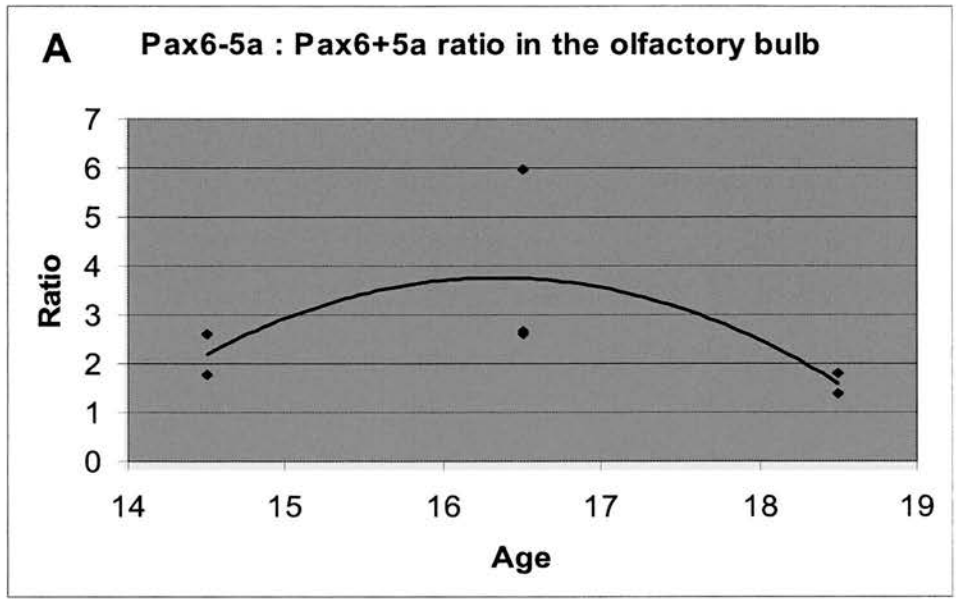

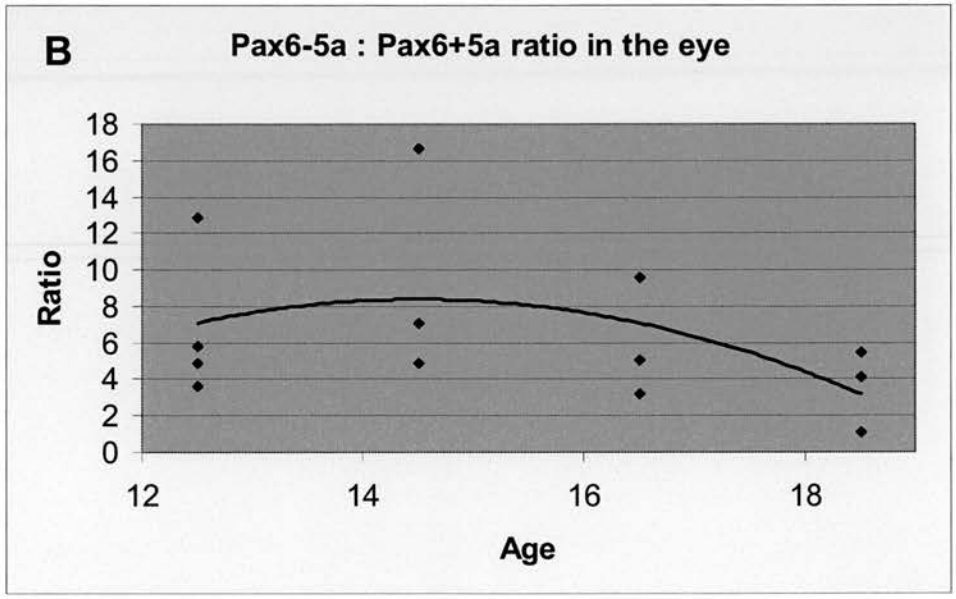

Figure 2.10 Scatter plot of *Pax6-5a* : *Pax6+5a* ratio in **A**, olfactory bulb from E14.5 to E18.5. **B**, eye from E12.5 to E18.5.

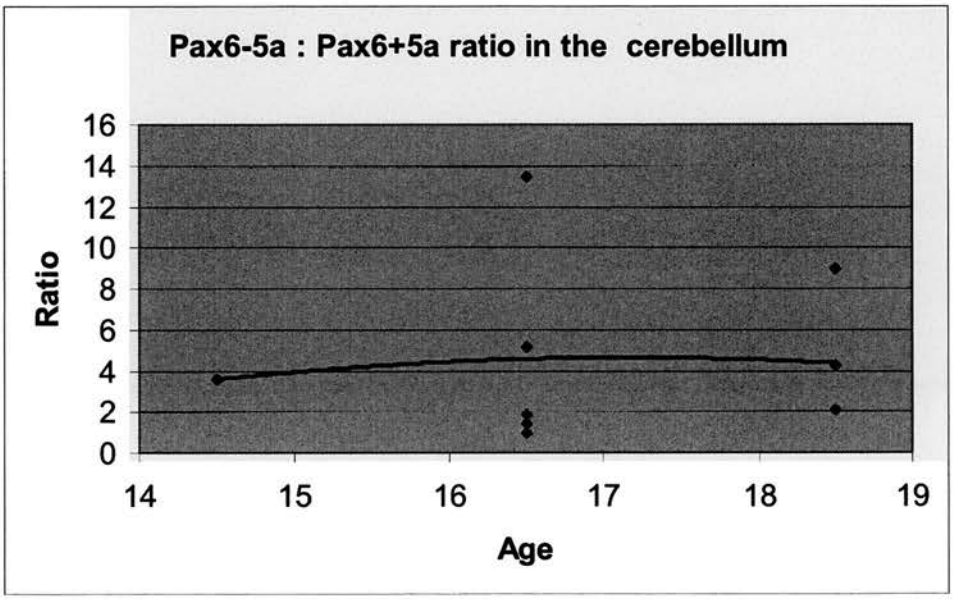

Figure 2.11 Scatter plot of *Pax6-5a* : *Pax6+5a* ratio in cerebellum from E14.5 to E18.5

The alternative splicing of exon 6 of the *Pax6* gene has been documented a number of times. Carriere et al. (1993) described an mRNA isolated from quail neuroretina in which the 3' 198bp of exon 5 (*Pax-QNR* exon 5 corresponds to human and mouse *Pax6* exon 6) was removed due to the usage of an unusual splice donor site 15bp into exon 5, allowing splicing straight onto sequence at the 5' end of exon 6 (human and mouse exon 7). The splice donor site described in this example is conserved across mouse and man, and this splice variant has also been described in the bovine eye (Jaworski et al., 1997). *Pax6* missing the entire of exon 6 has been cloned from the U373-MG glioblastoma cell line (T.I.Simpson pers. comm.). Each of these potential splice variants would be detected by the riboprobe pJP6.20, which spans exons 6 and 7 of the *Pax6* transcript.

RPA was performed using this riboprobe on all tissues at E12.5. This age was chosen for a preliminary screen as it is around the peak of neurogenesis (E13.5) and the peak of *Pax6* expression (E10.5) (Walther and Gruss, 1991). Also, as seen in Chapter 3, a 43KDa Pax6 protein, thought to correspond to Pax6 lacking exon 6 (Carriere et al., 1993) is present in both brain and eye at E12.5.

A single band of 340bp was observed in all samples (**Figure 2.12**). Any shorter bands were low in abundance, and observed in hindfoot RNA, and therefore unlikely to represent *Pax6* splice variants. This result was surprising, as the alternative splicing of some or all of *Pax6* exon 6 is reasonably well documented. It is possible that this mRNA is present at low levels, below the limits of detection by RPA. However, western blot data indicates that the 43KDa protein is present in reasonably high levels in a number of tissues (Carriere et al., 1993; Turque et al., 1994; Chapter 3 of the present study). This could mean that the protein product of this mRNA is highly stable, and only low levels of transcript are required to create relatively high levels of protein. Alternatively, differential antibody binding kinetics could mean that although this isoform appears quite common by western blot, it is in fact quite rare, but preferentially detected by anti-Pax6 antibodies. A third explanation is that the 43KDa protein is not a result of alternative splicing of exon 6. Although these cDNAs have been described *in vivo*, and their predicted molecular mass after translation is 43KDa, they have never been shown to be directly responsible for the 43KDa band observed by western blot.

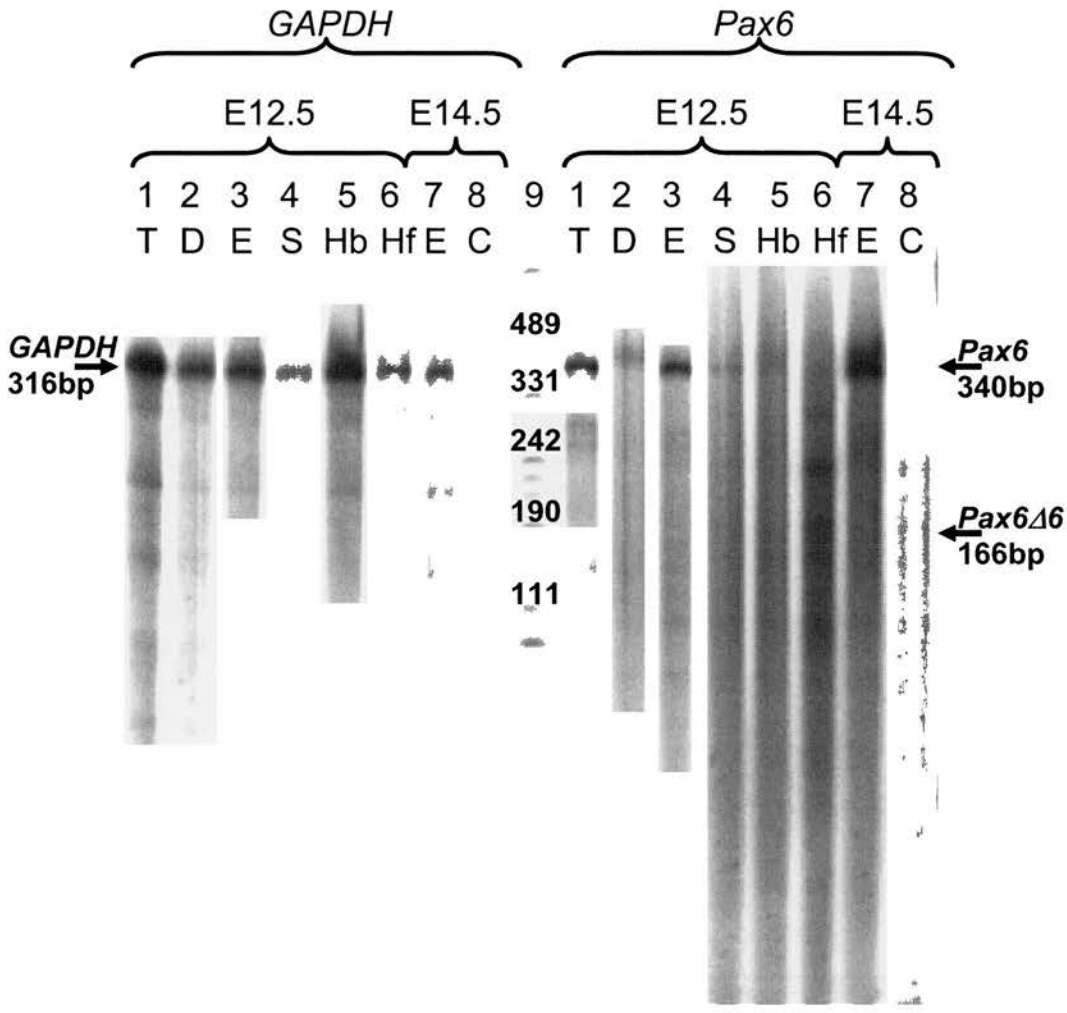

Figure 2.12, Example of GAPDH and *Pax6* signal detected by pTri-GAPDH and pJP6.20 in total RNA from E12.5 telencephalon (lane 1), E12.5 diencephalon (2), E12.5 eye (3), E12.5 spinal cord (4), E12.5 hindbrain (5) E12.5 hindfoot (6), E14.5 eye (7) and E14.5 cerebellum (8) 1µg total RNA was used in each sample. dsDNA ladder (9) allows approximate sizing of bands, fragment sizes are indicated above bands. A single band of 340bp is seen in all tissues except E12.5 hindfoot and E14.5 cerebellum, where *GAPDH* signal is weak. Any shorter bands are present in E12.5 hindfoot, therefore not *Pax6* specific. No clear 166bp *Pax6Δ6* band is visible in any tissue.

2.5: Discussion

2.5.1: Overall trends in *Pax6-5a* : *Pax6+5a* ratio in murine embryonic development

In all tissues, at all ages, *Pax6-5a* is more abundant than *Pax6+5a*.

The *Pax6-5a* : *Pax6+5a* ratio is shown to vary both spatially and temporally throughout murine neurogenesis. The most common pattern is observed in the telencephalon, diencephalon, spinal cord and hindbrain. In these tissues, the ratio starts high at E12.5, falls to around 2:1 by E16.5, then rises slightly to 3:1 at E18.5. Three of the tissues analysed in this study did not conform to that pattern; the olfactory bulb, the eye and the cerebellum. In the olfactory bulb, ratios are low, about 2:1 at E14.5. They then rise slightly at E16.5, before falling back to 2:1 at E18.5. In the eye, the ratio starts high, at around 8:1, then falls steadily to around 3:1 at E18.5. In the cerebellum, the ratio remains constant, at around 4:1.

2.5.2: Limitations of this analysis

Although RPA is theoretically a quantitative technique, in practice it was only possible to compare the amounts of transcript within a sample. Due to successive RNA precipitation steps in the protocol, sample was lost in some or all cases. As equal amounts of *Pax6-5a* and *Pax6+5a* mRNA are likely to be lost, their ratio within a sample should still be an accurate representation of the *in vivo* ratio.

Had this technique been quantitative between samples, it would have been interesting to compare data from the riboprobes pJP5.22 and pJP7.23. The former protects mRNA from exons 3 to 5a, and the latter from exons 7 to 11. *Pax6* transcripts have been described since the design of the riboprobes used here, in which transcription begins within intron 7 (Kleinjan et al., 2004), or various exons between 4 and 10 are absent (Gorlov and Saunders, 2002). These putative transcripts would be at least partially protected by the riboprobe pJP7.23, but not by pJP5.22. None of them, however, would give dsRNA fragments of a similar size to the short, ~240bp fragment observed occasionally with pJP7.23. A comparison in signal strength between the two riboprobes would have allowed an estimation of the levels of any 5'-truncated transcripts, had the technique proven to be quantitative. One RPA, in which

the two riboprobes were used in tandem on the same RNA samples, indicated that signal strength was indeed higher with pJP7.23 in the telencephalon and diencephalon, but not in the eye (**Figure 2.13**), however this data is likely to be qualitative at best.

Another obvious problem with assessing the levels of alternatively spliced *Pax6* mRNAs is that mRNA levels may not directly mirror protein levels. If one transcript is more stable, or translated with a higher efficiency, the observed *Pax6-5a* : *Pax6+5a* ratio may not be the same as the ratio between the two proteins. A comparison between these data and data from western blot analysis of whole brain and whole eye at E12.5 (see Chapter 3, **Figure 3.22** for further detail) implies that the mRNA ratio is similar to the protein ratio in the eye, and these data are probably an accurate representation of protein expression. In the brain, there is more disparity between the two values, which may be indicative of regulation at the protein level. This will be discussed in more detail in Section 3.6.2.

This technique was informative in looking at the development of the brain, as its constituent tissues were dissected out and analysed independently. However, the same is not true of the eye. Accurate conclusions cannot be drawn from the eye data presented here, as it involved the pooling of a number of different *Pax6* expressing tissues, most notably the neural retina and the lens.

2.5.3: Potential explanations for the developmentally regulated changes in *Pax6-5a* : *Pax6+5a* ratio

2.5.3.1: The telencephalon, diencephalon, spinal cord and hindbrain

That the telencephalon, diencephalon, spinal cord and hindbrain follow the same trends in *Pax6-5a* : *Pax6+5a* ratio implies that Pax6 may be playing a similar role in each tissue. In particular, from E14.5 to E18.5, results from the four tissues are virtually indistinguishable. It is possible that *Pax6* has a different action in each tissue at E12.5, but the same action from E14.5 onwards.

The fall in the ratio in these four tissues occurs whilst the proliferating precursor cell population begins to differentiate, and may be indicative of a switch in the role of

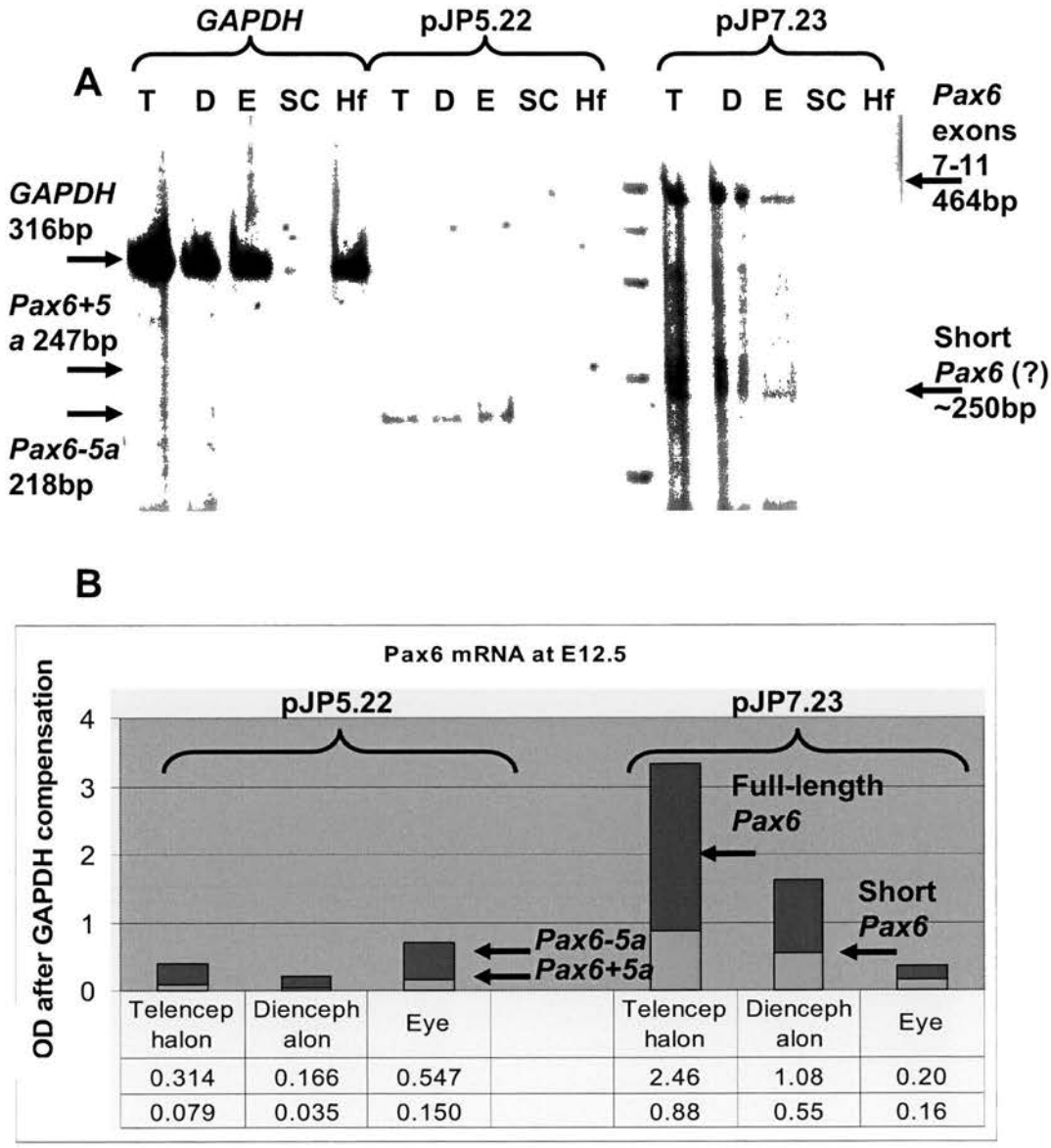

Figure 2.13, Comparison of *Pax6* signal strength from the probes pJP7.23 (spanning exons 7-11) and pJP5.22 (spanning exons 3-5a), analysed simultaneously. **A**, polyacrylamide gel. T, E12.5 telencephalon. D, E12.5 diencephalon. E, E12.5 eye. SC, E12.5 spinal cord (failed lane). Hf, E12.5 hindfoot. **B**, *Pax6* levels after compensation for *GAPDH*.

Pax6, from promoting proliferation to promoting differentiation. This will be discussed further in Section 2.5.3.5.

2.5.3.2: The olfactory bulb

The *Pax6-5a* : *Pax6+5a* ratio in the developing olfactory bulb is low at E14.5, coincident with both migration and proliferation contributing to the olfactory bulb cell population. It rises immediately after, as these proliferative precursor cells begin to differentiate. This is opposite to the effect seen in other CNS tissues, where the ratio falls at E16.5, as neuronal differentiation begins. These data suggest that *Pax6* may be playing another, as yet undefined role in olfactory bulb development. For example, the rise in ratio at E16.5 occurs as mitral cell axons begin to leave the olfactory bulb and innervate the olfactory cortex (Nomura and Osumi, 2004). Thus, Pax6 may be playing an important role in the regulation of cell adhesion molecules to control this migration.

By E18.5 the *Pax6-5a* : *Pax6+5a* ratio in the olfactory bulb has fallen again, and is close to that observed in other CNS tissues, about 2:1. By this point, development of all these structures is largely complete, and Pax6 could be playing a similar, maintenance role in each.

2.5.3.3: The eye

The eye is the most complex tissue used in this study, in terms of the number of tissues and cell types present. As such, this mRNA sample represented a number of *Pax6* expressing tissues which were pooled. It is likely that this led to the masking of some tissue-specific differences in ratio. As described in Section 2.2.1, the *Pax6-5a* : *Pax6+5a* ratio is best understood in the adult eye, largely as a result of two studies on the bovine eye (Jaworski et al., 1997) and the human lens, cornea and monkey retina (Zhang et al., 2001). Both of these studies indicated that there are indeed tissue-specific differences in the *Pax6-5a* : *Pax6+5a* ratio within the adult eye, an effect that is likely to extend to the developing murine eye.

Alternative *cis*-regulatory elements downstream of the *Pax6* gene direct its expression specifically in the neural retina (Griffin et al., 2002), or the lens (Dimanlig et al., 2001; Kammandel et al., 1999). The relative amounts of the *Pax6+5a* and

Pax6-5a splice forms vary markedly between these two tissues (Jaworski et al., 1997), a variation that would have been missed in this analysis.

For this reason, it is difficult to relate the *Pax6-5a* : *Pax6+5a* ratio observed in the eye to any specific role in development. What this data does show, however, is that there is a clear regulation of the ratio through murine eye development, and the general trend is similar to that observed in the majority of CNS tissues.

2.5.3.4: The cerebellum

Unlike all the other tissues analysed in this study, the *Pax6-5a* : *Pax6+5a* ratio does not appear to differ in the cerebellum between E14.5 and E18.5. One explanation for the difference in *Pax6* alternative splicing in the cerebellum when compared to other tissues is that Pax6 may be playing a different role here. As in the olfactory bulb, Pax6 is thought to be important for controlling cellular migration in the cerebellum (Engelkamp et al., 1999).

Unlike many of the other tissues analysed in this study, the cerebellum is known to continue developing beyond E18.5, and high levels of neurogenesis are known to occur postnatally (Altman and Bayer, 1978a; Altman and Bayer, 1978b). *Pax6* continues to be expressed at high levels in the adult mouse cerebellum (Stoykova and Gruss, 1994; Yamasaki et al., 2001), whilst expression in other brain tissues has fallen significantly. The maintenance of a relatively high *Pax6-5a* : *Pax6+5a* ratio in the cerebellum at E18.5 when compared to other brain tissues is consistent with the hypothesis that a high ratio is required for proliferation, whilst a lower ratio is required for subsequent neuronal differentiation.

2.5.3.5: Overall conclusions

Chauhan et al. (2004a) demonstrated that different *Pax6-5a* : *Pax6+5a* ratios had different transactivational activities on consensus Pax6 target sequences, within a cell culture system. Transactivation at both the P6CON and 5aCON sequences was highest with a ratio of 8:1 or 1:1, but lower at intermediate ratios. Two conclusions could be drawn from this information. It may be that transactivation of all Pax6 target genes is highest at ratios of 1:1 and 8:1. This would imply that Pax6 is most potent as a transcription factor in the diencephalon, for example, at E12.5 and E16.5, but less

so at E14.5 and E18.5. Alternatively, the change in ratio might lead to a switch in target genes, with the highest levels of transactivation at ratios of 2:1 and 4:1 occurring at sequences that were not analysed in that particular study. The latter scenario is consistent with the idea of the alternative splicing of exon 5a acting as a "molecular toggle", changing the set of Pax6 target genes (Epstein et al., 1994b).

The results described above suggest that an alteration in the *Pax6-5a* : *Pax6+5a* ratio in the majority of CNS tissues may be involved in a switch in *Pax6* activity, from promoting cellular proliferation to promoting differentiation.

A good model system to study the actions of Pax6-5a and Pax6+5a in these two processes is the fruit fly, *Drosophila melanogaster*. Rather than regulating PD-DNA interactions by alternative splicing, *Drosophila* have two *Pax6* homologues, *eyeless (ey)* and *eye gone (eyg)* (Jang et al., 2003). *ey* is homologous to *Pax6-5a*, whilst *eyg* is homologous to *Pax6+5a*, as it has a truncated PD containing only the C-terminal DNA-binding domain, thought to be the main DNA-binding domain in *Pax6+5a* (Xu et al., 1999). Expression of *ey* appears to promote proliferation in the developing eye, whilst a switch to expression of *eyg* promotes differentiation (Domínguez et al., 2004; Rodrigues and Moses, 2004).

Although the actions of *Pax6-5a* and *Pax6+5a* are likely to be more complex than those of *ey* and *eyg*, and the two isoforms are expressed together rather than independently, it is still a possibility that an alteration in the ratio between the two isoforms leads to a similar developmental switch; from proliferation to differentiation. It may be that the drop in ratio allows *Pax6* to act upon a different set of target genes, rather than just changing the level of transactivation of a constant set of targets, as suggested by Chauhan et al. (2004).

In the majority of the tissues analysed here, the *Pax6-5a* : *Pax6+5a* ratio has fallen by E18.5, shortly before birth, but transcript is still detected in all tissues at this age. The ratio is around 2:1 in all tissues except the cerebellum, which is still actively proliferating at E18.5 (Altman and Bayer, 1978a; Altman and Bayer, 1978b). That this ratio is similar implies that Pax6 may be playing a similar, maintenance role in each tissue.

2.5.4: Future work

An alternative technique for assessing mRNA levels in a tissue is quantitative RT-PCR (Q-PCR). Although this would allow direct comparison of mRNA levels between samples, it is less reliable for comparing the ratio of splice variants within a sample. PCR kinetics can vary between cDNAs, and one splice variant may be preferentially amplified over another. For this reason, Q-PCR could be used to compare the absolute levels of a transcript between tissues, but not the ratio of transcripts within a tissue.

A combination of RPA and Q-PCR could potentially address both factors in tandem; for example if RPA were used on a number of reference samples to determine the *Pax6-5a* : *Pax6+5a* ratio, followed by Q-PCR with primers specific to each isoform. The ratios observed by RPA could then be applied to all Q-PCR data, based on the assumption that two cDNAs may be amplified with different efficiencies, but this efficiency does not vary between repeats. This would be easier to achieve than RPA analysis of a large number of tissues, and could facilitate a much more extensive analysis, but is likely to be prone to error as it would involve significant extrapolation of data.

Another useful experiment would be to obtain RNA samples corresponding to different *Pax6* expressing components of the eye. Most notably, it would be interesting to compare the *Pax6-5a* : *Pax6+5a* ratio in the neural retina, a neurectoderm-derived structure, and the lens, a facial epithelial-derived structure.

It would also be interesting to extend this analysis to adult tissues. Pax6 expression is seen in adult corneal stem cells, and studies of *Sey/Sey* ↔ WT chimaeras have shown that it is necessary for the constant repair and replacement of damaged corneal cells (Collinson et al., 2003). Neural stem cells in the adult spinal cord also express Pax6 (Yamamoto et al., 2001), and it is possible that continued low-level expression of Pax6 in a number of CNS tissues after birth is essential for the maintenance of a stem cell population.

Ultimately, although the description of the relative levels of *Pax6-5a* and *Pax6+5a* is fundamental to our understanding of the role of these splice variants in embryonic development, it is also important to understand the regulation of Pax6 protein levels, and the functions of these proteins. These two issues will be addressed successively in Chapters 3 and 4.

Chapter 3: Analysing the Pax6 protein expression pattern in mice with various Pax6 alleles

3.1: Summary

Pax6 protein, as visualised by western blot, appears to exist as up to eight different isoforms. The presence or absence of these isoforms was characterised in *Pax6* mutant (*Sey*) mice, Pax6 over-expressing (PAX77) mice and WT mice at E12.5. Whole brain and whole eye extracts were analysed, and the relative amount of each isoform was compared across genotypes.

E12.5 was chosen for analysis of Pax6 protein expression for a number of reasons. Firstly, it is near to the peak period of neurogenesis (usually regarded as E13.5), a process in which Pax6 is involved. Secondly, levels of *Pax6* mRNA expression peak at E10.5, as measured by northern blot (Walther and Gruss, 1991). Although levels have fallen slightly by E12.5, this was considered an easier age to study, as tissue is more abundant, therefore more protein could be extracted. Also, as RPA data was collected for WT samples at E12.5 (see Chapter 2), comparisons could be made between RNA and protein data.

Two Pax6 isoforms were observed in brain extracts from E12.5 *Sey/Sey* mice, which contain a mutation in the *Pax6* locus, and were thought to be effectively Pax6-null. In order to determine the exact nature of these isoforms, their expression was compared to that seen in other Pax6 knockout mice, $Pax6^{LacZ\,LacZ}$ and Sey^{Neu}/Sey^{Neu}. A 32kDa Pax6 isoform was seen in each, whilst a 43kDa isoform was seen in *Sey/Sey*, but not $Pax6^{LacZ\,LacZ}$ or Sey^{Neu}/Sey^{Neu} brains.

3.2: Introduction

3.2.1: Pax6 protein isoforms

As described in Section 1.4, the alternative splicing of *Pax6* is well documented, and leads to the creation of a number of Pax6 protein isoforms.

The *Pax6* cDNA is described in **Figure 1.2**. The 422 amino acid protein resulting from translation of *Pax6-5a* has a molecular weight of 46kDa, whilst the 436 amino

acid Pax6+5a protein has a predicted molecular weight of 48kDa (Walther and Gruss, 1991). Both isoforms are visible by western blot, as a 46/48kDa doublet (Carriere et al., 1993).

A number of studies have looked at Pax6 protein isoform expression. Western blot analyses of Pax6 were first performed on quail neuroretina cells, using a series of polyclonal antibodies directed against the PD, PST-rich linker, HD and C-terminus of the Pax6 protein (Carriere et al., 1993; Turque et al., 1994). As well as the predicted 46/48kDa doublet, lower molecular weight bands were seen which appeared to be alternative Pax6 protein isoforms.

A single band was described at 42kDa, and is thought to correspond to Pax6Δ6, in which exon 6 of the transcript has been spliced out (Carriere et al., 1993; Jaworski et al., 1997). A band of approximately 42kDa is also seen in the adult mouse brain using a different anti-Pax6 C-terminus primary antibody (Davis and Reed, 1996). This band could also be due to the use of a cryptic splice site within intron 7, leading to a protein missing 36 amino acids of the PD, an event which has been documented in humans with mutations in the *PAX6* locus (www.hgu.mrc.ac.uk/Softdata/PAX6/).

Two further bands have been reported at 32/33kDa, and shown to be the result of internal translation initiation from an unspecified in-frame ATG residue within the *Pax6* transcript (Carriere et al., 1993). "Paired-less" *Pax6* transcripts have since been described in the mouse (Gorlov and Saunders, 2002; Kleinjan et al., 2004; Mishra et al., 2002) in which translation could only begin from an internal ATG, implying that the shorter Pax6 isoforms may be regulated at the transcript level as well as at the level of translation.

There is also a possibility that any Pax6 protein bands visible by western blot might be protein cleavage or degradation probucts.

3.2.2: Previous analyses of the Pax6 protein content of *Sey/Sey*, *Sey/+*, WT, PAX77$^{+/-}$ and PAX77$^{+/+}$ mice

Pax6 protein expression has been mainly studied in the WT mouse by immunohistochemistry (e.g. Dellovade et al., 1998; Ericson et al., 1997; Vitalis et al., 2000). Although this technique is useful in describing complex expression patterns

within a tissue, as well as local gradients of protein expression, it provides little information as to the protein isoforms that are being expressed.

In order to visualise the differential expression of Pax6 protein isoforms, the protein content of a tissue must be analysed by western blot, with a primary antibody that can detect all known isoforms. This has been performed in depth on protein extracts from the quail neuroretina (Carriere et al., 1993; Turque et al., 1994), (see Section 3.2.1) and the developing chick eye (Duncan et al., 2000; Koroma et al., 1997). Although these studies are fundamental to our understanding of the various Pax6 isoforms, this understanding remains largely confined to the quail neuroretina and chick eye model systems. The role of Pax6 has been most widely studied in murine development, therefore it is important to gain greater knowledge of the distribution of Pax6 isoforms in the developing mouse.

An antibody directed against the C-terminus of Pax6, and therefore likely to recognise all Pax6 isoforms, has been used for western blotting on a number of adult mouse tissues (Davis and Reed, 1996). A 46/48kDa doublet was seen in protein extracts from whole brain, whole eye, olfactory bulb and olfactory turbinates, indicating that both Pax6-5a and Pax6+5a were present in each of these tissues. Interestingly, the presence of lower molecular weight Pax6 proteins varied between tissues, in particular between brain and eye. A band of approximately 43kDa was seen exclusively in the brain, whilst a lower band of approximately 33kDa was seen exclusively in the eye, indicating that there may indeed be tissue-specific differences in Pax6 isoform expression (Davis and Reed, 1996).

A second study, using a different C-terminal Pax6 antibody, showed no obvious differences in Pax6 isoform content between adult mouse brain and adult mouse lens (Richardson et al., 1995). The disparity between results from the eye in these two studies is probably due to the use of whole eye extract in one (Davis and Reed, 1996), and lens extract in the other (Richardson et al., 1995), indicating that there may also be differences in Pax6 isoform expression between constituent tissues of the eye.

Using a set of antibodies directed against the N-terminus of Pax6, Engelkamp et al. (1999) demonstrated the presence of 46kDa and 48kDa Pax6 isoforms in the P1 mouse cerebellum. No other isoforms were seen in this case, as these antibodies would not pick up Pax6 proteins lacking the PD.

Whilst the current knowledge of differential Pax6 isoform expression in the WT mouse is limited, even fewer studies have been made of the Pax6 protein content of *Sey/Sey*, *Sey/+*, PAX77$^{+/-}$ or PAX77$^{+/+}$ mice. As the autoregulation of Pax6 has been demonstrated in a number of systems, (Okladnova et al., 1998; Plaza et al., 1993; Plaza et al., 1995; see Section 1.6.3), it seems pertinent to ask whether *Sey/+* mice do indeed express Pax6 at 50% of WT levels, and whether PAX77 hemizygote and homozygote mice express 4-fold and 7-fold more Pax6 than WT, as might be expected from genomic *Pax6* copy number. Knowledge of the Pax6 protein content of these mice is crucial to the correct interpretation of their phenotype.

3.2.3: Potential Pax6 protein synthesis in the *Sey/Sey* mouse

A Pax6 protein has been seen in the *Sey/Sey* mouse brain by immunohistochemistry with an antibody directed against the PD, which is thought to be an N-terminal fragment translated as far as the mutant STOP residue, and is detectable at low levels (Engelkamp et al., 1999). The functional capabilities of this protein have not been assessed, nor has its relative abundance.

There is also a possibility that an N-terminally truncated Pax6 protein could be made *via* internal translation initiation in the *Sey/Sey* and *Pax6*$^{LacZ\,LacZ}$ mouse. **Figure 1.3** describes the mutations found in the *Pax6* locus of the *Sey*, *Pax6*^{LacZ}, and *Sey*^{Neu} mice. There are four in-frame ATG residues within the central portion of the *Pax6* gene, from which translation could theoretically initiate. Where the mutation lies 5' of one or all of these internal ATG residues (**Figure 1.3 B** and **D,** *Sey* and *Pax6*^{LacZ}), an N-terminally truncated Pax6 could be made.

3.2.4: Aims

The aim of Chapter 3 was to study the levels of each Pax6 protein isoform in the E12.5 mouse brain and eye, by western blot.

The expression level of each isoform was compared between WT mice and *Sey/+*, *Sey/Sey*, PAX77$^{+/-}$ and PAX77$^{+/+}$ mice. This was done firstly to ascertain whether Pax6 protein levels were representative of *Pax6* copy number, and secondly to see if all Pax6 isoforms were regulated in the same manner across all five mouse strains.

Protein was taken from the brain and the eye at E12.5. The brain and the eye were chosen as they are both known to express high levels of Pax6, and the protein is thought to have a different role in the development of each. Protein was taken at E12.5 as this is during the peak period of neurogenesis (Gillies and Price, 1993; Levers et al., 2001), and also thought to be the age at which Pax6 expression is highest (Walther and Gruss, 1991). Thus, Pax6 is likely to be active in neurogenesis at this age.

The Pax6 protein content of E12.5 Sey^{Neu}/Sey^{Neu} and $Pax6^{LacZ\,LacZ}$ mouse brain was also determined by western blot. Any Pax6 protein isoforms seen in these mice were explained with reference to current knowledge of the mutation in each genotype, and of the molecular structure of the *Pax6* locus.

3.3: Methods

See **Appendix 1** for detailed protocols and lists of reagents.

3.3.1: Mouse strains used in this study

For all matings, the day on which a plug was found was designated embryonic day 0.5 (E0.5). Mice were harvested at E12.5.

CD1 mice were used as the wild type strain in this analysis. The *Sey* and PAX77 mutations were both maintained on the CD1 background, to allow an accurate comparison of Pax6 protein content between genotypes whilst minimising the risk of variation between strains contributing to the observed effects.

Sey/+, *Sey/Sey*, $PAX77^{+/-}$, $PAX77^{+/+}$, Sey^{Neu}/Sey^{Neu} and $Pax6^{LacZ\,LacZ}$ mice were also used (see Section 1.2 for a full description of *Pax6* mutant mouse strains). All embryos were phenotyped by visual inspection, *Sey*/+ embryos were genotyped by J.C. Quinn. $Pax6^{LacZ}$ embryos were provided by D.A. Kleinjan (MRC Human Genetics Unit, Edinburgh).

For a diagrammatical representation of the *Pax6* mutations in *Sey*, Sey^{Neu} and $Pax6^{LacZ}$, see **Figure 1.3**.

3.3.2: Extracting protein from murine embryonic tissues

All dissections were performed in ice-cold, sterile PBS. All tissues were collected within 90 minutes, and snap-frozen in liquid nitrogen as dry samples in cryovials. These were then stored at -70°C for up to 6 weeks before protein was harvested.

Whole brains were collected from all genotypes at E12.5. For each protein sample, two brains of the same genotype were combined.

Eyes were collected from all genotypes at E12.5. All eyes of the same genotype from a litter were pooled to obtain a high enough protein yield for immunoblotting.

Tissues were defrosted on ice, triturated in 50-200µl TENT buffer with protease inhibitors, and homogenised. Cells were allowed to lyse for 20 minutes at 4°C, then cellular debris was pelleted out by centrifugation at 13,000rpm for 15 minutes at 4°C. The supernatant, containing cellular proteins, was then decanted and stored at -70°C.

3.3.3: Quantitating protein samples

1µl and 2.5µl of each protein sample were quantitated alongside BSA standards.

BSA standards were made by dissolving 10µg.ml^{-1} to 1000µg.ml^{-1} BSA in PBS, and stored at 4°C for up to 6 weeks.

Quantitations were performed in 96-well plates using the colorimetric BCA assay, where OD at 565nm is proportional to protein concentration.

3.3.4: Protein denaturing polyacrylamide gel electrophoresis (SDS-PAGE)

All protein samples were resolved on 12% pre-cast tris-glycine gels. These were advantageous as they had high resolving power between bands of very similar molecular weight, and gave highly consistent results across repeats.

50µg of brain total protein or 10µg of eye total protein was loaded per well, made up to 20µl with 4X sample loading buffer and TENT buffer, and heated to 95°C for 5

minutes before loading, to denature all proteins. Gels were run for 1 hour 40 minutes at 150V, and each included 0.4µl of MagicMark (***Invitrogen***), a molecular weight ladder of bacterially-expressed proteins conjugated to protein G, and therefore detected by all secondary antibodies.

3.3.5: Protein transfer and western blotting

After resolution by SDS-PAGE, proteins were transferred onto either a PVDF (if using anti-Pax6 C-terminus primary antibody, see below), or a nitrocellulose (if using anti-Pax6 HD primary antibody, see below) membrane. Transfers were run at 50mA, 4°C overnight or 225mA, at room temperature for 2½ hours. Transfer efficiency was determined by staining the membrane in Ponceau's solution followed by two successive de-stains in ddH_2O.

Membranes were blocked in TBS-tween with 10% dried milk for 1 hour at room temperature. Primary antibodies were allowed to bind overnight at 4°C in sealed plastic bags.

Figure 3.1 shows the anti-Pax6 primary antibodies used for western blotting. Serum 13 anti-Pax6 HD (Carriere et al., 1993) was a kind gift from S.Saule (Institut Curie, Paris, France), and is a polyclonal antibody raised in rabbit and directed against the homeodomain of quail Pax6, PAX-QNR. The anti-Pax6 C-terminus antibody (***Chemicon***) is also a polyclonal antibody raised in rabbit, which is directed against the C-terminal TAD of mouse Pax6.

Following incubation in primary antibody, membranes were washed 3 times in TBS-tween to remove unbound antibody. Secondary antibodies were centrifuged and diluted in 10ml blocking buffer, and allowed to bind for one hour at room temperature on a shaking platform. All secondary antibodies were conjugated to horseradish peroxidase to allow chemiluminescent detection of bound primary antibody.

Membranes were washed 3 times in TBS-tween, to remove unbound secondary antibody. Bound antibody was then detected using the ECL+ chemiluminescent detection kit. Membranes were bathed for 5 minutes in ECL+ substrate, which was

Figure 3.1: Anti-Pax6 primary antibodies. The Pax6 cDNA is shown to scale. Red and Blue bars: Pax6 exons. Orange bar: Paired domain. Green bar: homeodomain. Black and white bars: internal ATG residues from which protein translation could initiate. Black lines: Pax6 polypeptide fragments against which the primary antibody was raised. N.B. Antibodies have not been epitope mapped.

broken down by horseradish peroxidase, causing the emission of light. Signal was then detected by exposure to photographic film for 1–45 minutes.

Where relative quantitation of Pax6 protein levels was required, membranes were washed 3 times in TBS-tween after chemiluminescent detection and re-probed for β-actin as described above. Densitometric analysis of gel films was performed as described in Section 2.3.4.

3.3.6: Cloning of *Pax6+5a* and *Pax6-5a*

Total RNA was obtained from the U373-MG human glioblastoma cell line using an RNeasy mini kit (***Qiagen***). cDNA synthesis was performed on total RNA using oligo d(T) primers, to amplify all poly(A)$^+$ mRNA species.

PCR was then performed using the "Human Pax6 Full 5' XbaI" and "Human Pax6 Full 3' XbaI" primers (see Appendix 2 for primer sequences and optimal annealing temperatures) to amplify full-length Pax6 with *Xba*I recognition sites both 5' and 3' of the gene. This PCR was performed using Expand DNA polymerase, combining high-fidelity amplification by the proofreading *Pfu* DNA polymerase with the speed of *Taq* DNA polymerase. PCR products of approximately 1.3kb, corresponding to full-length *Pax6+5a* and *Pax6-5a* combined, were purified by agarose gel extraction.

Expand DNA polymerase (***Roche***) yields PCR products that have a mixture of blunt ends from *Pfu* DNA polymerase amplification, and A-overhanging ends from *Taq* DNA polymerase amplification. Cloning can be aimed at either of these DNA sequence types. In this case, blunt-ended fragments were cloned using the Zero Blunt TOPO cloning system (***Invitrogen***). The reaction product was transformed into chemically-competent TOP-10 *E.coli* and grown on LB agar plates with kanamycin selection (50μg.ml^{-1}), allowing only transformed bacteria to grow.

After 24 hours at 37°C, 14 bacterial clones were isolated. These were frozen as glycerol stocks at -70°C, and colony PCR was performed to confirm the presence of *Pax6* sequence, and ascertain whether *Pax6+5a* or *Pax6-5a* was present.

Of the 14 clones isolated, 5 appeared to correspond to *Pax6+5a*, 7 to *Pax6-5a* (**Figure 3.2**). One appeared negative for *Pax6*, which was most likely due to failure

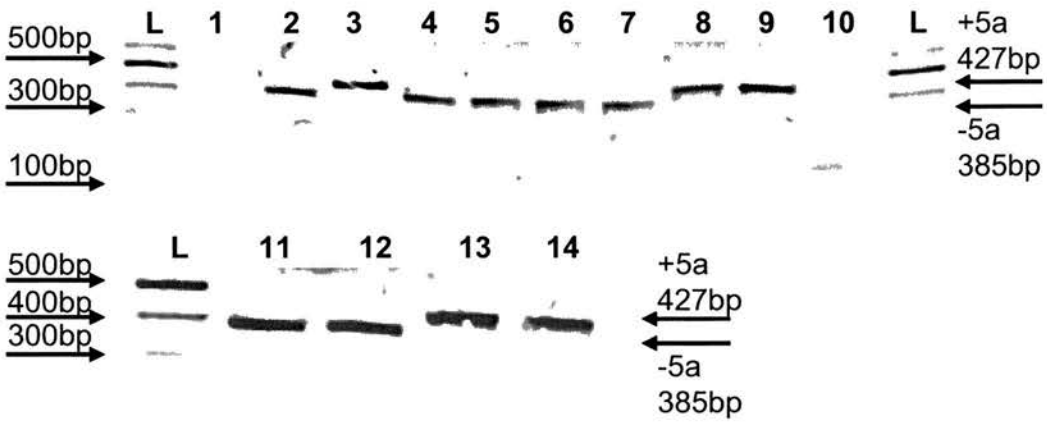

Figure 3.2: Colony PCR on plasmids pJP1.1 – pJP1.14 using the "Pax6 Exon 5F", and "Pax6 Exon 7R" primers. A 427bp PCR product indicates *Pax6+5a*. A 385bp PCR product indicates *Pax6-5a*. The ~170bp fragment from pJP1.10 could correspond to *Pax6-5aΔ6,* with a predicted size of 169bp.

of the PCR reaction. One gave a band of approximately 170bp, which appeared to correspond to the *Pax6-5aΔ6* splice variant, giving a predicted size of 169bp.

Clones pJP1.3 (*Pax6+5a*) and pJP1.11 (*Pax6-5a*) were sequenced across the *Pax6* insert in both orientations. Both had sequence corresponding exactly to EMBL entry BX640762, except for a single synonymous substitution. pJP1.3 contained an A→ C substitution at cDNA residue 1251, predicted to change a GTT (valine) codon to GTC (valine). pJP1.11 contained a A → C substitution at cDNA residue 1257, predicted to change a CCA (proline) codon to CCC (proline). Neither of these synonymous substitutions affect the protein sequence. Clones pJP1.3 and pJP1.11 were used as *Pax6+5a* and *Pax6-5a* clones for all further work.

See **Figure 3.3** for a plasmid map of pJP1.3 and pJP1.11

3.3.7: Inserting *Pax6+5a* and *Pax6-5a* into pSP64 for *in vitro* protein synthesis

Full length *Pax6-5a* and *Pax6+5a* were cloned into pSP64 (***Promega***) for *in vitro* protein synthesis. *Pax6* clones pJP1.3 and pJP1.11 were used, as they had been sequence-verified. The pSP64 vector was chosen as it has an SP6 transcription site immediately 5' of the multiple cloning site, with no intervening ATG start codons, from which ectopic protein translation could initiate. There is also a Poly(A) stretch immediately 3' of the multiple cloning site, to encourage efficient mRNA processing by the rabbit reticulate lysate in the TNT system.

Full length *Pax6* was removed from pJP1.3 and pJP1.11 by digestion with *Xba*I, and inserted into linearised pSP64 using T4 DNA ligase. Ligation products were used to transform chemically-competent TOP-10 *E.coli*, and colonies were grown overnight at 37°C with ampicillin (100μg.ml^{-1}) to allow only the growth of transformed bacteria.

Clones pJP8.6 (*Pax6-5a*) and pJP9.3 (*Pax6+5a*) were found to have *Pax6* inserted in the correct orientation for *in vitro* protein synthesis. The full length *Pax6* insert in both pJP8.6 and pJP9.3 was then sequenced in both directions to confirm that the intended *Pax6* sequence was present, and that no mutations had been introduced during the cloning process. As expected, the same synonymous substitutions were

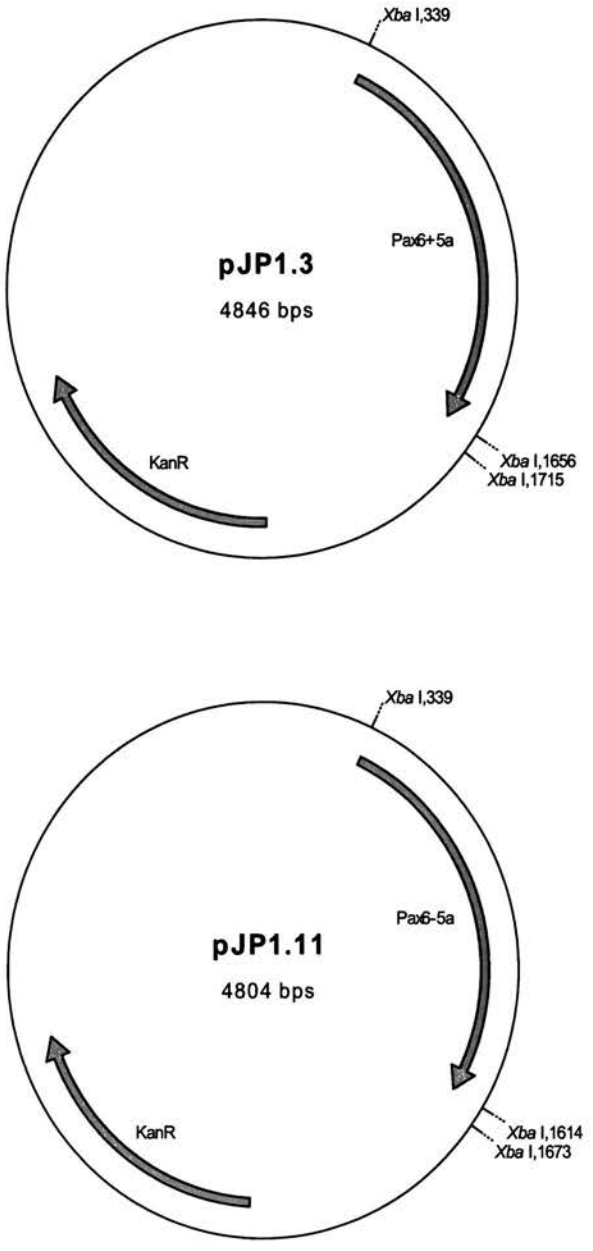

Figure 3.3: pJP1.3 / pJP1.11, full-length Pax6+5a / Pax6-5a in pCR-BluntII-TOPO. Red arrows: Human Pax6 sequence, and the Kanamycin resistance gene.

found as in the donor plasmids pJP1.3 and pJP1.11. The plasmids pJP8.6 and pJP9.3 were used for all further *in vitro* protein synthesis applications.

See **Figure 3.4** for plasmid maps of pJP8.6 and pJP9.3

3.3.8: *in vitro* protein synthesis

Pax6+5a and *Pax6-5a* were synthesised *in vitro* from the plasmid templates pJP9.3 and pJP8.6, to act as positive controls for western blotting analysis. Proteins were synthesised using the TNT Quick Coupled Transcription / Translation System (***Promega***). The TNT system then allowed simultaneous transcription from the SP6 site and translation of *Pax6*.

3.4: Results: Pax6 protein isoforms in the brain of various *Pax6* mutant mice at E12.5

3.4.1: Western blot analysis of Pax6 protein isoforms in the E12.5 mouse brain

Up to six E12.5 whole brain samples (each containing 2 brains) were obtained from *Sey/Sey, Sey/+*, WT, PAX77$^{+/-}$ and PAX77$^{+/+}$ mice. Samples were analysed a number of times by western blot to detect the presence of Pax6, and allow its quantitation.

Each sample was analysed by western blot between 2 and 6 times, and data from all repeats of all samples was pooled and analysed together.

Two whole brains were obtained from E12.5 Sey^{Neu}/Sey^{Neu} and $Pax6^{LacZ/LacZ}$ mice, and each was analysed by western blot twice, alongside *Sey/Sey, Sey/+* and WT brain samples.

Figure 3.5 shows the result of a typical western blot on E12.5 whole brain protein extract using both anti-Pax6 HD (**Fig 3.5 A**) and anti-Pax6 C-terminus (**Fig 3.5 B**) primary antibodies. All indicated bands were up-regulated in PAX77 mice compared to WT, therefore it is very likely that they are Pax6-specific rather than a result of non-specific antibody binding. The results from western blots using both antibodies were combined, as each appeared to recognise the same set of Pax6 isoforms.

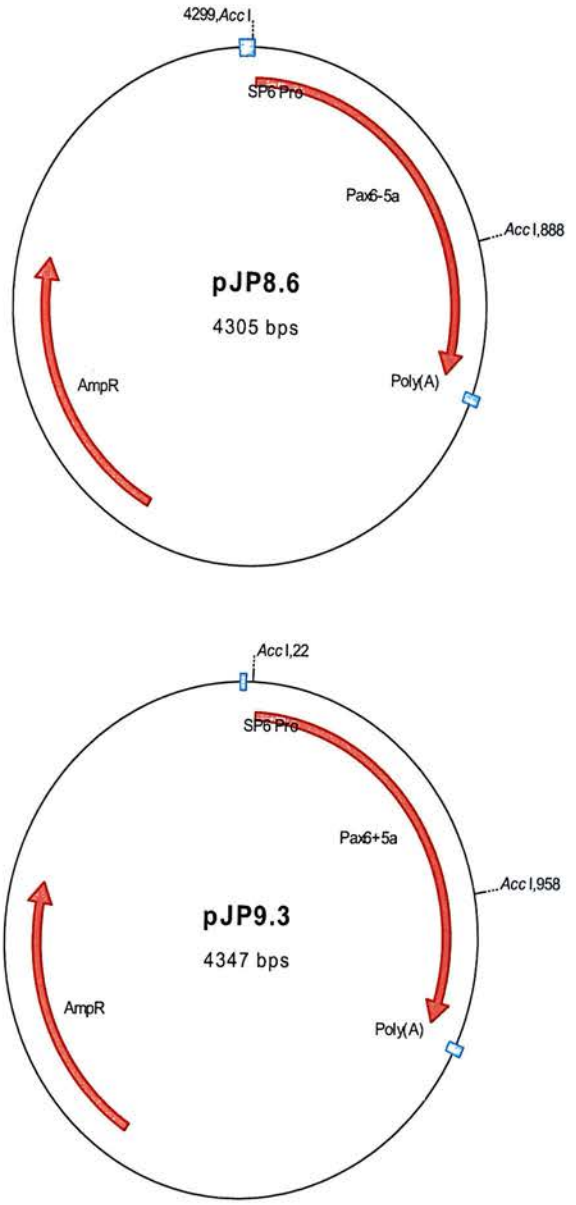

Figure 3.4: pJP8.6 / pJP9.3, full-length Pax6-5a / Pax6+5a in pSP64. Red arrows: Human Pax6 sequence for *in vitro* protein synthesis, and the Ampicillin resistance gene. Blue bars: SP6 promoter and Poly(A) sequences that allow efficient transcription and post-transcriptional modification of the insert.

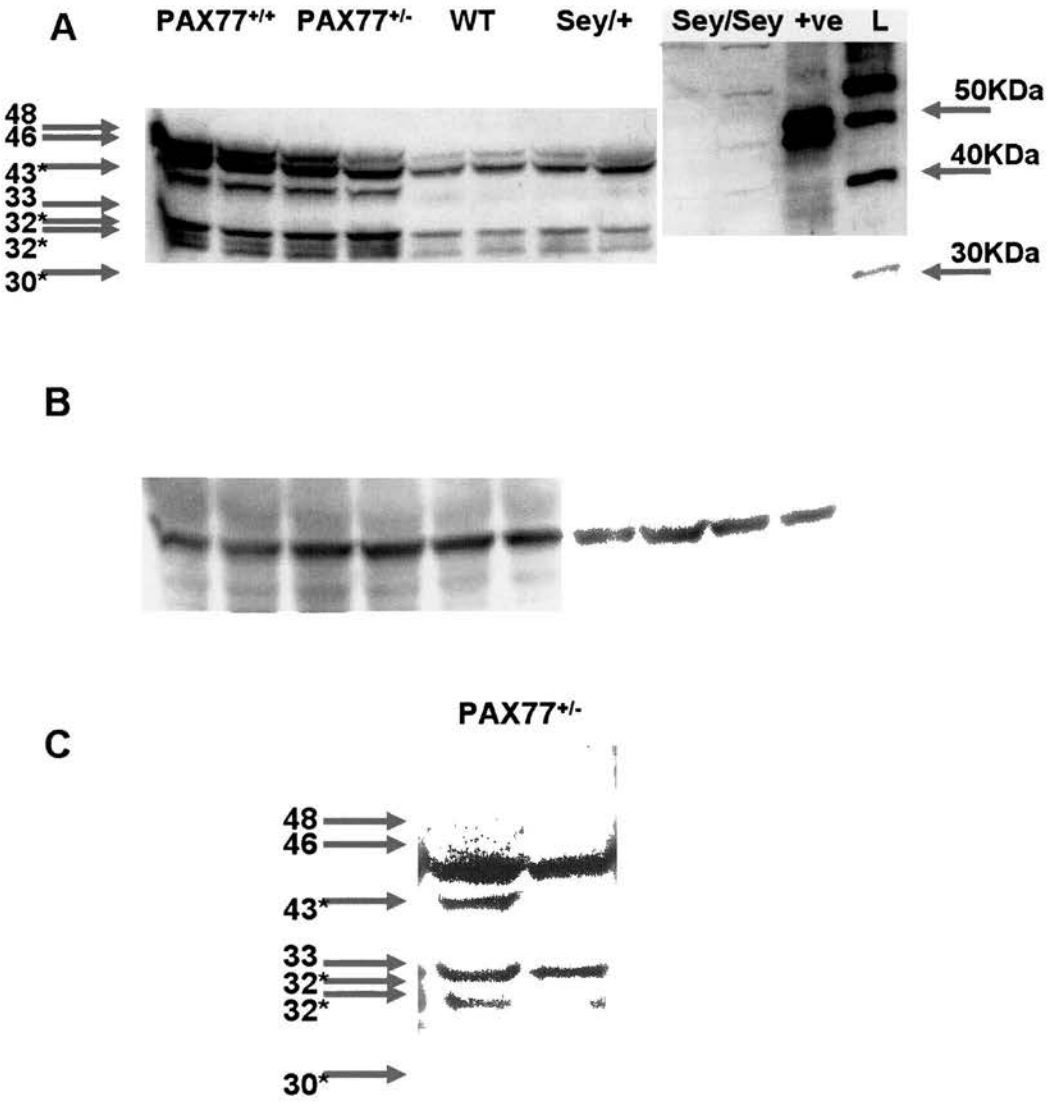

Figure 3.5: Typical results from western blot of E12.5 whole brain protein extract across a number of genotypes. A) Using serum 13 anti-HD primary antibody. B) Membrane seen in A, re-probed for β-actin. C) Using anti-Pax6 C-terminal primary antibody. Arrows indicate the bands observed, and their estimated mass in Kilodaltons (KDa). Bands with asterisks (*) were either not resolved on all gels, or not observed on all gels due to low sensitivity of the western. +ve, *in vitro*-synthesised positive controls. L, molecular weight ladder.

The highest molecular weight bands, a 46/48kDa doublet, correspond to Pax6-5a and Pax6+5a, respectively (**Fig 3.6 B, C**) (Carriere et al., 1993; Walther and Gruss, 1991).

The observed differences in molecular weight between this doublet and that of the *in vitro*-synthesised positive control doublet, which is slightly retarded on all gels, is probably due to the absence of post-translational modification in the TNT rabbit reticulate lysate system. Pax6 is known to be phosphorylated in the zebrafish, at residues within the C-terminal transactivation domain which are highly conserved between species as diverse as sea urchin and man (Mikkola et al., 1999). Phosphorylation of the quail Pax6 homologue, Pax-QNR, has also been demonstrated (Carriere et al., 1993). In addition to this, there is evidence for *O*-glycosylation in Pax-QNR in the quail neuroretina (Lefebvre et al., 2002), possibly at sites within the paired domain. Any of these post-translational modifications could account for differences in size between endogenous and *in vitro*-synthesised Pax6 proteins.

A second doublet is seen at approximately 42/43kDa. In some cases this appears as a single band, but this is probably due to a lack of resolution on the gel rather than absence of one of the bands. A 43kDa Pax6 band was first described by Carriere et al. (1993), using the serum 13 anti-Pax6 HD antibody. It was also seen with antibodies against the Gln/Gly-rich linker sequence between the PD and the HD (serum 12), and against the C-terminus of the protein (serum 14). This band was not observed, however, with an antibody directed against the PD. Using an antibody directed against the C-terminus of Pax6, Davis and Reed (1996) described a 43kDa band in adult mouse eye. As antibodies directed against the Pax6 HD and C-terminus can detect the 42/43kDa Pax6 doublet, but those directed against the PD cannot, it is thought to correspond to forms of Pax6 lacking the paired domain.

The most obvious mechanism leading to a "paired-less" form of Pax6 is alternative splicing of exon 6. As described in Chapter 2, the removal of the majority of exon 6 has been documented in both quail and cow (Carriere et al., 1993; Jaworski et al., 1997). RT-PCR for *Pax6* on mRNA extracted from the human glioblastoma cell line U373-MG has identified mRNA species lacking the entire of exon 6 in both *Pax6-5a* and *Pax6+5a* forms (T.I. Simpson, pers. comm.). Both mechanisms of excluding this exon would give a predicted protein of approximately 43kDa (**Fig 3.6 D, E**). The existence of a doublet could be explained by the presence or absence of exon 5a, or could be due to post-translational modification.

Figure 3.6 Possible explanations for the numerous Pax6 bands seen by western blot. Red and blue bars represent Pax6 exons. Orange bar: paired domain, Green bar: homeodomain, Black bars: internal ATG codons 2, 3, 4 and 5 (*Sey*STOP ATG). Canonical translation from ATG1 begins at the 3' end of exon 4. A, Full-length Pax6 cDNA. Magenta arrow, location of *Sey* STOP codon. B-K, translated exons found in each isoform. Predicted molecular weight was calculated using the Protein Molecular Weight algorithm at the Sequence Manipulation Suite (www.ualberta.ca/~stothard/javascript/)

The third set of bands picked up by both anti-Pax6 antibodies appears to be a triplet, migrating at approximately 32-33kDa, with a fourth, weaker band at 30kDa. Like the 43kDa bands, these were first described by Carrière et al. (1993), where they were detected by sera 12 (anti-linker region), 13 (anti-HD) and 14 (anti-C-terminus). In this case, a doublet was described, but again this could be due to lack of resolution rather than absence of bands. These bands are thought to be the result of internal translation initiation. To confirm this, Carriere et al. (1993) created a 5'-truncated Pax6 cDNA missing the first ATG start codon, and used it as a template for *in vitro* protein synthesis. The product migrated as a 32/33kDa doublet. There are four in-frame ATGs within the Pax6 gene from which translation initiation could occur, all of which lie in the Gln/Gly-rich linker sequence between the PD and the HD (**Fig 3.6 H-K**). Two studies have described *Pax6* mRNA species lacking the 5' portion of the gene, in which translation could only initiate from an internal ATG residue (Kleinjan et al., 2004; Mishra et al., 2002).

There are also nine more in-frame ATGs at the 3' end of the cDNA, but these would all lead to a protein less than 15kDa in molecular weight, the presence of which has not been demonstrated by western blotting using any of the available anti-Pax6 primary antibodies.

It is worth noting that where predicted protein molecular weights do not agree exactly with observed molecular weight after gel electrophoresis, this could be due to inaccuracies in the protein molecular weight algorithm, or most likely due to post-translational modification of the protein.

Other *Pax6* splice variants have been isolated by RT-PCR on total RNA from mouse brain and eye (Gorlov and Saunders, 2002), but their abundance has not been assessed *in vivo*, and it is still unclear whether these are due to low-frequency splicing errors, or whether they represent functional, regulated splice variants. For this reason, these newly-isolated splice variants were not considered to be likely explanations for Pax6 bands seen by western blotting.

3.4.2: Quantitation of bands observed by western blot

Although the relative levels of each Pax6 isoform within a sample are similar using either serum 13 or anti-Pax6 C-terminus primary antibodies (i.e. in all cases the upper 33kDa band of the triplet gives the strongest signal, compare **Figure 3.5 A** with **Fig 3.5 B**), this cannot be taken as an indicator of the relative abundance of each isoform

within a sample. Differential antibody-binding kinetics might lead to one protein isoform binding more efficiently to the antibody than a different isoform. For this reason, it may be inappropriate to compare relative abundances of the various Pax6 forms within a sample. However, it is worth noting that the shorter forms of Pax6 (i.e <46kDa) do appear to make a significant contribution to the Pax6 content of the brain, albeit on a qualitative level.

The only likely exception to this rule is the comparison between Pax6+5a and Pax6-5a. These two isoforms are known to be responsible for the 46/48kDa Pax6 doublet seen by western blot (Carriere et al., 1993; Walther and Gruss, 1991). Both antibodies used in this analysis were raised against peptide fragments within the C-terminal portion of the protein (see **Figure 3.1**), whilst the insertion of exon 5a should only affect protein structure at the N-terminus of the protein, in the paired domain. For this reason, it is likely that the two full-length isoforms have the same antibody-binding kinetics, and their relative abundance can be compared within a sample. As the exact protein sequence responsible for the other Pax6 bands has not been determined, and the explanation for each is an estimation based on known mRNA splice variants and sequence analysis, the same assumption cannot be made for other bands observed by western blot.

The amount of each isoform detected by western blot was quantitated, and compared between samples. Each different molecular weight band was considered as a separate entity, and compared across all genotypes. The relative intensity of each band was determined, and divided by the intensity of the β-actin band (**Figure 3.5 C**) obtained for that sample, to account for inaccurate protein quantitation and problems with gel loading.

The intensity of the WT bands (usually two WT samples were included per gel) was then averaged, and assigned an arbitrary value of 1. The intensity of the corresponding band in each sample was divided by that of the WT samples, to give the relative concentration of a Pax6 isoform within each protein sample, as compared to WT. For example, the amount of Pax6+5a in the $PAX77^{+/+}$ mouse could be compared to the amount of Pax6+5a in the WT (given a value of 1), or the amount of Pax6+5a in the *Sey*/+ mouse, but could not be compared to the amount of 33kDa Pax6 in the same $PAX77^{+/+}$ sample.

Analysis of Variance (ANOVA) was performed on the values for each protein isoform, using the InStat software package, to determine whether there was

statistically significant variance within the data set. If the ANOVA yielded a P-value <0.05, this was deemed significant, and *t*-tests were carried out. Protein levels were compared between all genotypes and WT, between *Sey/Sey* and *Sey/+* and between PAX77$^{+/-}$ and PAX77$^{+/+}$. *t*-tests were carried out in Microsoft Excel.

3.4.3: Pax6 protein levels in the brain of E12.5 *Sey/Sey, Sey/+*, WT, PAX77$^{+/-}$ and PAX77$^{-/-}$ mice

The most immediately striking observation is that PAX77$^{+/+}$ and PAX77$^{+/-}$ brains contain higher levels of all Pax6 isoforms than WT and *Sey/+*, and that most isoforms are absent from the *Sey/Sey* brain (**Figure 3.5, Figure 3.7**).

For more detailed analysis of the relative expression of Pax6 across genotypes, each band will be considered in turn.

3.4.3.1: 48kDa band, Pax6+5a

A 48kDa band corresponding to full-length Pax6+5a was observed in all PAX77$^{+/+}$, PAX77$^{+/-}$, WT and *Sey/+* brain extracts, but not *Sey/Sey* extracts (**Figure 3.8 A**). Relative levels of Pax6+5a were averaged from 16 repeats, and error was calculated as Standard Error of the Mean (SEM).

There are error bars on WT values, even though all other samples have been normalised to WT=1. This is because each individual western blot contained two WT samples, and the value for each was normalised to the average value of the two samples.

Significant differences in the level of Pax6+5a are seen between *Sey/Sey* and *Sey/+* brains (P<0.001), and between *Sey/Sey* and WT brains (P<0.001). This is to be expected, as there is no Pax6+5a present in the *Sey/Sey* mouse. Surprisingly, there is also more Pax6+5a in the *Sey/+* brain than in the WT (P<0.05).

Both PAX77$^{+/-}$ and PAX77$^{+/+}$ brains contain more Pax6+5a than WT, by three-to four-fold (P<0.001). There is no difference in the level of Pax6+5a between PAX77$^{+/-}$ and PAX77$^{+/+}$ brains.

Pax6 Isoform	*Sey/Sey* vs. *Sey/+*	*Sey/Sey* vs. WT	*Sey/+* vs. WT	WT vs. PAX77$^{+/-}$	WT vs. PAX77$^{+/+}$	PAX77$^{+/-}$ vs. PAX77$^{+/+}$
Pax6+5a	$1.62X10^{-5}$	$1.04X10^{-11}$	0.0148	$2.99X10^{-5}$	$8.53X10^{-4}$	0.309
Pax6-5a	$1.09X10^{-7}$	$3.205X10^{-15}$	0.443	0.0147	0.0241	0.297
43KDa	0.224	0.112	0.203	0.00157*	$7.47X10^{-4}$*	0.584*
42KDa	$5.721X10^{-6}$	$2.76X10^{-11}$	$7.48X10^{-5}$	0.150		
33KDa	$1.57X10^{-5}$	$6.94X10^{-18}$	0.0363	0.00141	$7.88X10^{-4}$	0.128
32.5KDa	0.0336	0.0022633	0.0982	0.0547*	0.0176*	0.3621*
32KDa	0.148	0.225	0.242	0.00224*	0.0149*	0.965*

P<0.05
P<0.01
P<0.001

Figure 3.7 Results of *t*-tests and Mann-Whitney U-tests where appropriate on combined data from E12.5 brain extracts (3 s.f.). Significant results are highlighted. A statistical comparison was not possible with PAX77$^{+/+}$ data for the 42KDa band, as it was only observed once. Starred (*) results indicate Mann-Whitney U-tests.

A

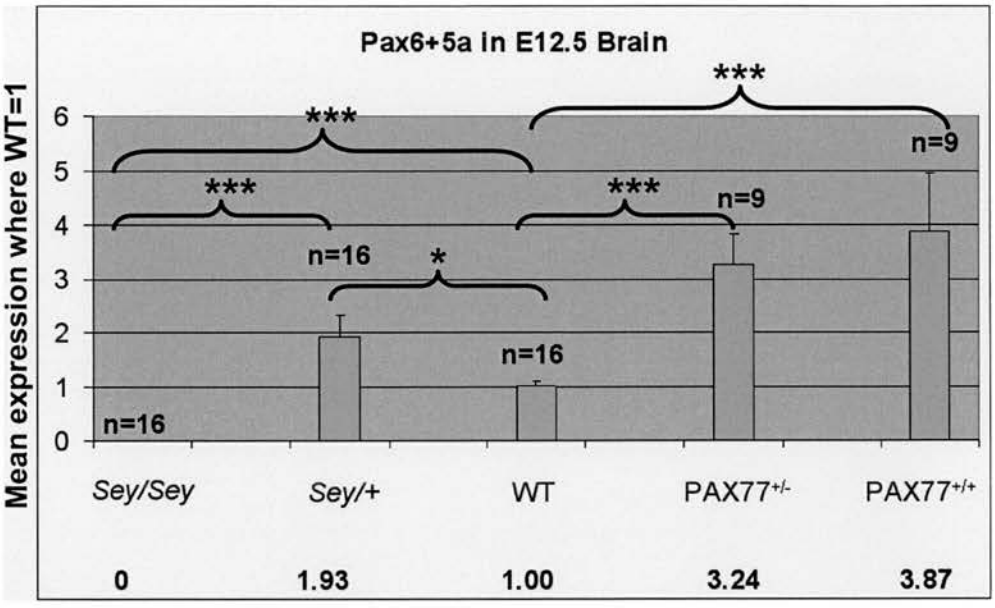

ANOVA P<0.0001, considered extremely significant

B

t-test	P-value
Sey/Sey vs. *Sey/+*	<0.001
Sey/Sey vs. WT	<0.001
Sey/+ vs. WT	<0.05
WT vs. PAX77$^{+/-}$	<0.001
WT vs. PAX77$^{+/+}$	<0.001
PAX77$^{+/-}$ vs. PAX77$^{+/+}$	>0.05

Figure 3.8: Full-length Pax6+5a in E12.5 mouse brain. A, Mean values. All values are normalised to WT=1. The number of samples analysed is shown above each bar. Error bars represent SEM. Values are given in numerical form below each bar. B, Results of paired *t*-test between genotypes. Significant results are highlighted. *=P<0.05; **=P<0.01; ***=P<0.001

In general, results for Pax6+5a in E12.5 brain show it is absent in *Sey/Sey* mice. *Sey*/+ mice express it at higher levels than WT. Both PAX77$^{+/-}$ and PAX77$^{+/+}$ mice express significantly more than WT, but there is no clear difference in the levels of Pax6+5a between PAX77$^{+/-}$ and PAX77$^{+/+}$ brain.

3.4.3.2: 46kDa band, Pax6-5a

A 46kDa band corresponding to full-length Pax6-5a was observed in all PAX77$^{+/+}$, PAX77$^{+/-}$, WT and *Sey*/+ brain extracts, but not *Sey/Sey* extracts.

Results for Pax6-5a are similar to those observed for Pax6+5a (compare **Figures 3.8 3.9**). In both cases, Significant differences are seen between *Sey/Sey* and *Sey*/+ ($P<0.001$), and *Sey/Sey* and WT samples ($P<0.001$), as would be expected, given that *Sey/Sey* mice cannot produce this protein. Unlike Pax6+5a, there is no significant difference in Pax6-5a levels between *Sey*/+ and WT brains.

PAX77$^{+/-}$ and PAX77$^{+/+}$ mice both express more Pax6-5a in the brain than WT ($P<0.05$), and again there is no difference between PAX77 hemizygotes and homozygotes.

Differences between the level of Pax6+5a and Pax6-5a in the PAX77 mice compared to WT can be interpreted as a difference in the ratio between the two isoforms, which will be discussed in more detail in section 3.4.5.

3.4.3.3: 43kDa band, Pax6+5aΔ6

A 43kDa Pax6 band, thought to correspond to Pax6+5aΔ6, was observed in E12.5 brain extract from all genotypes, including *Sey/Sey* (**Figure 3.10**).

Results for the 43kDa band are very different to those seen for full-length Pax6. *Sey/Sey*, *Sey*/+ and WT all express similar levels of this isoform. PAX77$^{+/-}$ and PAX77$^{+/+}$, on the other hand, express 144- and 56-fold more than WT. Due to this high level of over-expression, there were likely to be inaccuracies in the data collected from both PAX77 genotypes for this isoform. Where a WT band was visible on a film, the PAX77 band was often saturated. An accurate densitometric value for the PAX77 band could be obtained using a lower exposure, but the WT band was no

A

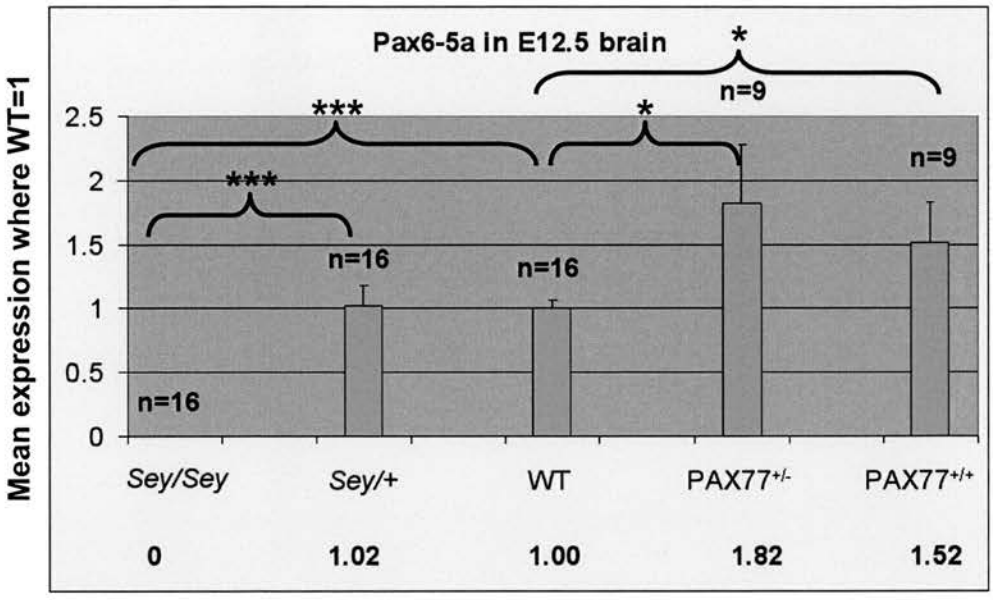

ANOVA P<0.0001, considered extremely significant

B

t-test	P-value
Sey/Sey vs. *Sey/+*	<0.001
Sey/Sey vs. WT	<0.001
Sey/+ vs. WT	>0.05
WT vs. PAX77$^{+/-}$	<0.05
WT vs. PAX77$^{+/+}$	<0.05
PAX77$^{+/-}$ vs. PAX77$^{+/+}$	>0.05

Figure 3.9: Full-length Pax6-5a in E12.5 mouse brain. A, Mean values. All values are normalised to WT=1. The number of samples analysed is shown above each bar. Error bars represent SEM. Values are given in numerical form below each bar. B, Results of paired *t*-test between genotypes. Significant results are highlighted. *=P<0.05; **=P<0.01; ***=P<0.001

A

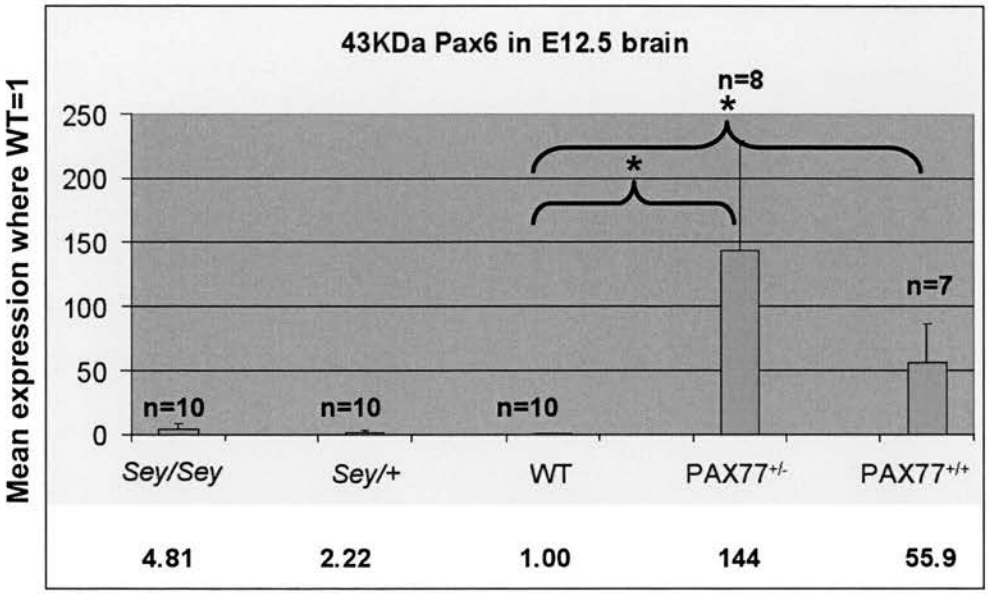

ANOVA P=0.0028, considered very significant

B

t-test	P-value
Sey/Sey vs. *Sey/+*	>0.05
Sey/Sey vs. WT	>0.05
Sey/+ vs. WT	>0.05
WT vs. PAX77$^{+/-}$	<0.05
WT vs. PAX77$^{+/+}$	<0.05
PAX77$^{+/-}$ vs. PAX77$^{+/+}$	>0.05

Mann-Whitney U-test
P-value
<0.01
<0.001
>0.05

Figure 3.10: 43KDa Pax6 in E12.5 mouse brain. A, Mean values. All values are normalised to WT=1. The number of samples analysed is shown above each bar. Error bars represent SEM. Values are given in numerical form below each bar. B, Results of paired *t*-test and Mann-Whitney U-test where appropriate between genotypes. Significant results are highlighted. *=P<0.05; **=P<0.01; ***=P<0.001

longer visible, therefore the value could no longer be normalised to WT, and accurate comparisons could no longer be drawn. Due to this saturation of bands, the PAX77 data for 43kDa Pax6 is unlikely to be normally distributed, therefore the *t*-test is no longer valid. Instead, Mann-Whitney U-tests were performed using the SPSS software package, to compare $PAX77^{+/-}$ and $PAX77^{+/+}$ with WT and with each other. The Mann-Whitney U-test shows that both $PAX77^{+/-}$ and $PAX77^{+/+}$ brains have higher levels of 43kDa than WT ($P<0.01$, $P<0.001$), but there is no difference between the two genotypes.

As the *Sey* mutation would render *Sey/Sey* mice incapable of producing Pax6+5aΔ6 protein, an alternate explanation for the presence of this band in the brains of *Sey/*Sey mice must be sought. It seems likely that the 43kDa band seen in the other samples is a form of Pax6, as it is highly up-regulated in the Pax6-overexpressing PAX77 mice. One explanation is that a non-specific band is being recognised by both antibodies, which co-migrates with the 43kDa Pax6 band. This seems unlikely, however, as the two primary antibodies were raised against different peptides.

RPA data from Chapter 2 (**Figure 2.12**) show that the alternative splicing of exon 6 is undetectable in a number or *Pax6* expressing tissues at E12.5. If this isoform is indeed less common than had been previously suggested, a different explanation for the 43kDa Pax6 protein band seems likely.

Pax6 resulting from internal translation initiation 3' of the *Sey* STOP codon would yield a protein with a predicted molecular weight of 24kDa, and even after extensive post-translational modifications, an 18kDa discrepancy between predicted and observed molecular weight seems unlikely. 3'-truncated Pax6 resulting from translation initiation at the canonical ATG in exon 4 and running until the STOP codon in exon 8 would give a protein with a predicted molecular weight of 22kDa. Again, the discrepancy between predicted and observed molecular weight rules this out as an explanation.

It is possible that exon 8 could be spliced out of the *Pax6* transcript, thus bypassing the *Sey* mutation entirely. This would leave the protein in-frame, and would give a predicted molecular mass of 41/42kDa (-/+5a). This is one possible explanation for the presence of a 43kDa band in *Sey/Sey* brain, although this splicing event has not been documented *in vivo*.

3.4.3.4: 42kDa band, Pax6-5aΔ6

A 42kDa Pax6 band, thought to correspond to Pax6-5aΔ6 (Carriere et al., 1993), was observed in E12.5 brain extract from all genotypes, except *Sey/Sey* (**Figure 3.11**).

As the 43kDa band runs very close to the 42kDa band on a polyacrylamide gel, it was often difficult to resolve the two. Where a single band was seen, this was classed as a 43kDa band, as the higher band was much more abundant in all samples, and tended to obscure the 42kDa band. For this reason, only one value was recorded in $PAX77^{+/+}$ brain. Although this shows that the 42kDa isoform is indeed present, ANOVAs and *t*-tests cannot be performed on data including $PAX77^{+/+}$, as a sample number >1 is needed for these statistical tests. All analyses were therefore performed on *Sey/Sey, Sey/+*, WT and $PAX77^{+/-}$ samples alone

The ANOVA, excluding $PAX77^{+/+}$, gives a P value <0.001, considered extremely significant, so there is variation within the data set and *t*-tests are valid.

As the *Sey/Sey* brain does not contain 42kDa Pax6, *t*-tests are significant between *Sey/Sey* and *Sey/+*, and between *Sey/Sey* and WT (both, $P<0.001$). Although the values do not appear very different in **Figure 3.11**, and the number of repeats is lower than seen for other bands, the comparison between *Sey/+* and WT is statistically significant ($P<0.001$). 42kDa Pax6 is only expressed at 61% of WT level in *Sey/+* brain at E12.5. Levels of 42kDa Pax6 in $PAX77^{+/-}$ and $PAX77^{+/+}$ mice seem comparable to those observed in WT.

3.4.3.5: 33kDa band, 5'-Truncated Pax6

A 33kDa Pax6 band, thought to correspond to 5'-truncated Pax6 after internal translation initiation, was observed in E12.5 brain extract from all genotypes, except *Sey/Sey* (**Figure 3.12**).

The *Sey/Sey* brain contains no 33kDa Pax6. There are reduced levels of 33kDa Pax6 in the *Sey/+* brain when compared to WT ($P<0.05$).

Both PAX77 genotypes contain more 33kDa Pax6 than WT ($P<0.01$, $P<0.001$), but there is no difference in levels between $PAX77^{+/-}$ and $PAX77^{+/+}$.

A

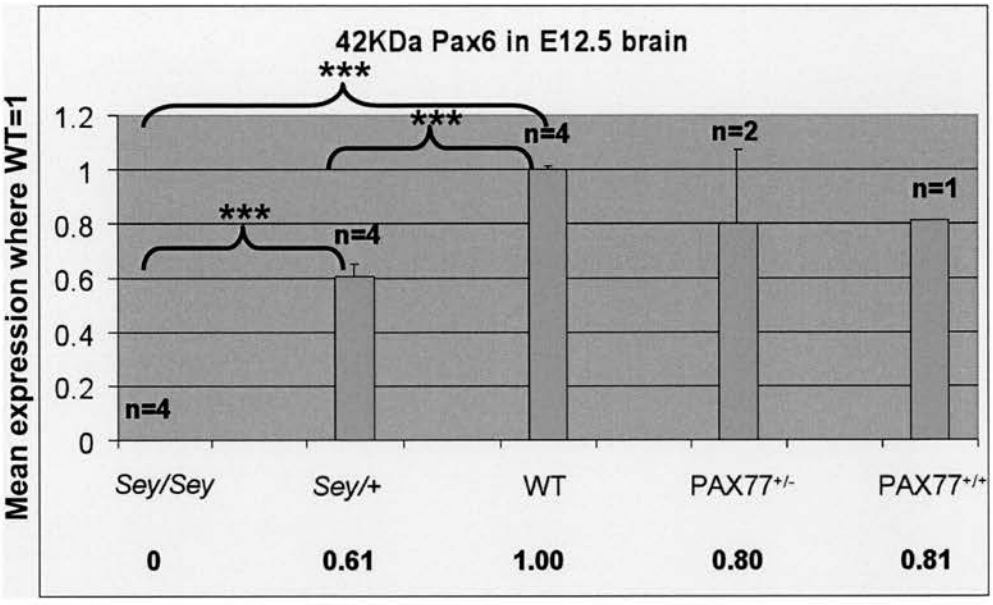

ANOVA (Not including Pax77$^{+/+}$) P<0.001, considered extremely significant.

B

t-test	P-value
Sey/Sey vs. *Sey/+*	<0.001
Sey/Sey vs. WT	<0.001
Sey/+ vs. WT	<0.001
WT vs. PAX77$^{+/-}$	>0.05
WT vs. PAX77$^{+/+}$	n/a
PAX77$^{+/-}$ vs. PAX77$^{+/+}$	n/a

Figure 3.11: 42KDa Pax6 in E12.5 mouse brain. A, Mean values. All values are normalised to WT=1. The number of samples analysed is shown above each bar. Error bars represent SEM. Values are given in numerical form below each bar. B, Results of paired *t*-test between genotypes. Significant results are highlighted. ANOVA and t-tests excluded PAX77$^{+/+}$ samples, as a 42KDa band was only seen once. *=P<0.05; **=P<0.01; ***=P<0.001

A

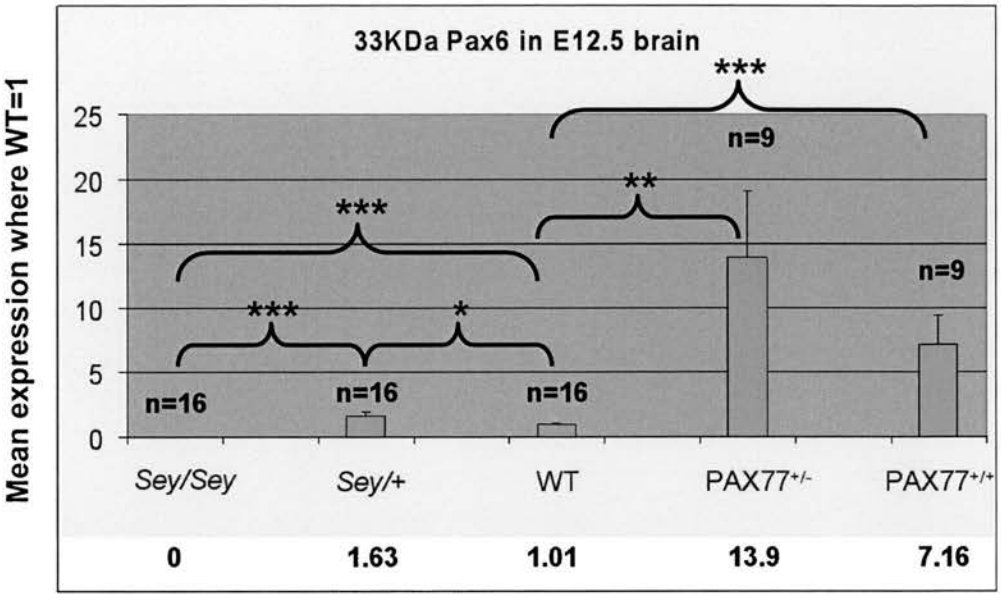

ANOVA P<0.0001, considered extremely significant

B

t-test	P-value
Sey/Sey vs. *Sey/+*	<0.001
Sey/Sey vs. WT	<0.001
Sey/+ vs. WT	<0.05
WT vs. PAX77$^{+/-}$	<0.01
WT vs. PAX77$^{+/+}$	<0.001
PAX77$^{+/-}$ vs. PAX77$^{+/+}$	>0.05

Figure 3.12: 33KDa Pax6 in E12.5 mouse brain. A, Mean values. All values are normalised to WT=1. The number of samples analysed is shown above each bar. Error bars represent SEM. Values are given in numerical form below each bar. B, Results of paired *t*-test between genotypes. Significant results are highlighted. *=P<0.05; **=P<0.01; ***=P<0.001

In general, this result differs from those seen for Pax6+5a, Pax6-5a and 43kDa Pax6, in that levels appear lower in both *Sey/Sey* and *Sey/+* than in WT. As observed with all other isoforms, levels are similar between $PAX77^{+/-}$ and $PAX77^{+/+}$. Levels of 33kDa Pax6 are raised in both PAX77 genotypes when compared to WT, as observed with most isoforms.

3.4.3.6: 32.5kDa band, 5'-Truncated Pax6

A 32.5kDa Pax6 band, thought to correspond to 5'-truncated Pax6 after internal translation initiation, was observed in E12.5 brain extract from all genotypes, except *Sey/Sey* (**Figure 3.13**).

There is no 32.5kDa Pax6 in the *Sey/Sey* brain. There is no difference in levels od 32.5KDa Pax6 between *Sey/+* and WT brains.

Although *t*-tests are significant between both PAX77 genotypes and WT, the high level of 33kDa Pax6 in these samples suggests that, as is the case for the 43kDa Pax6 isoform, these bands are in fact saturated. For this reason, the data are unlikely to be normally distributed, therefore the Mann-Whitney U-test was used to compare $PAX77^{+/-}$ and $PAX77^{+/+}$ data with WT and with each other. Only $PAX77^{+/+}$ brains contain more 33kDa Pax6 than WT ($P<0.05$), and no differences are seen between PAX77 hemizygotes and homozygotes.

In general, this result conforms to those seen for Pax6-5a and 43kDa Pax6, in that levels appear lower in both *Sey/Sey* and *Sey/+* than in WT, but there are no differences between *Sey/+* and WT. As observed with all other isoforms, levels are similar between $PAX77^{+/-}$ and $PAX77^{+/+}$, and levels are raised in $PAX77^{+/+}$ when compared to WT. In this case, however, there was no up-regulation in the $PAX77^{+/-}$ brain.

3.4.3.7: 32kDa band, 5'-Truncated Pax6

A 32kDa Pax6 band, thought to correspond to 5'-truncated Pax6 after internal translation initiation, was observed in E12.5 brain extract from all genotypes, including *Sey/Sey* (**Figure 3.14**).

A

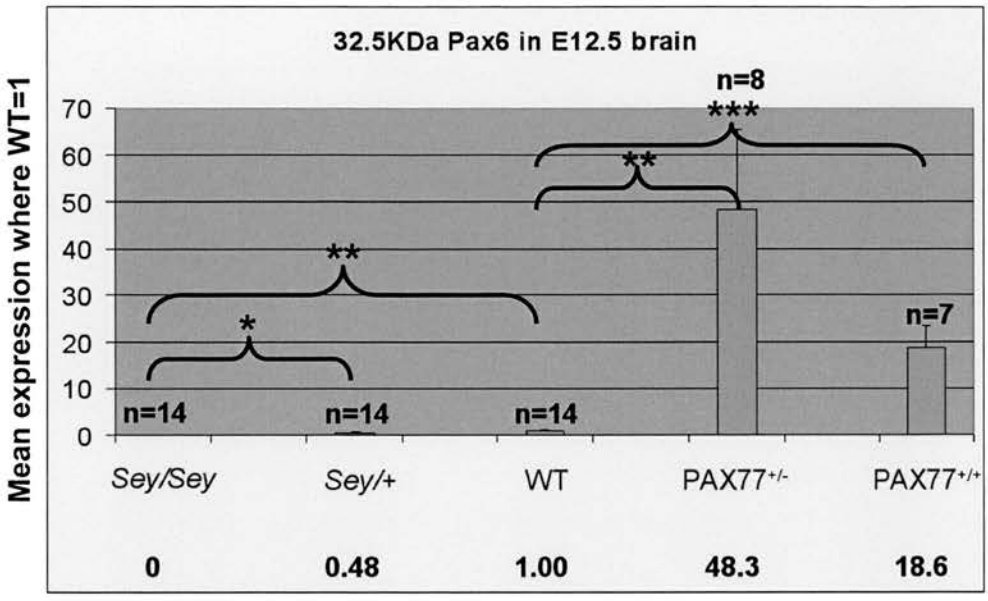

ANOVA P=0.0019, considered very significant

B

t-test	P-value
Sey/Sey vs. *Sey/+*	<0.05
Sey/Sey vs. WT	<0.01
Sey/+ vs. WT	>0.05
WT vs. PAX77$^{+/-}$	<0.01
WT vs. PAX77$^{+/+}$	<0.001
PAX77$^{+/-}$ vs. PAX77$^{+/+}$	>0.05

Mann-Whitney U-test
P-value
>0.05
<0.05
>0.05

Figure 3.13: 32.5KDa Pax6. in E12.5 mouse brain. A, Mean values. All values are normalised to WT=1. The number of samples analysed is shown above each bar. Error bars represent SEM. Values are given in numerical form below each bar. B, Results of paired *t*-test and Mann-Whitney U-test where appropriate between genotypes. Significant results are highlighted. *=P<0.05; **=P<0.01; ***=P<0.001

A

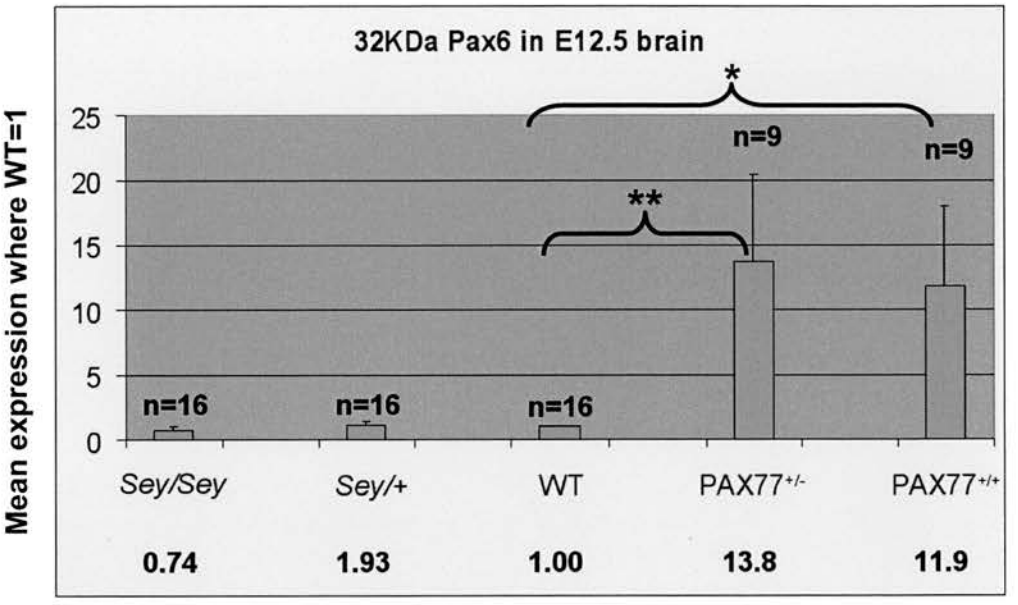

ANOVA P=0.0033, considered very significant

B

t-test	P-value
Sey/Sey vs. *Sey/+*	>0.05
Sey/Sey vs. WT	>0.05
Sey/+ vs. WT	>0.05
WT vs. PAX77$^{+/-}$	<0.01
WT vs. PAX77$^{+/+}$	<0.05
PAX77$^{+/-}$ vs. PAX77$^{+/+}$	>0.05

Mann-Whitney U-test
P-value
<0.01
<0.05
>0.05

Figure 3.14: 32KDa Pax6 in E12.5 mouse brain. A, Mean values. All values are normalised to WT=1. The number of samples analysed is shown above each bar. Error bars represent SEM. Values are given in numerical form below each bar. B, Results of paired *t*-test and Mann-Whitney U-test where appropriate between genotypes. Significant results are highlighted. *=P<0.05; **=P<0.01; ***=P<0.001

Sey/Sey, Sey/+ and WT brains all express similar levels of 32kDa Pax6. As with the 33kDa and the 32.5kDa bands, levels appear to rise dramatically in both $PAX77^{+/-}$ and $PAX77^{+/+}$ samples. Again, Man-Whitney U-tests were used to analyse these data, due to the problems with densitometric analysis described in Section 3.4.3.3. Both $PAX77^{+/-}$ and $PAX77^{+/+}$ brains contain more 32kDa Pax6 than WT ($P<0.01$, $P<0.05$), but there is no difference between the two genotypes.

In general, this result conforms to that seen for the 43kDa band. Both isoforms are present in the *Sey/Sey* brain, and are found at similar levels in *Sey/Sey*, *Sey/+* and WT. Both PAX77 homozygotes and hemizygotes express more 32kDa Pax6 than WT, but there is no difference between the two.

3.4.3.8: 30kDa Pax6, unexplained

A 30kDa band was observed in some western blots. It is likely to be a Pax6-specific band, as it was observed most frequently in just $PAX77^{+/-}$ and $PAX77^{+/+}$ samples (n=2), and once in WT, $PAX77^{+/-}$ and $PAX77^{+/+}$ samples (**Figure 3.15**). This is indicative of an up-regulation in PAX77 mice. Unfortunately, a comparison between PAX77 and WT levels is only possible using one data set, so statistical analyses could not be performed in the same manner as for the other Pax6 isoforms.

Figure 3.15 A appears to show a higher level in $PAX77^{+/+}$ than in $PAX77^{+/-}$, but that is contradicted by **Figure 3.15 C**. **Fig 3.15 B**, which includes WT, seems to show that levels do not vary greatly between the three genotypes, although this would not explain why the band was observed more often in the PAX77 brain samples.

The difficulties in detecting this band were largely due to its low abundance, being at the limits of detection by western blot. This could also be why a trend was not seen between the three genotypes, as weaker bands can be harder to quantitate densitometrically.

The presence of a 30kDa Pax6 band is difficult to explain given the current knowledge of Pax6 isoforms. The only known variants that would give Pax6 bands of approximately this size are those resulting from internal translation initiation. However, the smallest of these four possible proteins would be initiated from the ATG 3' of the *Sey* STOP codon, and that is the best explanation for the lower 32kDa

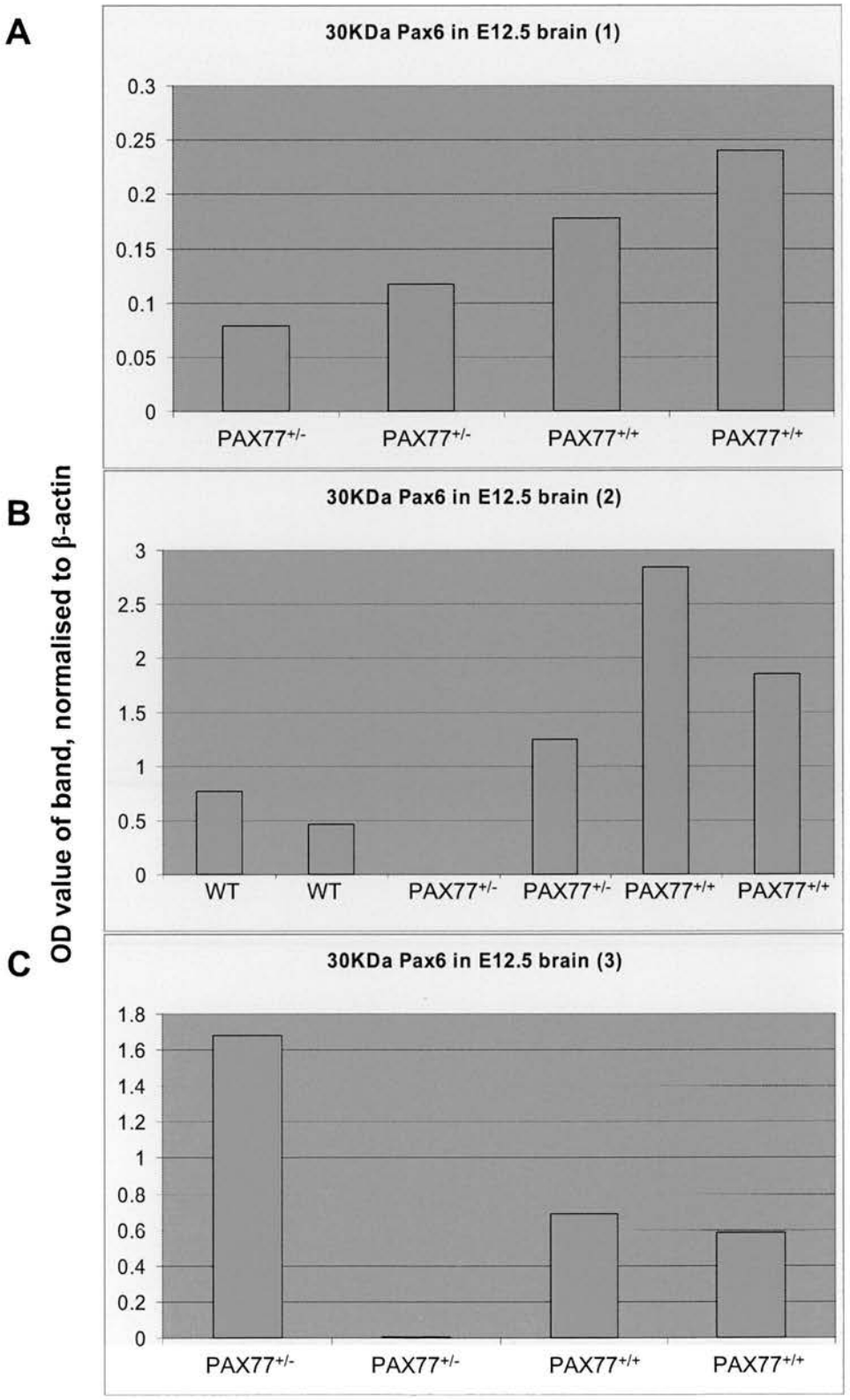

Figure 3.15: 30KDa Pax6 in E12.5 mouse brain. A, B, C, three separate western blots on which a 30KDa band was visible. All values are normalised to β-actin expression. Values are not directly comparable, as westerns 1 and 3 could not be normalised to WT.

band seen in all genotypes. A smaller, 30kDa band is not easily explained in this manner.

3.4.3.9: Overall patterns of Pax6 protein expression in E12.5 *Sey/Sey, Sey/+*. WT, PAX77$^{+/-}$ and PAX77$^{+/+}$ brain

The results described above follow a number of clear trends. Most obviously, the majority of Pax6 isoforms are not expressed in the *Sey/Sey* brain. Those which are expressed will be discussed in more detail in Section 3.7.

Protein levels of most Pax6 isoforms in the *Sey/+* brain are largely similar to those in the WT brain, although there are some notable exceptions. Intriguingly, Pax6+5a is up-regulated in the *Sey/+* brain. In contrast, the 42kDa and 33kDa bands are down-regulated.

The observation that all other Pax6 isoforms are expressed at the same levels in *Sey/+* and WT brains correlates well with the lack of an obvious phenotype in the *Sey/+* brain. Although some heterozygous effects have been described, they are far less pronounced than those seen in the homozygote brain. It is possible that the *Sey/+* brain has a regulatory mechanism in place by which it compensates for the lower *Pax6* copy number by increasing the amount of protein produced by the remaining, intact locus. In the *Sey/Sey* mouse, *Pax6* mRNA is easily detected by *in situ* hybridisation (Warren and Price, 1997), and *Pax6*$^{+/+}$ ↔ *Pax6*$^{-/-}$ chimeras show higher levels of *Pax6* expression in *Pax6*$^{-/-}$ cells than their WT counterparts (Collinson et al., 2003). Although this is not an accurate method of quantitating mRNA levels, this observation is consistent with an attempt to compensate for the absence of Pax6 protein by up-regulating *Pax6* mRNA transcription from the single remaining intact *Pax6* locus. Pax6 autoregulation is also suggested by the rise in levels of Pax6+5a in the *Sey/+* brain described here, and this is an indication that autoregulatory effects may be isoform-specific.

The existence of a brain phenotype, albeit a mild one, in the *Sey/+* brain can be reconciled with the data described above in two ways. Firstly, there may be regional variations in the regulation of Pax6. The protein samples used in this analysis were whole brain extracts, and any subtle variation in levels between brain regions would have been masked. It is therefore possible that the levels of all Pax6 isoforms differ

between *Sey/+* and WT in a tissue-specific manner not detected using the methods described here. Alternatively, the heterozygote brain phenotype may be entirely due to the differences in levels of Pax6+5a, 42kDa Pax6, and 33kDa Pax6, which do differ between *Sey/+* and WT.

Levels of all Pax6 isoforms are raised in the $PAX77^{+/+}$ mouse brain, and all but two are also up-regulated in the $PAX77^{+/-}$ brain. This is to be expected, as these mice carry 6 and 12 extra copies of the *Pax6* locus. What is unexpected is the similarity in Pax6 levels between the two genotypes. No statistically significant differences were observed between $PAX77^{+/-}$ and $PAX77^{+/+}$ brain extracts. This could again be due to autoregulation of Pax6 levels in the developing mouse brain, an argument which is supported by the fact that a number of isoforms are not expressed at 6- or 12-fold WT levels, as would be expected from the *Pax6* copy number. Just as the *Sey/+* brain appears to up-regulate the expression of most isoforms to near WT levels, similar mechanisms may down-regulate the expression of some Pax6 isoforms in the PAX77 brain. This is an indication that Pax6 dosage is important in the developing brain, and mechanisms exist to keep protein levels close to those found in the WT.

The degree of Pax6 up-regulation in PAX77 brains seems to vary between isoforms, with the most striking increases in protein level occurring for the shorter isoforms, rather than the better understood Pax6-5a and Pax6+5a isoforms. It is clear that the levels of Pax6 protein are being regulated in these mice, but the mechanism behind this regulation is not known.

Despite a clear upregulation of most Pax6 isoforms in PAX77 brain samples, the PAX77 brain does not exhibit an obvious phenotype (Schedl et al., 1996; M.Manuel, pers. comm.). The reason for this is unclear, but it is possible that the relative levels of expression of the different isoforms are an important factor. In particular, it may be the case that the ratio of Pax6-5a to Pax6+5a is as important as the absolute levels of these isoforms in controlling the activity of Pax6 (Chauhan et al., 2004a). This will be discussed in greater detail in Section 3.6.

3.5: Results: Pax6 protein isoforms in the eye of various *Pax6* mutant mice at E12.5

3.5.1: Pax6 protein levels in the eye of E12.5 *Sey/Sey, Sey/+*, WT, PAX77$^{+/-}$ and PAX77$^{+/+}$ mice

Up to four E12.5 eye samples (each containing up to 12 eyes) were obtained from *Sey/Sey, Sey/+*, WT, PAX77$^{+/-}$ and PAX77$^{+/+}$ mice. Each sample was analysed by western blot 3 times, and data from all repeats of all samples was pooled and analysed together.

Figure 3.16 shows the typical Pax6 content of E12.5 mouse eye across the five genotypes. Protein loading was less even than for brain extracts (**Figure 3.5**), as eye protein extracts were lower in concentration, therefore more prone to error in quantitation. Pax6 is more abundant in the eye, so a lower amount of total protein was used than for brain extracts (10μg as opposed to 50μg).

Both anti-Pax6 HD primary antibody (**Fig 3.16A**) and anti-Pax6 C-terminus primary antibody (**Fig 3.16B**) revealed an identical set of bands. This indicates that they are all Pax6-specific.

Both antibodies detect more 43/42kDa Pax6 and 33/32kDa Pax6 than full-length 48/46kDa Pax6. It is invalid to compare the intensity of bands within a lane, as the binding kinetics of the antibody may differ for different isoforms, and this result does not necessarily mean that the two full-length Pax6 forms are not the most abundant in the eye. However, a visual comparison can be made between **Fig 3.5**, with whole brain protein extracts and **Fig 3.16**, with eye extracts. The protein composition of the two tissues is different, and the shorter forms make a more significant contribution in the eye than in the brain.

Due to difficulties in collecting enough E12.5 eye protein from the five genotypes, the number of repeats in the eye was lower than in the brain. For this reason, error was higher, and fewer of the results are statistically significant. Only those seen for full-length Pax6+5a are significant by ANOVA. These will be described first, followed by a general discussion of the qualitative expression levels of other Pax6 forms in the eye.

3.5.2: 48kDa band, Pax6+5a in the eye

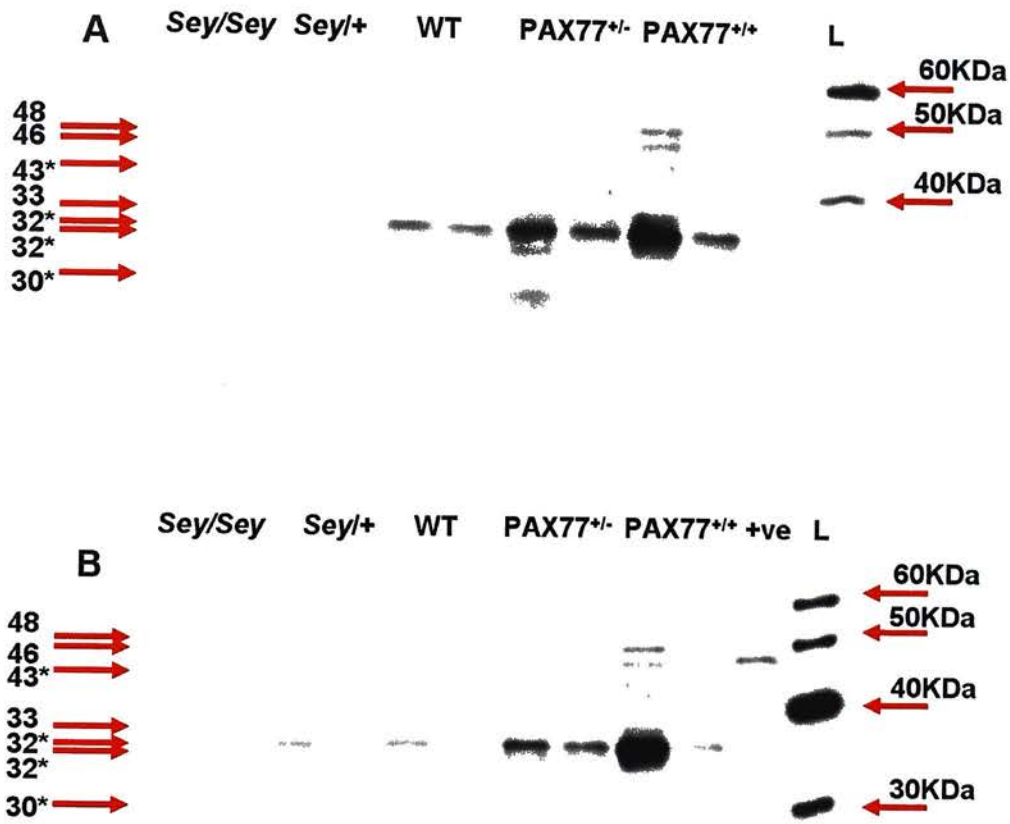

Figure 3.16: Typical results from western blot of E12.5 whole eye protein extract across a number of genotypes. A) Using serum 13 anti-HD primary antibody. B) Using anti-Pax6 C-terminus primary antibody. Arrows indicate the bands observed, and their estimated mass in Kilodaltons (KDa). Bands with asterisks (*) were either not resolved on all gels, or not observed on all gels due to low sensitivity of the western. +ve, *in vitro*-synthesised positive controls. L, molecular mass ladder.

A 48kDa band corresponding to full-length Pax6+5a was observed in all PAX77$^{+/+}$, PAX77$^{+/-}$, WT and *Sey*/+ eye extracts, but not *Sey/Sey* extracts (**Figure 3.17A**).

As with brain extracts, *t*-tests were carried out between all genotypes and WT, between *Sey/Sey* and *Sey*/+ and between PAX77$^{+/-}$ and PAX77$^{+/+}$ (**Figure 3.17 B**).

The only statistically significant result is the comparison between WT and PAX77$^{+/+}$ ($P<0.05$), in which levels are raised.

On a qualitative level, Pax6+5a protein expression appears to correspond more tightly to *Pax6* copy number in the eye than in the brain (compare **Figure 3.8** with **Figure 3.17**).

3.5.3: Other Pax6 isoforms in the eye

Although none of the results for other Pax6 bands in the E12.5 eye are statistically significant, all bands seem to follow similar trends, implying that the expression of each is regulated in a similar way across the five genotypes.

Unlike in the developing brain, the 42kDa band is only seen in one PAX77$^{+/+}$ sample. However, this could be due to the much higher abundance of the 43kDa band, obscuring the lower band in all cases.

Each graph (**Figures 3.18-3.20**) shows a similar pattern. In all cases, *Sey*/+ eyes express less Pax6 protein than WT. This is to be expected, given that there is only one functional copy of the gene, but is not seen in E12.5 whole brain. The autoregulatory mechanism which is hypothesised to up-regulate the amount of Pax6 protein in a heterozygous brain seems to be absent from the heterozygous eye. For most bands, the level observed in *Sey*/+ eye is approximately half that of the WT. The only isoforms obviously differing from this pattern are the 32.5kDa and 32kDa bands, expressed at 14% (32.5kDa) and 7% (32kDa) of WT levels.

PAX77$^{+/-}$ and PAX77$^{+/+}$ eyes both contain more Pax6 than WT. Unlike in the brain, Pax6 levels in the eye seem to vary between PAX77$^{+/-}$ and PAX77$^{+/+}$ mice. All but one isoform, the 30kDa band, are in greater abundance in the PAX77$^{+/+}$ eye. Again,

A

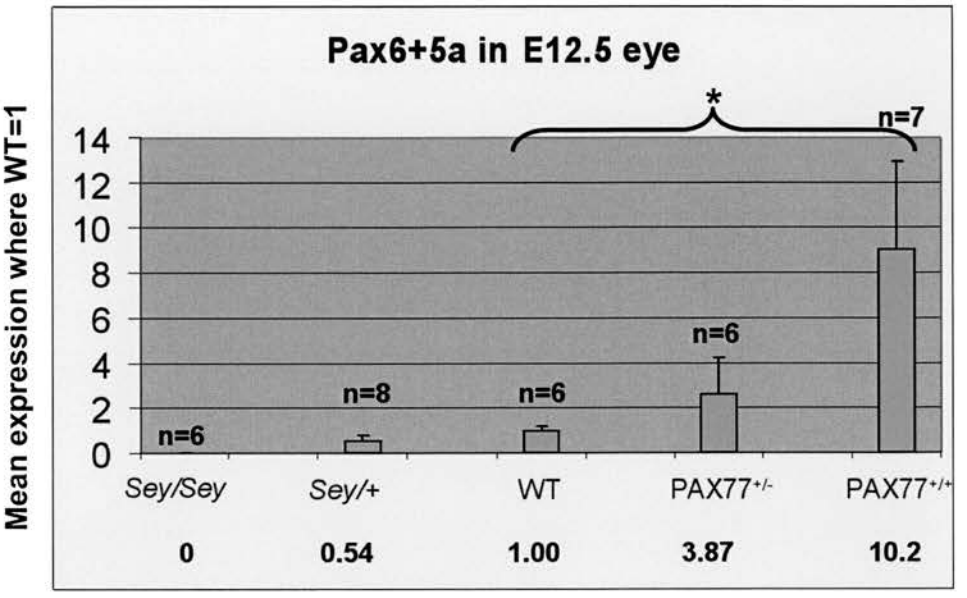

ANOVA P=0.0141, considered significant

B

t-test	P-value
Sey/Sey vs. *Sey/+*	>0.05
Sey/Sey vs. WT	>0.05
Sey/+ vs. WT	>0.05
WT vs. PAX77$^{+/-}$	>0.05
WT vs. PAX77$^{+/+}$	<0.05
PAX77$^{+/-}$ vs. PAX77$^{+/+}$	>0.05

Figure 3.17: Pax6+5a in E12.5 mouse eye. A, Mean values. All values are normalised to WT=1. The number of samples analysed is shown above each bar. Error bars represent SEM. Values are given in numerical form below each bar. B, Results of paired *t*-test between genotypes. Significant results are highlighted.

A

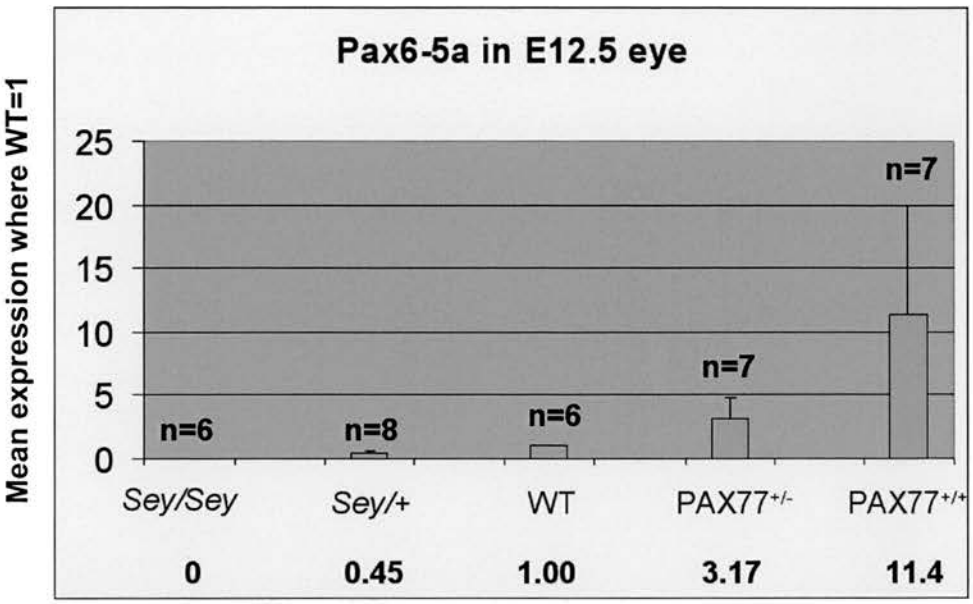

ANOVA P=0.259, not considered significant

B

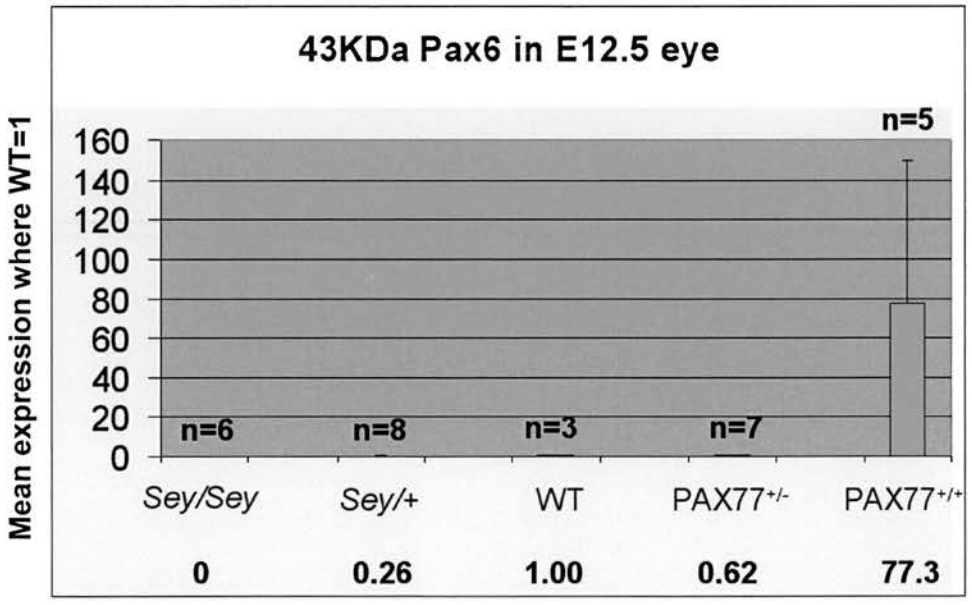

ANOVA P=0.317, not considered significant

Figure 3.18: Pax6-5a (A) and 43KDa Pax6 (B) in E12.5 mouse eye. All values are expressed as means, normalised to WT=1. The number of samples analysed is shown above each bar. Error bars represent SEM. Values are given in numerical form below each bar.

A

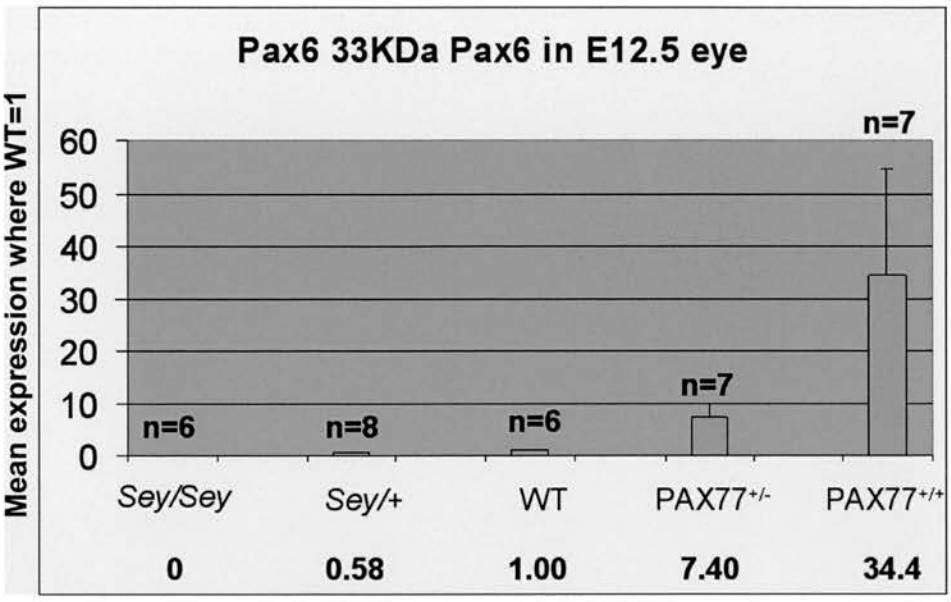

ANOVA P=0.0761, considered not quite significant

B

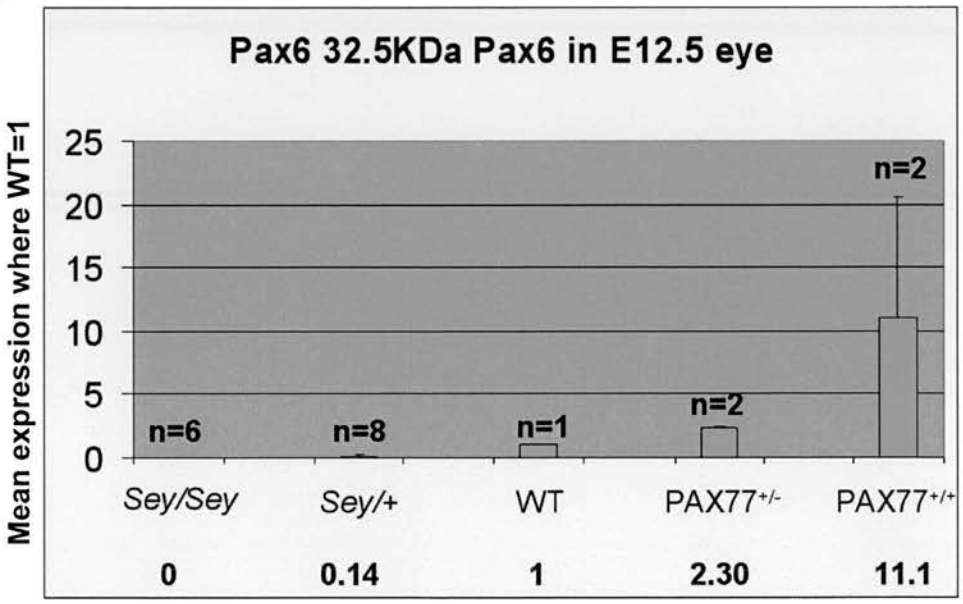

ANOVA P=0.317, not considered significant

Figure 3.19: 33KDa Pax6 (A) and 32.5KDa Pax6 (B) in E12.5 mouse eye. All values are means, normalised to WT=1. The number of samples analysed is shown above each bar. Error bars represent SEM. Values are given in numerical form below each bar.

A

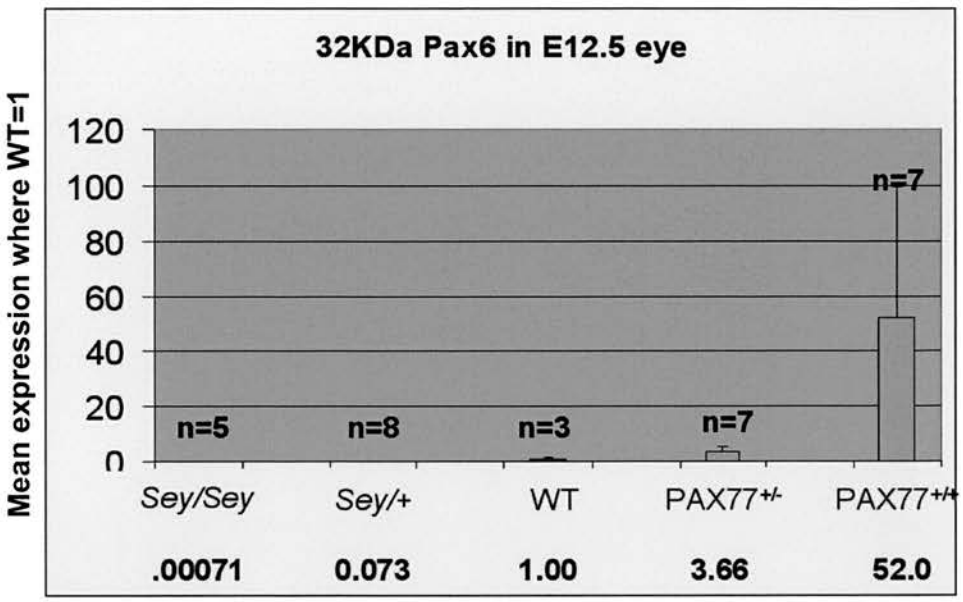

ANOVA P=0.3689, not considered significant

B

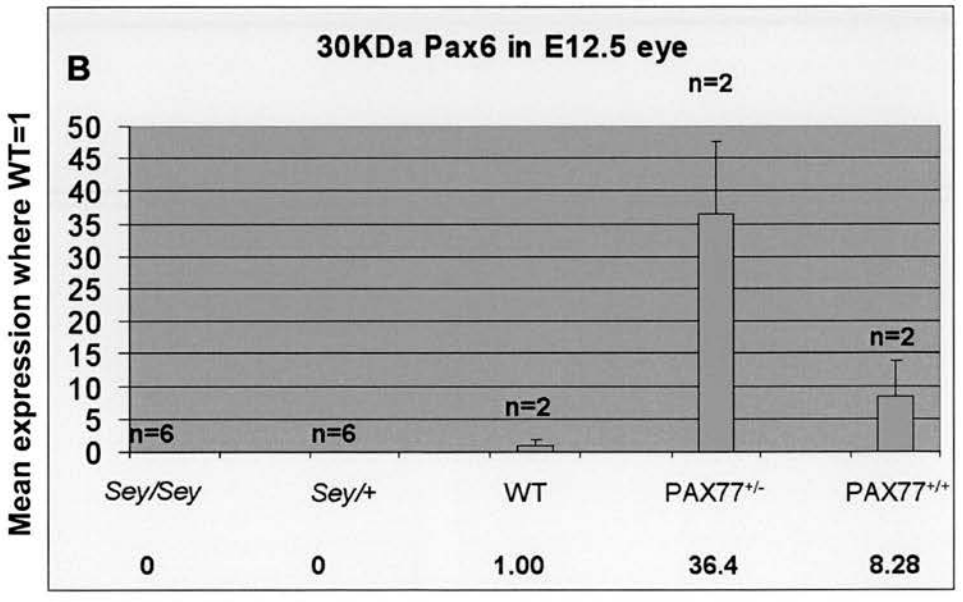

ANOVA P=0.4286, not considered significant

Figure 3.20: 32KDa Pax6 (A) and 30KDa Pax6 (B) in E12.5 mouse eye. All values are means, normalised to WT=1. The number of samples analysed is shown above each bar. Error bars represent SEM. Values are given in numerical form below each bar.

an autoregulatory mechanism which is hypothesised to stabilise Pax6 levels in the brain appears to be absent in the eye at E12.5.

The level of upregulation seen in PAX77$^{+/-}$ and PAX77$^{+/+}$ eyes seems to vary highly between isoforms. This is most dramatic in homozygotes, where upregulation ranges from 8-fold (30kDa band) to 77-fold (43kDa band). This may be due in part to the large error in these samples, but it seems likely that in some cases, upregulation is greater than the 12-fold which might be expected in a mouse with 12 extra copies of the gene.

Both 43kDa and 32kDa bands were observed in the brain of *Sey/Sey* mice at E12.5. The 43kDa band was not observed in the eye at this age, and the 32kDa band was only seen once. This might represent a genuine absence of these proteins in the *Sey/Sey* eye, or it may be due to the fact that levels are below the limits of detection. Given the high levels of 43kDa Pax6 in the eye of other genotypes, it seems likely that its absence from *Sey/Sey* samples is a genuine result. The lower 32kDa band is less abundant in other genotypes, and was observed once in *Sey/Sey*, so might be present at very low levels.

3.6: Results: The Pax6-5a : Pax6+5a protein ratio

As discussed in Chapter 2, the ratio between the two full-length *Pax6* mRNA splice variants, *Pax6+5a* and *Pax6-5a*, is an important aspect of the role of *Pax6* as a transcription factor. Despite this, the differential distribution of Pax6-5a and Pax6+5a proteins has yet to be studied in any organism, at any age.

3.6.1: Pax6-5a : Pax6+5a ratios in the eye and brain of E12.5 *Sey/+*, WT, PAX77$^{+/-}$ and PAX77$^{+/+}$ mice

In the brain, the ratio of Pax6-5a : Pax6+5a protein is 4:1 for WT, and 3:1 for *Sey/+* (**Figure 3.21 A**). These two results are not significantly different. The comparisons between WT and PAX77 brains, however, are statistically significant. In the PAX77$^{+/-}$ brain, the ratio falls to approximately 2:1. In the PAX77$^{+/+}$ brain, it is closer to 1.5:1.

A

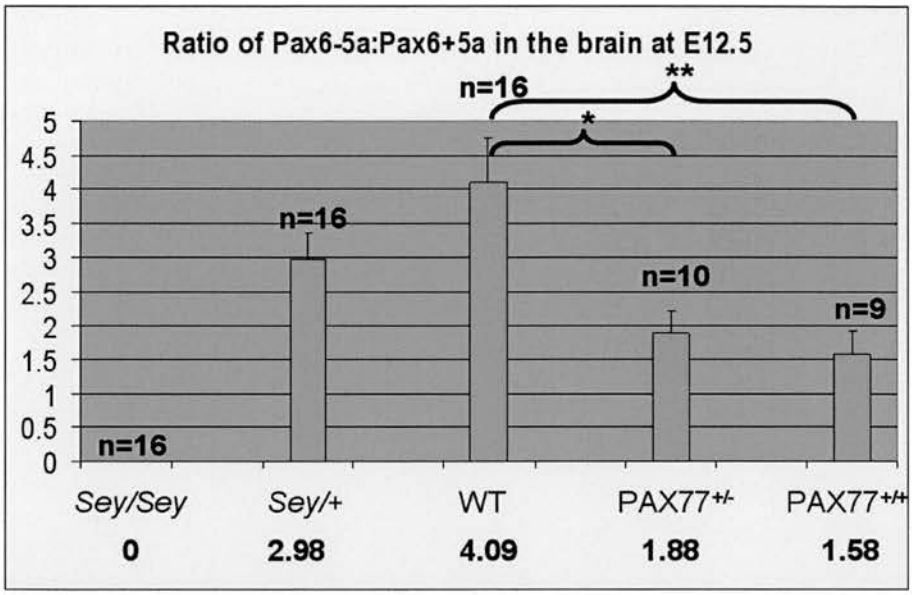

ANOVA P=0.0058, considered very significant

B

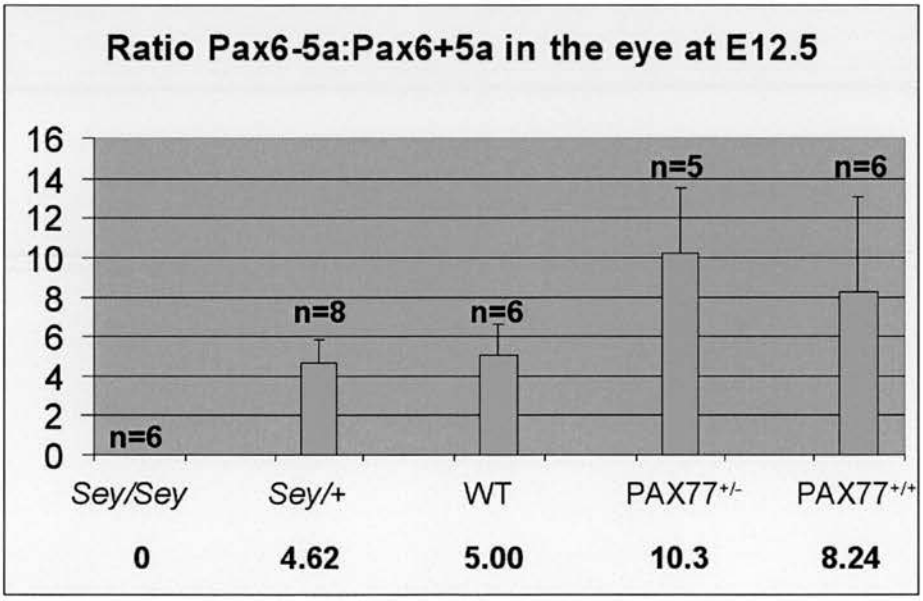

ANOVA P=0.490, not considered significant

Figure 3.21: Ratio of Pax6-5a:Pax6+5a in all genotypes at E12.5 in the brain (A) and eye (B). The ratio is expressed as total amount Pax6-5a / total amount Pax6+5a, thus a positive number indicates Pax6-5a in excess over Pax6+5a.All values are expressed as means. The number of samples analysed is shown above each bar. Error bars represent SEM. Values are given in numerical form below each bar. * *t*-test significant to P<0.5. **P<0.01

The WT figure of 4:1 is somewhat different from the *Pax6-5a* : *Pax6+5a* mRNA ratios described in the literature. A comparison between these figures and those seen for *Pax6* mRNA in Chapter 2 indicates that ratios observed for RNA are indeed recapitulated at the protein level. The relationship between *Pax6* mRNA levels and Pax6 protein levels as determined by this study will be discussed in more detail in section 3.6.2. Richardson et al. (1995) cloned full-length *Pax6* cDNAs from adult mouse brain, and found an equal representation of *Pax6+5a* and *Pax6-5a*, although this analysis was by no means quantitative. In contrast, Kozmik et al. (1997) saw a ratio of 8:1 in whole head from E12.5 – E16.5, and in adult whole brain. Although RPA, the technique used in this analysis (see Chapter 2) is quantitative, any ratio from whole head RNA would include eye, brain and nasal epithelia, and thus is not directly comparable with the results presented here.

In the eye, the ratio between Pax6-5a and Pax6+5a is 5:1 in the WT, and approximately 4.5:1 in *Sey/+*, results that are not significantly different (**Figure 3.21 B**). In the $PAX77^{+/-}$ eye this rises to 10:1, similar to the 8:1 seen in $PAX77^{+/+}$ eye. Although these figures are higher than in the WT eye, they are not significantly different.

As with the brain, the Pax6-5a : Pax6+5a ratio in E12.5 WT eye described here differs from some previously published data. Two studies have addressed this issue in the eye, although both were conducted at the mRNA level. The relative abundance of Pax6 protein isoforms has not been studied to date. Jaworski et al. (1997) used RT-PCR to amplify *Pax6* exons 4 to 7 from bovine retina, lens, iris and cornea. Based on the intensity of PCR products as visualised by agarose gel electrophoresis, they described a prevalence of *Pax6-5a* in the retina and lens, whilst the two isoforms were more equally represented in the iris and cornea. Zhang et al (2001) looked in the adult human lens and cornea, and the monkey retina, using RT-PCR reactions spiked with known amounts of "mimic" fragments, to obtain semi-quantitative results. Equal amounts of the two isoforms were seen in all tissues. Whilst these results seem contradictory, it is worth bearing in mind the different species being examined, and the different methods used. The results described here are an average of the ratio across whole eye, so tissue-specific effects will be masked, but are consistent with *Pax6-5a* being preferentially expressed.

It is interesting to note that the brain of $PAX77^{+/-}$ and $PAX77^{+/+}$ mice appears unaffected by the presence of extra copies of the *Pax6* gene (Schedl et al., 1996;

M.Manuel, pers. comm.), whereas the eye is severely affected in both cases (Schedl et al., 1996). It is clear that the absolute levels of Pax6 protein have an effect on the PAX77 mouse phenotype, but it is also possible that the difference in Pax6-5a : Pax6+5a ratio may play a part in this phenotype.

In the brain, the ratio drops significantly, from around 4:1 in the WT to below 2:1 in PAX77 mice. This is because Pax6-5a is up-regulated by less than two-fold, whereas Pax6+5a shows a higher level of up-regulation in both $PAX77^{+/-}$ and $PAX77^{+/+}$ brain, by a factor of 3 or 4. The alteration of the Pax6-5a:Pax6+5a ratio could alter the transcriptional activity of Pax6 protein, as seen in Chauhan et al. (2004), and may have an effect on *Pax6* autoregulation.

In the eye, the ratio between Pax6-5a and Pax6+5a in PAX77 mice does not alter significantly (**Figure 3.21 B**). The PAX77 eye displays micropthalmia (Schedl et al., 1996), and thus appears to be sensitive to *Pax6* dosage.

In contrast to the eye, there is no discernible PAX77 hemizygous or homozygous brain phenotype (Schedl et al., 1996; M. Manuel pers. comm.), and thus the brain is less sensitive to *Pax6* gene dosage. Here, the Pax6-5a : Pax6+5a ratio does differ significantly from that in the WT (**Figure 3.21 A**). It is possible that this alteration in ratio is the result of an autoregulatory mechanism, and one of the reasons for the lack of a strong brain phenotype.

3.6.2: Comparing Pax6-5a : Pax6+5a ratios at the mRNA and the protein level

Figure 3.22 allows a general comparison between the WT *Pax6-5a* : *Pax6+5a* mRNA ratios described in Chapter 2, and the WT protein ratios described here. The easiest comparison to make is that between whole eye mRNA and whole eye protein. The ratios are 6.8:1 and 5:1 respectively. When compared by *t*-test, these two results are not significantly different (P=0.35), indicating that the *Pax6-5a* : *Pax6+5a* mRNA ratio is representative of the Pax6-5a : Pax6+5a protein ratio. This suggests that regulation of the Pax6-5a : Pax6+5a protein ratio in the eye occurs largely at the

A

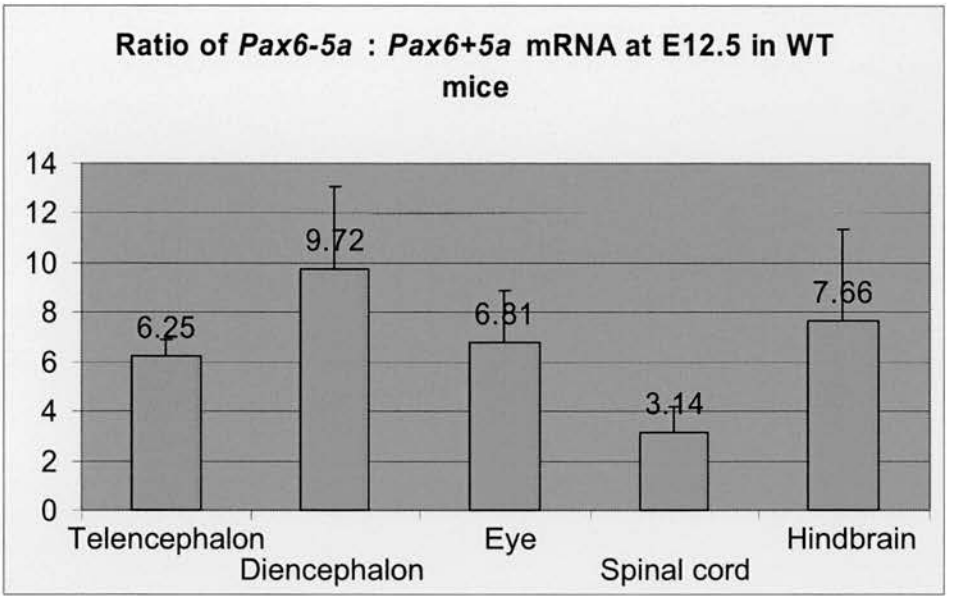

B

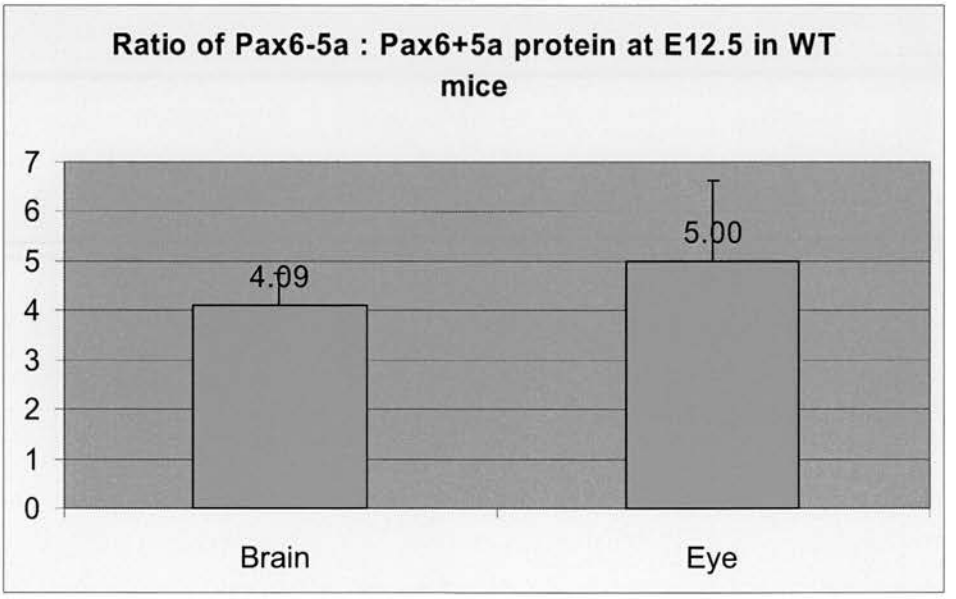

Figure 3.22: Comparison between *Pax6-5a* : *Pax6+5a* mRNA ratio and protein ratio at E12.5. A, mRNA ratio as determined by RPA. Error bars represent SEM. Values are given in numerical form above each bar. B, protein ratio as determined by western blot

mRNA level rather than the protein level, although it is still unclear whether this regulation occurs *via* changes in alternative splicing or changes in transcript stability.

In the brain the comparison between mRNA data and protein data becomes more complex, as mRNAs were divided by tissue to allow more in-depth analysis, whereas whole brain protein samples were used, as the technique was less sensitive. *Pax6* mRNA is expected to be most abundant in the telencephalon and diencephalon at E12.5, so a ratio from total brain will be skewed towards the ratio in these two tissues. At the protein level, the ratio is 4.1:1 (**Figure 3.22 B**). The ratio in the brain tissues analysed varies between 6.3:1 in the telencephalon and 9.7:1 in the diencephalon. The difference between the mRNA ratio and the protein ratio could be due to differential regulation of the two protein isoforms.

3.7: Results: Pax6 in the brain of E12.5 *Sey/Sey*, *Pax6*$^{LacZ/LacZ}$ and *Sey*^{Neu}/*Sey*^{Neu} mice

The 43kDa and 32kDa Pax6 bands were observed in E12.5 *Sey/Sey* brain extracts on 10 and 13 occasions, respectively. **Figure 3.23** shows three of these western blots. All three clearly show the 32kDa band, and **Fig 3.23 B + C** also show the 43kDa band in *Sey/Sey* samples.

As described in 3.4.3.3 and 3.4.3.7, these isoforms seem as common in the *Sey/Sey* brain at E12.5 as they are in the WT brain.

In order to determine the protein responsible for these two bands, western blots were performed on E12.5 brain samples collected from two other Pax6 mutants, *Pax6*$^{LacZ\,LacZ}$ and *Sey*^{Neu}/*Sey*^{Neu} (**Figure 3.24**). All genotypes appear to contain the 32kDa band, whilst only *Sey/Sey, Sey/+* and WT brains contain the 43kDa band.

Although the nature of the 43kDa band seen in the *Sey/Sey* brain is unknown, the fact that it is highly upregulated in the PAX77$^{+/-}$ and PAX77$^{+/+}$ brain and eye (**Figure 3.11** and **Figure 3.19**) is evidence for it being a *Pax6*-derived protein. One possible explanation is that the 43kDa band may be due to the splicing out of exon 8, which contains the *Sey* STOP codon. The corresponding protein would not be made in either *Pax6*$^{LacZ\,LacZ}$ or *Sey*^{Neu}/*Sey*^{Neu} mice, and the band would not be observed in either sample.

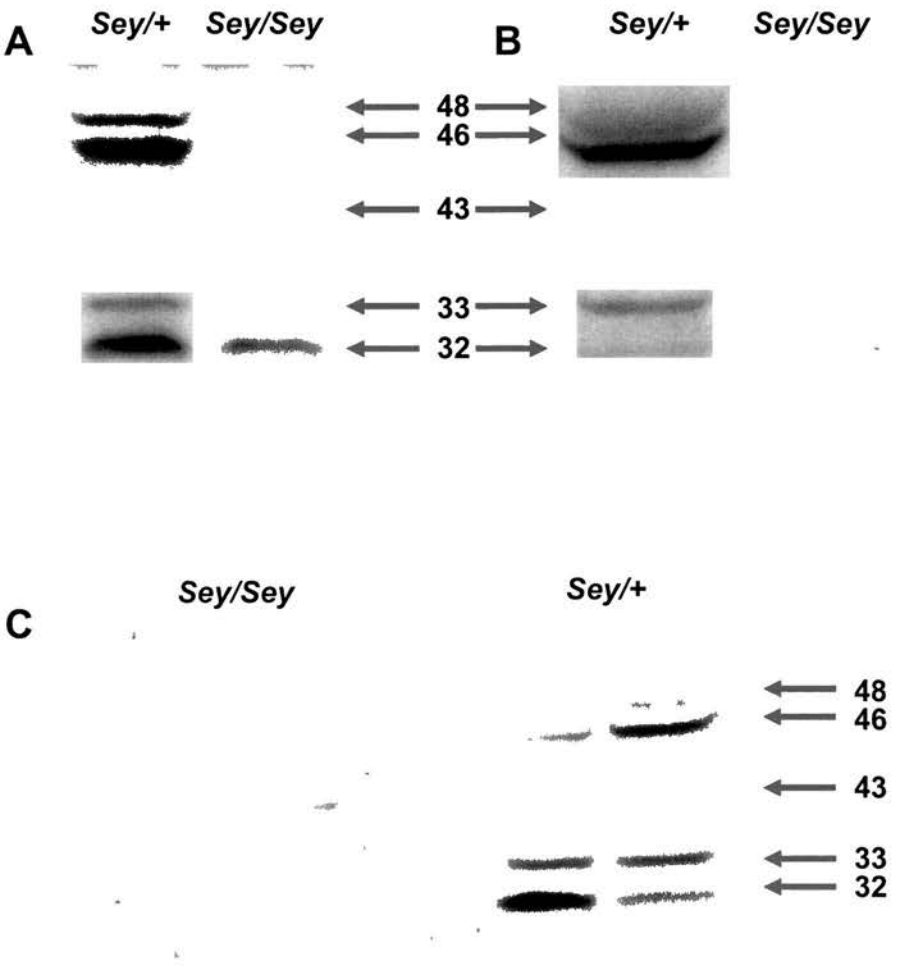

Figure 3.23: Typical results from western blot of E12.5 whole brain protein extract from *Sey/Sey* and *Sey*/+ mice. A, B, C, three separate repeats. All show the presence of the 32KDa band in *Sey/Sey* brain. B and C also show the presence of the 43KDa Pax6 band. Arrows indicate the bands observed, and their estimated mass in KiloDaltons (KDa).

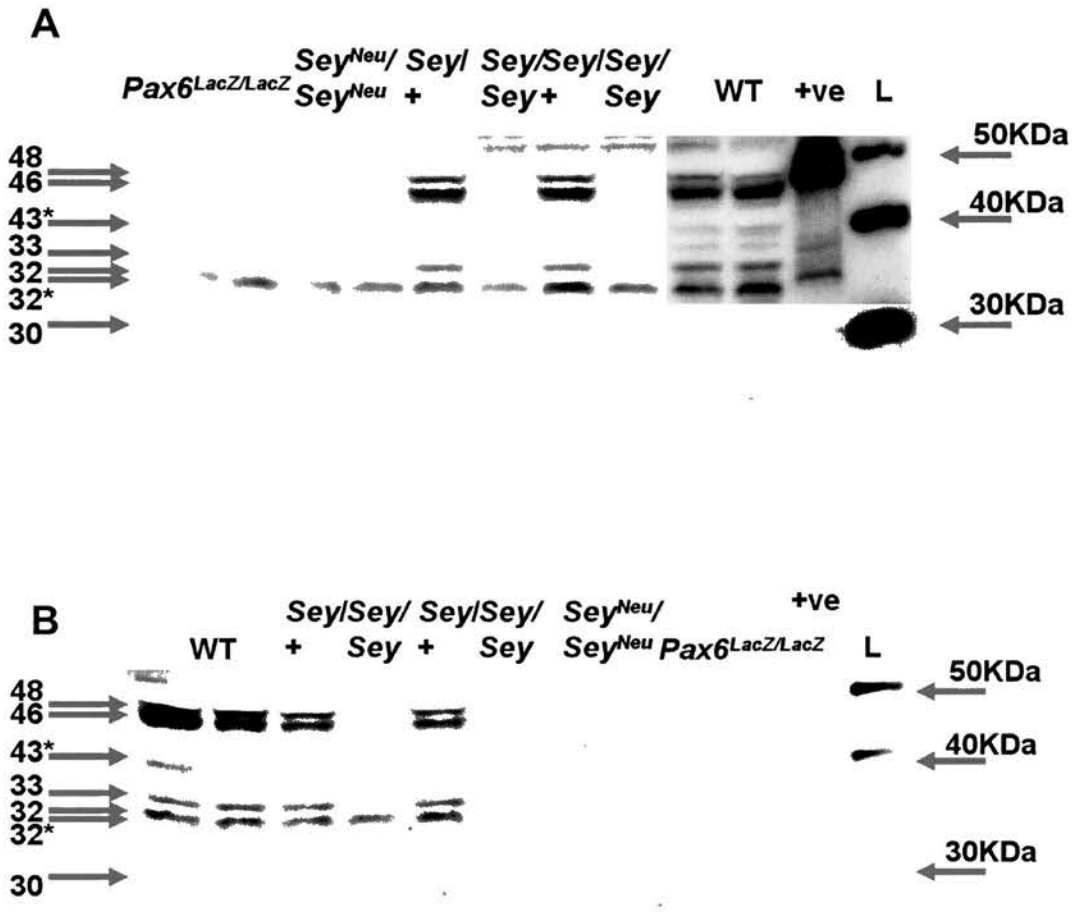

Figure 3.24: Typical results from western blot of E12.5 whole brain protein extract from *Pax6*$^{LacZ/LacZ}$, *Sey*^{Neu}/*Sey*^{Neu}, *Sey/Sey*, *Sey*/+ and WT mice. A, B, separate repeats on the same samples. All genotypes show the presence of the 32KDa band. The 43KDa Pax6 band, on the other hand, is only seen in *Sey/Sey, Sey*/+ and WT. Arrows indicate the bands observed, and their estimated mass in Kilodaltons (KDa). Bands over 50KDa are assumed to be non-specific. +ve, *in vitro*-synthesised positive control Pax6. L, molecular weight ladder.

The predicted molecular weight of a Pax6 protein resulting from translation of the *Sey Pax6* transcript from the first ATG to the STOP mutation (as described in Engelkamp et al., 1999) is 22.5kDa, making this an unlikely explanation for the 43kDa Pax6 *Sey/Sey* band. Indeed, no band of this molecular weight was seen in *Sey/Sey* brain or eye at E12.5, implying that the truncated protein is not made in sufficient quantities to be functionally significant.

As it is present in $Pax6^{LacZ\,LacZ}$ and Sey^{Neu}/Sey^{Neu} mouse brain extracts, the 32kDa Pax6 band can no longer be explained as a result of internal translation initiation. Although this would still be possible in the $Pax6^{LacZ\,LacZ}$ mouse, the Sey^{Neu} mutation would disrupt the 5'-truncated protein. The 32kDa band in the Sey^{Neu}/Sey^{Neu} brain may be the result of an unknown form of *Pax6* mRNA or protein processing, or it may be a non-specific band migrating at the same molecular weight as a Pax6-specific band. Given either explanation, it is still entirely plausible that the 32kDa band observed in $Pax6^{LacZ\,LacZ}$ and *Sey/Sey* brain at E12.5 is a genuine *Pax6*-derived protein.

3.8: Discussion

3.8.1: Overall trends in Pax6 protein isoform expression in the embryonic brain and eye across genotypes

At least eight isoforms of Pax6 can be detected by western blot of brain and eye tissue from E12.5 mice. The majority of isoforms are upregulated in both $PAX77^{+/-}$ and $PAX77^{+/+}$ mice. In the brain, there is no significant difference in expression levels between hemizygous and homozygous PAX77 mice. In the eye, levels of all but one of the Pax6 proteins are higher in the $PAX77^{+/+}$ mouse than in the $PAX77^{+/-}$ mouse. This is to be expected from the extra six copies of the *Pax6* gene in this mouse.

The *Sey/+* mouse brain shows similar expression levels to the WT for most Pax6 isoforms, which is surprising given that it is missing one copy of the gene. In the eye, expression levels of all isoforms appear to be reduced in the *Sey/+* mouse.

The only isoforms which do not seem to conform to this general rule are the Pax6+5a, 42kDa and 33kDa forms. Pax6+5a is the only isoform to be expressed at higher levels in the *Sey/+* brain than in the WT brain. Unlike the other isoforms, both the 42kDa

and the 33kDa Pax6 proteins are found at reduced levels in the *Sey/Sey* and the *Sey/+* brain when compared to WT.

The 43kDa isoform shows a very different expression pattern, as it is dramatically upregulated in PAX77 mice, by 144-fold in hemizygotes, and 56-fold in heterozygotes. It is also expressed in *Sey/Sey* mice, at a level that is not significantly different from the WT level.

At times the 42kDa and 43kDa bands were difficult to resolve by SDS-PAGE, and when a single band was seen, this was designated a 43kDa band. For this reason, it is possible that some signal from the 42kDa band may have been included as data for the 43kDa band. However, the 43kDa band was in great excess over the 42kDa band on all gels (see **Figure 3.5**), so this is unlikely to have contributed to the massive up-regulation of the 43kDa band observed in PAX77 mice. Also, where the 42kDa band was clearly resolved in one lane of a gel, it was clearly resolved in all lanes. Comparisons in its levels between these lanes were therefore valid, and not contaminated with information from the 43kDa band.

The Pax6-5a : Pax6+5a ratio in the eye is similar at the protein level to that observed at the RNA level by RNase protection assay. This indicates that control of expression of these two isoforms occurs largely at the mRNA level, and direct studies of mRNA levels, in this case at least, are a valid indicator of the protein content of a cell. It is difficult to compare mRNA data to protein data collected from the brain, as the brain was divided into constituent *Pax6* expressing tissues for mRNA analysis, whilst protein was analysed across the whole brain. There do, however, appear to be discrepancies between the *Pax6-5a* : *Pax6+5a* mRNA ratio and the corresponding protein ratio in the brain. This may be indicative of regulation of the Pax6 isoforms at the protein level.

The Pax6-5a : Pax6+5a protein ratio in the brain is consistent between *Sey/+* and WT samples. The ratio falls significantly in the PAX77 brain, both in hemizygotes and homozygotes. In the eye, there are no significant differences in the Pax6-5a : Pax6+5a protein ratio across all genotypes studied.

That the ratio between the two major Pax6 isoforms varies in the brain but not in the eye is consistent with the conclusion that Pax6 is more tightly autoregulated in the brain. A mechanism appears to be in place whereby the differential regulation of

Pax6 isoforms in the developing brain varies dependent on *Pax6* copy number. In the eye, this does not occur; Pax6-5a and Pax6+5a are not differentially regulated.

3.8.2: Limitations of this analysis

Analysis of Pax6 isoforms in whole brain and eye by western blot is a powerful tool for furthering our understanding of the roles of the various Pax6 isoforms in embryonic development. Pax6 protein level is not always representative of *Pax6* copy number, therefore insights into the autoregulation of Pax6 can be gained. Despite this, there are a number of limitations which must be borne in mind when discussing the results of this analysis.

Most obviously, protein extracts were taken from whole brain and whole eye at E12.5. Using just one embryonic age allows us to view a snapshot of development, around the peak of neurogenesis, but offers no indications as to whether the levels of any of these isoforms alter through development. The results from RNase protection assays (Chapter 2) clearly show that *Pax6* expression varies throughout development, an observation that is unlikely to be confined to *Pax6-5a* and *Pax6+5a*, the 46kDa and 48kDa protein isoforms. Understanding this developmental variation may give further insights into the roles of Pax6 isoforms in embryonic development.

The analysis of $PAX77^{+/-}$ and $PAX77^{+/+}$ samples alongside the same amount of total protein from WT samples led to difficulties in comparing signal strength between lanes. Where photographic film was exposed for sufficient length of time to observe some bands in the WT (e.g. the 43kDa, 33kDa and 32.5kDa bands), these bands were saturated in PAX77 samples, and could not be accurately quantitated. Retrospectively, this problem could have been solved by loading less PAX77 protein than WT protein, but this may have led to difficulties in relative quantitation where the levels of protein did not vary as markedly between genotypes (e.g. the 42kDa and 30kDa bands).

Comparisons with mRNA expression data from Chapter 2 reveal another weakness of this type of analysis. **Figure 2.9**, for example, shows a clear difference in *Pax6* isoform expression between telencephalon and diencephalon at E12.5. For western blot analysis, these two tissues were pooled as part of a whole brain protein extract. This was because western blot is a much less sensitive technique than RPA, and more tissue is needed to obtain accurate results.

Pooling such diverse tissues as lens and retina to obtain whole eye protein samples, or hindbrain and telencephalon to obtain whole brain protein samples, is likely to mask a number of interesting variations in Pax6 expression. For example, differential regulation of *Pax6* transcripts has been well documented in the developing eye, as described in Section 2.2.1. Alternative *cis*-regulatory elements downstream of the *Pax6* gene direct its expression specifically in the neural retina (Griffin et al., 2002), or the lens (Dimanlig et al., 2001; Kammandel et al., 1999). The relative amounts of the *Pax6+5a* and *Pax6-5a* splice forms vary markedly between these two tissues (Jaworski et al., 1997), and it seems likely that this differential regulation extends to the other alternative Pax6 isoforms, which this analysis would not have picked up.

Although differential regulation of most Pax6 isoforms is seen between the genotypes analysed, it is difficult to draw conclusions based on their roles in embryonic development without being entirely sure what Pax6 isoforms these bands represent. Studies have indicated what some of these bands might be (Carriere et al., 1993; present study) by over-expression of *in vitro* synthesised proteins in immortalised cell lines, but this is by no means proof of their identity. Unexpected Pax6 protein bands may exist as the result of a number of mechanisms, including protein cleavage, post-translational modifications, or unknown splice variants. Had the western blot technique been successful with the anti-Pax6 PD antibody, it would have been possible to differentiate between proteins created by these mechanisms, and those which were the result of internal translation initiation. Ultimately, until the precise protein sequence of these bands, has been determined, it is difficult to draw accurate and detailed conclusions from studies such as these.

3.8.3: Autoregulation of Pax6 protein in the E12.5 brain

PAX77$^{+/-}$ mice contain approximately 6 inserted copies of the human *PAX6* locus, and PAX77$^{+/+}$ mice contain approximately 12 extra copies. If there were a linear relationship between copy number and protein expression level, the PAX77$^{+/-}$ mouse brain would express four times more Pax6 than the WT brain (with eight total copies, as opposed to two), and the PAX77$^{+/+}$ mouse brain seven times more (with fourteen total copies, as opposed to two). Although Pax6 protein is clearly overexpressed in the PAX77 brain, the rise in expression of many isoforms, such as Pax6+5a and Pax6-5a is not that dramatic. In particular, no statistically significant increases in expression were detected between hemizygotes and homozygotes; if anything, hemizygotes express slightly more of most isoforms than homozygotes. This is likely

to be due to autoregulation. The mechanism behind this is unclear, but it may also help explain why there is no obvious brain phenotype in these mice (Schedl et al., 1996; M.Manuel, pers. comm.).

The majority of Pax6 isoforms are expressed at the same level in *Sey/+* and WT brains at E12.5, despite *Sey/+* mice only having one functional copy of the *Pax6* gene. In this case, a regulatory mechanism is seen to increase the levels of Pax6, up to those seen in the WT. Unlike the PAX77 brain, the *Sey/+* brain does have a phenotype (Estivill-Torrus et al., 2001; Mastick et al., 1997), but it is very subtle when compared to that seen in the *Sey/Sey* brain. It is possible that the upregulation of Pax6 to normal levels in the *Sey/+* brain is tissue-specific, and this technique would not be sensitive enough to detect regional variances in Pax6 levels. Alternatively, the brain phenotype in *Sey/+* mice could be due to the effects of the three isoforms, Pax6+5a, 42kDa Pax6 and 33kDa Pax6, that are seen at different levels between *Sey/+* and WT brains.

In the eye, this autoregulation is no longer evident. Pax6 expression levels seem to correlate much more tightly with *Pax6* copy number, and regulatory mechanisms to control its levels do not seem to be present. Expression of all Pax6 isoforms appears to be reduced in the *Sey/+* eye when compared to WT. Reduced transcription of *Pax6* has been previously demonstrated in the *Sey/+* lens (Chauhan et al., 2004b), which is consistent with the reduced levels of Pax6 protein observed here. All Pax6 isoforms except the 30kDa form are found at higher levels in the $PAX77^{+/+}$ eye than in the $PAX77^{+/-}$ eye, again indicating that a relationship between *Pax6* copy number and Pax6 protein expression is maintained in the eye.

Sey/+ eyes are severely reduced in size (Hill et al., 1991), as are those of the $PAX77^{+/-}$ and $PAX77^{+/+}$ mice, although eye size is more variable in the PAX77 mutant (Schedl et al., 1996). This similarity in phenotype is difficult to explain, given the large differences in Pax6 protein levels, but it is clear that the eye is highly sensitive to Pax6 protein dosage.

3.8.4: Over-expression of the human *Pax6* locus in mice

An important issue to bear in mind when comparing Pax6 expression between WT and PAX77 mice is that the extra copies of *PAX6* are under the control of the human

regulatory elements contained in the 420kb YAC. This is a possible explanation for differences in Pax6 regulation between WT and PAX77 mice.

Whilst most Pax6 isoforms are expressed at levels which are loosely comparable to *Pax6* copy number in the PAX77$^{+/+}$ brain and eye, extremely high levels of the 43kDa band are found in both tissues (56-fold more than WT in the brain, and 77-fold more in the eye). The PAX77$^{+/-}$ brain also exhibits very high levels of this isoform (144 times more than found in the WT brain), although no great upregulation is seen in the PAX77$^{+/-}$ eye. This is a much higher increase in protein level than would be predicted by *Pax6* copy number alone, and it remains a possibility that this isoform is expressed at higher levels because it is under the control of human regulatory sequences that differ markedly from those present in the mouse.

This is also a possible explanation for the difference in Pax6-5a : Pax6+5a ratio observed in the brain of both hemizygous and homozygous PAX77 mice.

Although most studies of *Pax6* expression have been conducted in mouse (e.g. Kozmik et al., 1997; Richardson et al., 1995), a few have analysed expression in other species, such as cow (Jaworski et al., 1997) and monkey (Zhang et al., 2001). It is difficult to make direct comparisons between these studies, as they involve mRNA characterisation of a number of tissues using different techniques. However, there are indications that species-specific differences may well occur. Zhang et al. (2001) described a 1:1 ratio between *Pax6-5a* and *Pax6+5a* in human lens epithelium, whilst Jaworski et al. (1997) and Richardson et al. (1995) observed more *Pax6-5a* in the cow and mouse lens. No other studies have yet been conducted comparing protein isoform expression between species.

3.8.5: Pax6 protein expression in the *Sey/Sey* mouse, and other Pax6 mutants

Some isoforms of Pax6 protein are present in the *Sey/Sey* brain at E12.5, but they are not detectable in the eye. The 43kDa band is expressed at similar levels to WT, whilst the 32kDa band is upregulated by approximately four-fold. If these bands are functional in the WT mouse, they may therefore also be contributing to the phenotype of *Sey/Sey* mice. The increased levels of *Pax6* mRNA in the *Sey/Sey* mouse

(Collinson et al., 2003; Warren and Price, 1997) may also explain the increased levels of 32kDa Pax6 protein.

43KDa Pax6 is found in the *Sey/Sey* brain at E12.5, but is not detectable in *Sey/Sey* eye, or in either tissue from $Pax6^{LacZ/LacZ}$ or Sey^{Neu}/Sey^{Neu} mice. The absence of this Pax6 band from two of the three *Pax6* mutant mice could be due to expression below the limits of detection by western blot, or it could indicate that these two genotypes are incapable of producing a 43kDa Pax6 protein.

The 43kDa Pax6 protein was previously thought to be the result of alternative splicing of exon 6 (Carriere et al., 1993), but two lines of evidence from this study suggest that an alternative explanation for the 43kDa band must now be sought. Firstly, it is present in the *Sey/Sey* brain, which is theoretically incapable of producing full-length Pax6Δ6 protein due to the presence of an internal STOP codon. Secondly, RPA data from Chapter 2 (**Figure 2.12**) show that the alternative splicing of exon 6 is undetectable in a number of *Pax6* expressing tissues at E12.5; unless the Pax6Δ6 protein is significantly more stable than other Pax6 isoforms at this age, other Pax6 proteins must be contributing to the 43kDa Pax6 band. One possible explanation is the alternative splicing of exon 8, leaving an in-frame protein with a predicted molecular mass of 41/42kDa (-/+5a).

32kDa Pax6 is present in the brain of *Sey/Sey*, $Pax6^{LacZ/LacZ}$ and Sey^{Neu}/Sey^{Neu} mice at E12.5, but is not detected in the eye. Again, protein may have been present in the eye of these strains, but at below the limits of detection by western blot. An explanation for the presence of this short Pax6 isoform in all three *Pax6* mutant mouse strains is harder to come by, but it is likely to be a Pax6 protein product, as it is over-expressed in the PAX77 brain and eye. One possibility is that it may result from internal translation initiation, giving rise to an N-terminally truncated Pax6 isoform, lacking the PD. Another is that it may be a protein cleavage product.

Although the protein sequence of the 43kDa and 32kDa Pax6 bands is unknown, it is clear that Pax6 protein is present at detectable levels in the brain of *Sey/Sey*, $Pax6^{LacZ/LacZ}$ and Sey^{Neu}/Sey^{Neu} mice, and may be contributing to their phenotype. The presence of 43kDa Pax6 isoform in just one of these mouse strains, *Sey/Sey,* also suggests that any differences in phenotypes between the strains might be explained by the presence of a short Pax6 isoform.

A possible role for N-terminally truncated Pax6 protein will be discussed further in Chapter 4.

3.8.6: Future work

Data from RNase protection assays on *Pax6* mRNA (Chapter 2) show tissue-specific and developmental stage-specific variations in the *Pax6-5a* : *Pax6+5a* ratio. For example, the ratio falls with time in the telencephalon and diencephalon, whilst it remains constant in the cerebellum. Although it would be impractical to extend this protein expression analysis to all Pax6 expressing tissues at all time points, a detailed protein expression analysis could be conducted in tissues or at time points which show interesting patterns of *Pax6* mRNA regulation. Tissues such as the telencephalon, from which large amounts of protein could easily be obtained, are particularly amenable to this type of analysis. It would be interesting to look at the levels of the shorter Pax6 isoforms in the developing telencephalon, to establish whether this fall in *Pax6-5a* : *Pax6+5a* ratio is coincident with changes in the levels of other Pax6 proteins, which would shed some light on their roles in cortical development.

Pax6 is known to have multiple roles, even within the developing cortex. It is expressed in both neural progenitor cells and glia (Gotz et al., 1998) and the different cell types may well express the various Pax6 isoforms at different levels. Double immunocytochemistry with a neural progenitor cell marker such as MAP2 and a glial cell marker such as RC2 would permit flow cytometric sorting of these two cell types. The two separate populations could then be subjected to western blot analysis, and an expression profile of the different Pax6 isoforms across cell types could be obtained.

The present analysis of E12.5 mouse brain has revealed that a 43kDa Pax6 isoform is present in the *Sey/Sey* mouse, but not Sey^{Neu}/Sey^{Neu} or $Pax6^{LacZ/LacZ}$ mice. A 32kDa Pax6 isoform is present in all three genotypes. A tissue-specific analysis of regions of the embryonic brain may highlight areas in which this short isoform is seen at relatively high levels. A phenotypic comparison between the three *Pax6* mutant mice in this tissue would shed further light on the *in vivo* roles of these short proteins.

It is difficult to draw conclusions as to the role of the Pax6 isoforms described here without knowing their exact protein sequence. By performing 2-dimensional gel

electrophoresis on PAX77 brain samples, these Pax6 bands could be separated from other proteins present in whole brain extract. Alternatively, samples could be enriched for Pax6 by immunoprecipitation. If two polyacrylamide gels were run simultaneously, western blot for Pax6 could be performed on one, to determine the exact location of each isoform. They could then be excised from the second gel, and N-terminal and C-terminal sequencing could be used to obtain an exact protein sequence for each, including post-translational modifications.

Finally, after characterisation of the expression levels of Pax6 isoforms, the next step is to define a functional role for each isoform. Although it is likely that the various Pax6 proteins interact with each other in a complex manner, an initial analysis could be conducted by forcing their expression in a cell culture system. Full-length Pax6-5a and Pax6+5a, alongside an N-terminally truncated Pax6 have been overexpressed in two cell lines, and preliminary analysis of the phenotype of these cell lines is described in Chapter 4.

Chapter 4: Analysing the effects of Pax6-5a and Pax6+5a over-expression in immortalised cell lines

4.1: Summary

Four cell lines were selected for preliminary study. These were H36CE2, a human lens cell line; Neuro2A, a murine neuroblastoma cell line; NIH3T3, a murine fibroblast cell line, and U373-MG, a human glioblastoma cell line. The levels of Pax6 expression were determined in each cell line, and transient transfections were performed with over-expression plasmids containing EGFP and Pax6, to determine transfection efficiency.

Two cell lines were then selected for the creation of stable transgenic Pax6-overexpressing cell lines. Neuro2A was selected as it expresses endogenous Pax6, is easy to culture, grows quickly, and is highly amenable to lipofection. NIH3T3 was selected as it expresses no endogenous Pax6 protein, but is also easy to culture, grows quickly, and is highly amenable to lipofection.

It was found that, in both cell lines, the addition of either Pax6-5a or Pax6+5a led to the over-expression of both splice variants. Cell lines were selected that over-expressed Pax6 at varying levels.

Pax6 over-expression was found to promote neuronal differentiation in the Neuro2A cell line, an effect which was most profound in the cell line with highest levels of Pax6 protein.

4.2: Introduction

4.2.1: Methods previously used to analyse the effects of Pax6 over-expression on cellular behaviour

The over-expression of Pax6 was first studied by Maulbecker and Gruss (1993), who transplanted Pax6 over-expressing cells into WT mice, and observed tumour formation, implying that Pax6 has a role in controlling cellular proliferation. The *Pax6* expression construct used by Maulbecker and Gruss contained *Pax6-5a*, and no similar experiments have been carried out to date using other *Pax6* isoforms.

Duncan et al. (2002) created a transgenic mouse in which *Pax6+5a* was specifically over-expressed in the lens, which led to the formation of cataracts, and the up-regulation of the cell adhesion molecules paxillin, $p120^{ctn}$ and $\alpha5\beta1$ integrin, but again the reciprocal experiment was not performed with *Pax6-5a*.

The PAX77 transgenic mouse (Schedl et al., 1996) (see Section 1.5.4) was engineered to allow the over-expression of all isoforms of PAX6 in all tissues with endogenous Pax6 expression. This was achieved by the addition of a number of copies of a YAC containing the human *PAX6* locus, and all known surrounding regulatory elements. Chapter 3 of the present study describes raised levels of Pax6 protein in both hemizygous and homozygous PAX77 mice, proving that all PAX6 isoforms were indeed over-expressed. The phenotype of the $PAX77^{+/-}$ and $PAX77^{+/+}$ mice mirrors that of the *Sey/+* mouse, with a reduction in eye size and no obvious phenotype in the brain (Schedl et al., 1996; M. Manuel, pers. comm.).

Little work has been done on the PAX77 mouse line to further characterise the effects of Pax6 over-expression, which would shed valuable light onto the normal function of Pax6 during development.

The effects of Pax6 over-expression have been more extensively studied *in vitro*, by transient transfection of immortalised cell lines. Most of these studies have focussed on the effects of Pax6 on various promoters, in particular the Pax6 P0 and P1 promoters (Aota et al., 2003; Plaza et al., 1993; Plaza et al., 1995) and the effects of Pax6 on the canonical binding sequences P6CON and 5aCON (Epstein et al., 1994b; Yamaguchi et al., 1997). Little work has been done to assess the cellular behaviour of Pax6 over-expressing cells. In a number of studies, conclusions have been made from the phenotype of cells after the introduction of one *Pax6* isoform, without any attempt to characterise the protein content of transfected cells (Carriere et al., 1995; Chauhan et al., 2004a; Heins et al., 2002; Yamaguchi et al., 1997). Given that Pax6 is known to transactivate its own promoter (Okladnova et al., 1998; Plaza et al., 1993; Plaza et al., 1995; see Section 1.6.3), it is difficult to assess the effects of Pax6 over-expression *in vitro* without first characterising the Pax6 protein content of transfected cells.

4.2.2: Stable cell lines as a model system for studying Pax6 over-expression

Cell lines are a good model system for studying the effects of gene over-expression. Circularised plasmid constructs containing the gene of interest, in this case *Pax6*, can be transiently transfected into cell lines, leading to very high levels of over-expression which peaks 48-72 hours after transfection. Alternatively, linearised plasmid constructs containing the gene of interest and a second gene conferring resistance to gentamycin (G-418) can be transfected into a cell line using the same protocol, and G-418 selection can be used to create stable transgenic lines.

Stable cell lines are particularly useful, as they are clonal in origin, and should express consistent levels of the transgene. Repeated experiments can be performed on stable cell lines to look at the effects of transgene over-expression, without the risk of inconsistent levels of over-expression leading to difficulties in the interpretation of results.

Cell lines can be chosen which endogenously express the gene of interest, and are therefore likely to be expressing co-factors necessary to mediate an over-expression phenotype. In addition, cell lines can also be chosen which do not endogenously express the gene of interest, in order to assess the effects of ectopic introduction of a gene.

NIH3T3 (European Collection of Cell Cultures, ECACC 93061524) is a murine fibroblast cell line (Jainchill et al., 1969) which does not express endogenous Pax6 (Okladnova et al., 1998; Turque et al., 1994). The necessary co-factors to mediate a Pax6 over-expression phenotype might not be present in this cell line. If a phenotype were seen, this would be an indication that Pax6 was acting as a "master regulator" of transcription (Halder et al., 1995; Harris, 1997; Onuma et al., 2002), and activating a cascade of downstream genes that might not already be expressed by NIH3T3 cells.

Neuro2A (ECACC 89121404) is a murine neuroblastoma-derived cell line. As the phenotype of these cells is thought to mirror that of partially differentiated neurons (Fischer et al., 1986; Prasad and Hsie, 1971), they are likely to express Pax6, as it is crucial for neuronal differentiation (Heins et al., 2002; Mastick and Andrews, 2001; Plaza et al., 1995; Takahashi and Osumi, 2002; Warren et al., 1999). This cell line is likely to express co-factors that are necessary to mediate a Pax6 over-expression phenotype. Any effect of Pax6 over-expression on the behaviour of this cell line should provide an insight into the role of Pax6 in neuronal differentiation.

U373-MG (ECACC 89081403) is a human glioblastoma-derived cell line (Ponten and Macintyre, 1968). The process of glial differentiation requires Pax6 (Heins et al., 2002), and this cell line is known to express Pax6 (C.T.Yap, Pers. Comm.). Therefore, it is also likely to be expressing co-factors necessary to mediate a Pax6 over-expression phenotype. Any effect of Pax6 over-expression on the behaviour of this cell line should provide an insight into the role of Pax6 in glial differentiation.

H36CE2 (a kind gift from A. Seawright, MRC Human Genetics Unit, Edinburgh) is a human lens-derived cell line (Lengler et al., 2001). As the human lens is known to express Pax6 (Glaser et al., 1992; Nishina et al., 1999), this cell line is likely to also express Pax6, alongside co-factors necessary to mediate a Pax6 over-expression phenotype. Any effect of Pax6 over-expression on the behaviour of this cell line should provide an insight into the role of Pax6 in lens formation.

4.2.3: The use of dbcAMP to promote neuronal differentiation in the Neuro2A cell line

In culture, a low percentage of Neuro2A cells spontaneously differentiate down a neuronal lineage, but the effect is enhanced by the addition of dibutyryl adenosine 3':5'-cyclic monophosphate (dbcAMP; Prasad and Hsie, 1971). The cells form axon-like processes (Fischer et al., 1986) which express neurofilament proteins (Shea et al., 1988), and the axonal markers MAP1B and Tau1 (Shea and Beermann, 1994).

Pax6 is known to be important in the process of neuronal differentiation (Heins et al., 2002; Plaza et al., 1997; Scardigli et al., 2003; Warren and Price, 1997), but the exact role of Pax6 in this process is still unknown. If the over-expression of Pax6 is sufficient to induce neuronal differentiation in the Neuro2A cell line, the effects of this over-expression should be similar to the effects of dbcAMP treatment.

4.2.4: The role of N-terminally truncated Pax6

Chapter 3 describes the use of western blot to detect Pax6-specific protein bands in *Sey/Sey* mice. These mice have a mutation in the *Pax6* gene, leading to the introduction of a STOP codon just 5' of the HD (see **Figure 1.3**).

As shown in **Figure 3.23**, a 32kDa protein is seen in E12.5 *Sey/Sey* brain extract, which could potentially be the result of internal translation initiation from an ATG residue 3' of the STOP mutation. This short Pax6 protein is also observed in WT E12.5 brain, and is therefore likely to be a functional Pax6 isoform (see **Figure 3.5**).

The protein produced from such an internal translation initiation event would have a functional DNA-binding domain, the HD, and a functional TAD. However, it would lack the N-terminal DNA-binding domain, the PD. The existence of *Pax6* transcripts in the mouse which are lacking the PD (Gorlov and Saunders, 2002; Kleinjan et al., 2004; Mishra et al., 2002), and of a "paired-less" form of *Pax6* in *C. elegans* (Zhang and Emmons, 1995) lend further functional significance to this putative protein.

Dimerisation of Pax proteins *via* the HD has been demonstrated (Wilson et al., 1993). Although many Pax6 HD-DNA interactions are thought to occur co-operatively with an intact PD (Mikkola et al., 2001; Mishra et al., 2002; Singh et al., 2000), this PD can be provided *in trans* by a different Pax6 molecule (Miskiewicz et al., 1996). Therefore, it is possible that "paired-less" Pax6 can dimerise with full-length Pax6, or other HD-containing genes, and affect the transactivation of target sequences. It is also not inconceivable that a "paired-less" Pax6 could bind DNA as a monomer, *via* the HD, and also exert a transactivational effect.

4.2.5: Aims

The aim of Chapter 4 was to study the effects of Pax6 over-expression in a cell culture system.

In particular, *Pax6-5a*, *Pax6+5a* and 5'-truncated *Pax6* constructs were introduced into cell lines both with and without endogenous Pax6 expression. If a difference in phenotype was seen after the introduction of these three constructs, this could be taken as an indication that different Pax6 isoforms had different effects on cellular behaviour.

Phenotypic analysis of Pax6 over-expressing cell lines was carried out with two main aims, to assess the effects of Pax6 isoform over-expression on autoregulation, and on neuronal differentiation.

4.3: Materials and Methods

4.3.1: Routine cell culture techniques

4.3.1.1: Maintenance of immortalised cell lines

The murine neuroblastoma line, Neuro2A, was obtained from the European Collection of Cell Cultures (ECACC; 89121404) and maintained in Minimal Essential Medium (MEM). The murine fibroblast line, NIH3T3 was also obtained from ECACC (93061524) and maintained in Dulbecco's Minimal Essential Medium (DMEM). The human lens cell line, H36CE2, was a kind gift from A. Seawright (MRC Human Genetics Unit, Edinburgh), and maintained in DMEM. The human glioblastoma line, U373-MG was obtained from ECACC (89081403), and maintained in DMEM.

All cells were routinely cultured at $37^{O}C$, 5% CO_2. When confluent, cells were dissociated in trypsin-EDTA, resuspended in 10 volumes of culture medium, and seeded onto fresh culture dishes at 1:2 (H36CE2) or 1:10 (Neuro2A, NIH3T3, U373-MG).

4.3.1.2: Freezing and defrosting cell lines

Cells were grown to confluence, dissociated in trypsin-EDTA and resuspended in 10 volumes of culture medium. They were then pelleted by centrifugation at 1000rpm for 5 minutes. Pellets were resuspended in 1ml freezing medium and transferred to a sterile cryovial. Freezing was achieved slowly to minimise cell damage, with cryovials being placed at $-20^{O}C$ for 2 hours, $-70^{O}C$ for up to 4 weeks, and stored in the long term in liquid nitrogen.

96-well plates were frozen by aspirating all culture medium, adding 200µl freezing medium per well, and freezing as above.

Cells frozen in cryovials were defrosted at $37^{O}C$, rescued in culture medium and seeded in a $25cm^2$ flask. Cells were allowed to adhere overnight, and culture medium was aspirated and replaced after 24 hours to avoid DMSO toxicity.

Cells frozen in 48-well plates were defrosted at 37^{O}C, and rescued in 1ml culture medium. This medium was immediately aspirated to remove most DMSO, leaving ~100µl in each well to ensure cells did not shear off. Fresh medium was added, and cells were allowed to recover overnight.

4.3.1.3: Transfection

Transient transfections were carried out initially to assess the efficiency with which cell lines overexpressed introduced genes. After the selection of appropriate cell lines, these were transfected with Pax6-5a and Pax6+5a over-expression constructs, and stable cell lines were created.

Cells were transfected with the plasmid pEGFPN1 (***Clontech***), which contained Enhanced Green Fluorescent Protein (EGFP) under the control of the strong viral CMV promoter. This allowed high levels of EGFP protein expression, and successfully transfected cells were easily visualised by microscopy after exposure to UV light at 488nm.

Cells were transfected using Lipofectamine 2000, according to the manufacturer's protocol. Briefly, cells were seeded at 5X10^{5} cells per well in 6-well plates 24 hours prior to transfection, in transfection medium. No antibiotic was added, as the lipofection reagent permeabilises cell membranes, and can render penicillin / streptomycin toxic to eukaryotic cells. Transfection efficiencies were highest using 8µl Lipofectamine and 10µg plasmid DNA (NIH3T3, U373-MG, H36CE2) or 8µl Lipofectamine and 4µg plasmid DNA (Neuro2A).

Transiently transfected cells were harvested 24 or 48 hours after introduction of the plasmid DNA.

4.3.2: Reverse-Transcriptase Polymerase Chain Reaction (RT-PCR)

RT-PCR was performed on tissue culture cells to assess their mRNA content (see Appendix 2 for primer sequences, product sizes and optimal annealing temperatures).

4.3.2.1: cDNA synthesis

In order to assess the presence or absence of *Pax6* mRNA in tissue culture cells, or to isolate *Pax6* cDNA for cloning, cDNA was synthesised from total RNA using Superscript reverse transcriptase (***Invitrogen***) and oligo d(T) primers. Oligo d(T) primers are complementary to poly(A) stretches found at the 3' end of all mRNAs, allowing synthesis of a cDNA population representing the entire mRNA population of a cell line.

cDNA synthesis was performed on 5µl total RNA. RNA was not quantitated prior to cDNA synthesis, as most RT-PCRs were designed only to measure the presence or absence of Pax6 mRNA, and in the case of real-time quantitative RT-PCR, a GAPDH internal standard was used to facilitate quantitation.

4.3.2.2: RT-PCR

To assess the *Pax6* mRNA expression status of cell lines, PCR was performed using *Taq* DNA polymerase. This allowed fast cDNA amplification, where high fidelity was not required as the product was not being used in any downstream cloning applications. Typically, 1µl cDNA was used in a 20µl PCR reaction with a 250nM concentration of each primer, and 200µM of each dNTP.

Colony PCRs were performed on bacterial clones to test for the presence of a cloned sequence, and assess cloning efficiency. PCRs were performed using *Taq* DNA polymerase. The proofreading ability of *Pfu* polymerase was not required, as the PCR products were not being used for any downstream applications. PCR reactions were conducted in 20µl volumes, and a sterile pipette tip was dipped in each bacterial colony, then in the corresponding PCR reaction. In this way, enough bacterial DNA was transferred to ensure amplification of target DNA if the transformation reaction had been successful.

4.3.2.3: Agarose gel electrophoresis

Agarose gel electrophoresis was used to visualise PCR products, and in some cases to separate target bands for gel extraction and cloning. For PCR products below 600bp, 1.5% agarose gels were used. For larger fragments, 0.8% gels were used. All gels contained ethidium bromide to allow visualisation of DNA under ultraviolet light.

Where PCR products were required for downstream cloning applications, gels were visualised with short exposures to low levels of ultraviolet light, in order to minimise DNA damage. Bands were excised using sterile scalpel blades to avoid contamination.

DNA was removed from agarose gel using a gel extraction kit (***Qiagen***). This involved dissolving the agarose in buffer at 55^0C, running the solution through a column to allow binding of DNA, washing away salts and other contaminants, and eluting the DNA in 50µl ddH_2O.

4.3.3: Quantitative RT-PCR (Q-PCR)

Quantitative RT-PCRs were performed using an Opticon DNA engine, to determine the relative levels of Pax6 mRNA in transiently and stably transfected cells. Separate primers were specifically designed for use in Q-PCR (see Appendix 2 for primer sequences, product sizes and optimal annealing temperatures). The optimal product size is 120bp, and Q-PCR reactions were optimised to proceed without the formation of primer dimmers or ectopic bands, which would interfere with quantitation.

PCRs were carried out in the presence of SYBR Green (***Qiagen***), a DNA intercalating reagent which binds to the minor groove of double-stranded DNA. In solution, fluorescence by the SYBR Green reagent is minimal. When double-stranded DNA PCR products are created, SYBR Green can bind, and fluoresces at 495nm.

After 35 PCR cycles, a melting curve of the PCR product was obtained by measuring the fluorescence emitted at decreasing temperature increments. At high temperatures, all DNA-DNA duplexes are denatured. SYBR Green cannot bind, therefore fluorescence falls to baseline levels. As the temperature falls, DNA-DNA duplexes can form at the optimal annealing temperature of the PCR product, SYBR Green can bind, and a rise in fluorescence is seen. A plot of fluorescence against temperature should form a sigmoidal curve. If a smooth sigmoid was seen, this was an indication that the only double-stranded DNA present in the PCR product was dimerised product, and no primer dimers or ectopic bands were contaminating the reaction. All fluorescence was therefore a result of the desired PCR product. Reaction conditions were optimised until a smooth sigmoidal melting curve was seen after each reaction.

A calibration standard was created for each primer set by serial dilution of the most concentrated DNA template. The number of cycles after which the fluorescence of a reaction rose above baseline was designated as the cycle threshold, c(t). As more DNA was included in a reaction, the c(t) dropped, and a calibration curve of volume of DNA against c(t) was plotted. The c(t) of each sample DNA was then plotted onto this calibration curve, thus allowing relative DNA quantitation across PCR reactions.

4.3.4: Inserting full-length *Pax6+5a* and *Pax6-5a* into pCMV-Script for over-expression analysis

Full-length *Pax6+5a* and *Pax6-5a* were cloned into pCMV-Script (***Stratagene***) for use in protein over-expression studies. The pCMV-Script vector contains a multiple cloning site 3' of the human cytomegalovirus (CMV) immediate early promoter, and 5' of an SV40 polyadenylation site. This allows over-expression of any gene placed in the correct orientation in the multiple cloning site. The vector also contains a neomycin-resistance gene which confers resistance to G-418, allowing selection for stable transfectants.

Full-length *Pax6* was removed from pJP1.3 and pJP1.11 (see Chapter 3) by digestion with *Xho*I and *Bam*HI, and inserted into linearised pCMV-Script using T4 DNA ligase. Ligation products were used to transform chemically-competent TOP-10 *E.coli*, and colonies were grown overnight at 37^{O}C with kanamycin (50μg.ml^{-1}) to allow only the growth of transformed bacteria. The human and murine Pax6 proteins are identical in sequence, therefore cDNAs cloned from the U373-MG cell line were appropriate for over-expression analysis in both human and murine cell lines.

The full length *Pax6* insert in both pJP13.1 (pCMV-Pax6+5a) and pJP14.1 (pCMV-Pax6-5a) was then sequenced in both directions to confirm that the intended *Pax6* sequence was present, and that no mutations had been introduced during the cloning process. As expected, the same synonymous substitutions were found as in the donor plasmids pJP1.3 and pJP1.11 (see Section 3.3.6). The plasmids pJP13.1 and pJP14.1 were used for all further over-expression studies, and for the creation of stable cell lines over-expressing Pax6.

See **Figure 4.1** for plasmid maps of pJP13.1 and pJP14.1

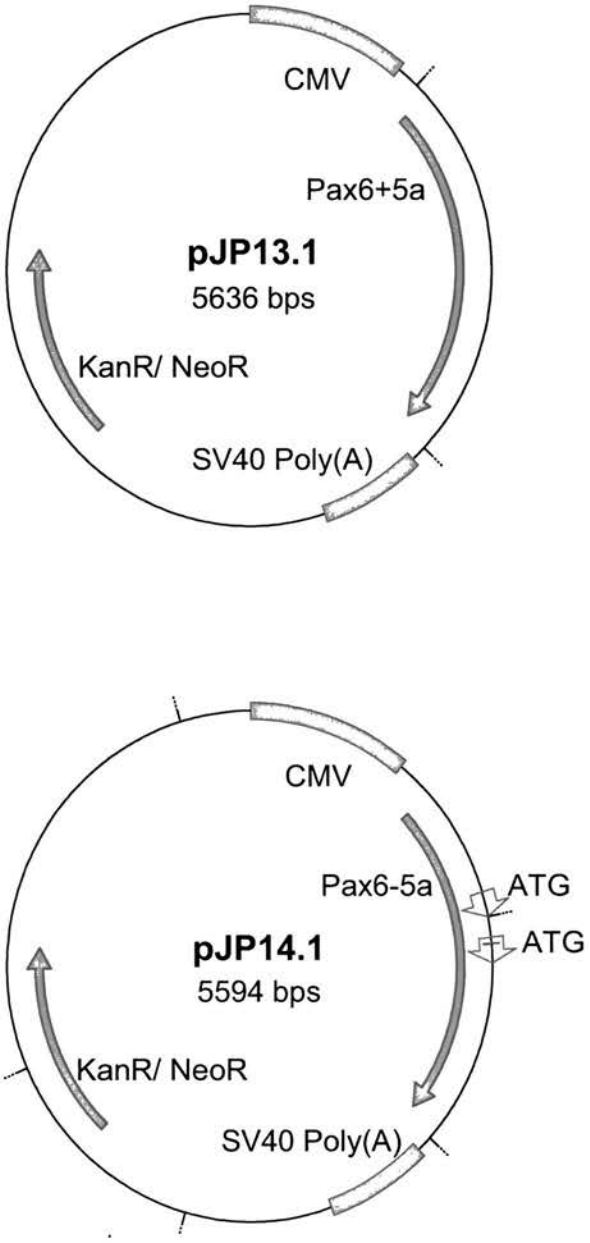

Figure 4.1: pJP13.1 / pJP14.1, full-length Pax6+5a / Pax6-5a in pCMV-Script. Red arrows: Human Pax6 sequence for overexpression, and the Kanamycin resistance gene. Blue bars: Strong viral CMV promoter and SV40 Poly(A) sequences that allow efficient transcription and post-transcriptional modification of the insert.

4.3.5: Inserting 5'-truncated *Pax6* into pCMV-Script for over-expression analysis

pJP15.12 was created to force Pax6 translation initiation from the internal ATG at amino acid residue 216 of the full-length protein. This ATG is 3' of the stop codon in the *Sey* mutation, and a hypothetical Pax6 protein could be made in the *Sey/Sey* mouse if translation could initiate here (see **Figure 1.3**)

Figure 4.2 outlines the cloning strategy used to construct pJP15.12. The donor plasmid pJP14.1 (**Fig 4.2, A**), containing full-length *Pax6-5a* in pCMV-Script, was first cut with *Bci*VI. *Bci*VI cuts within the *Pax6* locus, 5' of the ATG from which translation could initiate in the *Sey/Sey* mouse, but 3' of all other internal ATGs. In that way, if translation were seen from this product, it could only have initiated from the desired start codon. A protein made from this plasmid should be identical in sequence to the hypothetical protein that could be produced by internal translation initiation in the *Sey/Sey Pax6* gene.

The host vector, pCMV-Script (**Fig 4.2, D**) had no *Bci*VI-compatible restriction endonuclease sites, therefore the insert needed to be modified before ligation could take place. All *Bci*VI fragments were treated with T4 DNA polymerase, taking advantage of the fact that this enzyme possesses 3' exonuclease activity, to cut off the single base pair 3' overhang created by *Bci*VI digestion.

All four modified *Bci*VI digestion products were then subjected to a second restriction endonuclease digestion with *Xho*I **(Fig 4.2, B)**. This cuts only once within pJP14.1, immediately 3' of the Pax6 gene, thus cutting the largest *Bci*VI fragment in two, and producing an 820bp stretch of DNA with a blunt 5' end, and a *Xho*I-compatible 3' end (**Fig 4.2, C**). All other fragments present at this stage had two blunt ends.

pCMV-Script was then digested with *Xho*I and the blunt-cutting enzyme *Eco*RV, leaving a blunt DNA end 5' of the desired insertion site, and a *Xho*I-compatible end 3' of the insertion site.

A ligation was performed between the four modified *Bci*VI digestion products and the linearised pCMV-Script vector (**Fig 4.2, F**), and ligation could only occur

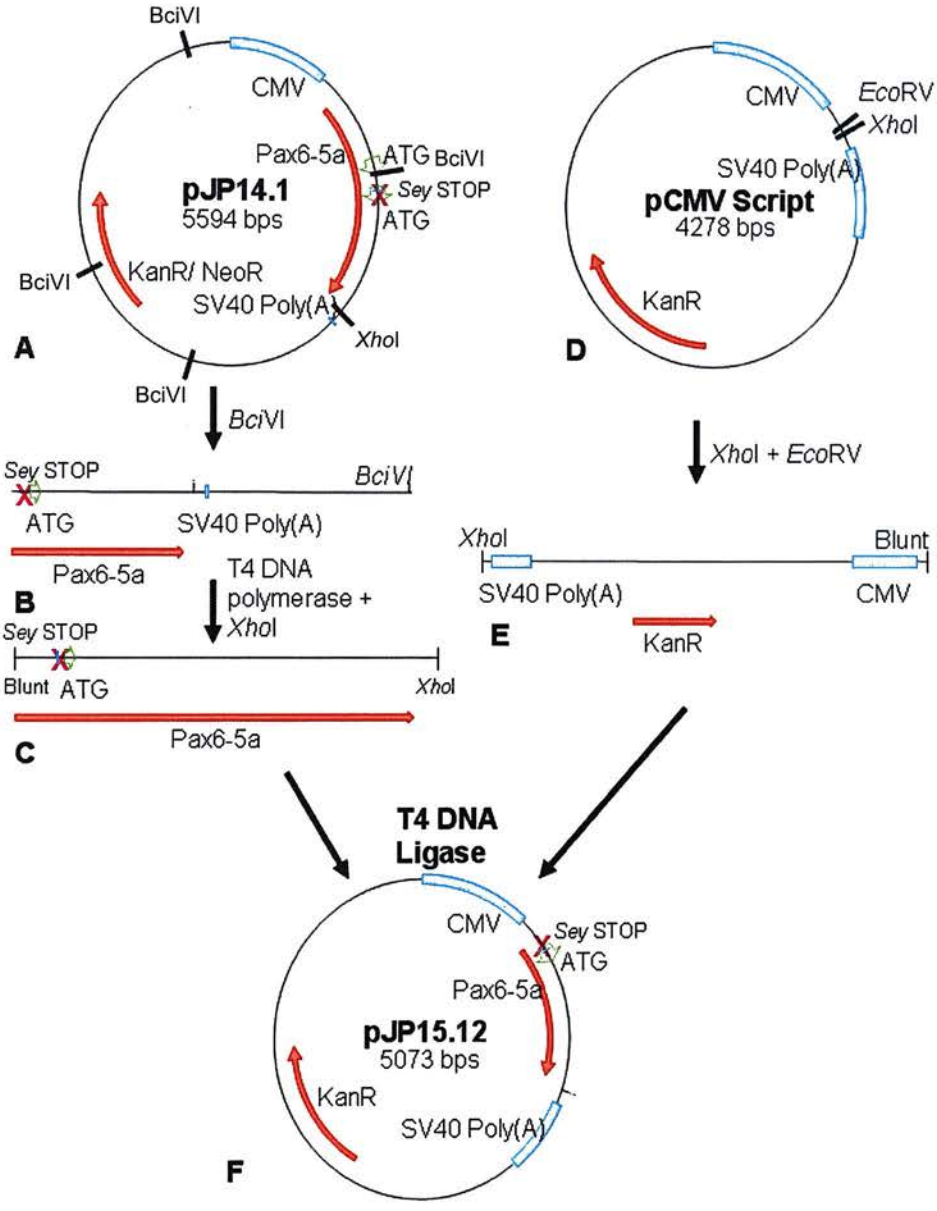

Figure 4.2: Construction of pJP15.12, 5'-truncated Pax6 in pCMV-Script. A, pJP14.1 donor plasmid showing in-frame ATGs within Pax6 (green arrows), and the STOP codon mutation in the *Sey* mouse (magenta X). B, *Bci*VI digestion product. C, 5'-truncated Pax6. D, pCMV-Script host plasmid. E, pCMV-Script after linearisation. F, pJP15.12

between the compatible 5'-truncated *Pax6* fragment and the host vector. This ligation was directional, as the insert could only ligate into the vector in the sense orientation. Ligation products were used to transform chemically-competent TOP-10 *E.coli*, and colonies were grown overnight at 37^{O}C with kanamycin (50μg.ml^{-1}) to allow only the growth of transformed bacteria.

The short *Pax6* insert in pJP15.12 was then sequenced in both directions to confirm that the intended *Pax6* sequence was present, and that no mutations had been introduced during the cloning process. As expected, the same synonymous substitution was found as in the donor plasmid pJP14.1. The plasmid pJP15.12 was used for all further over-expression studies, and for the creation of stable cell lines overexpressing 5'-truncated *Pax6*.

4.3.6: Creating stably transfected lines

Neuro2A and NIH3T3 cells were transfected as described in Section 4.2.1, with plasmids pJP13.1 and pJP14.1. Neuro2A was also transfected with pJP15.12. All plasmids were linearised with *Xho*I to allow integration into the host genome.

Cells were dissociated after 48 hours, and seeded in 10cm Petri dishes at 1:50, 1:100 and 1:200, in order to obtain clonal colonies of cells. Culture media were then supplemented with G-418 at 500μg.μl^{-1} (NIH3T3) (Roccato et al., 2003; Santos-Ocampo et al., 1996) or 600μg.μl^{-1} (Neuro2A) (Goshima et al., 1993; Kojima et al., 1996).

The active component of G-418, Geneticin, is derived from the antibiotic gentamicin and is usually toxic to eukaryotic cells. All over-expression plasmids contained the *Neo* DNA sequence, driven by the strong SV40 viral promoter. In successfully transfected cells, transcription of the *Neo* sequence led to expression of the bacterial aminoglycoside phosphotransferase 3' (I) gene, conferring G-418 resistance. Untransfected cells were killed.

Clones were allowed to grow for up to 2 weeks, before being picked with a sterile pipette tip and seeded onto 48-well plates for screening and maintenance of stable transfected cell lines.

4.3.7: Immunoblotting

Protein extracts from cell lines were immunoblotted for Pax6 to establish endogenous levels of expression, and to demonstrate and quantitate over-expression in stable cell lines.

4.3.7.1: Harvesting protein from tissue culture cells

For routine protein extraction, cells were seeded at $1X10^6$ cells.well^{-1} in 6-well plates, and collected after 48 hours.

All steps were carried out at $4^{O}C$ to avoid protein degradation

Cells were washed twice in ice-cold PBS to remove all traces of foetal bovine serum from the culture medium. Cells were then bathed in 1ml ice-cold PBS, scraped off using a sterile, disposable cell scraper, and pelleted. The pellet was then resuspended in 20-100µl TENT buffer with protease inhibitors. The mixture was homogenised using a motorised homogeniser and a disposable mini-pestle to break cellular and nuclear membranes, and left to lyse for 20 minutes. The lysate was then clarified by centrifugation, and the supernatant was stored at $-70^{O}C$.

Immunoblotting was carried out as described in Chapter 3.

4.3.8: Immunocytochemistry on tissue culture cells

Immunocytochemistry was performed on fixed monolayers of tissue culture cells to determine the sub-cellular localisation of both endogenous and over-expressed Pax6 by light- and confocal-microscopic analysis. This technique was also used to analyse the expression of genes whose expression is thought to be affected by Pax6, in order to determine the specific effects of Pax6 over-expression in immortalised cell lines.

In addition, immunocytochemistry was performed on fixed, dissociated tissue culture cells to ascertain the level of heterogeneity of Pax6 over-expression, and as a second measure of the level of over-expression, alongside immunoblotting.

Stably transfected cells were seeded at $5X10^5$ cells.well^{-1} on glass coverslips in 6-well plates, or $5X10^4$ cells.well^{-1} in 4-well dishes, and fixed after 48 hours. To assess transient transfections, cells were seeded at $1X10^5$ cells.well^{-1} on glass coverslips in 6-well plates, and transfections were performed 24 hours later.

Cells were fixed 48 hours after transfection, to allow maximal transcription and translation from the over-expression construct.

Monolayer cells were either fixed *in situ* for analysis by microscopy, or they were trypsinised, resuspended in PBS, and fixed as dissociated cells in solution to allow visualisation by flow cytometry.

All cells were fixed in 4% PFA for 30 minutes at room temperature and permeabilised in 100% ice-cold methanol for 10 minutes (anti-Pax6 PD) or 0.1% triton-X-100 (all other primary antibodies). Primary antibody incubations were carried out at $4^{O}C$ overnight in blocking buffer. Secondary antibody incubations were carried out at room temperature for an hour in the dark to avoid bleaching. For confocal microscopy, cells were counter-stained with TOPRO3, a fluorescent nuclear marker. Pax6-positive cells were visualised by fluorescence using either confocal microscopy for cells on coverslips or in 4-well plates, or an Epics-XL sorter (***Coulter***) for dissociated cells.

4.3.9: cAMP-Induced differentiation of Neuro2A cells

Neuronal differentiation was induced in the Neuro2A murine neuroblastoma cell line, both in stably transfected cells and negative, untransfected cells. The aim of this experiment was to see whether the introduction of *Pax6+5a* or *Pax6-5a* affected their capacity for neuronal differentiation.

2'-O-dibutyryladenosine 3', 5'-cyclic monophosphate (dbcAMP) was introduced to cells at a concentration of 1mM, and cells were harvested after 72 hours. Cells were then fixed in 4% PFA, and immunostained for a number of markers of neuronal differentiation. After counterstaining to visualise unstained cells, all cells were counted, and the number of differentiated cells was compared across genotypes, both with and without the addition of dbcAMP.

4.4: Results: Assessing the suitability of the cell lines H36CE2, Neuro2A, NIH3T3 and U373-MG for the creation of stable Pax6 transfectants

4.4.1: Morphology

All four cell lines cells grew well in standard tissue culture conditions, although the human lens cell line, H36CE2, grew more slowly than the other three, and could not be seeded at below 50% density without detrimental effects. The morphology of each cell line was as previously described (**Figure 4.3**), with a certain amount of heterogeneity in the H36CE2 and Neuro2A cell lines.

4.4.2: Pax6 expression by western blot

Western blot was performed on whole cell extract from each cell line to assess their Pax6 expression status. The anti-Pax6 HD antibody (see **Figure 3.1** for an explanation of the anti-Pax6 primary antibodies used in this study, and the epitopes against which they are directed) was used, as it detects all known Pax6 isoforms. Results of this western blot analysis are shown in **Figure 4.4**. As described by Turque et al. (1994) and Okladnova et al., (1998), the NIH3T3 line does not express Pax6. The other three cell lines, however, did contain Pax6 protein. Chapter 3 contains a detailed description of the Pax6 bands observed by western blotting, and the protein sequence thought to be responsible for each. Full-length Pax6+5a and Pax6-5a migrate as a 48/46kDa doublet, and their location on each gel is clear from a comparison with the positive control lanes, which contain *in vitro* synthesised Pax6-5a and Pax6+5a. Shorter Pax6 forms are seen in all three cell lines, but are most abundant in U373-MG.

4.4.3: Pax6 expression by immunocytochemistry

Anti-Pax6 immunocytochemistry was performed on all four cell lines to determine the subcellular location of Pax6 expression, and whether either location or expression levels varied between cells (**Figure 4.5**). NIH3T3 cells are entirely negative, as supported by western blot data. Neuro2A cells do express Pax6, but at low levels. Expression appears to be nuclear, and mostly uniform. U373-MG cells contain very

Figure 4.3 Morphology of untransfected cell lines, as observed by light microscopy. A, B, NIH3T3: Murine fibroblast cell line. Cells are homogeneous in size and shape, with a long cytoplasm that tapers away from the nucleus. C, D, Neuro2A: Murine neuroblastoma cell line, the majority of cells are homogeneous in size and shape, most are rounded with little cytoplasm, and have short dendrite-like processes. Occasionally larger cell types are observed (arrow). E, F, U373-MG: Human glioblastoma-derived cell line. Cells are largely homogeneous in size and shape, and have a thick, ruffling membrane at one pole. Lamellipodia are also seen (arrow). G, H, H36CE2: Human immortalised lens cell line. Cells were highly heterogeneous, often multinucleate, and spontaneously produced aggregates of lens-like, reflective material (arrow).

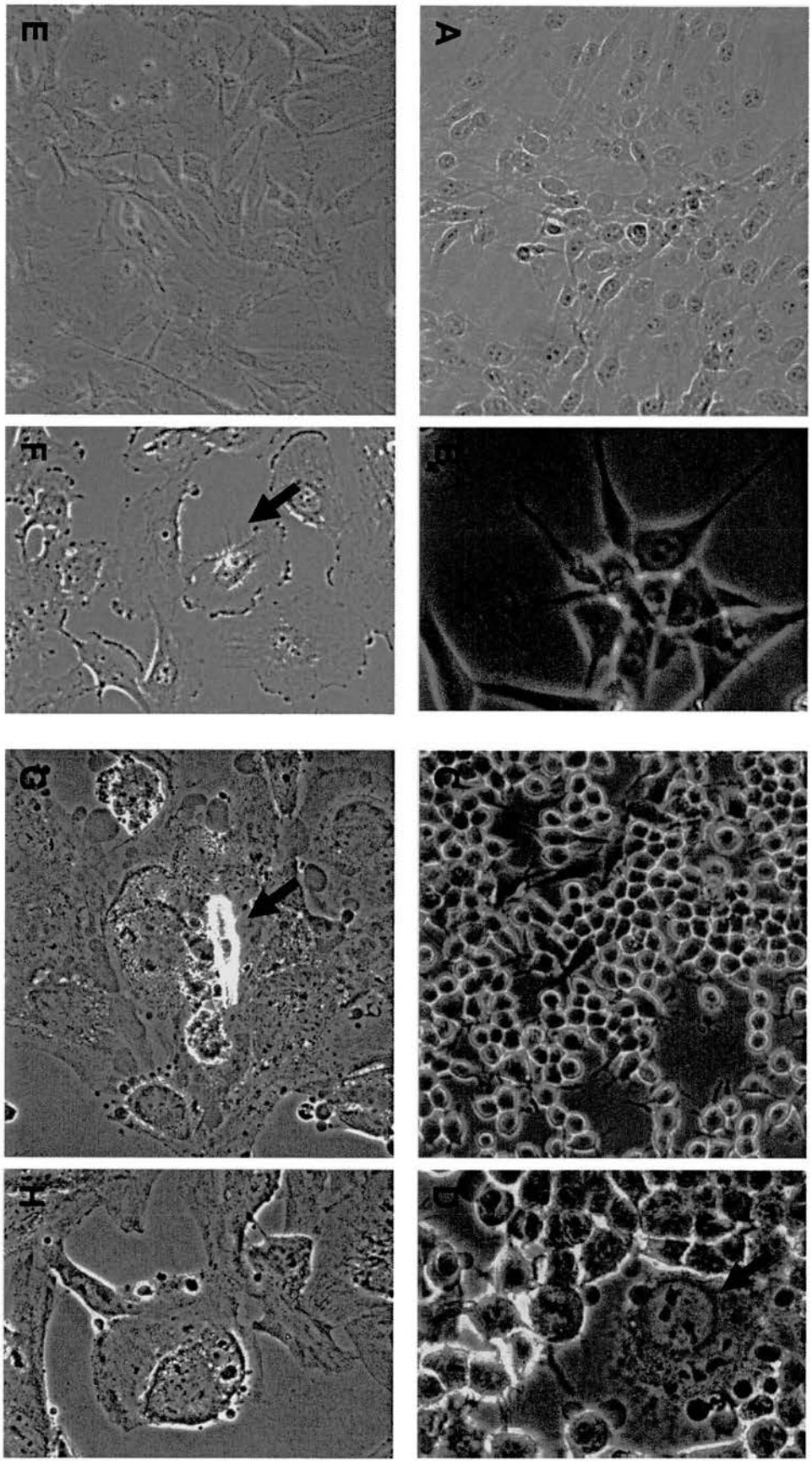
E
A
F
B
G
C
H
D

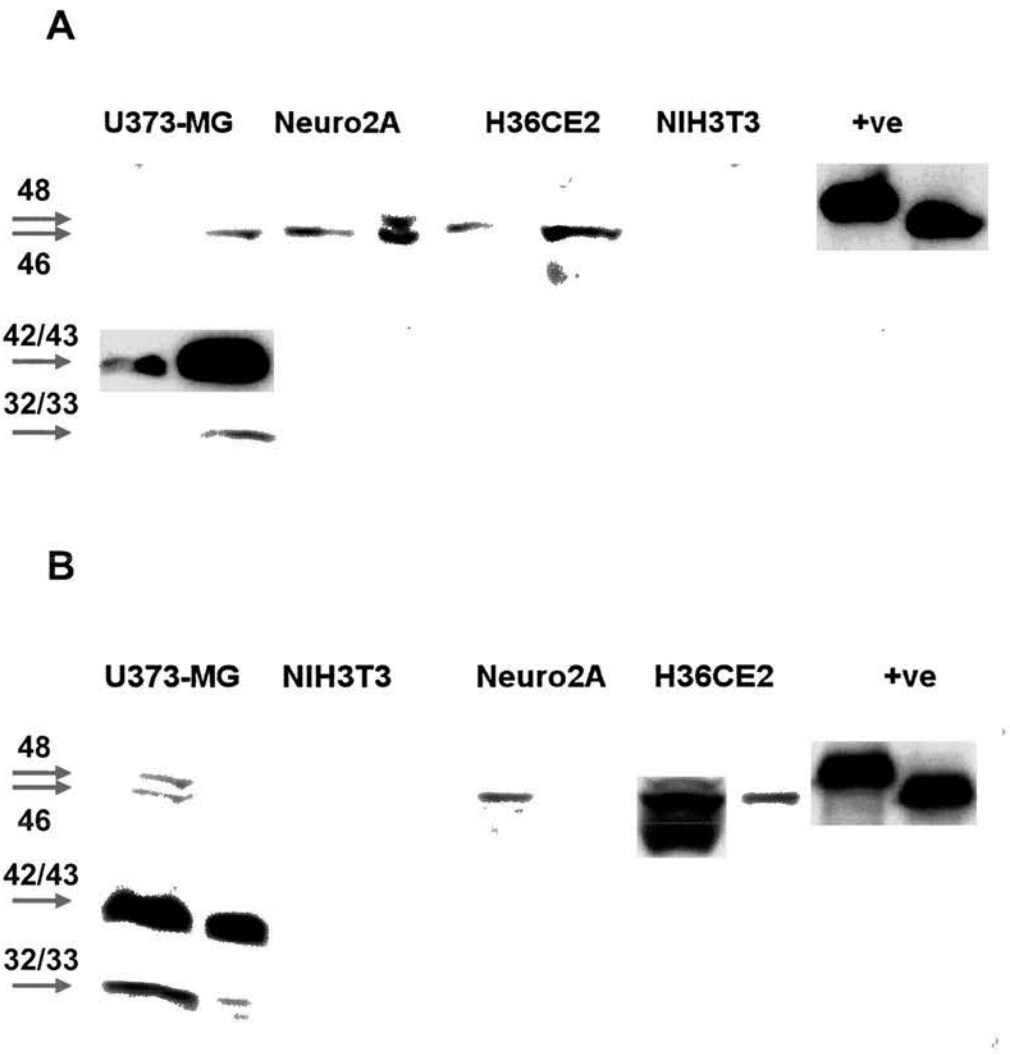

Figure 4.4: Pax6 expression in untransfected cell lines, by western blot. Two independent cell extracts from each line were analysed. A, B, separate repeats. +ve, *in vitro* synthesised positive control Pax6+5a (upper band) and Pax6-5a (lower band). Molecular weight of bands is indicated, in kDa. See Chapter 3 for further description of the numerous Pax6 bands. Full-length Pax6+5a and Pax6-5a are present in three of the four cell lines, with the highest concentration seen in the human lens line, H36CE2. Lower molecular weight Pax6 bands are seen in all three Pax6-positive lines, but are most abundant in the human glioblastoma cell line, U373-MG.

Figure 4.5 Anti-Pax6 immunocytochemistry on untransfected cell lines. A, NIH3T3 TOPRO-3 nuclear counterstain. B, NIH3T3 anti-Pax6 immuno, showing no detectable Pax6 (Pax6 signal would be green). C, Neuro2A TOPRO-3 nuclear counterstain. D, Neuro2A anti-Pax6 immuno, showing low-level Pax6 expression throughout all cells (Pax6 signal is green). E, U373-MG transmitted light image. F, U373-MG anti-Pax6 immuno, showing Pax6 signal just at the limits of detection (Pax6 signal is green). G, H36CE2 TOPRO-3 nuclear counterstain. H, H36CE2 anti-Pax6 immuno, variable, but generally high-level expression in all cells (Pax6 signal is red).

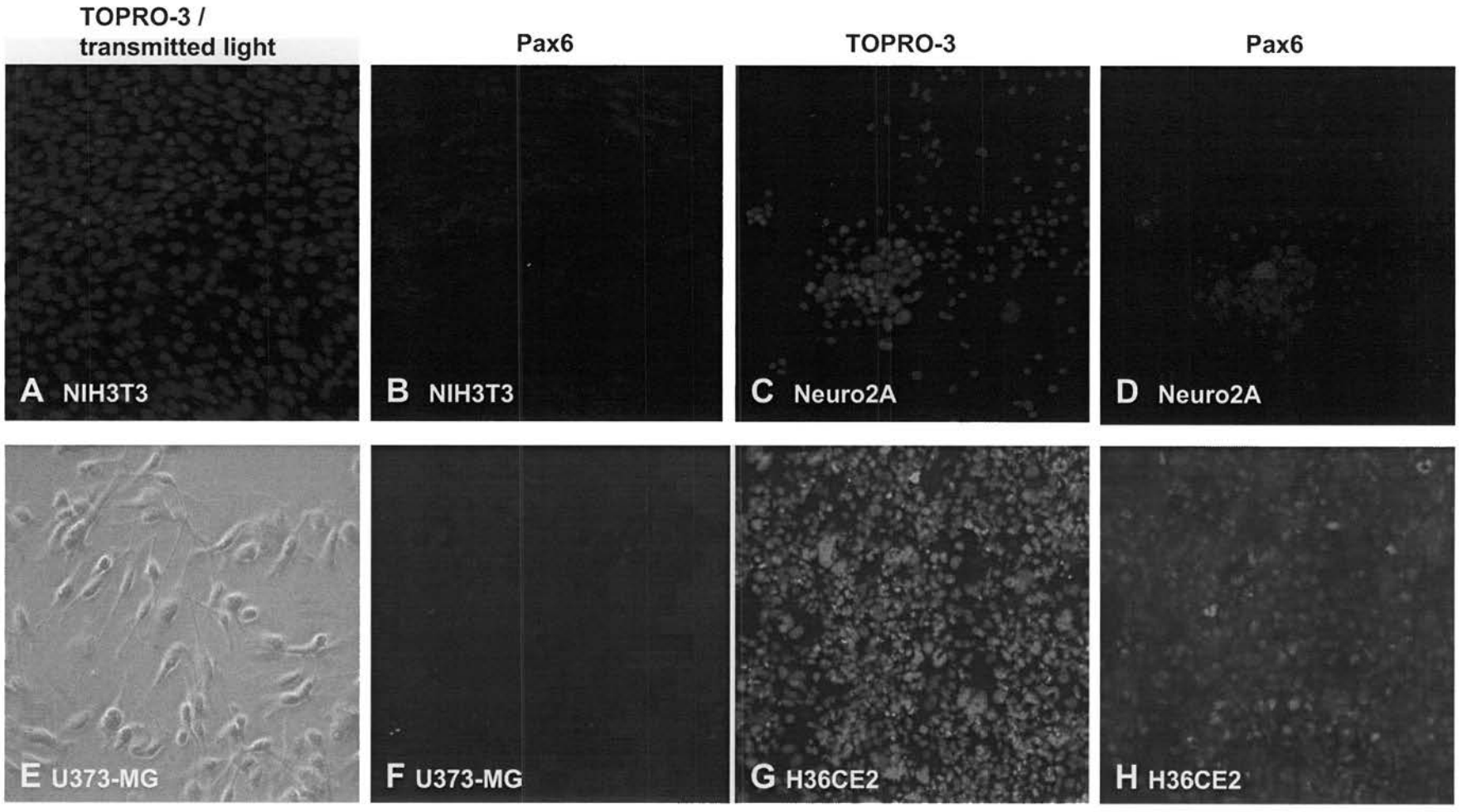
TOPRO-3 /
transmitted light
Pax6
TOPRO-3
Pax6
A NIH3T3
B NIH3T3
C Neuro2A
D Neuro2A
E U373-MG
F U373-MG
G H36CE2
H H36CE2

low levels of Pax6, at the limits of detection by immunocytochemistry. This is in contrast with western blot data, which shows reasonably high Pax6 expression in comparison with Neuro2A and H36CE2 protein extracts. This discrepancy may be due to the different primary antibodies used for the two techniques. For western blot, the anti-Pax6 HD antibody was used. This picks up a number of bands, and it is clear that a shorter form of Pax6 (~42/43kDa) is the most abundant in U373-MG cells. For immunocytochemistry, anti-Pax6 PD primary antibody was used. It is possible that the 42/43kDa band represents a "paired-less" form of Pax6, not recognised by this primary antibody. If that were the case, a weak signal might be expected from the low levels of full-length Pax6 present in the U373-MG cell line. The highest levels of Pax6 expression are seen in the H3CE2 cell line. As expected of a transcription factor, signal is largely nuclear. There is greater heterogeneity of Pax6 expression levels in this cell line, consistent with the greater heterogeneity of cell types.

4.4.4: Transfection efficiency

All four cell lines were transiently transfected with pEGFPN1 in order to qualitatively assess their transfection efficiency. **Figure 4.6** allows comparison of transfection efficiencies between the three cell lines. Transient transfections are most efficient in the Neuro2A line. A high percentage of cells are transfected, and EGFP expression is stronger than in the other three lines. The U373-MG line was also transfected with high efficiency on some occasions, as seen in **Fig 4.6**, but this was less repeatable. The NIH3T3 cell line consistently took in EGFP with a reasonably high efficiency, but protein expression is lower than seen in the other two lines. H36CE2 is the cell line least amenable to transfection, probably due to the heterogeneity of cell type, making it difficult to optimise conditions. Although some cells are seen to express high levels of EGFP, most are either untransfected, or only appear to express low levels of EGFP.

4.4.5: Selecting two cell lines for further study

On the basis of the above data, two cell lines were selected for further study, and to make stable clones with the *Pax6+5a*, *Pax6-5a* and 5'-truncated *Pax6* over-expression plasmids, pJP13.1, pJP14.1 and pJP15.12.

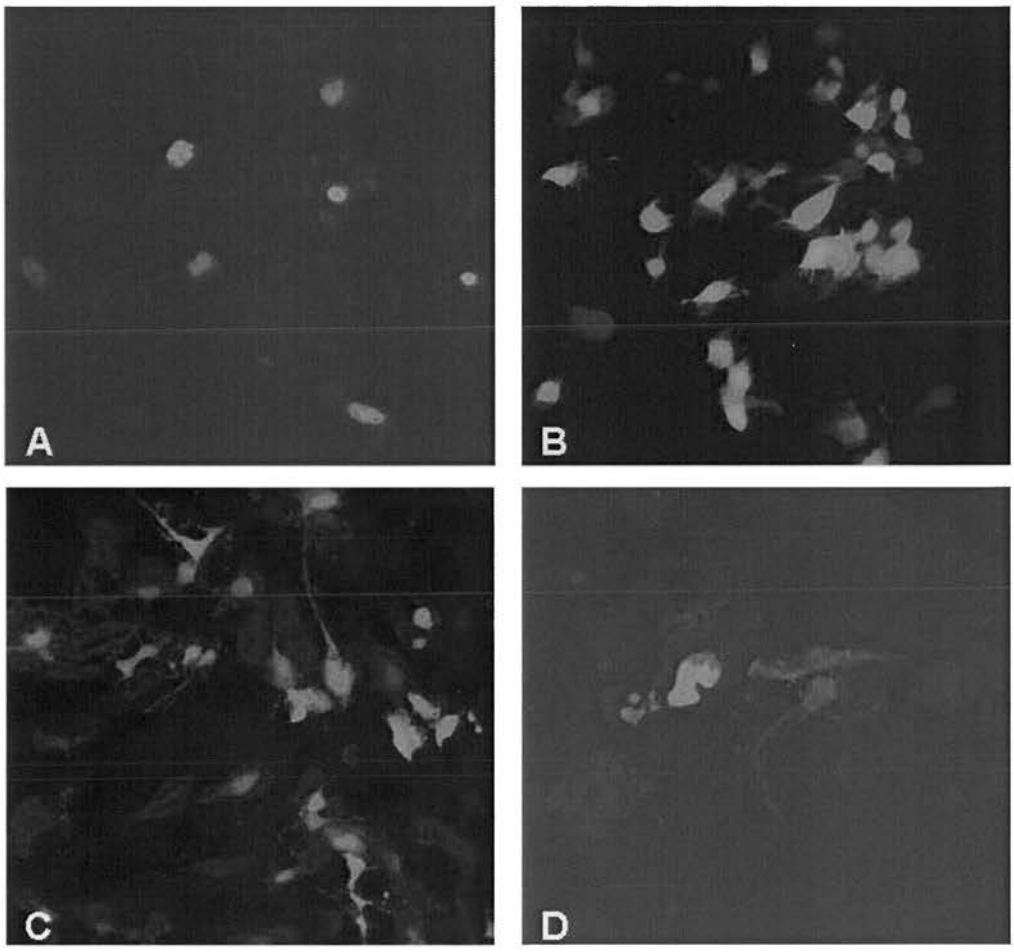

Figure 4.6 Cell lines after transient transfection with pEGFPN1. A, NIH3T3. B, Neuro2A. C, U373-MG. D, H36CE2

Neuro2A was chosen as it is easy to culture, grows rapidly, allows a high transfection efficiency, and endogenously expresses moderate levels of Pax6. NIH3T3 was chosen as it is easy to culture, grows rapidly, allows a reasonable transfection efficiency, and does not express endogenous Pax6.

These two cell lines also complement each other well as both are murine in origin; therefore species-specific differences could not interfere with the interpretation of a Pax6 over-expression phenotype.

The U373-MG cell line was excluded at this stage, because of its unreliable transfection efficiency.

The H36CE2 cell line was also excluded at this stage, because there were difficulties in culturing these cells. As their growth appears to be contact dependent, assays involving seeding at a low cell density and studying cell growth would be difficult to conduct.

4.5: Results: Transient over-expression of Pax6+5a and Pax6-5a in Neuro2A and NIH3T3 cells

Before making stable cell lines, Pax6 expression vectors were transiently transfected into NIH3T3 and Neuro2A cells. This was done to verify that Pax6 over-expression was indeed possible from the plasmids pJP13.1 and pJP14.1.

4.5.1: Quantitative RT-PCR (Q-PCR) analysis of *Pax6* over-expression in transiently transfected cells

The ability of the two plasmids to act as expression vectors was first assessed by Q-PCR. **Figure 4.7** and **Figure 4.8** show the results of PCR with primers specific to either *Pax6+5a* or *Pax6-5a*, after transfection with pJP13.1 (*Pax6+5a*) or pJP14.1 (*Pax6-5a*). All results are normalised to *Pax6* levels in the cell line with the lowest expression levels.

A) *Pax6+5a* levels in transfected and untransfected NIH3T3 cells	
Cells	***Pax6+5a* mRNA**
NIH3T3 + *Pax6-5a*	1.00
NIH3T3 + *Pax6-5a*	9.83
NIH3T3 + *Pax6+5a*	3230
NIH3T3 + *Pax6+5a*	13600
NIH3T3	5.17
NIH3T3	1.49

B) *Pax6-5a* levels in transfected and untransfected NIH3T3 cells	
Cells	***Pax6-5a* mRNA**
NIH3T3 + *Pax6-5a*	387
NIH3T3 + *Pax6-5a*	1420
NIH3T3 + *Pax6+5a*	1.67
NIH3T3 + *Pax6+5a*	25.7
NIH3T3	28.4
NIH3T3	1.00

Figure 4.7: Q-PCR analysis of Pax6 overexpression in transiently transfected NIH3T3 cells. A, *Pax6+5a* levels in NIH3T3. B, *Pax6-5a* levels in NIH3T3. RNA was collected from two separate transfections for each permutation. RNA levels that would be expected to rise are highlighted. All Pax6 mRNA levels are normalised to the lowest level, given an arbitrary value of 1 (All values expressed to 3 s.f.).

A) *Pax6+5a* levels in transfected and untransfected Neuro2A cells	
Cells	***Pax6+5a* mRNA**
Neuro2A + *Pax6-5a*	1.27
Neuro2A + *Pax6-5a*	1.10
Neuro2A + *Pax6+5a*	85.4
Neuro2A + *Pax6+5a*	159
Neuro2A	0.961
Neuro2A	1.04

B) *Pax6-5a* levels in transfected and untransfected Neuro2A cells	
Cells	***Pax6-5a* mRNA**
Neuro2A + *Pax6-5a*	17.2
Neuro2A + *Pax6-5a*	15.1
Neuro2A + *Pax6+5a*	0.778
Neuro2A + *Pax6+5a*	1.47
Neuro2A	0.780
Neuro2A	1.22

Figure 4.8: Q-PCR analysis of Pax6 overexpression in transiently transfected Neuro2A cells. A, *Pax6+5a* levels in Neuro2A. B, *Pax6-5a* levels in Neuro2A. RNA was collected from two separate transfections for each permutation. RNA levels that would be expected to rise are highlighted. All Pax6 mRNA levels are expressed as a proportion of untransfected Neuro2A levels (All values expressed to 3 s.f.).

Transfection efficiencies varied between runs, and these results are taken from just one run, but the effects of *Pax6* over-expression were clear. The introduced *Pax6* cDNA was upregulated by approximately 100-fold (*Pax6+5a*) or 16-fold (*Pax6-5a*) in the Neuro2A cell line. The NIH3T3 cell line also demonstrated marked up-regulation of the introduced transcript. Although this cell line does not express Pax6 protein, low levels of *Pax6* mRNA were occasionally observed by RT-PCR. Introduction of a *Pax6* over-expression construct caused a dramatic up-regulation in this mRNA level, by up to13,000-fold.

Due to the different PCR kinetics of the two reactions, comparisons could not be drawn between *Pax6-5a* and *Pax6+5a* levels, even within the same sample. It was consistently seen, however, that *Pax6+5a* up-regulation was more dramatic than *Pax6-5a* up-regulation in both cell types.

These results prove that the *Pax6* expression vectors pJP13.1 and pJP14.1 were capable of inducing *Pax6* mRNA over-expression in transfected cells.

4.5.2: Immunocytochemical analysis of Pax6 over-expression in transiently transfected Neuro2A cells

Transient transfections were performed to introduce pJP13.1 (*Pax6+5a*), pJP14.1 (*Pax6-5a)* and pJP15.12 (5'-truncated *Pax6*) into both the NIH3T3 and the Neuro2A cell lines. Over-expression was then analysed by immunocytochemistry, to ensure that a Pax6 protein product was indeed over-expressed in transfected cells, to get an idea of levels of over-expression within a successfully transfected cell, and to look at sub-cellular localisation of Pax6.

Untransfected NIH3T3 cells have no detectable Pax6 protein (**Figure 4.5**). Introduction of all three constructs leads to a high level of Pax6 expression in a few successfully transfected cells. The level of Pax6 expression seems high, as a comparison between **Figure 4.9 B, C, D** and **Figure 4.9 E** demonstrates. Untransfected Neuro2A cells express some Pax6, but signal is much weaker than in transfected NIH3T3 cells. Signal is mostly nuclear, which is consistent with the role of Pax6 as a transcription factor, but some cytoplasmic staining is observed. Interestingly, signal is observed in cells transfected with pJP15.12 (5'-truncated

Figure 4.9 Anti-Pax6 immunocytochemistry on cell lines transiently transfected with pJP13.1 (*Pax6+5a*), pJP14.1 (*Pax6-5a*), and pJP15.12 (5'-truncated *Pax6*). Blue, TOPRO-3 nuclear counterstain. Green, anti-Pax6 PD immunocytochemistry. A, NIH3T3 untransfected. B, NIH3T3 + *Pax6+5a*. C, NIH3T3 + *Pax6-5a*. D, NIH3T3 + 5'-truncated *Pax6*. E, Neuro2A untransfected. F, Neuro2A + *Pax6+5a*. G, Neuro2A + *Pax6-5a*. H, Neuro2A + 5'-truncated *Pax6*.

NIH3T3
Neuro2A
Untransfected
Pax6+5a
Pax6-5a
5'-truncated Pax6
A
B
C
D
E
F
G
H

Pax6; **Figure 4.9 D, H**). The primary antibody used for immunocytochemistry is directed against the Pax6 paired domain, but the protein product from pJP15.12 is a pairedless form, with translation initiating just 5' of the homeodomain. Therefore, any Pax6 signal seen in over-expressing cells must be a result of N-terminally truncated Pax6 acting to up-regulate full-length Pax6 from the endogenous genomic locus. This was later verified in stable cell lines (see Section 4.6.2).

Although levels are low, Pax6 signal is observed in untransfected Neuro2A cells, as was also seen in **Figure 4.5**. Introduction of all three constructs leads to a high level of Pax6 expression in a few successfully transfected cells. Signal is again largely nuclear, but some cytoplasmic staining is seen. **Fig 4.9 G** shows Pax6 labelling in a cellular process, which was observed on a number of occasions. Again, as with the NIH3T3 cell line, introduction of pJP15.12 into Neuro2A cells leads to an up-regulation of endogenous, full-length Pax6.

4.5.3: Western blot analysis of Pax6 over-expression in transiently transfected Neuro2A cells

Transient transfections were also performed to introduce pJP13.1 and pJP14.1 into the Neuro2A cell line, followed by western blot analysis (**Figure 4.10**). This was done to ascertain that Pax6 protein was over-expressed, to get an idea of levels of over-expression within a population of successfully and unsuccessfully transfected cells, and to check that the correct isoform was being expressed, i.e. Pax6+5a from pJP13.1, and Pax6-5a from pJP14.1.

Untransfected Neuro2A cells can be seen to express both splice variants, at a low level. Cells transfected with *Pax6-5a* express higher levels of Pax6-5a, as would be expected; however they no longer appear to express Pax6+5a, indicating that the addition of Pax6-5a might lead to the down-regulation of the other isoform. Cells transfected with *Pax6+5a* express higher levels of both splice variants than untransfected cells. This is likely to be due to Pax6+5a up-regulating the cell's endogenous Pax6-5a. It is not possible to ascertain whether the raised Pax6+5a levels in this case are entirely due to expression of the introduced plasmid, or whether some of the increase in signal is due to an increase in Pax6+5a expression from the endogenous genomic locus.

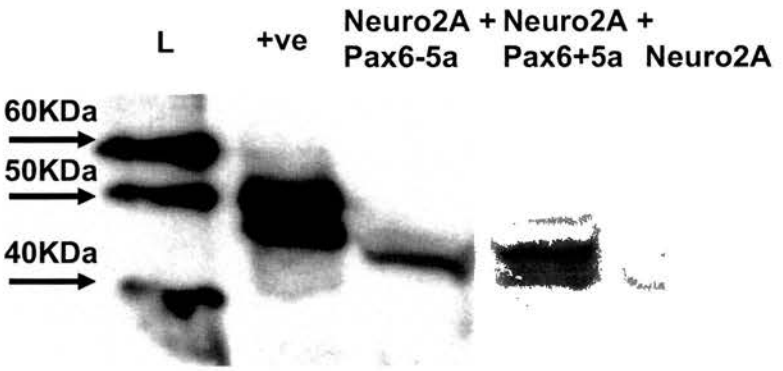

Figure 4.10: western blot analysis of Pax6 overexpression in transiently transfected Neuro2A cells. L, molecular weight ladder. +ve, *in vitro* synthesised control Pax6+5a and Pax6-5a.

4.6: Results: Stable over-expression of Pax6+5a, Pax6-5a and 5'-truncated Pax6 in Neuro2A and NIH3T3 cells

Although the introduction of Pax6 expression vectors leads to a more complicated Pax6 expression pattern than had been anticipated, it is clear from the above results that the plasmid vectors pJP13.1 and pJP14.1 are capable of causing over-expression of Pax6, in both Neuro2A and NIH3T3 cells. For this reason, stable cell lines were made with both plasmids, in both cell lines.

In addition, the plasmid pJP15.12 was introduced into the Neuro2A cell line. The only protein product that could be made from the pJP15.12 plasmid was an N-terminally truncated Pax6, thought to be responsible for the 32kDa band observed in western blot analysis of *Sey/Sey* mouse brain (see Chapter 3 for more details). If a phenotype was seen in this cell line, it was indicative that N-terminally truncated Pax6 could be contributing to the phenotype of *Sey/Sey* mice.

The plasmid pEGFPN1 was also introduced into both cell lines, and stable clones were obtained. This was done for two reasons. During the creation of stable cell lines, it allowed a measure of transfection efficiency in live cells, by microscopic visualisation of EGFP signal. After the creation of cell lines, the pEGFPN1 positive lines were used as experimental controls. They were proof that any phenotype seen in stable Pax6 over-expressing cell lines was indeed due to the presence of extra copies of *Pax6*, rather than the process of creating a stable, G-418 resistant cell line.

A number of cell lines were created from the insertion of each vector into each parental cell line. Up to 30 clones were screened from each, and the two clones that displayed the highest levels of Pax6 over-expression as assayed by a number of techniques (see below), were chosen for further study.

These cell lines were:
NIH3T3 + pJP13.1 (*Pax6+5a*) clones L and O
NIH3T3 + pJP14.1 (*Pax6-5a*) clones O and Q
NIH3T3 + pEGFPN1 clones A and B
Neuro2A + pJP13.1 clones H and Q
Neuro2A + pJP14.1 clones G and AD
Neuro2A + pJP15.12 (5'-truncated *Pax6*) clones A and E

Neuro2A + pEGFPN1 clones C and E

4.6.1: Confirmation of *Pax6* over-expression in stable cell lines by Q-PCR

Q-PCR was used to confirm over-expression of mRNA from the introduced cDNA in each cell line.

Adding *Pax6+5a* to the Neuro2A cell line leads to up-regulation between approximately 3- and 13-fold untransfected levels (**Figure 4.11 B**). The addition of *Pax6-5a*, however, has less of an effect on *Pax6-5a* mRNA levels, although they rise 1.3- and 1.4-fold in the two cell lines chosen (**Figure 4.11 A**).

There is no endogenous *Pax6* expression in the NIH3T3 cell line, but levels were normalised to the level of transcript in the cell line with the lowest level of *Pax6* expression, to create a reference point. NIH3T3 cells stably transfected with both *Pax6-5a* and *Pax6+5a* express the mRNA at between 2- and 9.5-fold untransfected Neuro2A levels (**Figure 4.11 A, B**). Expression levels vary between cell lines, probably due to position effects of vector integration into the host genome.

4.6.2: Confirmation of Pax6 over-expression in stable cell lines by western blot

In order to confirm that the increased levels of *Pax6* mRNA were accompanied by an increase in Pax6 protein levels, western blot analysis was performed on cell extracts from each cell line.

Pax6 protein over-expression is clear in the Neuro2A cell lines (**Figure 4.12**). Introduction of a *Pax6+5a* expression vector leads to between 20-and 40-fold over-expression of Pax6+5a. The addition of a *Pax6-5a* expression vector leads to much higher over-expression of Pax6-5a, from approximately 50- to 100-fold. The two cell lines transfected with the *Pax6-5a* vector did not show a great increase in *Pax6-5a* mRNA (**Figure 4.11**), but show a large increase in Pax6-5a protein (**Figure 4.12**). This is an indication that the level of *Pax6-5a* transcript is being tightly regulated in these cells, and that translation may be occurring with a higher efficiency from the ectopic transcript than from the endogenous genomic locus.

A) *Pax6-5a* mRNA in stable cell lines containing a *Pax6-5a* expression construct	
Cell line	***Pax6-5a* mRNA**
Neuro2A negative	1.00
NIH3T3 + *Pax6-5a* clone L	3.55
NIH3T3 + *Pax6-5a* clone O	1.00
Neuro2A + *Pax6-5a* clone G	1.43
Neuro2A + *Pax6-5a* clone AD	1.29

B) *Pax6+5a* mRNA in stable cell lines containing a *Pax6+5a* expression construct	
Cell line	***Pax6+5a* mRNA**
Neuro2A negative	1.00
NIH3T3 + *Pax6+5a* clone O	1.73
NIH3T3 + *Pax6+5a* clone Q	1.00
Neuro2A + *Pax6+5a* clone H	13.1
Neuro2A + *Pax6+5a* clone Q	2.70

Figure 4.11: Overexpression of introduced *Pax6* in stable cell lines, as determined by Q-PCR. All Neuro2A values are presented as a proportion of *Pax6* levels in untransfected Neuro2A cells, assigned an arbitrary value of 1. All NIH3T3 values are presented as a proportion of *Pax6* levels in the cell line with lowest expression, given an arbitrary value of 1 (all values expressed to 3 s.f.).

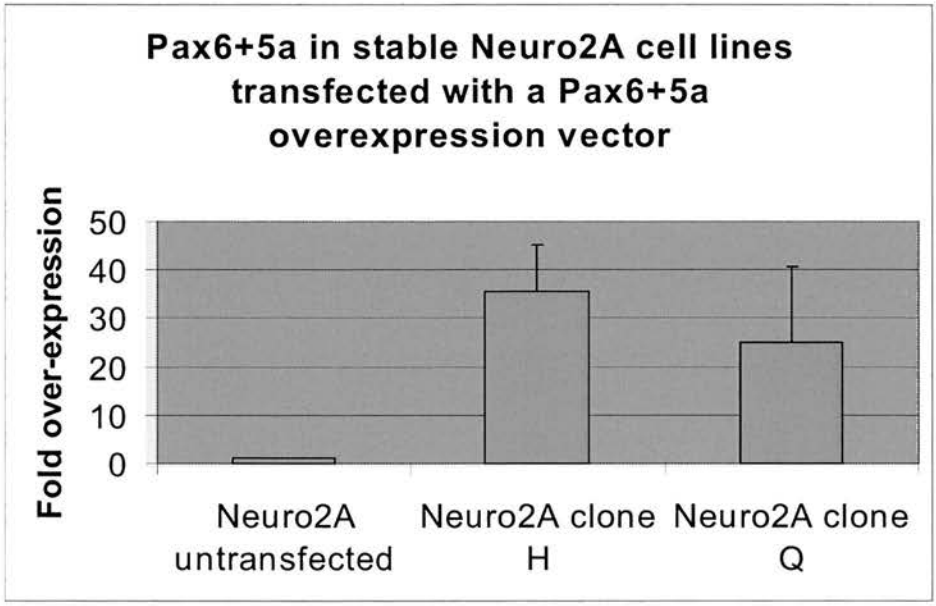

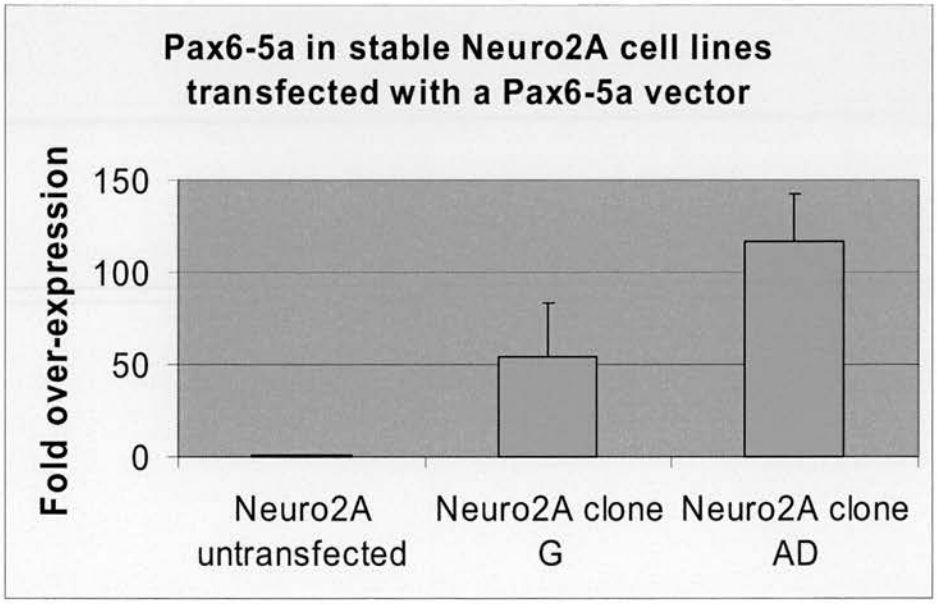

Figure 4.12 Expression of introduced Pax6 in stable Neuro2A cell lines, as determined by western blot. Values are expressed as a proportion of Pax6 levels in untransfected Neuro2A cells.

As the NIH3T3 cell line does not express Pax6, and was analysed in separate western blots to the Neuro2A cell line, there is no reference level of Pax6 with which to normalise data from this cell line. Values were therefore expressed as optical density of the appropriate band on photographic film (OD). Although this is an arbitrary measure, all four NIH3T3 cell lines containing *Pax6* expression vectors do produce Pax6 protein (**Figure 4.13**), and at varying levels, as was seen by Q-PCR.

4.6.3: The effect of Pax6 over-expression on the endogenous *Pax6* locus

Although the *Pax6* expression vectors contain human *Pax6*, and were introduced into murine cell lines, it is not possible to distinguish the two isoforms from the introduced *Pax6* mRNA or protein from that which originated from the endogenous locus. At the protein level, the two sequences are identical. There are differences at the mRNA level, but the primers used for Q-PCR are not in a position that can distinguish between the murine and human forms. This is because the 3'end of each primer must span an exon boundary, therefore they are restricted in position to a sequence that is conserved across the two species (see Appendix 2 **Figure A2.1** for a detailed description of Q-PCR primers).

The autoregulation of *Pax6* is well documented (Okladnova et al., 1998; Plaza et al., 1993; Plaza et al., 1995). This is likely to affect the Pax6 content of a cell transfected with a *Pax6* expression vector, and regulatory mechanisms have been hinted at by the previous mRNA and protein data (sections 4.5.1 and 4.5.2). Therefore, similar experiments were performed to assess the levels of the Pax6 splice form that had not been introduced into cell lines, i.e. the levels of Pax6-5a were determined in cell lines which had been stably transfected with *Pax6+5a*, and *vice versa*. Any mRNA or protein measured in these experiments must have been produced from the endogenous genomic locus, and is evidence for *Pax6* autoregulation.

Q-PCR demonstrates that the introduction of one isoform of *Pax6* into the NIH3T3 cell line does indeed lead to the up-regulation of mRNA corresponding to the other isoform (**Figure 4.14 A**). Although *Pax6-5a* levels are near to or below 1 in NIH3T3 cell lines with a *Pax6+5a* expression construct, these data are normalised to *Pax6* expression in the cell line with the lowest expression level. The NIH3T3 cell line has

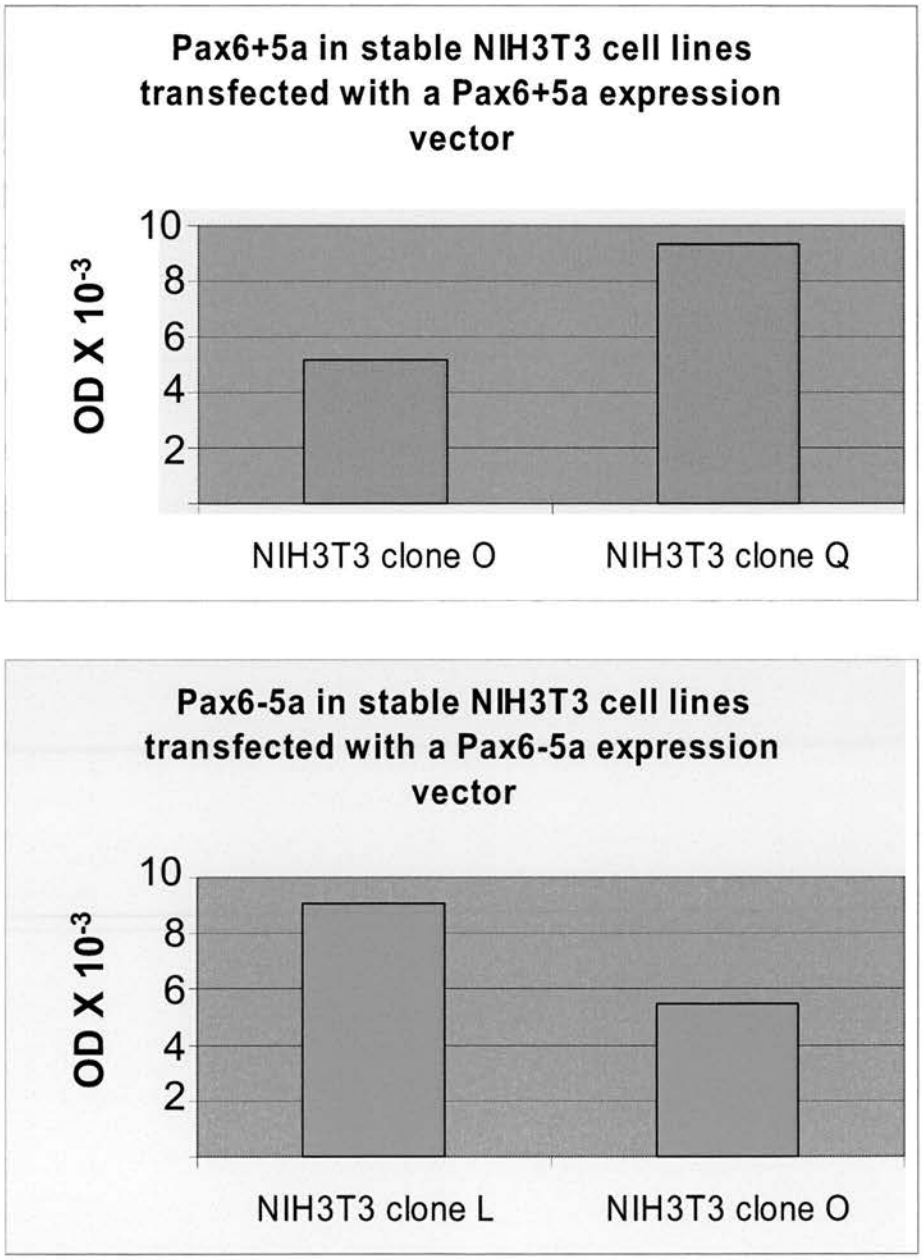

Figure 4.13 Expression of introduced Pax6 in stable NIH3T3 cell lines, as determined by western blot. Values cannot be normalised to untransfected cells, as these do not express endogenous Pax6. Instead, values are expressed as optical density (OD X 10^{-3}), an arbitrary measure of the signal strength of a band.

A) *Pax6+5a* mRNA in stable cell lines containing a *Pax6-5a* expression construct	
Cell line	***Pax6+5a* mRNA**
Neuro2A negative	1.00
NIH3T3 + *Pax6-5a* clone L	2.05
NIH3T3 + *Pax6-5a* clone O	1.00
Neuro2A + *Pax6-5a* clone G	1.44
Neuro2A + *Pax6-5a* clone AD	1.39

B) *Pax6-5a* mRNA in stable cell lines containing a *Pax6+5a* expression construct	
Cell line	***Pax6-5a* mRNA**
Neuro2A negative	1.00
NIH3T3 + *Pax6+5a* clone O	2.01
NIH3T3 + *Pax6+5a* clone Q	1.00
Neuro2A + *Pax6+5a* clone H	17.3
Neuro2A + *Pax6+5a* clone Q	1.39

Figure 4.14: Overexpression of endogenous *Pax6* in stable cell lines, as determined by Q-PCR. All values are presented as a proportion of *Pax6* levels in untransfected Neuro2A cells, assigned an arbitrary value of 1. All NIH3T3 values are presented as a proportion of *Pax6* levels in the cell line with lowest expression, given an arbitrary value of 1 (all values expressed to 3 s.f.).

no endogenous *Pax6* mRNA, thus any mRNA indicates up-regulation from the endogenous locus.

In the Neuro2A cell line, the results are slightly more complicated (**Figure 4.14 A, B**). *Pax6* mRNA levels from the endogenous locus are all above 1, but only Neuro2A + *Pax6+5a* clone H shows a large increase in levels when compared to untransfected cells (approximately 17-fold). However, this result is largely consistent with that described in section 4.5.1; often the *Pax6* mRNA levels are not raised, despite an increase in protein levels.

Western blot analysis was performed to detect any protein expression from these transcripts. These data clearly indicate that in both cell lines, there was a large increase in Pax6 protein levels from the endogenous locus (**Figures 4.15 and 4.16**).

4.6.4: Total Pax6 protein levels in stable cell lines

Figure 4.17 shows the combined western blot data from each cell line, giving an indication of the total Pax6 content of each line. All transfected NIH3T3 and Neuro2A cell lines express much more Pax6 protein than untransfected cells.

Variations in levels of expression between clones are probably due to position effects and variation in the number of copies of plasmid that were integrated into the genome. NIH3T3 + pJP13.1 clone Q expresses the highest amount of Pax6, and NIH3T3 + pJP14.1 clone O expresses the lowest amount. For the Neuro2A cell line, Neuro2A + pJP13.1 clone H expresses the highest amount of Pax6, whilst Neuro2A + pJP13.1 clone Q expresses the lowest amount, although this is still in great excess when compared to untransfected cells.

The introduction of a *Pax6* expression construct into Neuro2A cell lines also leads to the up-regulation of a shorter Pax6 isoform, the 32/33kDa band described in Chapter 3.

The ratio of Pax6-5a : Pax6+5a varies between cell lines (**Figure 4.18**), from 1.5:1 to 4:1 in NIH3T3 lines, and from 1:1 to 6:1 in Neuro2a cell lines. This is within the range of ratios described *in vivo* (see **Figure 3.22**).

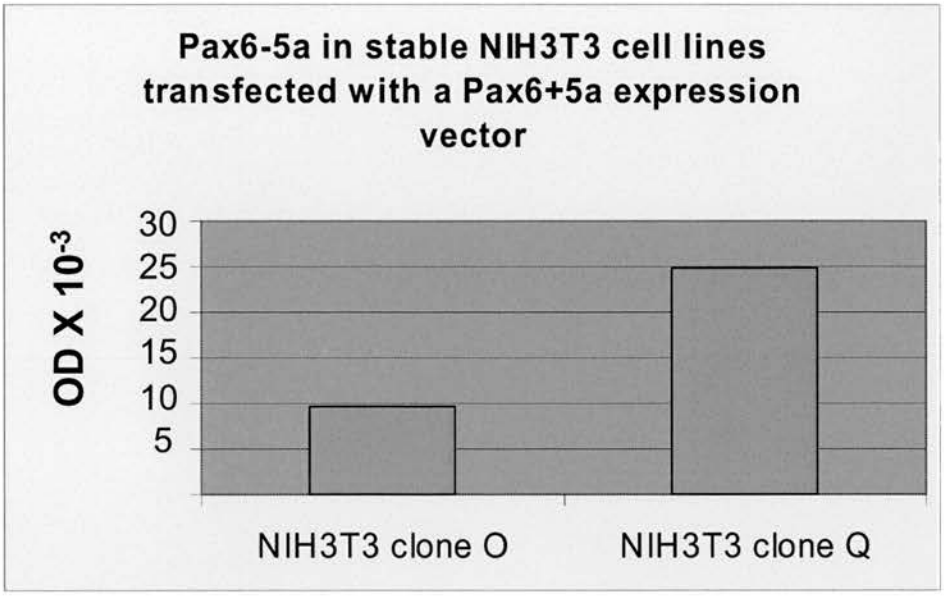

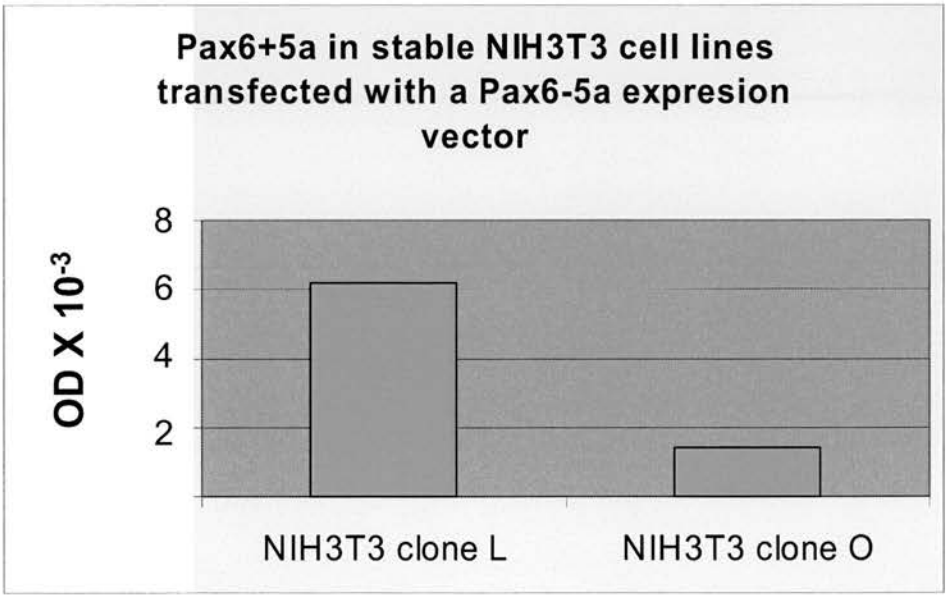

Figure 4.15 Expression of endogenous Pax6 in stable Neuro2A cell lines, as determined by western blot. Values cannot be normalised to untransfected cells, as these do not express endogenous Pax6. Instead, values are expressed as optical density (OD), an arbitrary measure of the signal strength of a band.

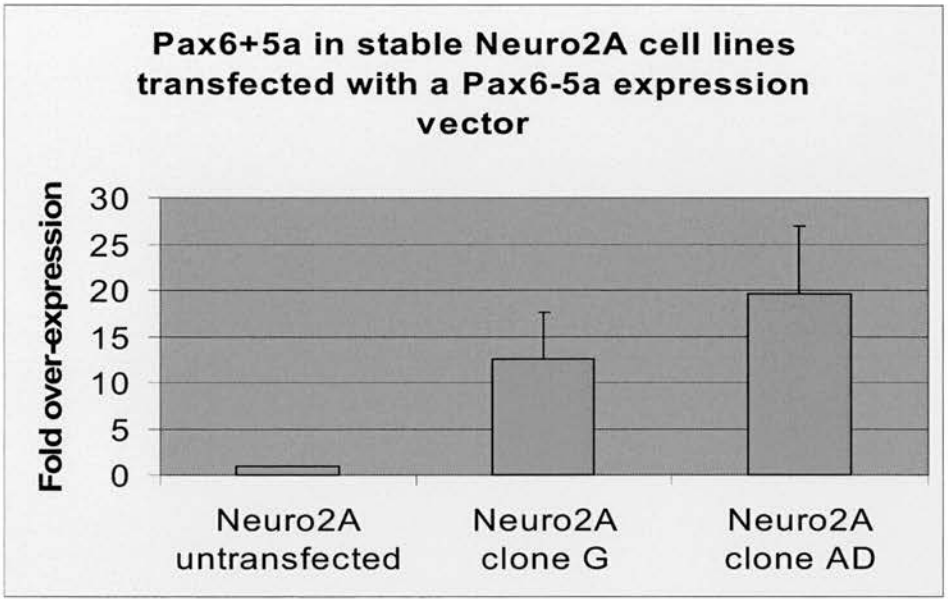

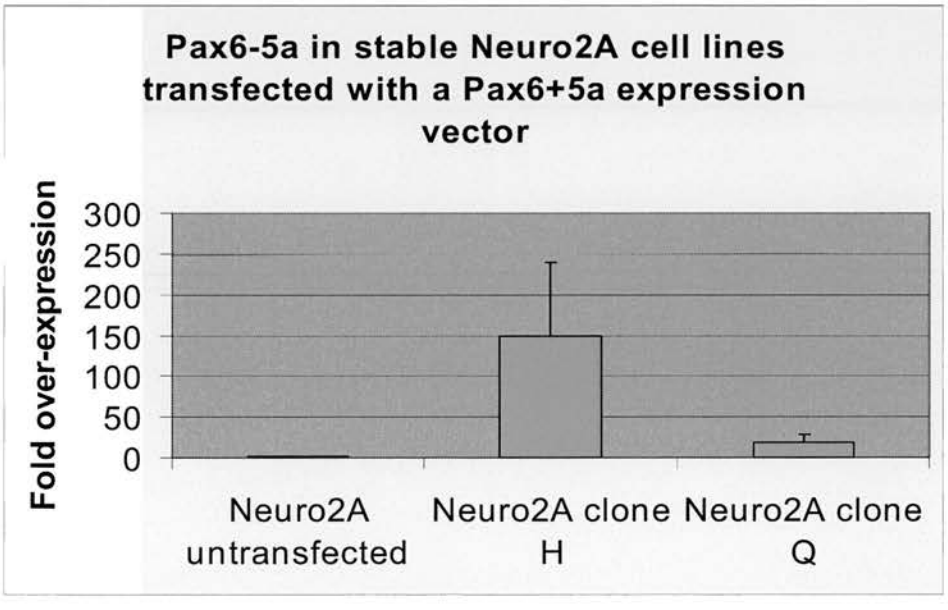

Figure 4.16 Expression of endogenous Pax6 in stable Neuro2A cell lines, as determined by western blot. Values are expressed as a proportion of Pax6 levels in untransfected Neuro2A cells.

Figure 4.17: Combined Pax6 protein levels in A, NIH3T3 (n=1) and B, Neuro2A (n=2, except 15.12, where n=1) cell lines after stable transfection with pJP13.1 (*Pax6+5a*), pJP14.1 (*Pax6-5a*) and pJP15.12 (5'-truncated *Pax6*). Error bars represent SEM. 5'-tr. *Pax6* = 5'-truncated *Pax6* **NB** All values in B are normalised to levels of Pax6-5a in untransfected cells. This value is only 0.15 for Pax6+5a protein in untransfected cells, therefore the values for Pax6+5a in other cell lines do not represent fold over-expression of the Pax6+5a isoform; they only represent levels relative to Pax6-5a over-expression.

A

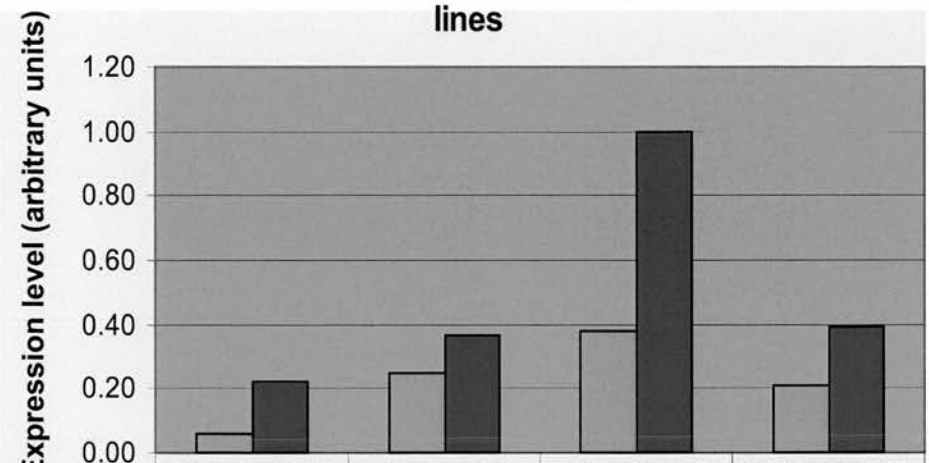

	14.1 clone O	14.1 clone L	13.1 clone Q	13.1 clone O
Pax6+5a	0.06	0.25	0.38	0.21
Pax6-5a	0.22	0.37	1.00	0.39
	Transfected with Pax6-5a		***Transfected with Pax6+5a***	

B

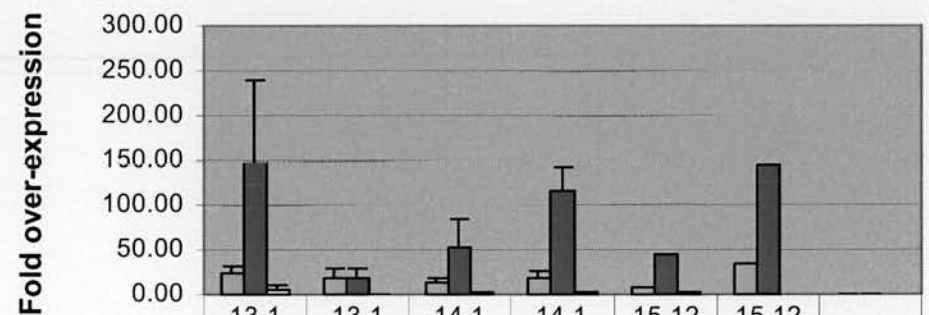

	13.1 clone H	13.1 clone Q	14.1 clone G	14.1 clone AD	15.12 clone A	15.12 clone E	-ve
Pax6+5a	24.55	17.34	12.52	19.63	7.33	35.36	0.15
Pax6-5a	148.46	18.20	53.76	116.50	45.95	145.93	1.00
Pax6 33KDa	5.81	0.31	3.94	3.53	2.64	0.00	0.00
	+ Pax6+5a		***+ Pax6-5a***		***+ 5'-tr. Pax6***		

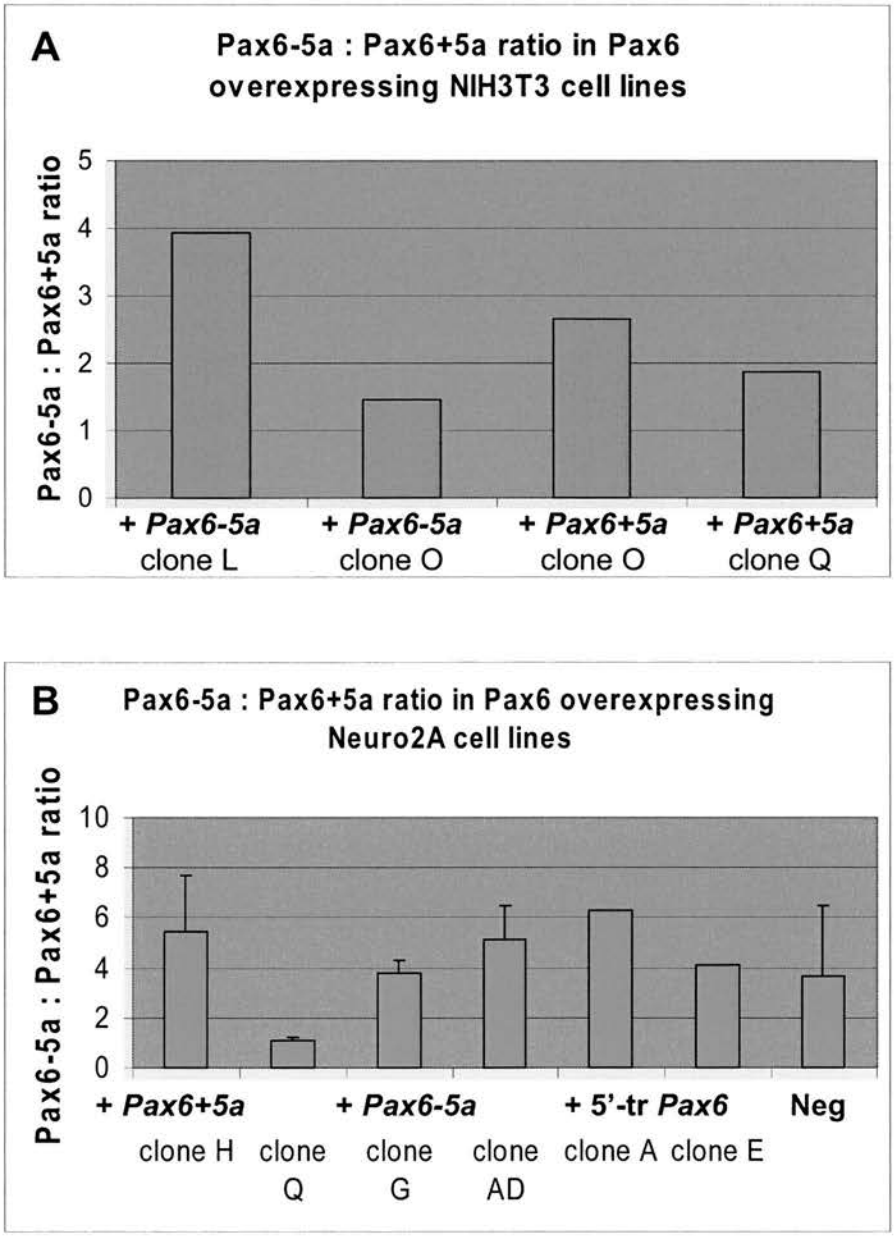

Figure 4.18: Pax6-5a : Pax6+5a ratio in A, NIH3T3 (n=1) and B, Neuro2A (n=2, except 15.12, where n=1) cell lines after stable transfection with pJP13.1 (*Pax6+5a*), pJP14.1 (*Pax6-5a*) and pJP15.12 (5'-truncated *Pax6*). Neg, untransfected Neuro2A. Error bars represent SEM.

Confirming the result seen by immunocytochemistry on transiently transfected cells (**Figure 4.9**), the addition of 5'-truncated *Pax6* leads to the up-regulation of both isoforms of full-length Pax6 (**Figure 4.17 B, Figure 4.18B**). This may have implications for the function of the 32kDa band observed by western blot in E12.5 mouse brain and eye, which will be discussed further in Section 4.8.4.

4.6.5: Confirmation of Pax6 over-expression in stable cell lines by immunocytochemistry and flow cytometry

Cell lines were also analysed by immunocytochemistry on dissociated cells using the anti-Pax6 PD antibody, to confirm Pax6 over-expression, and to ascertain whether levels were raised in a few cells, or all cells.

For the NIH3T3 cell lines, clear differences were seen between untransfected and transfected cell lines (**Figure 4.19**). A histogram showing FL1 fluorescence value against cell number was plotted for each genotype. A gate was drawn on the untransfected histogram, gating the 1% of cells with the highest fluorescence values. An increase in Pax6 signal is indicated by either an increase in the percentage of gated cells (more cells expressing high levels of Pax6), or by a shift in the mean FL1 value of the histogram (each cell expressing slightly more Pax6). Measured either way, the increase in Pax6 immunofluorescence is greatest in cell lines containing the Pax6-5a over-expressing construct, pJP14.1.

Flow cytometry proved a less reliable technique for the analysis of Pax6 over-expression in the Neuro2A cell line. Results seem to indicate that no Neuro2A cell lines had been created which over-expressed Pax6 (**Figures 4.20 and 4.21**). Analysis by western blot had proved this to be untrue (see sections 4.5.2 and 4.5.3), but immunocytochemistry was unable to detect Pax6 over-expression in stable Neuro2A cell lines.

One possible explanation for the observed discrepancy in results between immunocytochemistry and western blot lies in practical differences between the two techniques. Immunocytochemistry is a non-denaturing protocol, detecting proteins in their native form within the cell. Western blot, on the other hand, is a denaturing protocol; proteins were denatured to allow their resolution by SDS-PAGE. As the untransfected Neuro2A cell line normally expresses Pax6, other proteins with which

Figure 4.19 Flow cytometric immunocytochemical analysis of Pax6 expression in stable NIH3T3 cell lines. A, untransfected cells. B, no primary control reaction performed on untransfected cells. C, Stably transfected with pJP13.1 (*Pax6+5a*), clone O. D, Stably transfected with pJP14.1 (*Pax6-5a*), clone L. E, Stably transfected with pJP13.1, clone Q. F, Stably transfected with pJP14.1, clone O. Pax6 signal was detected in the FL1 channel, mean FL1 value is indicated below each histogram.

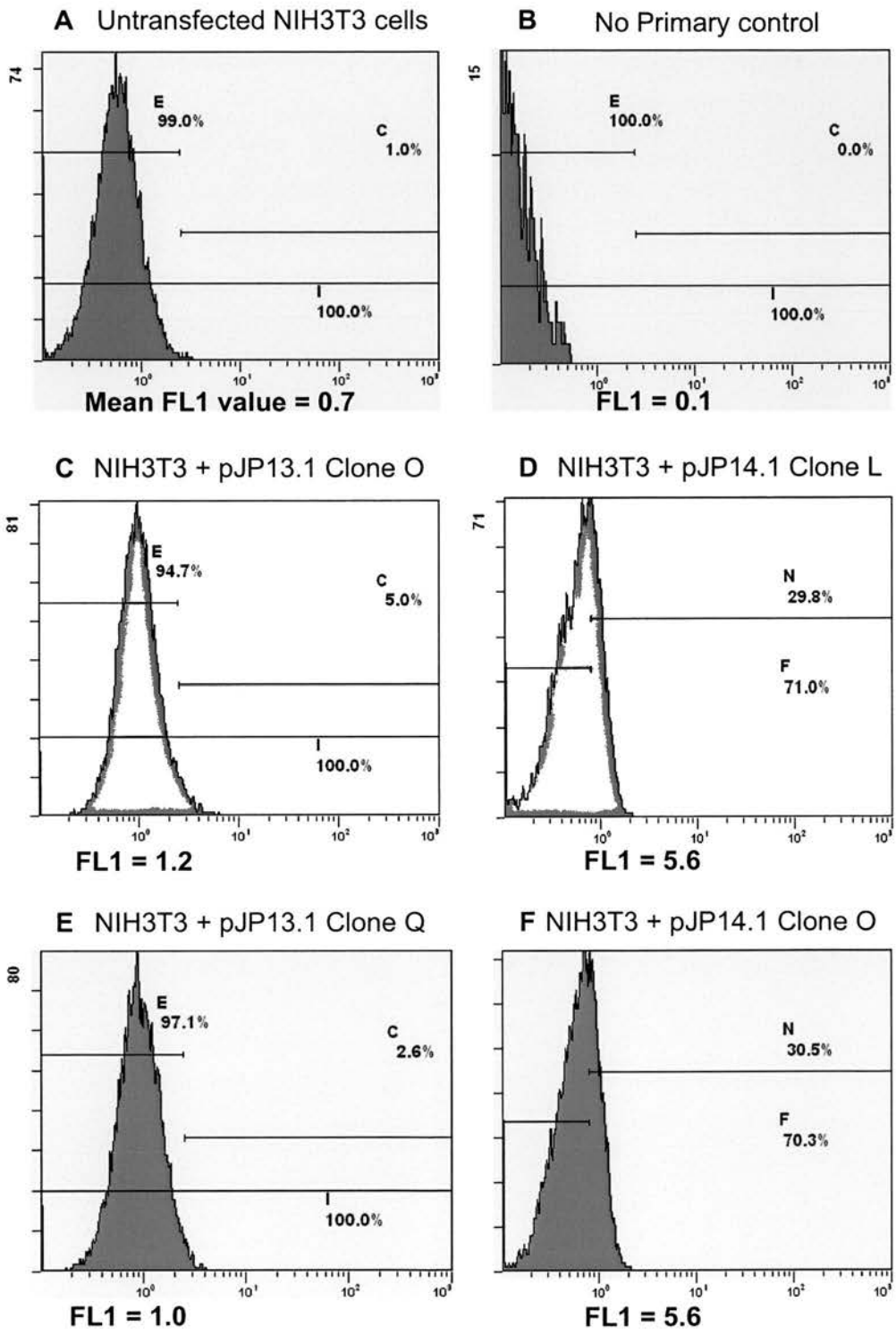
A Untransfected NIH3T3 cells
74
E
99.0%
C
1.0%
100.0%
Mean FL1 value = 0.7
B No Primary control
15
E
100.0%
C
0.0%
100.0%
FL1 = 0.1
C NIH3T3 + pJP13.1 Clone O
81
E
94.7%
C
5.0%
100.0%
FL1 = 1.2
D NIH3T3 + pJP14.1 Clone L
71
N
29.8%
F
71.0%
FL1 = 5.6
E NIH3T3 + pJP13.1 Clone Q
80
E
97.1%
C
2.6%
100.0%
FL1 = 1.0
F NIH3T3 + pJP14.1 Clone O
N
30.5%
F
70.3%
FL1 = 5.6

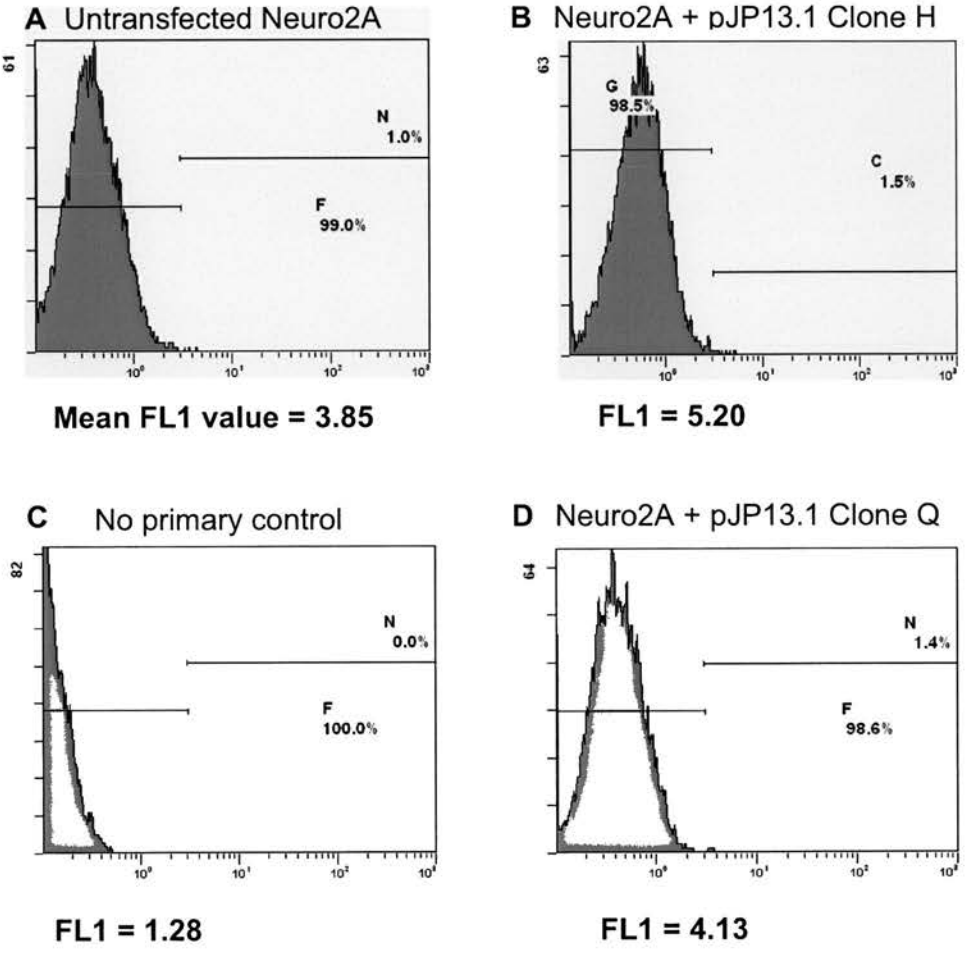

Figure 4.20 Flow cytometric immunocytochemical analysis of Pax6 expression in stable Neuro2A cell lines. A, untransfected cells. B, Stably transfected with pJP13.1 (Pax6+5a), clone H. C, no primary control reaction performed on untransfected cells. D, Stably transfected with pJP13.1, clone Q. Pax6 signal was detected in the FL1 channel, mean FL1 value is indicated below each histogram.

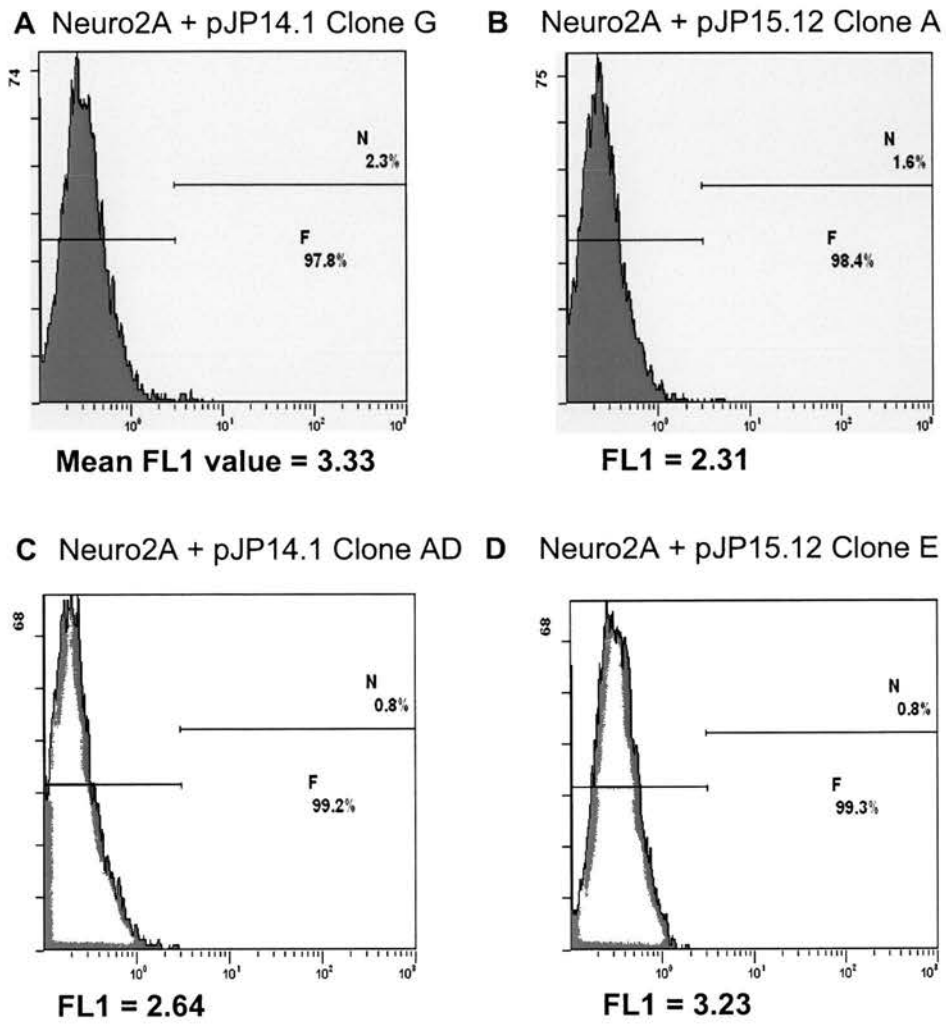

Figure 4.21 Flow cytometric immunocytochemical analysis of Pax6 expression in stable Neuro2A cell lines. A, Stable transfected with pJP14.1 (Pax6-5a) Clone G B, Stably transfected with pJP15.12 (5'-truncated Pax6) Clone A. C, Stably transfected with pJP14.1 Clone AD. D, Stably transfected with pJP15.12, clone E. Pax6 signal was detected in the FL1 channel, mean FL1 value is indicated below each histogram.

Pax6 can interact may also be present. In its native state, Pax6 may be complexed with these other proteins, and unrecognisable to the primary antibody. Denaturation would break up these complexes, allowing the primary antibody to recognise its epitope.

In accordance with this hypothesis, immunocytochemistry is capable of detecting over-expressed Pax6 in NIH3T3 cells (**Figure 4.19**). NIH3T3 cells do not express endogenous Pax6, and therefore might not be expected to express proteins which interact with Pax6.

These results demonstrate that the introduction of both major *Pax6* splice variants into either cell line did not lead to the intended model system, the production of clonal cell lines that expressed either one isoform or the other. However, it did result in a number of cell lines with a spectrum of Pax6 expression levels, and a spectrum of Pax6-5a : Pax6+5a ratios. Also, one set of cell lines demonstrates the effects of introducing *Pax6* into otherwise non-expressing cells, and the other set demonstrates the effects of *Pax6* over-expression.

This combination of factors makes the cell lines described above a useful model system for studying the roles of Pax6 at the cellular level.

4.7: Results: The effect of Pax6 over-expression on the neuronal differentiation of Neuro2A cells

When treated with 2'-O-dibutyryladenosine 3', 5'-cyclic monophosphate (dbcAMP), Neuro2A cells have been shown to differentiate along the neuronal lineage (Prasad and Hsie, 1971; Shea et al., 1988). They form axon-like, monopolar or bipolar processes, spanning many cell diameters (Fischer et al., 1986). Maximal differentiation is seen 72 hours after dbcAMP addition (Shea and Beermann, 1994).

4.7.1: Total cell number in differentiated Neuro2A cell lines

Prior to the induction of neuronal differentiation by dbcAMP, cells of all genotypes were seeded at the same density, $2.5X10^4 cells.cm^{-2}$. Throughout these analyses, Pax6 over-expressing cells seemed to exist at a lower density after 72 hours than

untransfected cells. This observation was made in both differentiated and undifferentiated cell lines.

Comparative cell counts were made 72 hours after seeding, both with and without the addition of dbcAMP after 24 hours (**Figure 4.22**), and at 96 hours with the addition of dbcAMP. After 72 hours, there are a higher number of untransfected cells per field of view than Pax6 over-expressing cells. This difference is statistically significant in all over-expressing cell lines without the addition of dbcAMP, and all but one after dbcAMP addition. By 96 hours, all dbcAMP treated Pax6 over-expressing cell lines have reached significantly lower numbers than untransfected cells. Total cell number increases between the two stages, indicating that cells are still proliferating in all cases, but the rate of proliferation has dropped in Pax6 over-expressing cell lines. EGFPN1 over-expressing cells behave as untransfected cells, indicating that the decrease in cell numbers is due to Pax6 over-expression rather than the process of transgene addition.

Undifferentiated Neuro2A cells have properties of neuronal precursor cells (Fischer et al., 1986). After the addition of dbcAMP, cell number is lower in Pax6 over-expressing cells than in WT cells. The decrease in proliferation is likely to be the result of increased differentiation, as cells exit the cell cycle. In the experiments described here, differentiation is induced either by Pax6 over-expression, by the addition of dbcAMP, or both.

According to this hypothesis, the drop in the rate of proliferation after neuronal differentiation is not due to a slowing of the cell cycle, but to an increased number of cells exiting the cell cycle and becoming post-mitotic.

4.7.2: β-3-tubulin expression in undifferentiated and differentiated Neuro2A cell lines

Anti-β-3-tubulin immunocytochemistry was used to visualise both undifferentiated (**Figure 4.23**) and differentiated (**Figure 4.24**) cells. The majority of cells of all genotypes are β-3-tubulin positive, both before and after the addition of dbcAMP; this indicates that even untreated Neuro2A cells are partially differentiated along the neuronal lineage. As anti-β-3-tubulin antibody labels both cell bodies and processes, it is useful for the study of cell morphology.

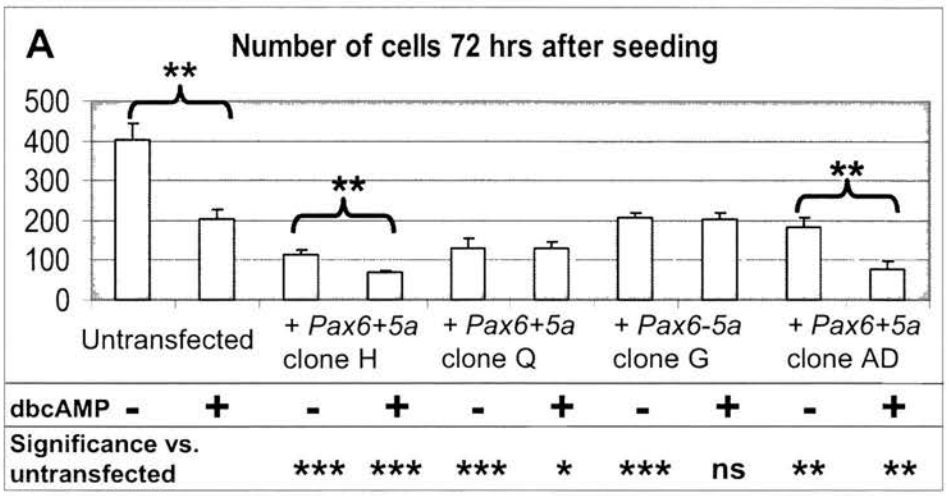

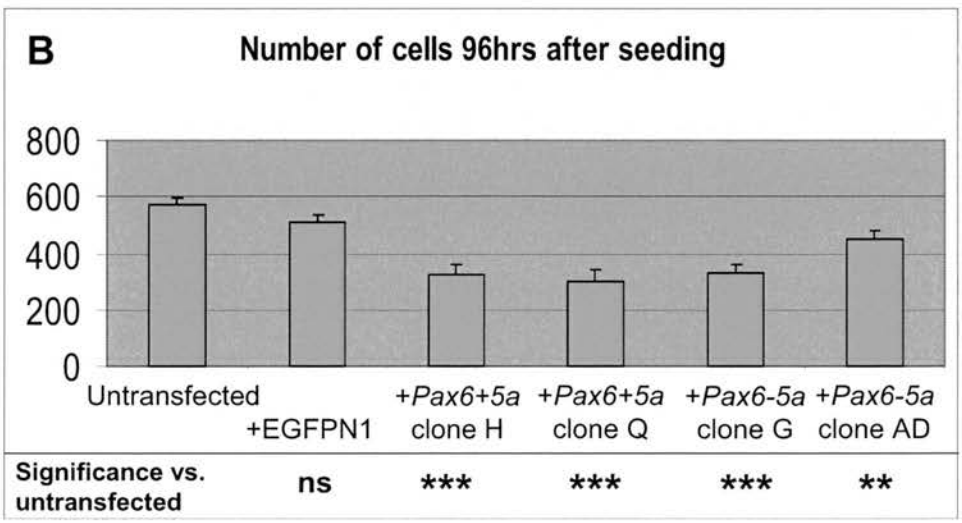

Figure 4.22: Cells per field of view after seeding $5X10^4$ cells.well^{-1} onto 4-well dishes, A, 72hrs, untreated and treated with 1mM dbcAMP after 24 hours. B, 96hrs, all dbcAMP treated. Error bars represent SEM.Below bars, *t*-test vs. untransfected cells * $P<0.05$, ** $P<0.01$, *** $P<0.001$. ns, not significant. Above bars, *t*-test without vs. with dbcAMP treatment.

Figure 4.23 β-3-Tubulin expression in untransfected and Pax6-overexpressing cells before treatment with dbcAMP. A, untransfected cells. B, Neuro2A + pJP13.1 (*Pax6+5a*) clone H, note the increased number of dendrites. C, Neuro2A + pJP14.1 (*Pax6-5a*) clone G. D, Neuro2A + pEGFPN1. E, Neuro2A + pJP13.1 clone Q. F, Neuro2A + pJP14.1 clone AD.

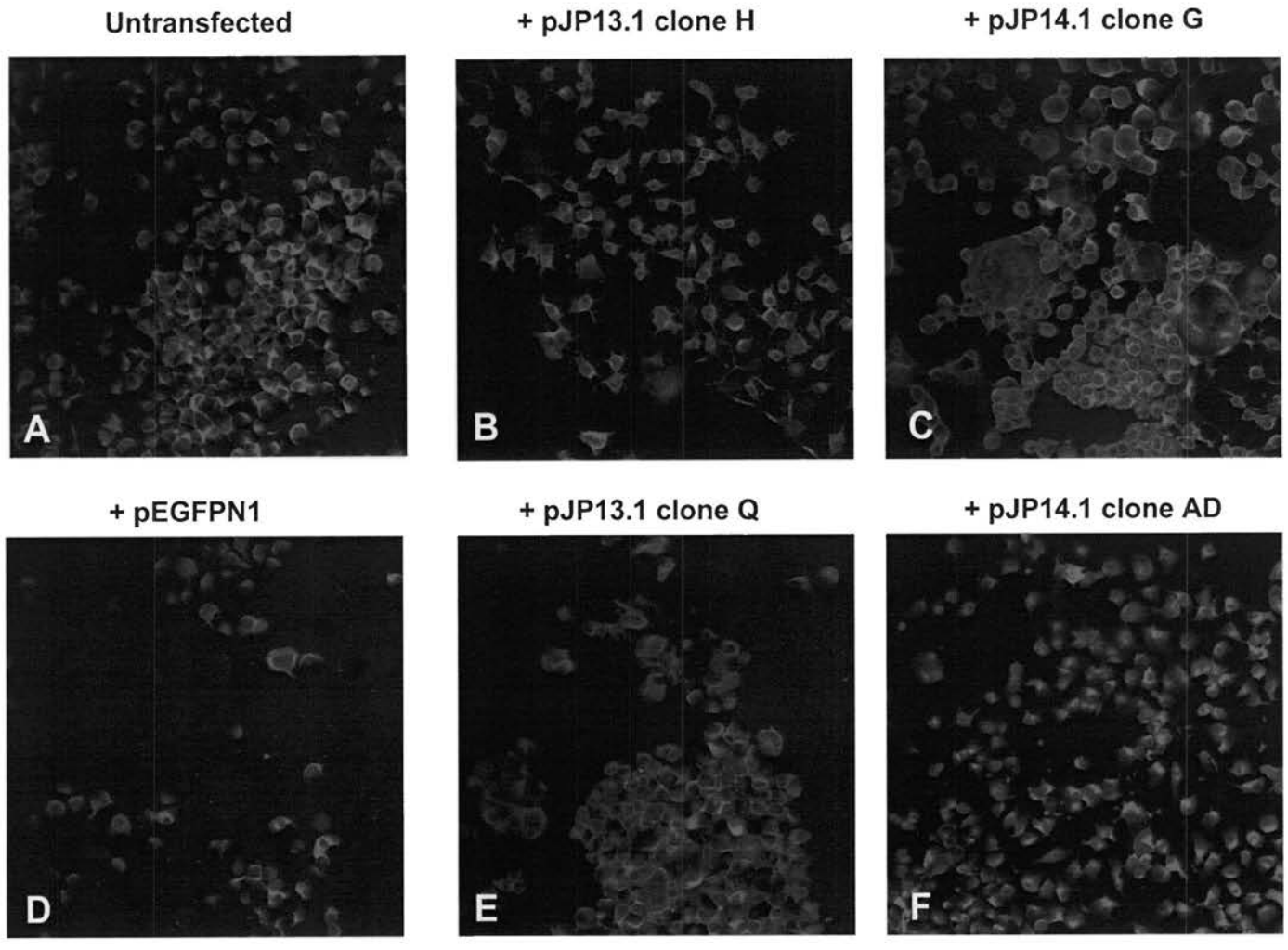
Untransfected
+ pJP13.1 clone H
+ pJP14.1 clone G
A
B
C
+ pEGFPN1
+ pJP13.1 clone Q
+ pJP14.1 clone AD
D
E
F

Figure 4.24 β-3-Tubulin expression in untransfected and Pax6-overexpressing cells after treatment with dbcAMP. A, untransfected cells. B, Neuro2A + pJP13.1 (*Pax6+5a*) clone H, note the high frequency of larger cell types with increased dendritogenesis (arrowhead) and smaller cells with long, axon-like processes (arrow). C, Neuro2A + pJP14.1 (*Pax6-5a*) clone G. D, Neuro2A + pEGFPN1. E, Neuro2A + pJP13.1 clone Q. F, Neuro2A + pJP14.1 clone AD.

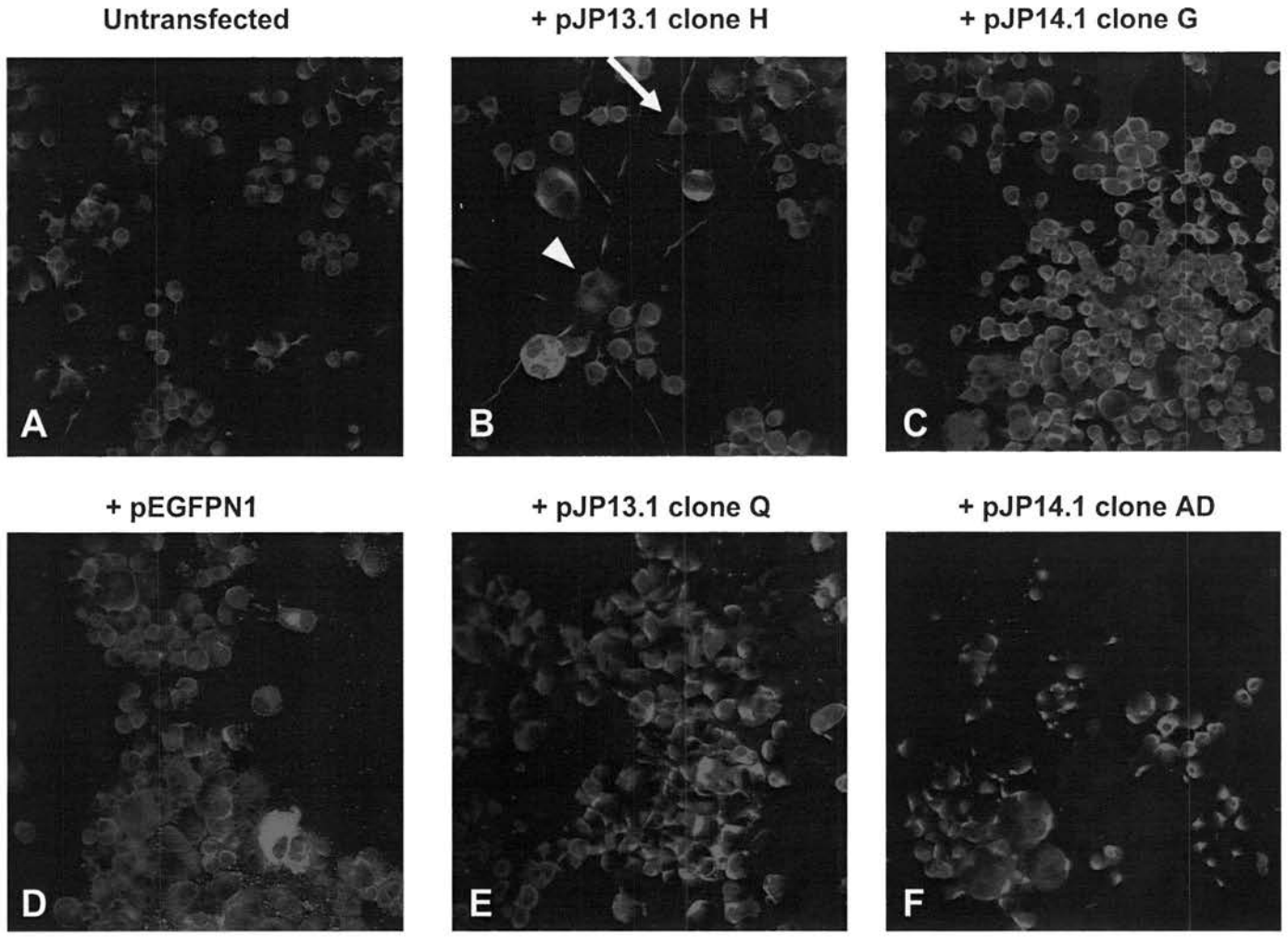
Untransfected
+ pJP13.1 clone H
+ pJP14.1 clone G
A
B
C
+ pEGFPN1
+ pJP13.1 clone Q
+ pJP14.1 clone AD
D
E
F

A comparison between untransfected cells before and after dbcAMP treatment (compare **Figure 4.23 A** with **Figure 4.24 A**) shows an increase in the number of larger cell types, and axon-like processes after dbcAMP treatment, as described by Fischer et al. (1986). This increase is most profound in Neuro2A + *Pax6+5a* clone H, the cell line with highest overall levels of Pax6 expression, and whilst most obvious in treated cells (**Figure 4.24 B**), it is also apparent without addition of dbcAMP (**Figure 4.23 B**). All Pax6 over-expressing cell lines exhibit this phenotype, whilst EGFP over-expressing cells behave more like untransfected cells.

Pax6 over-expressing cells from the cell line Neuro2A + *Pax6+5a* clone H show two obvious phenotypes. Many differentiated cells behave in a similar way to the untransfected population, growing bi-polar processes that resemble the "axon-like" phenotype described by Fischer et al., (1996) (arrow in **Figure 4.24 B**). In addition to this, cells are often seen with a large number of processes (arrowhead in **Figure 4.24 B**), more closely resembling the "dendrite-like" cells seen in the same study after retinoic acid-mediated differentiation. Other Pax6 over-expressing cell lines also appear to grow more processes than untransfected cells, although the effect is less profound. Control cells which over-express EGFP, and untransfected cells also change in morphology after dbcAMP treatment, most notably more large cells are seen, but the increase in the number of processes is less dramatic than in Pax6 over-expressing cells (**Figure 4.24 D**). In this respect, there appears to be a correlation between Pax6 expression levels, and the number of cells exhibiting altered morphology after dbcAMP treatment.

Although the majority of cells of all genotypes express β-3-tubulin, some cells (2 to 18%) do not (see **Figure 4.25**). This is characteristic of a heterogeneous cell population, in which cells are at various stages of neuronal differentiation. The least differentiated cells do not express β-3-tubulin. If Pax6 over-expression does indeed promote neuronal differentiation, as indicated by the altered morphology of Pax6 over-expressing cells, a higher percentage of the Pax6 over-expressing cell populations would be expected to express β-3-tubulin.

To test this hypothesis, the number of β-3-tubulin positive cells, expressed as a percentage of total cell number, was compared across genotypes (**Figure 4.25**). Before dbcAMP treatment, all Pax6 over-expressing cell lines have significantly more β-3-tubulin positive cells than the untransfected cell line, whilst the EGFPN1 cell line does not. After dbcAMP treatment, a similar effect is seen, but it is less

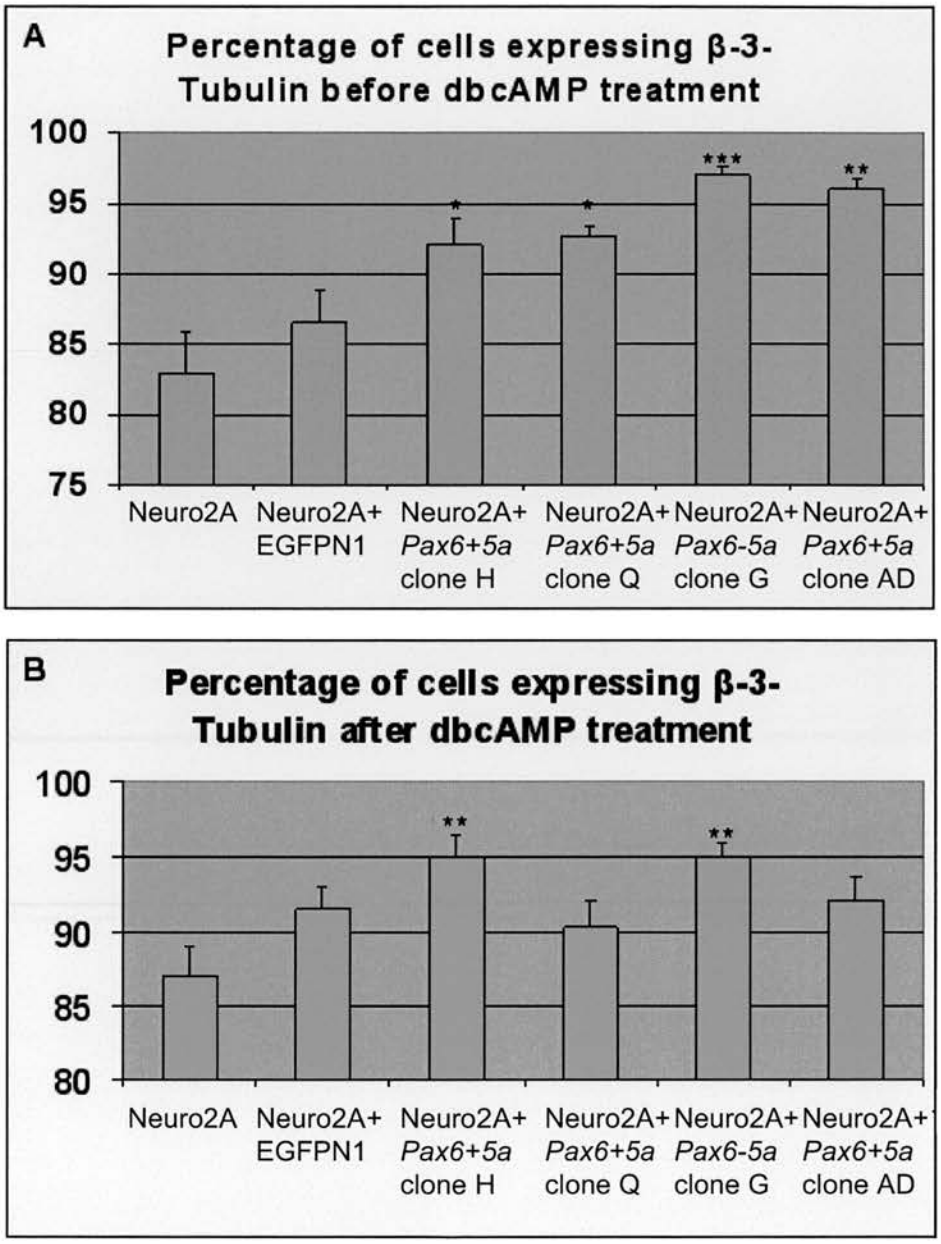

Figure 4.25: Percentage of β-3-tubulin positive cells A, before and B, after dbcAMP treatment of untransfected and Pax6 over-expressing Neuro2A cell lines. Error bars represent SEM. *t*-test vs. untransfected cells * P<0.05, ** P<0.01, *** P<0.001

pronounced; only two cell lines show significantly more β-3-tubulin positive cells. These are the cell lines with the highest, and the third highest level of Pax6 expression, implying that the more Pax6 protein is present in the cell line, the more β-3-tubulin positive cells are produced.

According to this analysis, Pax6 over-expression in the Neuro2A cell line leads to neuronal differentiation. The difference is most pronounced in untreated cells, and the addition of dbcAMP seems to mask the effect. dbcAMP treated, untransfected cells behave more like transfected cells.

4.7.3: MAP2 and Neurofilament expression in differentiated Neuro2A cell lines

As the processes observed in untransfected cells appeared to be largely "axon-like" in morphology, whilst those in Pax6 over-expressing cells appeared more "dendrite-like" (Fischer et al., 1986), dbcAMP treated cells were stained with antibodies against MAP2 and Neurofilament. The anti-neurofilament cocktail of primary antibodies should label all processes. MAP2, on the other hand, is specific to dendrites and should not label axons (Fischer et al., 1986).

This experiment was performed on untransfected cells and the cell line Neuro2A + pJP13.1 clone H, as the difference in morphology was most obvious between these two lines. As seen in **Figure 4.26**, both neurofilament and MAP2 are seen in all processes, in both genotypes. This is evidence for dbcAMP treatment promoting neuronal differentiation down the same pathway in all cells. The addition of extra Pax6 leads to a further increase in the number of differentiated cells, but does not appear to change their fate.

4.8: Discussion

Chapters 2 and 3 describe the Pax6 mRNA and protein content during development of the murine central nervous system. The next step in understanding the role of Pax6 in embryonic development is to gain an understanding of what role Pax6 may be playing in these tissues, and how alterations in the levels of various Pax6 isoforms can affect this role.

Figure 4.26 MAP2 and Neurofilament expression in untransfected and Pax6-overexpressing cells after treatment with dbcAMP. A-C, untransfected cells. D-F, Neuro2A + pJP13.1 clone H. Anti-MAP2 signal is red (A, D). Anti-neurofilament signal is green (B, E). When overlaid (C, F), the two protwins are seen to co-localise in all processes, whether dendrite-like, or axon-like.

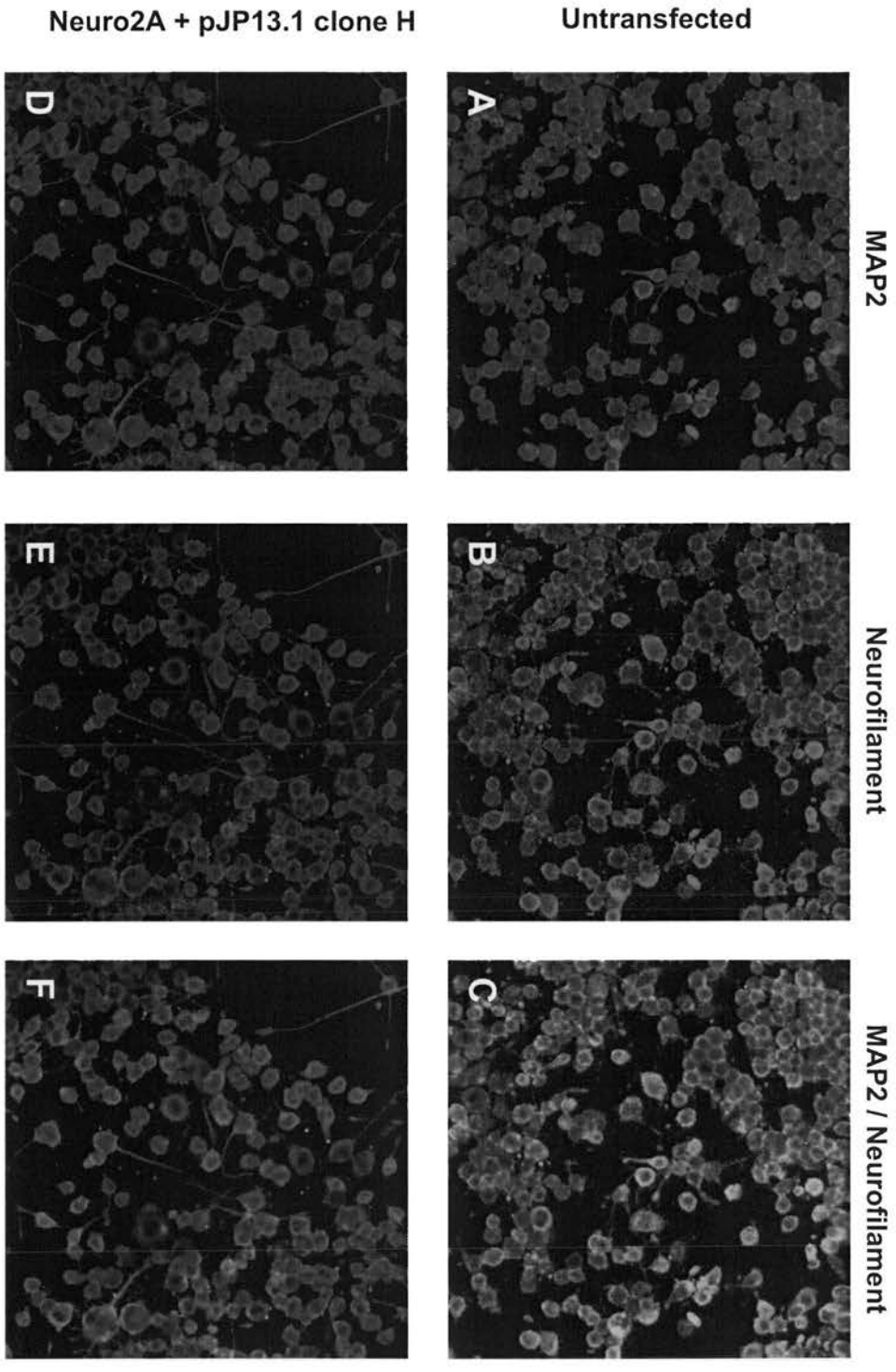
Untransfected
Neuro2A + pJP13.1 clone H
MAP2
Neurofilament
MAP2 / Neurofilament
A
B
C
D
E
F

4.8.1: Plasmid constructs can induce Pax6 over-expression in NIH3T3 and Neuro2A cell lines

The results described above demonstrate that constructs containing *Pax6-5a, Pax6+5a* and 5'-truncated *Pax6* can all induce Pax6 over-expression in the NIH3T3 and Neuro2A cell lines. In both cell lines, the addition of one splice variant leads to the up-regulation of both full-length *Pax6-5a* and *Pax6+5a*, from the endogenous genomic locus.

Stable over-expression of Pax6 has an autoregulatory phenotype in both cell lines. In the Neuro2A cell line, its role in neuronal differentiation can also be studied.

4.8.2: Limitations of this analysis

A cell culture system is an easily manipulable way of assessing the *in vivo* role of Pax6 in cell lines derived from a number of different tissues, in particular the effects of Pax6 over-expression, or of varying the levels of Pax6 isoforms.

One of the major limitations of this system is that immortalised cell lines represent an artificial system, which is at best an approximation of the environment in which the *Pax6* gene usually acts.

However, by comparing untransfected to Pax6 over-expressing cells, we can be confident that any difference in phenotype is due to the presence of the transgene. Use of EGFPN1 over-expressing cell lines rules out effects of the addition of a non-specific transgene. Creating a number of Pax6 over-expressing stable cell lines rules out position effects, due to transgene insertion interrupting genes whose function is necessary to maintain the normal cellular phenotype.

The use of only two cell lines is a further limitation of this study. Although the two cell lines were carefully chosen (see Section 4.4), they do not represent all the environments in which Pax6 can act. For example, it would have been interesting to assess the activity of Pax6 in a glial-derived cell line, and ascertain whether there were any phenotypic differences between this and the Neuro2A cell line in particular. It would also have been useful to use two different neuroblastoma cell lines, to see if the phenotype of Pax6 over-expression was the same in each, which would lend

credence to the results described above. However, it was not practical to extend this study to more cell lines, although this could be done in the future.

The aim behind using both *Pax6-5a* and *Pax6+5a* expression constructs was to assess the different activities of each isoform. The ability to perform this assessment was hampered by the fact that introduction of one full-length *Pax6* isoform led to the up-regulation of the other full-length *Pax6* isoform, as did the introduction of a 5'-truncated transcript. Although this initially seemed to be a significant limitation to this technique, it is actually more representative of the *in vivo* activity of *Pax6*. As shown in Chapters 2 and 3, the two *Pax6* isoforms are invariably co-expressed. What varies is their ratio to one another.

The cell culture system described here allows the analysis of cellular phenotype across a number of *Pax6-5a* : *Pax6+5a* ratios, all of which are within the range described in Chapter 2. The present study highlights the importance of the analysis of protein content even in transiently transfected cells. A number of studies have been conducted in which one *Pax6* isoform is introduced into cells, their phenotype is assessed, and conclusions are drawn as to the differential activity of the two isoforms (e.g. Chauhan et al., 2004b). The results described above demonstrate that these conclusions are invalid without an evaluation of the protein content of these cells after transfection.

4.8.3: Pax6 and autoregulation

Introduction of any isoform of *Pax6* into both Neuro2A and NIH3T3 cell lines leads to up-regulation of other Pax6 isoforms, from the endogenous genomic locus. Although the precise mechanism behind this up-regulation is unclear, it appears to vary between transient and stable transfections, and between stable cell lines. The variations between cell lines are likely to be due to position effects, as the chromosomal location into which the *Pax6* expression construct is inserted will have an effect on its regulation.

Despite the variation between cell lines, what is clear is that autoregulation is a strong, consistently observed phenomenon. In all cell lines, the introduction of a full-length *Pax6* isoform leads to some degree of up-regulation of the other full-length isoform, from the endogenous genomic locus.

The autoregulation of Pax6 was first documented by Plaza et al., (1993, 1995), who demonstrated that quail Pax6, PAX-QNR, could bind to both of its known promoters, P0 and P1, and could activate transcription from each. The data presented here show that the over-expression of either Pax6-5a or Pax6+5a leads to the up-regulation of the other major Pax6 isoform from the endogenous *Pax6* locus. In quail neuroretina cells, however, only Pax6-5a can transactivate the P0 and P1 promoters; Pax6+5a cannot (Plaza et al., 1993; Plaza et al., 1995). Similarly, Pax6-5a but not Pax6+5a can activate *Pax6* transcription *via* P0 in the presence of head surface ectoderm-specific enhancer sequences (Aota et al., 2003).

The discrepancy between the ability of Pax6+5a to up-regulate *Pax6* transcription in the cell culture system described here, but not in other systems, may be due in part to species-specific differences in the autoregulation of Pax6. Human PAX6, for example, can only activate *PAX6* transcription from the PB promoter (equivalent to P1), and not from the PA promoter (equivalent to P0) (Okladnova et al., 1998). A second explanation for the discrepancies in observed results is that the autoregulation of Pax6 may be tissue-specific, perhaps dependent on the expression of co-factors. PAX6 activates transcription from promoter PB in one cell line, whilst it represses transcription from the same promoter in a different cell line (Okladnova et al., 1998).

In the Neuro2A cell line, the over-expression of 5'-truncated *Pax6* also leads to up-regulation of both Pax6-5a and Pax6+5a. The activity of a "paired-less" Pax6 protein has been studied in the quail neuroretina model system, and it was unable to transactivate either the P0 or P1 promoters (Plaza et al., 1993; Plaza et al., 1995). The data described here are the first evidence that "paired-less" Pax6 act to autoregulate full-length Pax6.

It is also worth noting that the 32kDa isoform of Pax6, thought to result from internal translation initiation (see Chapter 3) is also up-regulated in all Pax6 over-expressing Neuro2A cell lines, although this was not seen in NIH3T3 cell lines. The up-regulation of this protein could be due to an increase in full-length transcript, from which internal translation may initiate. Alternatively, it could be due to an increase in the levels of 5'-truncated transcripts. A murine "paired-less" transcript is initiated from within intron 7, a region which contains a number of *Pax6* regulatory elements, some of which are known to be bound by Pax6 protein (Kleinjan et al., 2004).

The existence of Pax6 autoregulatory mechanisms *in vivo* was first proposed by Grindley et al. (1997), who observed reduced areas of *Pax6* mRNA expression in the caudal *Sey/Sey* diencephalon, implying that Pax6 protein was required for the maintenance of Pax6 protein expression. *In situ* hybridisation analysis of the *Pax6* mRNA content of $Pax6^{+/+} \leftrightarrow Pax6^{-/-}$ chimaeric mice shows that *Pax6* transcript levels are raised in $Pax6^{-/-}$ cells in the retina and in the dorsal telencephalon (Collinson et al., 2003; J.C. Quinn, pers. comm.). These two findings appear to be contradictory, the first indicating that Pax6 can activate its own transcription, the second indicating that Pax6 represses its own transcription in WT cells. Pax6-5a over-expression in the mouse lens leads to increased transcription of both *Pax6-5a* and *Pax6+5a*, consistent with Pax6 acting to up-regulate its own transcription (Chauhan et al., 2002a). The data presented in Chapter 3, however, indicate that Pax6 has a largely negative autoregulatory effect in the brain as a whole, and no discernable autoregulatory effect in the eye. Again, the mechanisms governing Pax6 autoregulation may vary in a tissue-specific manner, dependent on the expression of co-factors.

One way in which the expression of co-factors is known to influence *Pax6* transcription is by acting upon different *cis*-regulatory elements. For example, transactivation of the mouse P0 promoter in a cell culture system is stronger in the presence of a 5' enhancer sequence, and strongest when co-transfected with *Sox2* or *Sox3* (Aota et al., 2003). Transcription factors can bind to a number of regulatory elements both 5' and 3' of the *Pax6* gene, and can direct transcription in different tissues from different promoters (Anderson et al., 2002; Kammandel et al., 1999). Recapitulation of the complete *Pax6* expression pattern requires the presence of up to 420kb of flanking sequence (Fantes et al., 1995; Schedl et al., 1996) and Pax6 is likely to exert different autoregulatory effects at different *cis*-regulatory elements.

In general, the data presented here add weight to the hypothesis that Pax6 protein can regulate *Pax6* transcription. The precise nature of this interaction varies between experimental systems and between tissues in the developing mouse, and this variation is likely to be due to the differential expression of co-factors.

4.8.4: Pax6 over-expression induces neuronal differentiation in the Neuro2A cell line

The Neuro2A neuroblastoma cell line spontaneously differentiates along what is thought to be a neuronal pathway in culture (Fischer et al., 1986). This effect is enhanced by Pax6 over- expression and treatment with dbcAMP. Both manipulations appear to drive differentiation along the same pathway. This conclusion is supported by the fact that the effects of Pax6 over-expression are less profound in dbcAMP-treated cells than in their untreated counterparts.

After both types of treatment, cells grow an increased number of MAP2- and neurofilament-expressing processes, which are thought to be axonal rather than dendritic (Fischer et al., 1986).

The growth of more axonal-like projections in Pax6 over-expressing Neuro2A cells after dbcAMP-induced differentiation is consistent with the observation that *Sey/Sey* cerebellar cells do not form neuronal processes in culture, unlike their wild type counterparts (Engelkamp et al., 1999). A similar effect is also seen in the rat *rSey/rSey* hindbrain, where axon growth is stunted (Osumi et al., 1997).

Two observations can be made from the Pax6 over-expressing cell populations in this study, based on cellular morphology. Firstly, more cells become differentiated, as described above. Secondly, of the differentiated cells, cells with more than two processes are more common in the Pax6 over-expressing lines. Another study of cultured cerebellar cells, from the rat $rSey^2/rSey^2$ (rat small eye) mutant, supports this finding. These mutant cells showed disordered neural morphology; in particular fewer long bipolar neurites were formed (Yamasaki et al., 2001).

It is worth noting that the changes in cellular morphology described here were not observed in Pax6 over-expressing NIH3T3 cells, although this was not confirmed at a molecular level. These cells do not express endogenous Pax6 and, unlike Neuro2A cells, do not spontaneously differentiate in culture. From these observations it can be concluded that Pax6 over-expression can enhance the differentiation of neuronal precursor cells, but is not sufficient to cause transdifferentiation in a non-neuronal cell type.

Pax6 is known to be important in the switch from proliferation to differentiation in neuronal precursor cells. This is perhaps best demonstrated in *D. melanogaster*, where the *eyegone* gene, paralogous to *Pax6+5a,* promotes cellular proliferation, whilst the *eyeless* gene, paralogous to *Pax6-5a,* promotes differentiation (reviewed in

Rodrigues and Moses, 2004). The two genes are expressed in a sequential manner in *Drosophila* eye development, and the switch in expression is coincident with a switch from proliferation to differentiation (Dominguez et al., 2004).

In the murine pancreas, Pax6 is required for the differentiation of islet cells (Dohrmann et al., 2000; St-Onge et al., 1997), and in the eye it is involved in fate restriction of retinal progenitor cells (Marquardt et al., 2001).

Previous studies have suggested that Pax6 promotes neuronal differentiation. It is known to be a direct regulator of the proneural genes *Neurogenin2* (Scardigli et al., 2003), *Math5* and *Mash1* (Marquardt et al., 2001), which are crucial for specifying a neuronal cell fate (reviewed in Bertrand et al., 2002). Pax6 is required for the normal differentiation of glia (Gotz et al., 1998), and Pax6 over-expression in radial glial cells leads to the generation of neurons (Heins et al., 2002). The increased level of neuronal differentiation in Pax6 over-expressing Neuro2A cells described here is consistent with Pax6 acting to promote neuronal differentiation.

Some evidence from the developing *Sey/Sey* cortex, however, indicates that Pax6 may inhibit neuronal differentiation. An abnormally high proportion of *Sey/Sey* cortical cells undergo asymmetrical division between E12.5 and E15.5 (Estivill-Torrus et al., 2002), suggesting that Pax6 is required to maintain proliferation in these cells. Sey^{Neu}/Sey^{Neu} cortical plate neurons cease differentiation earlier than those in the WT (Schmahl et al., 1993), which also suggests that Pax6 is crucial for inhibiting neuronal differentiation in early cortical development.

One hypothesis that might reconcile these seemingly disparate results is that Pax6 may have a role in controlling both proliferation and differentiation of neural progenitor cells. Early in neurogenesis, Pax6 may act to promote symmetrical cell division within the cortex, thereby maintaining a proliferative precursor cell pool. Later in neurogenesis, the role of Pax6 may switch to promoting neuronal differentiation by activating proneural genes.

The temporal and spatial differences in the role played by Pax6 may vary dependent on the expression of co-factors, such as other HD-containing genes. Pax genes can dimerise *via* their HDs and bind to target DNA (Wilson et al., 1993), and a number of other Pax genes (*Pax2, Pax3, Pax5, Pax7* and *Pax8*) are co-expressed with *Pax6* in some regions of the developing murine brain (Stoykova and Gruss, 1994), (see

Figure 1.1). The two Pax6 DNA-binding domains can also interact with one other, either within a Pax6 molecule or between co-expressed Pax6 molecules (Mikkola et al., 2001; Mishra et al., 2002; Singh et al., 2000). As suggested in Chapter 2, developmentally-regulated changes in the ratio of Pax6-5a : Pax6+5a might also play a part in changing the action of Pax6. Although the cell lines described here express Pax6-5a and Pax6+5a in a variety of ratios, and all display a similar increase in the rate of differentiation, the role of the Pax6-5a : Pax6+5a ratio in regulating neuronal differentiation may also be dependent on the expression of other genes.

4.8.5: A possible role for N-terminally truncated Pax6 in WT, *Sey/Sey* and *Pax6*$^{LacZ/LacZ}$ mice

Transient transfections in both cell lines and stable transfections in the Neuro2A cell line indicate that 5'-truncated *Pax6* is capable of up-regulating full-length Pax6 protein. As the "paired-less" Pax6 protein synthesised from the 5'-truncated construct is shown to have transactivational properties (**Figure 4.9, Figure 4.17**), it could potentially affect the transcription of other Pax6 target genes. This has implications for the *Sey/Sey* and *Pax6*$^{LacZ\ LacZ}$ mutant mice. Both of these mice have mutations in the 5' portion of the *Pax6* gene. Internal translation initiation from within the *Pax6* gene could theoretically lead to the production of an N-terminally truncated Pax6 protein in either mouse mutant. In the *Pax6*$^{LacZ\ LacZ}$ mouse, there are four in-frame ATG residues 3' of the inserted *LacZ* gene. In the *Sey/Sey* mouse, the mutation is further on in the gene, and translation of a wild type Pax6 protein could only initiate from the most 3' of these ATG residues.

The plasmid pJP15.12, containing 5'-truncated *Pax6* cDNA, forces translation initiation from this 3' ATG residue. The resultant protein would still contain an intact DNA binding domain (HD) and TAD (Tang et al., 1998; Walther and Gruss, 1991), thereby fulfilling the basic requirements of a transcription factor. The presence of short, 32/33kDa Pax6 isoforms in mouse brain and eye (see Chapter 3), which are thought to be the result of just such an internal translation initiation mechanism (Carriere et al., 1993), is compelling evidence that these Pax6 variants have an important role *in vivo*. More work is needed to define this role, but it seems increasingly likely that the *Sey/Sey* and *Pax6*$^{LacZ\ LacZ}$ mice express some functional Pax6, and therefore can no longer be considered Pax6-null.

These protein isoforms are expressed at similar levels in *Sey/Sey* and WT mice, suggesting that any functional role may be maintained across the two genotypes. Part of the mutant phenotype in *Sey/Sey*, and by implication $Pax6^{LacZ/LacZ}$ mice may indeed be due to the presence of short Pax6 forms, rather than the absence of full-length Pax6, as was previously assumed.

The role of N-terminally truncated Pax6 has yet to be established, either in a WT or a *Pax6* mutant context, but a number of studies have addressed the possible transactivational abilities of Pax6 proteins lacking the PD. The homeodomain of a "pairedless" Pax6 protein can bind to canonical homeodomain binding sites, but in doing so does not activate transcription (Mishra et al., 2002). However, this Pax6 isoform can interact with full-length Pax6, and promote transcriptional activation *via* consensus Pax6 binding sites (Mikkola et al., 2001). The results described here demonstrate that short Pax6 isoforms can have a transcriptional effect not only on consensus binding sequences, but also on a known target gene, as they are able to upregulate full-length Pax6.

As seen in Chapter 3, the *Sey/Sey* mouse brain contains some short Pax6 isoforms, thought to be lacking a paired domain as a result of internal translation initiation. Whilst the up-regulation of full-length Pax6 protein by this "pairedless" form would not be possible in these mice, it is likely to affect other transcriptional targets. The data described above lend weight to the idea that short forms of Pax6 have a functional role in the *Sey/Sey* mouse.

4.8.6: Future work

The phenotypic analysis of Pax6 over-expressing cells described here is preliminary. Whilst it demonstrates that Pax6 over-expression has an effect on Pax6 autoregulation and neuronal differentiation of cultured cells, further studies are needed to define these effects, and the molecular mechanisms which underpin them.

After dbcAMP-induced differentiation, there is a clear difference in phenotype between untransfected and Pax6 over-expressing cells. Pax6 over-expressing cells produce more dendrite-like processes, whilst untransfected cells produce mainly axon-like processes. On the other hand, the markers of neuronal cell type used in this study failed to distinguish between the two phenotypes; they indicated that differentiation was proceeding down the same pathway in both genotypes. A PCR-

based screen of a larger number of cell type markers would enable a distinction to be drawn between these two scenarios.

Pax6 over-expression can also be predicted to have an effect on cellular proliferation (Estivill-Torrus et al., 2002; Maulbecker and Gruss, 1993; Mikkola et al., 2001; Warren et al., 1999; Warren and Price, 1997). Analysis of the cell cycle in untransfected and Pax6 over-expressing cells could be performed using the thymidine analogue, bromodeoxyuridine (BrdU).

Another important role of Pax6, which was not addressed here, is in the control of cellular adhesion. Cell adhesion defects have been demonstrated in the *Sey/Sey* mouse (Stoykova et al., 1997; Tyas et al., 2003). Pax6 is known to be a direct transcriptional regulator of cell adhesion molecules such as L1 (Meech et al., 1999) and NCAM (Edelman and Jones, 1995), and is also thought to interact with R-cadherin (Andrews and Mastick, 2003). These genes and a number of other regulators of cell adhesion could be included in a PCR-based screen of untransfected and Pax6 over-expressing cell lines.

The major drawback of the Pax6 over-expression system described in this chapter is that it did not lead to the creation of cell lines over-expressing either just Pax6-5a or just Pax6+5a. Whilst Pax6 autoregulation is an interesting phenotype in itself, and worthy of further study, it sheds no light on the differential activity of the two best know *Pax6* splice variants. One way to address this problem would be to introduce the constructs pJP13.1 and pJP14.1 into a *Sey/Sey* embryonic stem (ES) cell line. Although this study has shown that *Sey/Sey* mice are capable of expressing some short Pax6 forms, the up-regulation of both full-length splice forms could not occur in *Sey/Sey* ES cells. Any phenotype could only be caused by the introduced construct, as the endogenous locus is mutated, therefore cannot respond by producing full-length Pax6. The *Sey/Sey* ES cell line would also be a useful tool in assessing the role of N-terminally truncated Pax6.

Chapter 5 : Conclusions

5.1: Chapter 2: The *Pax6-5a* : *Pax6+5a* ratio in embryonic development

RNase protection assay was used to determine the *Pax6-5a* : *Pax6+5a* mRNA ratio in the telencephalon, diencephalon, eye, spinal cord and hindbrain from E12.5 to E18.5, and in the olfactory bulb and cerebellum from E14.5 to E18.5.

In all tissues studied, *Pax6-5a* is expressed at a higher level than *Pax6+5a.* The ratio between the two splice variants is regulated in a tissue-specific and developmental stage-specific manner. The telencephalon, diencephalon, spinal cord and hindbrain appear to be regulated in a similar way; the ratio is generally high but variable at E12.5, ranging from 2:1 to 18:1. It then falls to around 2:1 by E16.5, then rises slightly to approximately 4:1 at E18.5. The fact that the ratio follows a similar trend in these four tissues implies that Pax6 is playing a similar role in each. The fall in ratio may lead to a change in Pax6 target genes, and is coincident with a change in Pax6 activity, from a role in cellular proliferation to a role in neuronal differentiation.

In the olfactory bulb, the *Pax6-5a* : *Pax6+5a* ratio is around 2:1 from E14.5 to E18.5, and may rise slightly at E16.5. In the eye, the ratio is consistently higher than that in other tissues studied; 7:1 at E12.5, falling to around 3:1 at E18.5. In the cerebellum, the ratio remains largely constant, at around 4:1.

At E12.5, transcripts lacking exon 6 (*Pax6Δ6*) could not be detected in any tissue, suggesting that this transcript may not be as common as previously thought.

The tissue-specific differences in *Pax6-5a* : *Pax6+5a* ratio described here suggest that Pax6 activity varies, and differential *Pax6* isoform expression is developmentally regulated, between tissues.

5.2: Chapter 3: Analysing the Pax6 protein expression pattern in mice with various *Pax6* alleles

The Pax6 protein content of E12.5 whole brain and whole eye from, PAX77$^{+/-}$, PAX77$^{+/+}$ WT, *Sey/+* and *Sey/Sey* mice was analysed by western blot using an antibody that detects all known Pax6 isoforms.

The various Pax6 isoforms are differentially expressed between genotypes. Most isoforms are up-regulated in the brain of both PAX77 genotypes. Pax6 protein expression level is not directly proportional to *PAX6* copy number, and varies between isoforms, suggesting autoregulation of the Pax6 product in order to minimise the effects of over-expression. This conclusion is further supported by the observation that no isoform is seen at higher levels in the PAX77$^{+/+}$ brain than in the PAX77$^{+/-}$ brain, despite there being six extra copies of the *PAX6* transgene.

All Pax6 isoforms also appear to be up-regulated in the eye of PAX77$^{+/-}$ and PAX77$^{+/+}$ mice at E12.5. In the eye, Pax6 expression is more representative of *PAX6* copy number than in the brain, suggesting that autoregulation does not occur in this tissue. This may be one reason why the eye is more sensitive than the brain to *PAX6* gene dosage. The Pax6-5a : Pax6+5a ratio is lower in the PAX77$^{+/-}$ and PAX77$^{+/+}$ brains than in the WT brain, but unaffected in the PAX77$^{+/-}$ and PAX77$^{+/+}$ eyes. Again, Pax6 autoregulation is occurring in the brain but not in the eye.

Pax6+5a is up-regulated in the *Sey/+* brain at E12.5, when compared to WT. Four other isoforms, Pax6-5a, 43kDa Pax6, 32.5kDa Pax6 and 32kDa Pax6, are expressed at the same level in *Sey/+* and WT brains. This is evidence that autoregulation also occurs to control the Pax6 protein level when the *Pax6* copy number is reduced, and that this effect varies between isoforms. As was observed with the PAX77 eye, the *Sey/+* eye does not seem to have a Pax6 autoregulatory mechanism, as all isoforms appear to be down-regulated when compared to WT. This could explain why the *Sey/+* eye phenotype is stronger than the *Sey/+* brain phenotype.

Although previously believed to be functionally null for Pax6, the *Sey/Sey* mouse does express some Pax6 isoforms in the brain; 43kDa Pax6 and 32kDa Pax6. These two isoforms are expressed at the same levels in the *Sey/Sey* and the WT brain, and it is possible that they are contributing to its phenotype. Neither isoform was seen in the *Sey/Sey* eye.

The Pax6 protein content of two further *Pax6* mutant mice, Sey^{Neu}/Sey^{Neu} and $Pax6^{LacZ\,LacZ}$ was also analysed by western blot. Both were found to express 32kDa

Pax6 in the brain at E12.5, therefore this isoform may be contributing to the phenotype of all three *Pax6* null mice. Neither Sey^{Neu}/Sey^{Neu}, nor $Pax6^{LacZ/LacZ}$ mice express 43kDa Pax6 in the brain at E12.5, therefore any differences between the phenotype of these two mutant mice and that of *Sey/Sey* mice may be due to the presence of 43kDa Pax6 in the developing *Sey/Sey* brain. The 43kDa Pax6 band was previously thought to be the result of alternative splicing of exon 6, but this would not explain the presence of a band in the *Sey/Sey* mutant, therefore an alternative explanation must be sought. One possibility is that it is due to alternative splicing of exon 8, which would remove the *Sey* STOP mutation.

5.3: Chapter 4: Analysing the effects of Pax6-5a and Pax6+5a over-expression in immortalised cell lines

Expression constructs were made containing *Pax6-5a*, *Pax6+5a*, and 5'-truncated *Pax6* under the control of the strong viral CMV promoter. Transient and stable transfections were carried out to introduce all three constructs into the Neuro2A murine neuroblastoma cell line, and *Pax6-5a* and *Pax6+5a* into the NIH3T3 murine fibroblast cell line.

Transient transfection of both Pax6 isoforms into both cell lines leads to the up-regulation of the introduced transcript. In the Neuro2A cell line, transient introduction of *Pax6-5a* leads to an increase in the level of Pax6-5a protein, and a decrease in the level of Pax6+5a protein, suggesting that complex Pax6 autoregulation of the type observed in Chapter 3 can occur in a cell culture system. Transient introduction of *Pax6+5a* into the Neuro2A cell line leads to an increase in the level of both Pax6-5a and Pax6+5a protein.

Stable transfection of all three *Pax6* expression constructs into the Neuro2A cell line causes a rise in the levels of the introduced protein. There is also a rise in the protein levels of the other full-length Pax6 isoform(s), indicating autoregulation of Pax6 from the endogenous locus, after the introduction of either *Pax6-5a*, *Pax6+5a*, or 5'-truncated *Pax6*.

5'-truncated *Pax6* is capable of regulating the expression of Pax6, and may therefore be able to act on other Pax6 target genes. As the *Sey/Sey* and $Pax6^{LacZ/LacZ}$ mutant mice contain mutations in the 5' portion of the *Pax6* gene, they are theoretically

capable of producing "paired-less" Pax6 from the same transcript as that used in the present study. As suggested by the results of Chapter 3, it is possible that short isoforms of Pax6 may be contributing to the phenotype of these mice, and that of the Sey^{Neu}/Sey^{Neu} mouse, and that they are not entirely null for Pax6, as was previously thought.

Pax6-5a and *Pax6+5a* were also introduced into the NIH3T3 cell line, which does not express endogenous Pax6, by stable transfection. As with the Neuro2A cell line, both Pax6-5a and Pax6+5a proteins are up-regulated, indicating that Pax6 autoregulation can occur in a system in which Pax6 is not normally expressed.

Pax6 over-expression promotes neuronal differentiation in the Neuro2A cell line. The low level of spontaneous neuronal differentiation seen in this cell line is known to be increased by the addition of dbcAMP. This study shows that Pax6 over-expression promotes an exit from the cell cycle, and a concomitant increase in the level of neuronal differentiation, along the same pathway as that mediated by dbcAMP treatment.

Appendix 1 – Reagents and Protocols

Cell culture reagents

Minimal Essential Medium (MEM; for Neuro2A)
MEM (***Gibco***)
1% Non-essentail amino acids (***Gibco***)
1% Penicillin-streptomycin-L-glutamine (***Gibco***)
10% Foetal bovine serum (***Gibco***)

Dulbecco's Minimal Essential Medium (DMEM; for NIH3T3, H36CE2 and U373MG)
DMEM-F12 (***Gibco***)
1% Penicillin-streptomycin-L-glutamine (***Gibco***)
10% Foetal bovine serum (***Gibco***)

Transfection medium
RPMI 1640 (***Gibco***)
10% Foetal bovine serum (***Gibco***)
1% L-Glutamine (***Gibco***)

Trypsin-EDTA (***Gibco***)

Freezing medium
Foetal Bovine Serum (***Gibco***)
1% DMSO

Lipofectamine 2000 transfection reagent (***Invitrogen***)

G-418 stock
Geneticin (G-418 sulfate) (***Gibco***) to 200$\mu g.\mu l^{-1}$
1mM HEPES buffer (***Gibco***) in 1X PBS
Filter sterilised at 0.2μm to ensure there are no undissolved particles

Reagents for cAMP-Induced differentiation of Neuro2A cells

2'-O-dibutyryladenosine 3', 5'-cyclic monophosphate sodium salt (dbcAMP) (***Sigma***)
$100mg.ml^{-1}$ stock solution:
25mg dbcAMP salt
dissolve in 250μl ddH_2O
Use at 1mM, i.e. $509.4\mu g.ml^{-1}$
i.e. $5.094\mu l.ml^{-1}$

cAMP-Induced differentiation of Neuro2A cells

1) Seed cells 24 hours before induction of differentiation at $5X10^5$ $cells.well^{-1}$ in 6-well plates on sterile glass coverslips
2) Incubate at 37^0C, 5% CO_2 overnight
3) After 24 hours, change medium. Replace with 1.5ml medium
4) Add 7.64μl of $100mg.ml^{-1}$ dbcAMP stock solution per well
5) Return to incubator, collect after 48 or 72 hours

Protein Isolation and Quantitation Reagents

TENT buffer
20mM Tris-HCl (pH=8.0)
2mM EDTA
150mM NaCl
1% (v/v) Triton-X100
add one Complete Mini protease inhibitor cocktail tablet (***Roche***) per 10ml buffer, store aliquots at -20^{0}C

BSA Stock
BSA Fraction V 10mg.ml^{-1} in TENT buffer
Make serial dilutions 10-1000µg.ml^{-1} in PBS

BCA Protein Assay Reagents (***Pierce***)

Protein Isolation

From Tissue Culture Cells

1) Wash cells 2X in ice-cold PBS
2) Bathe in 1ml ice-cold PBS
3) Scrape cells off dish using a sterile, disposable cell-scraper
4) Decant into a 1.5ml microfuge tube
5) Pellet by centrifugation at 1,000g for 10 minutes at 4^{0}C
6) Discard supernatant, and resuspend cells in 20-100µl TENT buffer with protease inhibitors
7) Homogenise using a motorised homogeniser and a disposable mini-pestle
8) Allow lysis to occur for 20 minutes at 4^{0}C
9) Pellet out cell debris by centrifugation at 10,000g for 10 minutes at 4^{0}C
10) Remove supernatant and store at -70^{0}C for up to 6 months

From Embryonic Tissue

Dissections should be carried out in ice-cold, sterile PBS, within 90 minutes of harvesting embryos.
Freeze tissue dry in cryovials, by immersion in liquid nitrogen. Tissue can then be stored at -70^{0}C until protein extraction.

1) Defrost tissue on ice
2) Add 50-200µl TENT buffer with protease inhibitor, triturate
3) Continue as protein isolation from tissue culture cells, from step 7).

Reagents for *in vitro* Protein Synthesis

pJP8.6 (Pax6-5a), pJP9.3 (Pax6+5a) ans pJP17.x (5'-truncated Pax6) at 1µg.µl^{-1}

TNT Quick Coupled Transcription / Translation System (***Promega***)

in vitro Protein Synthesis

1) Prepare the following mastermix:
TNT Quick Mastermix 40.0µl

1mM Methionine	1.0µl
Template DNA (1µg.µl^{-1})	1.0µl
ddH_2O	8.0µl

2) Incubate at 30^{0}C for 90 minutes
3) Store at -70^{0}C for 12 months

Protein Quantitation

Perform all quantitations in 96-well plates

1) Dilute BSA stock solution to a range of concentrations from 10µg.ml^{-1} to 1000µg.ml^{-1} in TENT buffer
2) Aliquot 25µl of each standard into a separate well, alongside a blank well with just 25µl TENT buffer
3) Aliquot 1µl and 2.5µl of each protein sample into separate wells, and make up to 25µl with TENT buffer
4) Make BCA working reagent; 200µl per well *n* wells +1; by combining reagents A and B in a 50:1 ratio
5) Add 200µl working reagent to each well, incubate at 37^{0}C for 30 minutes
6) Allow to cool to room temperature, and measure absorbance at 565nm on a microplate reader
7) Using values from BSA standards, plot a regression in Excel of µg BSA against OD at 565nm
8) If the R^2 value of the regression is >0.95, use the equation generated to calculate the absolute amount of protein present in each sample
9) If only one value for a sample falls within the standard curve, discount the second value. If both values for a sample fall within the standard curve, average the two values

Protein Denaturing Polyacrylamide Gel Electrophoresis (SDS-PAGE) Reagents

Novex 12% Tris-Glycine Gel, 1.0mm thick, 12 well (***Invitrogen***)

5X SDS Running Buffer (pH=8.3)
- 0.125M Tris base
- 0.96M Glycine
- 0.5% (w/v) SDS

4X SDS Sample Loading Buffer
- 62.5mM Tris-HCl (pH=6.8)
- 2% (w/v) SDS
- 10% (v/v) Glycerol
- 5% (v/v) β-Mercaptoethanol (Add fresh, store for up to 6 weeks at room temperature)
- 0.005% (w/v) Bromphenol Blue

MagicMark Western Protein Size Standard (***Invitrogen***)

Protein Denaturing Polyacrylamide Gel Electrophoresis (SDS-PAGE)

1) For each lane, prepare 50µg protein, make up to 15µl with TENT buffer, and add 5µl 4X SDS loading buffer
2) Heat to 95^{0}C for 5 minutes, and load immediately

3) For Pax6 positive control lane use 1µl 1:10 *in vitro* synthesised Pax6+5a and Pax6-5a with 13µl TENT buffer and 5µl 4X SDS loading buffer; heat at 65^0C for 3 minutes, and load immediately
4) For MagicMark protein molecular weight ladder, use 4µl 1:10 MagicMark with 11µl TENT buffer and 5µl 4X SDS loading buffer. Do not heat prior to gel loading
5) Prepare the Novex gel:
Remove outer packaging
Rinse in ddH_2O to remove storage buffer
Remove protective strip from bottom of gel
Remove comb and wash wells repeatedly in 1X SDS running buffer
Place gel in tank alongside buffer dam, and tighten
Fill upper chamber with 1X SDS running buffer
6) Load 20µl sample per well, fill lower chamber with 1X SDS running buffer and run at 150V for 1 hour 40 minutes

Protein Transfer and Western Blotting Reagents

Transfer Buffer: **prepare fresh**
200mM Glycine
24mM Tris base
20% (v/v) Methanol

TBS-Tween
100mM Tris base (pH=7.5)
150mM NaCl
0.1% (v/v) Tween 20

Blocking Buffer: prepare fresh
TBS-Tween
5% (w/v) Marvel
Microwave to dissolve

Immuno-Blot PVDF membrane, 0.2 µm (***BioRad***)

Nitrocellulose Membrane, 0.2 µm (***BioRad***)

Ponceau's solution (***Sigma***)

ECL Plus (***Amersham Pharmacia Biotech***)

18X24cm Photographic Film (***Sigma***)

Protein Transfer and Western Blotting

For detection with DSHB anti-Pax6 or Chemicon anti-Pax6 primary antibody, proteins were transferred to PVDF membranes. For detection with serum 13 anti-Pax6, proteins were transferred to nitrocellulose membranes.

Prepare transfer buffer fresh on day of transfer

1) Pre-soak 2X sponges and 4X filter papers per gel in transfer buffer
2) Pre-soak nitrocellulose membranes in transfer buffer; permeabilise PVDF membranes in 100% methanol for 5 minutes before pre-soaking in transfer buffer

3) Remove gel from plastic casing, and prepare the transfer cell in the following order:
-ve; 1X sponge; 2X filter papers; gel; membrane; 2X filter papers; 1X sponge; +ve
4) Smoothe out bubbles, close the cassette tightly and place in the transfer tank
5) Fill tank with transfer buffer and transfer overnight at 50mA, 4^0C
6) Stain the membrane with Ponceau's solution, and de-stain with 2X ddH_2O washes to check transfer efficiency
7) Membranes can be wrapped in saran wrap and scanned in using the GS-710 densitometer to record transfer efficiency and protein loading accuracy
8) Block membranes in blocking buffer for 1 hour at room temperature, with shaking
9) Prepare primary antibody solutions by centrifuging antibodies at 13000rpm for 5 minutes, and dilute to the required concentration in 600µl – 1ml blocking buffer
10) Incubate membranes with primary antibody solutions in sealed plastic bags at 4^0C overnight
11) Wash 3X 10 minutes in TBS-tween
12) Prepare secondary antibody solutions by centrifuging antibodies at 13000rpm for 5 minutes, and dilute to the required concentration in 10ml blocking buffer
13) Incubate membranes with secondary antibody solutions for 1 hour at room temperature with shaking
14) Wash 3X 10 minutes in TBS-tween
15) Prepare ECL+ solution by mixing 1ml solution A and 25µl solution B per membrane
16) Bathe the membrane in ECL+ solution for 5 minutes
17) Dab off excess ECL+ solution onto a tissue, wrap the membrane in saran wrap, and expose to photographic film to visualise
18) If β-actin detection is required to allow relative quantitation of proteins, wash 3X 10 minutes in TBS-tween and repeat from step 9)

Reagents for Innunocytochemistry on Tissue Culture Cells

4% PFA in PBS

Blocking Solution:
15% BSA
10% goat serum
in PBS
Passed through 0.22µm filter to remove undissolved BSA crystals
Serum should be from the species in which the secondary antibody was raised

100% Methanol pre-cooled to -20^0C

TOPRO3 (***Molecular Probes***) diluted 1:5000 in PBS, with 1:1000 RNaseA (***Sigma***)
Boil RNaseA for 30 minutes before use to remove DNase activity

Vectashiled (***Vector Laboratories***) diluted 1:10 in PBS

Confocal Immunocytochemistry on Tissue Culture Cells

For stably transfected cells: Seed at $5X10^5$ cells.well^{-1} on glass coverslips in 6-well plates. Fix after 48 hours
For transiently transfected cells: Seed at $1X10^5$ cells.well^{-1} on glass coverslips in 6-well plates. Transfect after 24 hours, fix a further 48 hours after transfection

1) On ice, remove media and wash in ice cold PBS X2

2) Remove PBS and cover in 4% PFA in PBS, take off ice
3) Incubate at room temperature for 30 minutes
4) Remove fix by washing in PBS
5) Remove PBS, permeabilise the cells by incubating in pre-cooled 100% Methanol at -20^{0}C for 10 minutes
6) Wash 2X with PBS
7) Incubate cells in blocking solution for 30 minutes at room temperature
8) Microfuge primary antibody at 13000rpm for 15 minutes at 4^{0}C. Prepare correct dilutions (usually 1:75, 90µl is adequate to cover one coverslip, prepare 100µl each) of primary antibodies in blocking solution
9) Apply 90µl of the primary antibody and incubate in a sealed, humid, container at 4^{0}C overnight – can put PBS-soaked tissue paper in the gaps between wells, put the lid on, and leave in fridge
10) Wash 2X with PBS
11) Dilute the secondary antibody 1:200 in blocking solution (again, 90µl per coverslip, make 100µl each) **NB** may help if direct light is avoided from this stage onwards, although alexa-conjugated antibodies are less sensitive to photo-degradation than some fluorescent conjugates
12) Apply 90µl diluted secondary antibody to the cells and incubate in a sealed, humid, dark container at room temperature for 1 hour (as above, but covered to keep light out)
13) Wash the cells 2X in ddH_2O (can use PBS, but this leaves crystals)
14) Aspirate PBS, cover in TOPRO3/RNaseA mix in PBS, incubate at room temperature for 30 minutes
15) Wash 2X in ddH_2O
16) Mount on a microscope slide using 10% Vectashield, visualise within 48 hours

Flow Cytometric Immunocytochemistry on Tissue Culture Cells

Cells should be seeded as for confocal immunocytochemistry
Before fixation, trypsinise cells and resuspend in 1ml PBS
Pellet cells by centrifugation at 5000rpm for 4 minutes at 4^{0}C
All wash and incubation steps should be carried out in 100µl solution, followed by pelleting cells and removing supernatant
Immunocytochemistry is performed as for confocal microscopy, but without the addition of TOPRO3 nuclear counterstain
Cells are then run through an Epics-Coulter-XL flow cytometer. Voltages are kept constant for each set of samples to allow comparison between cell populations
Alexa-488-conjugated secondary antibody can be detected in the FL1 channel

Reagents for RNA Extraction from Tissue Culture Cells

RNeasy mini kit (***Qiagen***)
Buffer RWL supplemented with 1% β-mercaptoethanol (fresh)

RNA Extraction from Tissue Culture Cells

All RNA work must be performed in RNase-free conditions. Scrub benches with 70% ethanol before starting. Where possible, all solutions should be treated with DEPC, and filter tips should be used throughout

1) Seed cells at 1X10^6 cells per 25cm^2 flask
2) Collect after 48 hours by trypsinisation
3) Pellet cells by centrifugation at 1000 rpm for 5 minutes, discard medium
4) Wash in PBS, repeat centrifugation, and discard PBS

5) Resuspend pellet in 700µl RWL buffer with β-mercaptoethanol
6) Carry out RNA extraction as per manufacturer's protocol
7) Elute sample in 50µl RNase-free H_2O
8) Samples can be stored at -70^{0}C for up to 6 months

Reagents for RNA Extraction from Embryonic Tissue

RNagents Total RNA Isolation System (***Promega***)

75% Ethanol, 25% DEPC-treated H_2O, ice-cold

RNA Extraction from Embryonic Tissue

Dissections should be carried out in ice-cold, sterile PBS, within 90 minutes of harvesting embryos
Freeze tissue dry in cryovials, by immersion in liquid nitrogen. Tissue can then be stored at -70^{0}C until RNA extraction

1) Resuspend tissue in the appropriate volume of denaturing solution:
Olfactory bulb (pool as many as possible)
120µl
Telencephalon (pool 2-4 telencephalic vesicles, depending on age)
300µl
Diencephalon (pool as many as possible at E12.5, decreasing to 2-3 by E18.5)
120µl
Eye (pool as many as possible)
120µl
Spinal cord (pool as many as possible at E12.5, decreasing to 2-3 by E18.5)
120µl
Hindbrain (pool 2-3, exclude cerebellum from E16.5)
300µl
Cerebellum (pool 2-3, only E16.5 and E18.5)
300µl
Hindfoot (pool as many as possible)
300µl
Where very small amounts of tissue are present in a sample, 60µl of denaturing buffer can be used, but RNA yield will be low, as RNA may be lost during successive precipitations
2) Homogenise using a motorised homogeniser and a disposable mini-pestle
3) Proceed with RNA extraction as per manufacturer's protocol
4) Resuspend RNA pellet in RNase free H_2O. Generally, where 300µl denaturing solution was used, resuspend in 150µl; where 120µl denaturing solution was used, resuspend in 50µl.
5) RNA can be stored at -70^{0}C for up to 12 months

Reagents for RNA Quantitation

RiboGreen RNA quantitation kit (***Molecular Probes***)

PicoFuor bench-top fluorimiter (***Turner Designs***)

RNA Quantitation

N.B. RiboGreen is photosensitive, keep lights dimmed at all times
1) Dilute appropriate amount of RiboGreen 1:1000 in 1X TE

80µl per sample if trying 2 different dilutions + 40µl per standard (usually X8)

2) Dilute rRNA standard to 100ng.ml^{-1} in 1X TE

3) Prepare the following rRNA standards:

Total ng RNA	µl of 100ng.ml^{-1}stock rRNA	µl TE	Final conc (ng.ml^{-1})
4	40	0	50
2.4	24	16	30
2	20	20	25
1.6	16	24	20
1.2	12	28	15
0.8	8	32	10
0.4	4	36	5
0	0	40	0

4) Dilute sample RNA in 1X TE (usually use 0.2µl and 0.02µl, to ensure than one is within the range of the assay) to 40µl

5) Add 40µl sample/standard RNA (in 1X TE) to 40µl 1:1000 RiboGreen. Mix well, incubate at room temperature for 5 minutes

6) Calibrate PicoFluor using the 4ng standard and the blank (0ng)

- Switch ON
- Check it's set to blue, not UV
- Set "STANDARD" value to 400 (arbitrary, but in this case, 400 = 4ng RNA)
- Press "CAL", Calibrate according to the instructions it gives you (use 4ng as calibration standard, 0ng as blank)
- After calibration, insert sample and press "READ"

7) Take readings first for all standards, then for all sample RNAs

8) In Excel, use standards to plot a regression, and use the equation of the regression to calculate total RNA in each sample

Reagents for Riboprobe Synthesis

Maxiscript SP6 Kit (***Ambion***)

Linearised template DNA at 0.5µg.µl^{-1}

^{32}P UTP at 800Ci/mmol, 10mCi/ml (***Sigma***)

MicroSpin G-25 columns (***Amersham Pharmacia Biotech***)

Acrylamide / bis-acrylamide 40% solution (***Sigma***)

RepelcoteVS (***BDH***)

Ammonium persulphate 10% (Make fresh)

Dissolve 1g in 10ml ddH_2O, mix thoroughly

TEMED (N,N,N',N'-Tetramethyl-1,2-diaminomethane) (***Sigma***)

6% acrylamide, 8M Urea solution

Make up 100 ml acrylamide:
10ml 10XTBE
15ml Acrylamide/Bis-acrylamide (40% mix)
46.0g Urea

Make up to 100ml with water (not very much)
Mix until dissolved
Filter to remove any undissolved urea
Keep in the dark @4^{0}C for 14 days, after which crystals of acrylamide start to form

Riboprobe Synthesis

Preparation of a 6% polyacrylamide, 8M urea denaturing gel:
1) Clean 2 glass plates with water and 70% ethanol
2) Coat front plate with repelcote, marking the outer surface, rub in with a tissue, and wash off with 100% ethanol X2
3) Assemble the gel, washing alignment card with ethanol first. Check for a seal against the gasket at the bottom of the gel
3) Make fresh 10% APS
4) To polymerise 100ml of 6% acrylamide, 8M urea solution (need ~60ml per gel, if it doesn't leak) add:
100µl TEMED
1ml APS
5) Pour immediately, avoiding bubbles and leakage, insert comb before gel sets
6) Once the gel has set, soak 2X Whatman strips in 1X TBE and lay over either end of gel
7) Wrap in Saran wrap and place in fridge for 30 minutes, to harden the wells. Can be left overnight.

Transcription Reaction
1) In lab, make up the following:

	Nuclease free water	to 20.0µl total
	Linearised DNA	2.0µl (@0.5µg/µl)
	10X Buffer	2.0µl
	10mM ATP	1.0µl
	10mM GTP	1.0µl
	10mM CTP	1.0µl
For GAPDH probe:	1mM UTP	1.0µl

2) In radioactivity room, add:

^{32}P UTP	4.0µl	800Ci/mmol, 10mCi/ml
RNA polymerase		2.0µl

3)Mix well and incubate at 37^{0}C for 10 minutes
4) Add 1µl DNaseI to remove template and incubate at 37^{0}C for 15 minutes
5) Add 1µl 0.5M EDTA (pH8.0) to stop the reaction

G25 sepharose column purification of probe:
1) Vortex G25 column briefly to resuspend resin
2) Loosen cap ¼ and snap off bottom
3) Place in a clean 1.5ml eppendorf, spin at 3000rpm (785g in benchtop microfuge in room 350) for 1 min
4) Place in a clean 1.5ml eppendorf, spin at 3000rpm for 2 minutes
5) Collect eluate, store at -20^{0}C for 48 hours. After this time, radiolysis begins to occur
Verification of probe integrity:
1) Aliquot 1µl into a fresh microfuge tube with 5µl Gel Loading Buffer
2) Heat to 95^{0}C for 5 minutes
3) Load onto a 6% Polyacrylamide, 8M Urea gel (usually 1.5mm thick with 1cm wells), and run at 400V for ~1 hour
4) Visualise by exposure to photographic film for 30 minutes

Riboprobe quantitation
This was achieved by cerenkov counting
1) Aliquot 1µl and 2µl of each probe into 2ml ddH_2O in scintillation vials. Also include a blank, with just 2ml ddH_2O.
2) Measure fluorescence at 420nm
3) Compensate for the inefficiency of cerenkov counting by multiplying all cpm values by 3.33

Reagents for RNase Protection Assay (RPA)

Purified and quantitated target RNA (see above for methods of purification and quantification of RNA)

Radiolabelled, Quantitated Antisense RNA Probe (see above)

HybSpeed RPA Kit (***Ambion***)

Gel fixation buffer
5% Glacial acetic acid
15% Methanol
to 1 litre in ddH_2O

RNase Protection Assay (RPA)

Hybridisation of Probe and target RNA:
1) Aliquot 80,000cpm (Pax6) or 40,000cpm (GAPDH) of probe into a 2ml, snap-cap, RNase-free eppendorf.
2) Add a known amount of target RNA, 1µg for E12.5 and E14.5 RNAs, 4µg for E16.5 and E18.5
3) Make up to 50µg with yeast tRNA
4) For each probe, prepare a no target positive control reaction, with 50µg yeast tRNA
5) For each RPA, also prepare a no target negative control reaction with one probe and 50µg yeast tRNA
6) Precipitate the probe – target mix by adding 1/10 volume of 5M ammonium acetate and 2.5 volumes of 100% ethanol
7) Place on dry ice >20 minutes
8) Microfuge at 13000rpm at 4^0C for 15 minutes
9) Turn on 95^0C hotblock, defrost HybSpeed Hybridisation Buffer, and pre-heat to ~90^0C (at 95^0C it can be difficult to aliquot)
10) Using gel-loading tips, remove all ethanol, being careful not to disturb the precipitate
11) Add 10µl pre-heated Hybridisation buffer, immediately place the tube in the 95^0C hotblock. Do not let the samples drop below 65^0C after the addition of Hybridisation buffer
12) Vortex each sample for 15 seconds, then return to the hotblock to regain heat. Repeat 3 times.
13) Incubate samples for 2-3 minutes at 95^0C after vortexing the final sample.
14) In the hotblock, quickly transport 5 or 6 tubes at a time to the 68^0C oven.
15) Incubate overnight (>10 hours, or signal will be lower than anticipated) at 68^0C

RNase Digestion
1) Make up RNase digestion mastermix (*n* total number of tubes – positive controls + 1)

100µl HybSpeed RNase Digestion Buffer
2µl RNase cocktail / RNase A/T1 mix

2) Centrifuge samples briefly
3) Add 100µl mastermix to each sample except positive controls, vortex
4) Add 100µl RNase digestion buffer to each positive control sample, vortex
5) Incubate at 37^{0}C for 30 mins, vortex after 15 minutes
6) Add 150µl HybSpeed Inactivation/Precipitation Mix to each tube, vortex
7) Place on dry ice >20minutes
8) Microfuge at 13000rpm at 4^{0}C for 15 minutes

Detection on a Denaturing Polyacrylamide Gel:

1) Pre-run a 6% polyacrylamide, 8M urea gel at 400V for >15 minutes, washing the wells with 1XTBE to remove accumulated urea and polyacrylamide
2) Turn on 95^{0}C hotblock, defrost Gel loading buffer and radio-labelled dsDNA ladder (see below)
3) Using gel-loading tips, very carefully remove supernatant, a second brief microfuge step is usually necessary to ensure all traces of ethanol are removed
4) Resuspend the pellet in 4µl gel loading buffer
5) Vortex each sample for 60 seconds to ensure the pellet is fully resuspended
6) In a separate eppendorf, aliquot 4µl loading buffer, and add 2µl DIG-labelled DNA ladder
7) Heat tubes to 95^{0}C for 3-4 minutes to solubilise and denature the RNA
8) During this denaturation step, wash each well of the gel a second time with 1XTBE
9) Using a Hamiltonian syringe and custom-made 0.43mm thick loading tips, carefully load the gel, rinsing the loading tip after each well
10) Run at 450V for 2½ hours, using a cooling jacket filled with running cold water to stop the glass plates cracking through over-heating
11) Peel off the smaller, front glass plate
12) Keeping the gel attached to the back plate for support, immerse in gel fixation buffer for 1 hour
13) Transfer from glass plate onto filter paper, cover in saran wrap and dry overnight using a vacuum drier
14) Expose to photographic film at -70^{0}C using an intensifying screen for 14 days

Reagents for Synthesis of Radiolabelled dsDNA Ladder

^{32}P[dCTP] 3000 Ci/mmol, 10mCi/ml (***Sigma***)

pUC 19/*Hpa* II Digested dsDNA Markers (***Ambion***)

Klenow DNA Polymerase (5u.µl^{-1}) (***Promega***)

100mM dATP, dGTP, dTTP and dCTP (***Roche***)

MicroSpin G-50 columns (***Amersham Pharmacia Biotech***)

Synthesis of Radiolabelled dsDNA Ladder

1) Prepare the following in a 500µl microfuge tube:

pUC19/*Hpa*II Digested dsDNA markers	1.0µl
10X Klenow DNA Polymerase Reaction Buffer	2.0µl
1mM dATP	1.0µl
1mM dTTP	1.0µl
1mM dGTP	1.0µl

1mM dCTP	0.1µl
3000 Ci/mmol, 10mCi/ml ^{32}P[dCTP]	1.0µl
ddH_2O	11.9µl
Klenow DNA Polymerase	1.0µl

2) Mix well and incubate at 37^{0}C for 15 minutes
3) Prepare a G-50 column: Shake well
Snap off bottom, place in an empty microfuge tube
Microfuge at 3000rpm for 1 minute
Place in a fresh microfuge tube
4) Aliquot the reaction product (20µl) into the column, microfuge at 3000rpm for 1 minute
5) Store at -20^{0}C for up to 2 weeks

Reagents for cDNA Synthesis

First Strand cDNA Synthesis Kit (***Invitrogen***)

cDNA Synthesis

Use 5µl total RNA per cDNA synthesis reaction
Use 1µl oligo d(T) primer (0.5µg.µl^{-1}) per reaction, to specifically amplify poly(A) mRNA
Carry out cDNA synthesis according to the manufacturer's instructions

Reagents for Reverse-Transcriptase Polymerase Chain Reaction (RT-PCR)

Expand DNA Polymerase (***Roche***)

Taq DNA Polymerase (***Promega***)

10X DNA polymerase buffer with 15mM $MgCl_2$ (***Promega***)

10mM dNTP solution - 10µl dATP (100mM, ***Roche***)
10µl dCTP (100mM, ***Roche***)
10µl dGTP (100mM, ***Roche***)
10µl dTTP (100mM, ***Roche***)
60µl ddH_2O

10µM each primer (***MWG***)

Reverse-Transcriptase Polymerase Chain Reaction (RT-PCR)

Expand PCR
1) Prepare 25µl Mastermix 1 for each sample
1X
0.75µl forward primer (10µM)
0.75µl reverse primer (10µM)
2.00µl dNTP (10mM)
1.00µl template DNA
20.50µl ddH_2O
2) Prepare 25µl Mastermix 2 for each sample, make enough for n+1 samples
1X
5.00µl 10X Expand reaction buffer
0.75µl Expand DNA polymerase
19.25µl ddH_2O

3) Combine each 25µl Mastermix 1 with 25µl of Mastermix 2
4) Perform PCR using the following programme:

2 minutes at 94^0C		
15 seconds at 94^0C	|	
30 seconds at annealing temperature	|	X10 cycles
3 minutes at 68^0C	|	
15 seconds at 94^0C	|	
30 seconds at annealing temperature	|	
3 minutes and 5 seconds at 68^0C	|	X20 cycles
Plus 5 seconds per cycle at 68^0C	|	
5 minutes at 72^0C		
4^0C for ever		

5) Store PCR product at 4^0C, and use within 24 hours

Genotyping PCR
1) Prepare 19µl mastermix per sample, make enough for n+1 samples

1X
0.5µl forward primer (10µM)
0.5µl reverse primer (10µM)
0.4µl dNTP (10mM)
2.0µl 10X reaction buffer (incl. 15mM $MgCl_2$)
0.1µl *Taq* DNA polymerase
1.0µl template DNA
15.5µl ddH_2O

2) Perform PCR using the following programme:

5 minutes at 96^0C		
1 minute at 96^0C	|	
30 seconds at annealing temperature	|	X35 cycles
45 seconds at 72^0C	|	

Colony PCR
1) Prepare 20µl mastermix per sample, make enough for n+1 samples
2) Using a sterile pipette tip, touch the bacterial colony, then dip the tip into the PCR mix
3) Leave for 5 minutes, then expel any liquid within the tip and discard
4) Perform PCR using the following programme:

5 minutes at 96^0C		
1 minute at 96^0C	|	
30 seconds at annealing temperature	|	X35 cycles
45 seconds at 72^0C	|	

<u>Reagents for Agarose Gel Electrophoresis</u>

10X Gel loading buffer

20% Ficoll 400
0.1M disodium EDTA, pH8
1% sodium diodecyl sulphate
0.25% bromphenol blue
0.25% xylene cyanol

Ethidium bromide (***Fisher Scientific***)

10X TBE

890mM tris base
890mM boric acid
20mM disodium EDTA, pH8

Autoclave before use, dilute to 1X with ddH_2O

Agarose (***Sigma***)

Molecular weight ladders

DNA molecular weight marker XIV (***Roche***): for fragments <600bp
DNA molecular weight marker XVII (***Roche***): for fragments >600bp
DNA molecular weight marker X (***Roche***): for fragments of mixed sizes

Working dilutions:

5µl DNA molecular weight marker
6µl 10X gel loading buffer
49µl ddH_2O

Agarose Gel Electrophoresis

1) Prepare an agarose solution
   0.8% agarose (for DNA fragments >600bp): 40g agarose in 50ml 1X TBE
   1.5% agarose (for DNA fragments <600bp): 75g agarose in 50ml 1X TBE
2) Microwave on full power for 1 minute
3) Add 1µl ethidium bromide, mix gently
4) Pour into a gel casting tray, immediately insert comb
5) Allow to set for 30 minutes
6) Prepare sample DNA by adding 2µl 10X loading buffer per 20µl PCR reaction
7) Load 10µl sample per well
8) Load 5µl DNA molecular weight marker in one well per gel
9) Run gels at 50V for ~45 minutes, or until bands have resolved
10) Visualise by exposure to UV light

Reagents for DNA Extraction from Agarose Gels

Gel extraction mini kit (***Qiagen***)

DNA Extraction from Agarose Gels

Visualise gels with minimum exposure to UV light, to avoid DNA damage
Cut out bands with a sterile scalpel blade
Carry out gel extraction according to manufacturer's protocol
Elute in 50µl ddH_2O

Reagents for Quantitative RT-PCR

QuantiTect SYBR Green PCR kit (***Qiagen***):
A complete reaction mix containing reaction buffer, dNTPs, SYBR Green and DNA polymerase at 2X concentration

Primers at 20µM

Quantitative RT-PCR

1) For each set of primers, set up a template DNA dilution series to act as a standard curve. Ideally, these should be serial dilutions of the most highly concentrated template DNA:
0.001µl (1µl 1:1000)
0.01µl (1µl 1:100)
0.1µl (1µl 1:10)
1µl
2µl
For each other template DNA, make a 1:10 dilution and use 1µl per reaction (0.1µl template)
2) Make the template DNA solution up to 9.5µl with ddH_2O
3) Prepare 14µl mastermix per sample, make enough for n+1 samples
    1.5µl Forward primer (20µM)
    12.5µl 2X SYBR Green mix
4) Add 14µl mastermix to each diluted DNA template
5) Add 1.5µl Reverse primer (20µM) to each reaction
6) Perform PCR using the following programme:

15 minutes at 95^0C		
16 seconds at 94^0C	|	
30 seconds at annealing temperature	|	X35 cycles
30 seconds at 72^0C	|	
Plate read	|	
Melting curve analysis		

Reagents for TOPO Cloning of PCR Products

PCR product

Zero Blunt TOPO PCR Cloning Kit (***Invitrogen***)

Top-10 Chemically Competent *E.coli* (***Invitrogen***)

LB Agar plates
    3.5g LB Agar per 100ml
    Autoclave before use
    Pour plates at <50^0C
    Add antibiotic to cooled agar before cooling

Kanamycin (***Sigma***)
    Stock solution at 50mg.ml^{-1}
    Use at 1:1000, final concentration 50µg.ml^{-1}

TOPO Cloning of PCR Products

Perform PCR using Expand DNA polymerase.
Use 4µl fresh PCR product per TOPO cloning reaction
Carry out TOPO cloning according to the manufacturer's instructions
Transform into chemically competent TOP-10 *E.coli* according to the manufacturer's instructions
Spread 10µl, 50µl and 100µl transformed *E.coli* onto LB agar-kanamycin plates, allow to grow at 37^0C overnight
Transformed bacteria on LB agar plates can be stored at 4^0C for up to 14 days

Reagents for DNA Ligation

T4 DNA ligase (***Promega***)

T4 DNA ligase buffer (***Promega***)

Quantitated, linearised vector and insert DNA

DNA Ligation

Use 1 molecule vector per 10 molecules insert
1) Set up the following reaction:

Vector DNA	*n*µl
Insert DNA	*n*µl (100ng)
T4 DNA ligase	1.0µl
T4 DNA ligase buffer	2.5µl
ddH_2O	to 25.0µl

2) Incubate at 4^0C overnight
3) Transform into chemically competent TOP-10 *E.coli* as described above

Reagents for Glycerol Bacterial Strain Storage

Glycerol strain storage mix
- 65% Glycerol
- 0.1M $MgSO_4$
- 25mM Tris-Hcl pH8.0

LB broth
- 4g Bacto-tryptone
- 4g yeast extract
- 2g NaCl
- 400ml ddH_2O
- Autoclave before use

Kanamycin (see above)

Ampicillin (***Sigma***)
- Stock solution at 100mg.ml^{-1} in 50% ethanol
- Use at 1:1000, final concentration 100µg.ml^{-1}

Glycerol Bacterial Strain Storage

1) Seed 1ml LB broth containing the appropriate selective antibiotic with the bacterial clone
2) Grow at 37^0C overnight with shaking
3) Add 1ml glycerol strain storage mix
4) Store at -70^0C for up to 18 months

Reagents for Plasmid Minipreps and Midipreps

LB broth (see above)

Kanamycin (see above)

Ampicillin (see above)

QIAprep Spin Miniprep Kit (***Qiagen***)

HiSpeed Plasmid Midi Kit (***Qiagen***)

Plasmid Minipreps and Midipreps

1) Seed 2ml (miniprep) or 150ml (midiprep) LB broth containing the appropriate selective antibiotic with the bacterial clone
2) Grow at 37^0C overnight with shaking
3) Pellet cells by centrifugation at 10,000*g* for 1 minute (miniprep), or 6000*g* for 15 minutes at 4^0C (midiprep)
4) Remove LB broth, and resuspend the pellet in the appropriate amount of buffer P1
5) Carry out plasmid prep according to the manufacturer's instructions

Antibodies

Primary Antibodies

Anti-Pax6 PD (***Developmental Studies Hybridoma Bank***)

Monoclonal antibody, raised in mouse and directed against the paired domain (amino acids 1-122) of chick Pax6. Will detect both human and murine Pax6, as peptide sequence is identical across the three species.

Use in immunocytochemistry at 1:75, detect with direct fluorescence

Anti-Pax6 HD, Serum 13 (***Carriere et al., 1992***)

Antipeptide serum raised against the homeodomain of quail Pax6 (Pax QNR)

Use in Western Blotting at 1:200 in blocking buffer

Each aliquot can be re-used up to 3 times

Anti-Pax6 C-terminus (***Chemicon***)

Antipeptide serum raised against a C-terminal portion of mouse Pax6

Use in western blotting at 1:500 in blocking buffer

Use in immunocytochemistry at 1:500

Each aliquot can be re-used up to 2 times

Anti β-Actin (***Sigma***)

Monoclonal antibody, raised in mouse and directed against the N-terminal portion of β-actin

Use in western blotting at 1:1000 in TBS-Tween

Anti β-Tubulin Isotype III (***Sigma***)

Monoclonal antibody, raised in mouse and directed against the C-terminal portion of human β-III-tubulin

Use in immunocytochemistry at 1:1000 in blocking buffer

Anti-MAP2 (***Sigma***)

Monoclonal antibody, raised in mouse and directed against all mouse MAP2 forms. Does not cross react with tubulin from other microtubule associated proteins

Use in immunocytochemistry at 1:200

Anti-Tau1 (***Chemicon***)

Monoclonal antibody, raised in mouse and directed against bovine Tau-1. Recognises both mouse and human Tau-1

Use in immunocytochemistry at 1:200

Secondary Antibodies: Immunocytochemistry

AlexaFluor 448- conjugated anti-mouse IgG1 (***Molecular Probes***)
secondary antibody, raised in goat
Use in Immunocytochemistry at 1:200

Alexa-Fluor 568-conjugated anti-mouse IgG1 (***Molecular Probes***)
Secondary antibody, raised in rabbit
Use in immunocytochemistry at 1:200

R-PE- conjugated anti-mouse IgG1 (***Molecular Probes***)
secondary antibody, raised in goat
Use in Immunocytochemistry at 1:75

Biotin-Anti-Mouse
Biotin-conjugated anti-mouse IgG secondary antibody, raised in goat
Use in Immunocytochemistry at 1:500

Streptavidin AlexaFluor 488 conjugate (***Molecular Probes***)
AlexaFluor 488- conjugated streptavidin
Use in immunocytochemistry at 1:1000

Secondary Antibodies: Western Blotting

HRP-Anti-mouse (***SAPU***)
Horseradish Peroxidase- conjugated anti-mouse IgG secondary antibody, raised in sheep
Use in Western blotting at 1:1000 in blocking buffer

HRP-Anti-Rabbit (***Sigma***)
Horseradish Peroxidase- conjugated anti-rabbit IgG secondary antibody, raised in donkey
Use in Western blotting at 1:10000 in blocking buffer

Appendix 2 - Primer sequences and optimal annealing temperatures for PCR

PCR primers

Human Pax6 Full 5' XbaI
5' AAT CTA GAA TGC AGA ACA GTC ACA GC 3' Anneal: 63^0C

Human Pax6 Full 3' XbaI
5' AAT CTA GAT TAC TGT AAT CTT GGC CA 3' Anneal: 59^0C

Product size:1327bp/1285bp (Full-length Pax6+5a / Full-length Pax6-5a)

These primers were designed by Dr T. I. Simpson to amplify full-length Pax6 from the U373-MG cell line. These primers were specific to sequence within the 5' and 3' UTRs of the human Pax6 gene. The 5' end of each primer contained an *Xba*I recognition site. As primer specificity is conferred by 3' sequence, the presence of this 5' restriction endonuclease recognition site did not adversely affect primer-cDNA binding. However, cDNA clones obtained this way could then be cut with the restriction endonuclease *Xba*I, and cloned into sites with compatible cohesive DNA ends.

Pax6 Exon 5 F
5' GTC ACA GCG GAG TGA ATC AG 3' Anneal: 58.5^0C

Pax6 Exon 7 R
5' CTA GCC AGG TTG CGA AGA AC 3' Anneal: 58.5^0C

Product size: 385/427bp (-5a /+5a) 169/211bp (-5aΔ6 /+5aΔ6)

These primers were designed by Dr. T. I. Simpson to amplify a region between exons 5 and 7 of the Pax6 cDNA. Due to the high degree of sequence conservation at the Pax6 locus between mouse and human, these primers were 100% complementary to cDNA from both species. This PCR spans two intron-exon boundaries, thus eliminating the risk of amplifying any contaminating genomic DNA and obtaining false positive results. It also spans the alternatively spliced exons 5a and 6, giving four PCR products corresponding to Pax6+5a, Pax6-5a, Pax6+5aΔ6, and Pax6-5aΔ6, with product sizes from 169bp to 427bp, which are easily resolved by agarose gel electrophoresis.

Pax6 exon 9 F
5' CAT CCT TTA CCC AAG AGC AA 3' Anneal: 58^0C

Pax6 BR
5' GTA TGA GGA GGT CTG GCT GG 3' Anneal: 61^0C

These primers were used to amplify the 5'-truncated Pax6 form in pJP15.12. "Pax6 exon 9 F" anneals within exon 9 of the human Pax6 gene, after the internal ATG putative translation start site. "Pax6 BR" anneals within exon 12. They allowed amplification of the inserted short form of Pax6 by colony PCR, to confirm its presence after cloning.

GAPDH F
5' GGG TGG AGC CAA ACG GGT C 3' Anneal: 58.5^{0}C

GAPDH R
5' GGAGTTGCTGTTGAAGTCGCA 3' Anneal: 58.5^{0}C

Product size: 532bp

These primers were designed to allow amplification of the murine glyceraldehyde-3-phosphate dehydrogenase (GAPDH) cDNA. This is a housekeeping gene expressed in all mammalian cells, and was used to confirm the presence of cDNA in samples which were being tested for Pax6, in order to confirm that negative results were due to the absence of Pax6 expression rather than cDNA degradation or problems with cDNA synthesis.

GAPDH F Light
5' GGG TGT GAA CCA CGA GAA AT 3' Anneal: 58^{0}C

GAPDH R Light
5' CCT TCC ATG CCA AAG TT 3' Anneal: 56^{0}C

Product size: 120bp

These primers were designed to allow amplification of the murine GAPDH cDNA for quantitative real-time PCR. This was used to confirm the presence of cDNA in samples which were being tested for Pax6, in order to confirm that negative results were due to the absence of Pax6 expression rather than cDNA degradation or problems with cDNA synthesis. Levels of GAPDH cDNA as determined by this primer set were also used to create quantitative standards, to allow the exact quantitation of Pax6 in cDNA samples.

Pax6 Exon 5F light
5' GCT TGG TGG TGT CTT TGT CA 3' Anneal: 55^{0}C

Pax6 Exon 56R light
5' TCA CAC AAC CGT TGG ATA CC 3' Anneal: 55^{0}C

Pax6 Exon 55aR light
5' TTT GCA TCT GCA TGG GTC T 3' Anneal: 55^{0}C

Product size Exon 5F light / Exon 56R light: 131bp
Exon 5F light / Exon 55aR light: 129bp

These primers (see **Figure A2.1**) were designed to allow amplification of the Pax6 gene between exons 5 and 6. Exon 5F light binds within exon 5 of the Pax6 cDNA, and should bind all Pax6 cDNA present in a sample. Exon 56R light takes advantage of the fact that primer binding specificity is conferred by 3' sequence, to allow selective amplification of the Pax6-5a splice form. 19bp of this primer corresponds to sequence in the 5' end of exon 6. The most 3' residue, however, binds to the G residue at the 3' end of exon 5. Thus, this primer can only bind target cDNA when exon 5 is spliced directly onto exon 6, and exon 5a is absent. In a similar manner, the Exon 55aR light primer spans the junction between exons 5 and 5a, and can only bind to the Pax6+5a splice form.

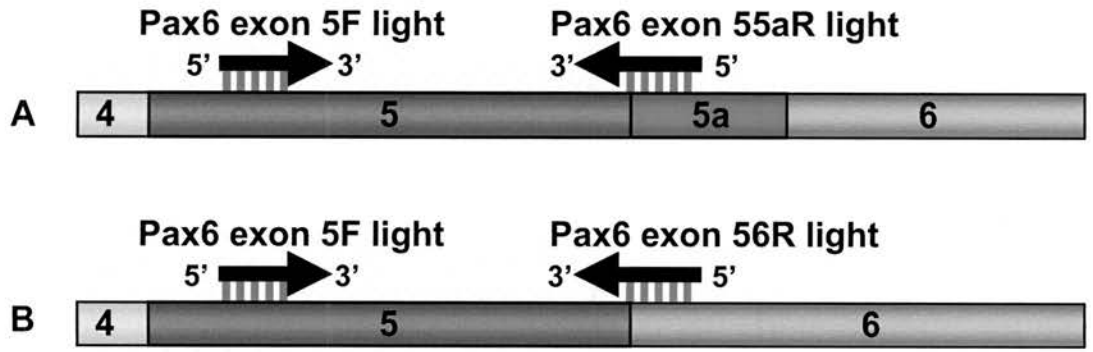

Figure A2.1 Q-PCR primers used to distinguish *Pax6-5a* and *Pax6+5a*. One forward primer, "Pax6 exon 5F light", is used for both PCR reactions, as it binds to sequence within exon 5 of the *Pax6* cDNA. **A**, The reverse primer "Pax6 exon 55aR light" anneals to sequence spanning the junction between exons 5 and 5a. The 3' 3bp of the primer, which are crucial for primer binding, cross the exon boundary. If exon 5a is absent, this primer cannot bind. **B**, The reverse primer "Pax6 exon 56R light" anneals to sequence spanning the junction between exons 5 and 6. The 3' 3bp of the primer crosses the exon boundary. If exon 5a is present, this primer cannot bind. Coloured bars, *Pax6* exons. Arrows, Q-PCR primers.

Pax6 MMu Exon 3F
5' AAG TGG ACG TAT ATC CCA GTT CTC 3' Anneal: 49^{0}C

Pax6 MMu Exon 5AR
5' AGC ACC TGG ACT TTT GCA TC 3' Anneal: 49^{0}C

Product size: 247bp

These primers were designed to amplify murine Pax6 between exon 3, in the 5'UTR of the gene, and exon 5a. Products created in this way were subsequently cloned and used as templates for riboprobe synthesis.

Pax6 MMu Exon6F
5' GAG ACT GGC TCC ATC AGA CC 3' Anneal: 65^{0}C

Pax6 MMu Exon7R
5' CTT GCG TGG GTT GCC CTG GT 3' Anneal: 65^{0}C

Product size: 340bp

These primers were designed to amplify murine Pax6 between exon 6 and exon 7. Products created in this way were subsequently cloned and used as templates for riboprobe synthesis.

Pax6 MMu RiboF
5' AGG GCA ACC CAC GCA AGA 3' Anneal: 63^{0}C

Pax6 MMu Exon11R
5' TGG TGA GGG CGG TGT CTG TTC 3' Anneal: 63^{0}C

Product size: 464bp

These primers were designed to amplify murine Pax6 between exon 7 and exon 11. Products created in this way were subsequently cloned and used as templates for riboprobe synthesis.

Sequencing Primers:

Pax6 AF
5' TTT GCC CGA GAA AGA CTA GC 3' Anneal: 61^{0}C

Pax6 AR
5' AAC TCT TTC TCC AGG GCC TC 3' Anneal: 61^{0}C

Pax6 BF
5' CCA GCC AGA CCTACCTACAT AC 3' Anneal: 61^{0}C

Pax6 BR
5' GTA TGA GGA GGT CTG GCT GG 3' Anneal: 61^{0}C

These primers were designed to anneal at intervals within the Pax6 coding sequence. In combination with M13 primers either side of the multiple cloning site into which Pax6 was inserted, they were used to sequence all Pax6 over-expression constructs in both directions.

M13F
5' GTA AAA CGA CGG CCA G 3' Anneal: 52^0C

M13R
5' CAG GAA ACA GCT ATG AC 3' Anneal: 52^0C

These primers were used to sequence all Pax6 over-expression constructs and riboprobe template constructs in both directions.

Bibliography

Altman, J. and Bayer, S. A. (1978a). Prenatal development of the cerebellar system in the rat. I. Cytogenesis and histogenesis of the deep nuclei and the cortex of the cerebellum. *J Comp Neurol* **179**, 23-48.

Altman, J. and Bayer, S. A. (1978b). Prenatal development of the cerebellar system in the rat. II. Cytogenesis and histogenesis of the inferior olive, pontine gray, and the precerebellar reticular nuclei. *J Comp Neurol* **179**, 49-75.

Anderson, T. R., Hedlund, E. and Carpenter, E. M. (2002). Differential Pax6 promoter activity and transcript expression during forebrain development. *Mech Dev* **114**, 171-5.

Andrews, G. L. and Mastick, G. S. (2003). R-cadherin is a Pax6-regulated, growth-promoting cue for pioneer axons. *J Neurosci* **23**, 9873-80.

Aota, S., Nakajima, N., Sakamoto, R., Watanabe, S., Ibaraki, N. and Okazaki, K. (2003). Pax6 autoregulation mediated by direct interaction of Pax6 protein with the head surface ectoderm-specific enhancer of the mouse Pax6 gene. *Dev Biol* **257**, 1-13.

Ashery-Padan, R. and Gruss, P. (2001). Pax6 lights-up the way for eye development. *Curr Opin Cell Biol* **13**, 706-14.

Baumer, N., Marquardt, T., Stoykova, A., Ashery-Padan, R., Chowdhury, K. and Gruss, P. (2002). Pax6 is required for establishing naso-temporal and dorsal characteristics of the optic vesicle. *Development* **129**, 4535-45.

Baumer, N., Marquardt, T., Stoykova, A., Spieler, D., Treichel, D., Ashery-Padan, R. and Gruss, P. (2003). Retinal pigmented epithelium determination requires the redundant activities of Pax2 and Pax6. *Development* **130**, 2903-15.

Bertrand, N., Castro, D. S. and Guillemot, F. (2002). Proneural genes and the specification of neural cell types. *Nat Rev Neurosci* **3**, 517-30.

Bishop, K. M., Rubenstein, J. L. and O'Leary, D. D. (2002). Distinct actions of Emx1, Emx2, and Pax6 in regulating the specification of areas in the developing neocortex. *J Neurosci* **22**, 7627-38.

Briscoe, J. and Ericson, J. (1999). The specification of neuronal identity by graded Sonic Hedgehog signalling. *Semin Cell Dev Biol* **10**, 353-62.

Burrill, J. D., Moran, L., Goulding, M. D. and Saueressig, H. (1997). PAX2 is expressed in multiple spinal cord interneurons, including a population of EN1+ interneurons that require PAX6 for their development. *Development* **124**, 4493-503.

Bustin, S. A. (2000). Absolute quantification of mRNA using real-time reverse transcription polymerase chain reaction assays. *J Mol Endocrinol* **25**, 169-93.

Callaerts, P., Halder, G. and Gehring, W. J. (1997). PAX-6 in development and evolution. *Annu Rev Neurosci* **20**, 483-532.

Caric, D., Gooday, D., Hill, R. E., McConnell, S. K. and Price, D. J. (1997). Determination of the migratory capacity of embryonic cortical cells lacking the transcription factor Pax-6. *Development* **124**, 5087-96.

Carriere, C., Plaza, S., Caboche, J., Dozier, C., Bailly, M., Martin, P. and Saule, S. (1995). Nuclear localization signals, DNA binding, and transactivation properties of quail Pax-6 (Pax-QNR) isoforms. *Cell Growth Differ* **6**, 1531-40.

Carriere, C., Plaza, S., Martin, P., Quatannens, B., Bailly, M., Stehelin, D. and Saule, S. (1993). Characterization of quail Pax-6 (Pax-QNR) proteins expressed in the neuroretina. *Mol Cell Biol* **13**, 7257-66.

Chauhan, B. K., Reed, N. A., Yang, Y., Cermak, L., Reneker, L., Duncan, M. K. and Cvekl, A. (2002a). A comparative cDNA microarray analysis reveals a spectrum of genes regulated by Pax6 in mouse lens. *Genes Cells* **7**, 1267-83.

Chauhan, B. K., Reed, N. A., Zhang, W., Duncan, M. K., Kilimann, M. W. and Cvekl, A. (2002b). Identification of genes downstream of Pax6 in the mouse lens using cDNA microarrays. *J Biol Chem* **277**, 11539-48.

Chauhan, B. K., Yang, Y., Cveklova, K. and Cvekl, A. (2004a). Functional interactions between alternatively spliced forms of Pax6 in crystallin gene regulation and in haploinsufficiency. *Nucleic Acids Res* **32**, 1696-709.
Chauhan, B. K., Yang, Y., Cveklova, K. and Cvekl, A. (2004b). Functional properties of natural human PAX6 and PAX6(5a) mutants. *Invest Ophthalmol Vis Sci* **45**, 385-92.
Chauhan, B. K., Zhang, W., Cveklova, K., Kantorow, M. and Cvekl, A. (2002c). Identification of differentially expressed genes in mouse Pax6 heterozygous lenses. *Invest Ophthalmol Vis Sci* **43**, 1884-90.
Collinson, J. M., Chanas, S. A., Hill, R. E. and West, J. D. (2004). Corneal development, limbal stem cell function, and corneal epithelial cell migration in the Pax6(+/-) mouse. *Invest Ophthalmol Vis Sci* **45**, 1101-8.
Collinson, J. M., Hill, R. E. and West, J. D. (2000). Different roles for Pax6 in the optic vesicle and facial epithelium mediate early morphogenesis of the murine eye. *Development* **127**, 945-56.
Collinson, J. M., Quinn, J. C., Hill, R. E. and West, J. D. (2003). The roles of Pax6 in the cornea, retina, and olfactory epithelium of the developing mouse embryo. *Dev Biol* **255**, 303-12.
Cremer, H., Lange, R., Christoph, A., Plomann, M., Vopper, G., Roes, J., Brown, R., Baldwin, S., Kraemer, P. and Scheff, S. (1994). Inactivation of the N-CAM gene in mice results in size reduction of the olfactory bulb and deficits in spatial learning. *Nature* **367**, 455-9.
Cvekl, A., Kashanchi, F., Brady, J. N. and Piatigorsky, J. (1999). Pax-6 interactions with TATA-box-binding protein and retinoblastoma protein. *Invest Ophthalmol Vis Sci* **40**, 1343-50.
Cvekl, A., Kashanchi, F., Sax, C. M., Brady, J. N. and Piatigorsky, J. (1995a). Transcriptional regulation of the mouse alpha A-crystallin gene: activation dependent on a cyclic AMP-responsive element (DE1/CRE) and a Pax-6-binding site. *Mol Cell Biol* **15**, 653-60.
Cvekl, A., Sax, C. M., Li, X., McDermott, J. B. and Piatigorsky, J. (1995b). Pax-6 and lens-specific transcription of the chicken delta 1-crystallin gene. *Proc Natl Acad Sci U S A* **92**, 4681-5.
Czerny, T. and Busslinger, M. (1995). DNA-binding and transactivation properties of Pax-6: three amino acids in the paired domain are responsible for the different sequence recognition of Pax-6 and BSAP (Pax-5). *Mol Cell Biol* **15**, 2858-71.
Czerny, T., Halder, G., Kloter, U., Souabni, A., Gehring, W. J. and Busslinger, M. (1999). twin of eyeless, a second Pax-6 gene of Drosophila, acts upstream of eyeless in the control of eye development. *Mol Cell* **3**, 297-307.
Davis, J. A. and Reed, R. R. (1996). Role of Olf-1 and Pax-6 transcription factors in neurodevelopment. *J Neurosci* **16**, 5082-94.
Dellovade, T. L., Pfaff, D. W. and Schwanzel-Fukuda, M. (1998). Olfactory bulb development is altered in small-eye (Sey) mice. *J Comp Neurol* **402**, 402-18.
Dimanlig, P. V., Faber, S. C., Auerbach, W., Makarenkova, H. P. and Lang, R. A. (2001). The upstream ectoderm enhancer in Pax6 has an important role in lens induction. *Development* **128**, 4415-24.
Dohrmann, C., Gruss, P. and Lemaire, L. (2000). Pax genes and the differentiation of hormone-producing endocrine cells in the pancreas. *Mech Dev* **92**, 47-54.
Dominguez, M., Ferres-Marco, D., Gutierrez-Avino, F. J., Speicher, S. A. and Beneyto, M. (2004). Growth and specification of the eye are controlled independently by Eyegone and Eyeless in Drosophila melanogaster. *Nat Genet* **36**, 31-9.
Duncan, M. K., Haynes, J. I., 2nd, Cvekl, A. and Piatigorsky, J. (1998). Dual roles for Pax-6: a transcriptional repressor of lens fiber cell-specific beta-crystallin genes. *Mol Cell Biol* **18**, 5579-86.
Duncan, M. K., Kozmik, Z., Cveklova, K., Piatigorsky, J. and Cvekl, A. (2000). Overexpression of PAX6(5a) in lens fiber cells results in cataract and upregulation of (alpha)5(beta)1 integrin expression. *J Cell Sci* **113 (Pt 18)**, 3173-85.

Edelman, G. M. and Jones, F. S. (1995). Developmental control of N-CAM expression by Hox and Pax gene products. *Philos Trans R Soc Lond B Biol Sci* **349**, 305-12.
Engelkamp, D., Rashbass, P., Seawright, A. and van Heyningen, V. (1999). Role of Pax6 in development of the cerebellar system. *Development* **126**, 3585-96.
Epstein, J., Cai, J., Glaser, T., Jepeal, L. and Maas, R. (1994a). Identification of a Pax paired domain recognition sequence and evidence for DNA-dependent conformational changes. *J Biol Chem* **269**, 8355-61.
Epstein, J. A., Glaser, T., Cai, J., Jepeal, L., Walton, D. S. and Maas, R. L. (1994b). Two independent and interactive DNA-binding subdomains of the Pax6 paired domain are regulated by alternative splicing. *Genes Dev* **8**, 2022-34.
Ericson, J., Rashbass, P., Schedl, A., Brenner-Morton, S., Kawakami, A., van Heyningen, V., Jessell, T. M. and Briscoe, J. (1997). Pax6 controls progenitor cell identity and neuronal fate in response to graded Shh signaling. *Cell* **90**, 169-80.
Estivill-Torrus, G., Pearson, H., van Heyningen, V., Price, D. J. and Rashbass, P. (2002). Pax6 is required to regulate the cell cycle and the rate of progression from symmetrical to asymmetrical division in mammalian cortical progenitors. *Development* **129**, 455-66.
Estivill-Torrus, G., Vitalis, T., Fernandez-Llebrez, P. and Price, D. J. (2001). The transcription factor Pax6 is required for development of the diencephalic dorsal midline secretory radial glia that form the subcommissural organ. *Mech Dev* **109**, 215-24.
Fantes, J., Redeker, B., Breen, M., Boyle, S., Brown, J., Fletcher, J., Jones, S., Bickmore, W., Fukushima, Y., Mannens, M. et al. (1995). Aniridia-associated cytogenetic rearrangements suggest that a position effect may cause the mutant phenotype. *Hum Mol Genet* **4**, 415-22.
Favor, J., Neuhauser-Klaus, A. and Ehling, U. H. (1988). The effect of dose fractionation on the frequency of ethylnitrosourea-induced dominant cataract and recessive specific locus mutations in germ cells of the mouse. *Mutat Res* **198**, 269-75.
Fischer, I., Shea, T. B., Sapirstein, V. S. and Kosik, K. S. (1986). Expression and distribution of microtubule-associated protein 2 (MAP2) in neuroblastoma and primary neuronal cells. *Brain Res* **390**, 99-109.
Fujita, S. (1964). Analysis of Neuron Differentiation in the Central Nervous System by Tritiated Thymidine Autoradiography. *J Comp Neurol* **122**, 311-27.
Gillies, K. and Price, D. J. (1993). The fates of cells in the developing cerebral cortex of normal and methylazoxymethanol acetate-lesioned mice. *Eur J Neurosci* **5**, 73-84.
Glaser, T., Walton, D. S. and Maas, R. L. (1992). Genomic structure, evolutionary conservation and aniridia mutations in the human PAX6 gene. *Nat Genet* **2**, 232-9.
Gorlov, I. P. and Saunders, G. F. (2002). A method for isolating alternatively spliced isoforms: isolation of murine Pax6 isoforms. *Anal Biochem* **308**, 401-4.
Goshima, Y., Ohsako, S. and Yamauchi, T. (1993). Overexpression of Ca2+/calmodulin-dependent protein kinase II in Neuro2a and NG108-15 neuroblastoma cell lines promotes neurite outgrowth and growth cone motility. *J Neurosci* **13**, 559-67.
Gotz, M., Stoykova, A. and Gruss, P. (1998). Pax6 controls radial glia differentiation in the cerebral cortex. *Neuron* **21**, 1031-44.
Goudreau, G., Petrou, P., Reneker, L. W., Graw, J., Loster, J. and Gruss, P. (2002). Mutually regulated expression of Pax6 and Six3 and its implications for the Pax6 haploinsufficient lens phenotype. *Proc Natl Acad Sci U S A* **99**, 8719-24.
Goulding, M. D., Lumsden, A. and Gruss, P. (1993). Signals from the notochord and floor plate regulate the region-specific expression of two Pax genes in the developing spinal cord. *Development* **117**, 1001-16.
Griffin, C., Kleinjan, D. A., Doe, B. and van Heyningen, V. (2002). New 3' elements control Pax6 expression in the developing pretectum, neural retina and olfactory region. *Mech Dev* **112**, 89-100.
Grindley, J. C., Davidson, D. R. and Hill, R. E. (1995). The role of Pax-6 in eye and nasal development. *Development* **121**, 1433-42.
Grindley, J. C., Hargett, L. K., Hill, R. E., Ross, A. and Hogan, B. L. (1997). Disruption of PAX6 function in mice homozygous for the Pax6Sey-1Neu mutation produces

abnormalities in the early development and regionalization of the diencephalon. *Mech Dev* **64**, 111-26.
Halder, G., Callaerts, P. and Gehring, W. J. (1995). Induction of ectopic eyes by targeted expression of the eyeless gene in Drosophila. *Science* **267**, 1788-92.
Harris, W. A. (1997). Pax-6: where to be conserved is not conservative. *Proc Natl Acad Sci U S A* **94**, 2098-100.
Heins, N., Malatesta, P., Cecconi, F., Nakafuku, M., Tucker, K. L., Hack, M. A., Chapouton, P., Barde, Y. A. and Gotz, M. (2002). Glial cells generate neurons: the role of the transcription factor Pax6. *Nat Neurosci* **5**, 308-15.
Hill, R. E., Favor, J., Hogan, B. L., Ton, C. C., Saunders, G. F., Hanson, I. M., Prosser, J., Jordan, T., Hastie, N. D. and van Heyningen, V. (1991). Mouse small eye results from mutations in a paired-like homeobox-containing gene. *Nature* **354**, 522-5.
Hogan, B. L., Horsburgh, G., Cohen, J., Hetherington, C. M., Fisher, G. and Lyon, M. F. (1986). Small eyes (Sey): a homozygous lethal mutation on chromosome 2 which affects the differentiation of both lens and nasal placodes in the mouse. *J Embryol Exp Morphol* **97**, 95-110.
Holst, B. D., Wang, Y., Jones, F. S. and Edelman, G. M. (1997). A binding site for Pax proteins regulates expression of the gene for the neural cell adhesion molecule in the embryonic spinal cord. *Proc Natl Acad Sci U S A* **94**, 1465-70.
Jainchill, J. L., Aaronson, S. A. and Todaro, G. J. (1969). Murine sarcoma and leukemia viruses: assay using clonal lines of contact-inhibited mouse cells. *J Virol* **4**, 549-53.
Jang, C. C., Chao, J. L., Jones, N., Yao, L. C., Bessarab, D. A., Kuo, Y. M., Jun, S., Desplan, C., Beckendorf, S. K. and Sun, Y. H. (2003). Two Pax genes, eye gone and eyeless, act cooperatively in promoting Drosophila eye development. *Development* **130**, 2939-51.
Jaworski, C., Sperbeck, S., Graham, C. and Wistow, G. (1997). Alternative splicing of Pax6 in bovine eye and evolutionary conservation of intron sequences. *Biochem Biophys Res Commun* **240**, 196-202.
Jean, D., Ewan, K. and Gruss, P. (1998). Molecular regulators involved in vertebrate eye development. *Mech Dev* **76**, 3-18.
Jimenez, D., Garcia, C., de Castro, F., Chedotal, A., Sotelo, C., de Carlos, J. A., Valverde, F. and Lopez-Mascaraque, L. (2000). Evidence for intrinsic development of olfactory structures in Pax-6 mutant mice. *J Comp Neurol* **428**, 511-26.
Jones, L., Lopez-Bendito, G., Gruss, P., Stoykova, A. and Molnar, Z. (2002). Pax6 is required for the normal development of the forebrain axonal connections. *Development* **129**, 5041-52.
Jun, S. and Desplan, C. (1996). Cooperative interactions between paired domain and homeodomain. *Development* **122**, 2639-50.
Kamachi, Y., Uchikawa, M., Tanouchi, A., Sekido, R. and Kondoh, H. (2001). Pax6 and SOX2 form a co-DNA-binding partner complex that regulates initiation of lens development. *Genes Dev* **15**, 1272-86.
Kammandel, B., Chowdhury, K., Stoykova, A., Aparicio, S., Brenner, S. and Gruss, P. (1999). Distinct cis-essential modules direct the time-space pattern of the Pax6 gene activity. *Dev Biol* **205**, 79-97.
Kammermeier, L., Leemans, R., Hirth, F., Flister, S., Wenger, U., Walldorf, U., Gehring, W. J. and Reichert, H. (2001). Differential expression and function of the Drosophila Pax6 genes eyeless and twin of eyeless in embryonic central nervous system development. *Mech Dev* **103**, 71-8.
Kawakami, A., Kimura-Kawakami, M., Nomura, T. and Fujisawa, H. (1997). Distributions of PAX6 and PAX7 proteins suggest their involvement in both early and late phases of chick brain development. *Mech Dev* **66**, 119-30.
Kim, A. S., Anderson, S. A., Rubenstein, J. L., Lowenstein, D. H. and Pleasure, S. J. (2001). Pax-6 regulates expression of SFRP-2 and Wnt-7b in the developing CNS. *J Neurosci* **21**, RC132.

Kleinjan, D. A., Seawright, A., Childs, A. J. and van Heyningen, V. (2004). Conserved elements in Pax6 intron 7 involved in (auto)regulation and alternative transcription. *Dev Biol* **265**, 462-77.
Kojima, N., Tachida, Y., Yoshida, Y. and Tsuji, S. (1996). Characterization of mouse ST8Sia II (STX) as a neural cell adhesion molecule-specific polysialic acid synthase. Requirement of core alpha1,6-linked fucose and a polypeptide chain for polysialylation. *J Biol Chem* **271**, 19457-63.
Koroma, B. M., Yang, J. M. and Sundin, O. H. (1997). The Pax-6 homeobox gene is expressed throughout the corneal and conjunctival epithelia. *Invest Ophthalmol Vis Sci* **38**, 108-20.
Kozmik, Z., Czerny, T. and Busslinger, M. (1997). Alternatively spliced insertions in the paired domain restrict the DNA sequence specificity of Pax6 and Pax8. *Embo J* **16**, 6793-803.
Kralova, J., Czerny, T., Spanielova, H., Ratajova, V. and Kozmik, Z. (2002). Complex regulatory element within the gammaE- and gammaF-crystallin enhancers mediates Pax6 regulation and is required for induction by retinoic acid. *Gene* **286**, 271-82.
Kronhamn, J., Frei, E., Daube, M., Jiao, R., Shi, Y., Noll, M. and Rasmuson-Lestander, A. (2002). Headless flies produced by mutations in the paralogous Pax6 genes eyeless and twin of eyeless. *Development* **129**, 1015-26.
Lefebvre, T., Planque, N., Leleu, D., Bailly, M., Caillet-Boudin, M. L., Saule, S. and Michalski, J. C. (2002). O-glycosylation of the nuclear forms of Pax-6 products in quail neuroretina cells. *J Cell Biochem* **85**, 208-18.
Lengler, J., Krausz, E., Tomarev, S., Prescott, A., Quinlan, R. A. and Graw, J. (2001). Antagonistic action of Six3 and Prox1 at the gamma-crystallin promoter. *Nucleic Acids Res* **29**, 515-26.
Levers, T. E., Edgar, J. M. and Price, D. J. (2001). The fates of cells generated at the end of neurogenesis in developing mouse cortex. *J Neurobiol* **48**, 265-77.
Lewis, J. A. and Hodgkin, J. A. (1977). Specific neuroanatomical changes in chemosensory mutants of the nematode Caenorhabditis elegans. *J Comp Neurol* **172**, 489-510.
Lopez-Mascaraque, L. and de Castro, F. (2002). The olfactory bulb as an independent developmental domain. *Cell Death Differ* **9**, 1279-86.
Lopez-Mascaraque, L., Garcia, C., Valverde, F. and de Carlos, J. A. (1998). Central olfactory structures in Pax-6 mutant mice. *Ann N Y Acad Sci* **855**, 83-94.
Malatesta, P., Hack, M. A., Hartfuss, E., Kettenmann, H., Klinkert, W., Kirchhoff, F. and Gotz, M. (2003). Neuronal or glial progeny: regional differences in radial glia fate. *Neuron* **37**, 751-64.
Malatesta, P., Hartfuss, E. and Gotz, M. (2000). Isolation of radial glial cells by fluorescent-activated cell sorting reveals a neuronal lineage. *Development* **127**, 5253-63.
Mansouri, A., St-Onge, L. and Gruss, P. (1999). Role of Genes in Endoderm-derived Organs. *Trends Endocrinol Metab* **10**, 164-167.
Marquardt, T., Ashery-Padan, R., Andrejewski, N., Scardigli, R., Guillemot, F. and Gruss, P. (2001). Pax6 is required for the multipotent state of retinal progenitor cells. *Cell* **105**, 43-55.
Mastick, G. S. and Andrews, G. L. (2001). Pax6 regulates the identity of embryonic diencephalic neurons. *Mol Cell Neurosci* **17**, 190-207.
Mastick, G. S., Davis, N. M., Andrew, G. L. and Easter, S. S., Jr. (1997). Pax-6 functions in boundary formation and axon guidance in the embryonic mouse forebrain. *Development* **124**, 1985-97.
Matsunaga, E., Araki, I. and Nakamura, H. (2000). Pax6 defines the di-mesencephalic boundary by repressing En1 and Pax2. *Development* **127**, 2357-65.
Maulbecker, C. C. and Gruss, P. (1993). The oncogenic potential of Pax genes. *Embo J* **12**, 2361-7.
Mayanil, C. S., George, D., Freilich, L., Miljan, E. J., Mania-Farnell, B., McLone, D. G. and Bremer, E. G. (2001). Microarray analysis detects novel Pax3 downstream target genes. *J Biol Chem* **276**, 49299-309.

Mazet, F., Hutt, J. A., Millard, J. and Shimeld, S. M. (2003). Pax gene expression in the developing central nervous system of Ciona intestinalis. *Gene Expr Patterns* **3**, 743-5.
Meech, R., Kallunki, P., Edelman, G. M. and Jones, F. S. (1999). A binding site for homeodomain and Pax proteins is necessary for L1 cell adhesion molecule gene expression by Pax-6 and bone morphogenetic proteins. *Proc Natl Acad Sci U S A* **96**, 2420-5.
Mikkola, I., Bruun, J. A., Bjorkoy, G., Holm, T. and Johansen, T. (1999). Phosphorylation of the transactivation domain of Pax6 by extracellular signal-regulated kinase and p38 mitogen-activated protein kinase. *J Biol Chem* **274**, 15115-26.
Mikkola, I., Bruun, J. A., Holm, T. and Johansen, T. (2001). Superactivation of Pax6-mediated transactivation from paired domain-binding sites by dna-independent recruitment of different homeodomain proteins. *J Biol Chem* **276**, 4109-18.
Mishra, R., Gorlov, I. P., Chao, L. Y., Singh, S. and Saunders, G. F. (2002). PAX6, paired domain influences sequence recognition by the homeodomain. *J Biol Chem* **277**, 49488-94.
Miskiewicz, P., Morrissey, D., Lan, Y., Raj, L., Kessler, S., Fujioka, M., Goto, T. and Weir, M. (1996). Both the paired domain and homeodomain are required for in vivo function of Drosophila Paired. *Development* **122**, 2709-18.
Morgan, R. (2004). Conservation of sequence and function in the Pax6 regulatory elements. *Trends Genet* **20**, 283-7.
Muta, M., Kamachi, Y., Yoshimoto, A., Higashi, Y. and Kondoh, H. (2002). Distinct roles of SOX2, Pax6 and Maf transcription factors in the regulation of lens-specific delta1-crystallin enhancer. *Genes Cells* **7**, 791-805.
Muzio, L., DiBenedetto, B., Stoykova, A., Boncinelli, E., Gruss, P. and Mallamaci, A. (2002a). Conversion of cerebral cortex into basal ganglia in Emx2(-/-) Pax6(Sey/Sey) double-mutant mice. *Nat Neurosci* **5**, 737-45.
Muzio, L., DiBenedetto, B., Stoykova, A., Boncinelli, E., Gruss, P. and Mallamaci, A. (2002b). Emx2 and Pax6 control regionalization of the pre-neuronogenic cortical primordium. *Cereb Cortex* **12**, 129-39.
Nadarajah, B. and Parnavelas, J. G. (2002). Modes of neuronal migration in the developing cerebral cortex. *Nat Rev Neurosci* **3**, 423-32.
Nishina, S., Kohsaka, S., Yamaguchi, Y., Handa, H., Kawakami, A., Fujisawa, H. and Azuma, N. (1999). PAX6 expression in the developing human eye. *Br J Ophthalmol* **83**, 723-7.
Nomura, T. and Osumi, N. (2004). Misrouting of mitral cell progenitors in the Pax6/small eye rat telencephalon. *Development* **131**, 787-96.
Okladnova, O., Syagailo, Y. V., Mossner, R., Riederer, P. and Lesch, K. P. (1998). Regulation of PAX-6 gene transcription: alternate promoter usage in human brain. *Brain Res Mol Brain Res* **60**, 177-92.
Onuma, Y., Takahashi, S., Asashima, M., Kurata, S. and Gehring, W. J. (2002). Conservation of Pax 6 function and upstream activation by Notch signaling in eye development of frogs and flies. *Proc Natl Acad Sci U S A* **99**, 2020-5.
Osumi, N., Hirota, A., Ohuchi, H., Nakafuku, M., Iimura, T., Kuratani, S., Fujiwara, M., Noji, S. and Eto, K. (1997). Pax-6 is involved in the specification of hindbrain motor neuron subtype. *Development* **124**, 2961-72.
Plaza, S., Dozier, C. and Saule, S. (1993). Quail Pax-6 (Pax-QNR) encodes a transcription factor able to bind and trans-activate its own promoter. *Cell Growth Differ* **4**, 1041-50.
Plaza, S., Dozier, C., Turque, N. and Saule, S. (1995). Quail Pax-6 (Pax-QNR) mRNAs are expressed from two promoters used differentially during retina development and neuronal differentiation. *Mol Cell Biol* **15**, 3344-53.
Plaza, S., Grevin, D., MacLeod, K., Stehelin, D. and Saule, S. (1994). Pax-QNR/Pax-6, a paired- and homeobox-containing protein, recognizes Ets binding sites and can alter the transactivating properties of Ets transcription factors. *Gene Expr* **4**, 43-52.
Plaza, S., Langlois, M. C., Turque, N., LeCornet, S., Bailly, M., Begue, A., Quatannens, B., Dozier, C. and Saule, S. (1997). The homeobox-containing Engrailed (En-1) product down-regulates the expression of Pax-6 through a DNA binding-independent mechanism. *Cell Growth Differ* **8**, 1115-25.

Ponten, J. and Macintyre, E. H. (1968). Long term culture of normal and neoplastic human glia. *Acta Pathol Microbiol Scand* **74**, 465-86.
Prasad, K. N. and Hsie, A. W. (1971). Morphologic differentiation of mouse neuroblastoma cells induced in vitro by dibutyryl adenosine 3':5'-cyclic monophosphate. *Nat New Biol* **233**, 141-2.
Pratt, T., Quinn, J. C., Simpson, T. I., West, J. D., Mason, J. O. and Price, D. J. (2002). Disruption of early events in thalamocortical tract formation in mice lacking the transcription factors Pax6 or Foxg1. *J Neurosci* **22**, 8523-31.
Pratt, T., Vitalis, T., Warren, N., Edgar, J. M., Mason, J. O. and Price, D. J. (2000). A role for Pax6 in the normal development of dorsal thalamus and its cortical connections. *Development* **127**, 5167-78.
Punzo, C., Plaza, S., Seimiya, M., Schnupf, P., Kurata, S., Jaeger, J. and Gehring, W. J. (2004). Functional divergence between eyeless and twin of eyeless in Drosophila melanogaster. *Development* **131**, 3943-53.
Quiring, R., Walldorf, U., Kloter, U. and Gehring, W. J. (1994). Homology of the eyeless gene of Drosophila to the Small eye gene in mice and Aniridia in humans. *Science* **265**, 785-9.
Rakic, P. (1972). Mode of cell migration to the superficial layers of fetal monkey neocortex. *J Comp Neurol* **145**, 61-83.
Rakic, P. (2003). Developmental and evolutionary adaptations of cortical radial glia. *Cereb Cortex* **13**, 541-9.
Richardson, J., Cvekl, A. and Wistow, G. (1995). Pax-6 is essential for lens-specific expression of zeta-crystallin. *Proc Natl Acad Sci U S A* **92**, 4676-80.
Roccato, E., Pagliardini, S., Cleris, L., Canevari, S., Formelli, F., Pierotti, M. A. and Greco, A. (2003). Role of TFG sequences outside the coiled-coil domain in TRK-T3 oncogenic activation. *Oncogene* **22**, 807-18.
Rodrigues, A. B. and Moses, K. (2004). Growth and specification: fly Pax6 homologs eyegone and eyeless have distinct functions. *Bioessays* **26**, 600-3.
Sakai, M., Serria, M. S., Ikeda, H., Yoshida, K., Imaki, J. and Nishi, S. (2001). Regulation of c-maf gene expression by Pax6 in cultured cells. *Nucleic Acids Res* **29**, 1228-37.
Salem, C. E., Markl, I. D., Bender, C. M., Gonzales, F. A., Jones, P. A. and Liang, G. (2000). PAX6 methylation and ectopic expression in human tumor cells. *Int J Cancer* **87**, 179-85.
Santos-Ocampo, S., Colvin, J. S., Chellaiah, A. and Ornitz, D. M. (1996). Expression and biological activity of mouse fibroblast growth factor-9. *J Biol Chem* **271**, 1726-31.
Scardigli, R., Baumer, N., Gruss, P., Guillemot, F. and Le Roux, I. (2003). Direct and concentration-dependent regulation of the proneural gene Neurogenin2 by Pax6. *Development* **130**, 3269-81.
Schedl, A., Ross, A., Lee, M., Engelkamp, D., Rashbass, P., van Heyningen, V. and Hastie, N. D. (1996). Influence of PAX6 gene dosage on development: overexpression causes severe eye abnormalities. *Cell* **86**, 71-82.
Schmahl, W., Knoedlseder, M., Favor, J. and Davidson, D. (1993). Defects of neuronal migration and the pathogenesis of cortical malformations are associated with Small eye (Sey) in the mouse, a point mutation at the Pax-6-locus. *Acta Neuropathol (Berl)* **86**, 126-35.
Schwarz, M., Cecconi, F., Bernier, G., Andrejewski, N., Kammandel, B., Wagner, M. and Gruss, P. (2000). Spatial specification of mammalian eye territories by reciprocal transcriptional repression of Pax2 and Pax6. *Development* **127**, 4325-34.
Sharon-Friling, R., Richardson, J., Sperbeck, S., Lee, D., Rauchman, M., Maas, R., Swaroop, A. and Wistow, G. (1998). Lens-specific gene recruitment of zeta-crystallin through Pax6, Nrl-Maf, and brain suppressor sites. *Mol Cell Biol* **18**, 2067-76.
Shea, T. B. and Beermann, M. L. (1994). Respective roles of neurofilaments, microtubules, MAP1B, and tau in neurite outgrowth and stabilization. *Mol Biol Cell* **5**, 863-75.
Shea, T. B., Majocha, R. E., Marotta, C. A. and Nixon, R. A. (1988). Soluble, phosphorylated forms of the high molecular weight neurofilament protein in perikarya of cultured neuronal cells. *Neurosci Lett* **92**, 291-7.

Sidman, R. L., Miale, I. L. and Feder, N. (1959). Cell proliferation and migration in the primitive ependymal zone: an autoradiographic study of histogenesis in the nervous system. *Exp Neurol* **1**, 322-33.
Simpson, T. I. and Price, D. J. (2002). Pax6; a pleiotropic player in development. *Bioessays* **24**, 1041-51.
Singh, S., Mishra, R., Arango, N. A., Deng, J. M., Behringer, R. R. and Saunders, G. F. (2002). Iris hypoplasia in mice that lack the alternatively spliced Pax6(5a) isoform. *Proc Natl Acad Sci U S A* **99**, 6812-5.
Singh, S., Stellrecht, C. M., Tang, H. K. and Saunders, G. F. (2000). Modulation of PAX6 homeodomain function by the paired domain. *J Biol Chem* **275**, 17306-13.
St-Onge, L., Sosa-Pineda, B., Chowdhury, K., Mansouri, A. and Gruss, P. (1997). Pax6 is required for differentiation of glucagon-producing alpha-cells in mouse pancreas. *Nature* **387**, 406-9.
Stoykova, A., Fritsch, R., Walther, C. and Gruss, P. (1996). Forebrain patterning defects in Small eye mutant mice. *Development* **122**, 3453-65.
Stoykova, A., Gotz, M., Gruss, P. and Price, J. (1997). Pax6-dependent regulation of adhesive patterning, R-cadherin expression and boundary formation in developing forebrain. *Development* **124**, 3765-77.
Stoykova, A. and Gruss, P. (1994). Roles of Pax-genes in developing and adult brain as suggested by expression patterns. *J Neurosci* **14**, 1395-412.
Sun, T., Pringle, N. P., Hardy, A. P., Richardson, W. D. and Smith, H. K. (1998). Pax6 influences the time and site of origin of glial precursors in the ventral neural tube. *Mol Cell Neurosci* **12**, 228-39.
Takahashi, M. and Osumi, N. (2002). Pax6 regulates specification of ventral neurone subtypes in the hindbrain by establishing progenitor domains. *Development* **129**, 1327-38.
Talamillo, A., Quinn, J. C., Collinson, J. M., Caric, D., Price, D. J., West, J. D. and Hill, R. E. (2003). Pax6 regulates regional development and neuronal migration in the cerebral cortex. *Dev Biol* **255**, 151-63.
Tang, H. K., Singh, S. and Saunders, G. F. (1998). Dissection of the transactivation function of the transcription factor encoded by the eye developmental gene PAX6. *J Biol Chem* **273**, 7210-21.
Ton, C. C., Hirvonen, H., Miwa, H., Weil, M. M., Monaghan, P., Jordan, T., van Heyningen, V., Hastie, N. D., Meijers-Heijboer, H. and Drechsler, M. (1991). Positional cloning and characterization of a paired box- and homeobox-containing gene from the aniridia region. *Cell* **67**, 1059-74.
Turque, N., Plaza, S., Radvanyi, F., Carriere, C. and Saule, S. (1994). Pax-QNR/Pax-6, a paired box- and homeobox-containing gene expressed in neurons, is also expressed in pancreatic endocrine cells. *Mol Endocrinol* **8**, 929-38.
Tyas, D. A., Pearson, H., Rashbass, P. and Price, D. J. (2003). Pax6 regulates cell adhesion during cortical development. *Cereb Cortex* **13**, 612-9.
van Heyningen, V. and Williamson, K. A. (2002). PAX6 in sensory development. *Hum Mol Genet* **11**, 1161-7.
Vitalis, T., Cases, O., Engelkamp, D., Verney, C. and Price, D. J. (2000). Defect of tyrosine hydroxylase-immunoreactive neurons in the brains of mice lacking the transcription factor Pax6. *J Neurosci* **20**, 6501-16.
Walther, C. and Gruss, P. (1991). Pax-6, a murine paired box gene, is expressed in the developing CNS. *Development* **113**, 1435-49.
Warren, N., Caric, D., Pratt, T., Clausen, J. A., Asavaritikrai, P., Mason, J. O., Hill, R. E. and Price, D. J. (1999). The transcription factor, Pax6, is required for cell proliferation and differentiation in the developing cerebral cortex. *Cereb Cortex* **9**, 627-35.
Warren, N. and Price, D. J. (1997). Roles of Pax-6 in murine diencephalic development. *Development* **124**, 1573-82.
Wilson, D., Sheng, G., Lecuit, T., Dostatni, N. and Desplan, C. (1993). Cooperative dimerization of paired class homeo domains on DNA. *Genes Dev* **7**, 2120-34.

Xu, H. E., Rould, M. A., Xu, W., Epstein, J. A., Maas, R. L. and Pabo, C. O. (1999). Crystal structure of the human Pax6 paired domain-DNA complex reveals specific roles for the linker region and carboxy-terminal subdomain in DNA binding. *Genes Dev* **13**, 1263-75.
Yamaguchi, Y., Sawada, J., Yamada, M., Handa, H. and Azuma, N. (1997). Autoregulation of Pax6 transcriptional activation by two distinct DNA-binding subdomains of the paired domain. *Genes Cells* **2**, 255-61.
Yamamoto, S., Nagao, M., Sugimori, M., Kosako, H., Nakatomi, H., Yamamoto, N., Takebayashi, H., Nabeshima, Y., Kitamura, T., Weinmaster, G. et al. (2001). Transcription factor expression and Notch-dependent regulation of neural progenitors in the adult rat spinal cord. *J Neurosci* **21**, 9814-23.
Yamaoka, T., Yano, M., Yamada, T., Matsushita, T., Moritani, M., Ii, S., Yoshimoto, K., Hata, J. and Itakura, M. (2000). Diabetes and pancreatic tumours in transgenic mice expressing Pa x 6. *Diabetologia* **43**, 332-9.
Yamasaki, T., Kawaji, K., Ono, K., Bito, H., Hirano, T., Osumi, N. and Kengaku, M. (2001). Pax6 regulates granule cell polarization during parallel fiber formation in the developing cerebellum. *Development* **128**, 3133-44.
Zhang, W., Cveklova, K., Oppermann, B., Kantorow, M. and Cvekl, A. (2001). Quantitation of PAX6 and PAX6(5a) transcript levels in adult human lens, cornea, and monkey retina. *Mol Vis* **7**, 1-5.
Zhang, Y. and Emmons, S. W. (1995). Specification of sense-organ identity by a Caenorhabditis elegans Pax-6 homologue. *Nature* **377**, 55-9.